

Alma Mater Studiorum – Università di Bologna

**DOTTORATO DI RICERCA IN
SCIENZE VETERINARIE**

Ciclo 34

Settore Concorsuale: 07/H4 – CLINICA MEDICA E FARMACOLOGIA VETERINARIA

Settore Scientifico Disciplinare: CLINICA MEDICA VETERINARIA

NEW PERSPECTIVES OF GENETIC DISORDERS IN CATTLE

Presentata da: Joana Gonçalves Pontes Jacinto

Coodinatore Dottorato

Carolina Castagnetti

Supervisore

Arcangelo Gentile

Co-supervisore

Cord Drögemüller

Esame finale anno 2022

I Abstract

Improvement in productivity and performance has been observed in cattle production worldwide during the last decades as result of advances in e.g., nutrition, disease control and genetics. However, a negative trend in inbreeding has developed simultaneously and has predisposed to an increased significance of recessively inherited disorders. Although many of them occur sporadically, other, if not perceived in their real potentiality of spread, may constitute a concerning threat for the affected breed. The investigative strategy used in this thesis is called “forward genetic approach” (FGA), following the sequence of a clinical, genealogical, gross- and/or histopathological and genetic study of the affected individual(s). Genomic technologies, such as single nucleotide polymorphism (SNP), array genotyping and whole-genome sequencing (WGS), allowed for straightforward locus mapping and the identification of candidate causal variants in affected individuals or families. In particular a WGS trio-approach (patient, dam and sire) was applied.

The objectives of the current study were: a) to study genetic disorders deriving from the past or current caseload available as well as presented or submitted to the Clinic for Ruminants, Department of Veterinary Medical Sciences, University of Bologna, Italy (DIMEVET) and to the Institute for Genetics, Vetsuisse-Faculty, University of Bern, Switzerland (IGVFB) by applying a FGA; b) to estimate the prevalence of deleterious alleles responsible for Pseudomyotonia Congenita in Chianina, Romagnola and Marchigiana cattle, Paunch Calf Syndrome in Romagnola and Marchigiana cattle, Hemifacial microsomia (Romagnola), Congenital bilateral cataract (Romagnola), Ichthyosis congenita (Chianina), Ichthyosis fetalis (Chianina), Achromatopsia (Braunvieh) and Hypotrichosis (Belted-Galloway, Hereford); and c) to add well-characterized materials to the Biobank for Bovine Genetic Disorders at DIMEVET/IGVFB.

FGA allowed the identification of candidate variants for seven recessive and seven *de novo* dominant disorders in different breeds, associated with a large spectrum of phenotypes affecting different systems:

- skeletal (n=5):
 - two *de novo* variants in *COL2A1* (large deletions) causing Achondrogenesis type II,

- *de novo* variant in *COL1A1* (missense) causing Osteogenesis imperfecta,
- *de novo* variant in *MAP2K2* (missense) causing Skeletal-cardio-enteric dysplasia,
- recessively inherited variant in *KDM2B* (missense) causing Paunch calf syndrome,
- neuromuscular (n=1):
 - *de novo* variant in *KCNQ1* (missense) causing Congenital neuromuscular channelopathy, representing the first disorder associated with the *KCNQ1*,
- metabolic (n=1):
 - recessively inherited variant in *APOB* (gross insertion) causing Congenital Cholesterol Deficiency,
- integumentary (n=5):
 - *de novo* variant in *KRT5* (in-frame deletion) causing Epidermolysis Bullosa Simplex,
 - *de novo* variant in *COL5A2* (missense) causing Classical Ehlers-Danlos Syndrome,
 - recessively inherited variant in *FA2H* (frameshift insertion) causing Ichthyosis Congenita,
 - recessively inherited variant in *KRT71* (frameshift deletion) causing Hypotrichosis,
 - recessively inherited variant in *HEPHL1* (nonsense) causing Hypotrichosis,
- ocular and ears (n=2):
 - recessively inherited variant in *CNGB3* (missense) causing Achromatopsia,
 - recessively inherited variant in *LAMB1* (missense) causing Hemifacial Microsomia.

A further FGA carried out for a case of Generalized Juvenile Angiomatosis in a Simmental calf revealed to be inconclusive.

The allelic frequencies for the Pseudomyotonia congenita, Paunch calf syndrome, Hemifacial microsomia, Congenital bilateral cataract, Ichthyosis congenita, Ichthyosis fetalis, Achromatopsia and Hypotrichosis were calculated. Particular concerning was the finding of an allelic frequency of 12% for the Paunch calf syndrome in Romagnola cattle. With respect to the improvement of the Biobank for Bovine Genetic Diseases, biological materials of cases and their available relatives as well as controls used for the allelic

frequency estimations were stored at -20 °C. Altogether, around 16 000 samples were added to the biobank.

The performed research enabled a comprehensive clinicopathological and molecular genetic study. The given examples highlight the usefulness of genetically precise diagnosis for understanding rare disorders caused by *de novo* and recessively inherited variants, and the need for continuous monitoring of genetic disorders in cattle breeding. Furthermore, this research provides a DNA-based diagnostic tests for six recessively inherited disorders enabling the selection against the identified causal variants. Novel discoveries in large animals (specifically cattle) are useful as translational models for human diseases.

II Tables of contents, figures and tables

i Table of contents

I	Abstract	1
II	Tables of contents, figures and tables	4
i	Table of contents	5
ii	List of figures	7
iii	List of tables	8
iv	List of additional data in the appendix	9
1	Introduction	11
1.1	Recessively inherited disorders in cattle	12
1.2	Dominantly inherited disorders in cattle	14
1.3	X-linked inherited disorders in cattle	15
1.4	Clinicopathological approach to genetic disorders	16
1.4.1	Anamnesis	17
1.4.2	Clinical and pathological investigations	18
1.5	Genetic approach to disorders in cattle	19
1.5.1	Methods of the forward genetic approach	19
2	Objectives of thesis work	25
3	Materials and Methods	26
3.1	Study of the genetic disorders	26
3.2	Estimation of the frequency of deleterious alleles	33
3.3	Enrichment of the Biobank for Bovine Genetic Disorders	35
4	Results	36
4.1	Study of the genetic disorders	36
4.1.1	Skeletal disorders	39
4.1.2	Neuromuscular disorders	77
4.1.3	Metabolic disorders	91
4.1.4	Genodermatosis	96
4.1.5	Ocular and auricular disorders	166

4.2	Estimation of the frequency of deleterious alleles.....	190
4.3	Enrichment of the Biobank for Genetic Disorders.....	191
5	Discussion and Perspectives	192
6	Appendix	196
7	Curriculum Vitae	220
8	List of Publications.....	223
9	Conference oral communications and posters	225
10	References	227
11	Acknowledgements.....	240

ii List and legends of the figures

Figure 1: Possible causes of genetic disorders.	11
Figure 2: Illustration of the most common modes of recessively inherited disorders. (A) Classical recessive inheritance in non-lethal disorders. (B) Classical recessive inheritance in lethal disorders. (C) Co-dominant inherited disorders. Note that heterozygous animals of co- dominant disorders might be affected in a completely dominant manner, recessive manner, or any level in between.	13
Figure 3: Illustration of the most common modes of dominantly inherited disorders. (A and B) Classical dominant somatic inheritance. (C) <i>De novo</i> post-zygotic mutations during the early embryonic development of the calf. (D) <i>De novo</i> mutations in the germinal line of the sire. (E) <i>De novo</i> mutations in the germinal line of the dam.	15
Figure 4: Illustration of the most common modes of X-linked inherited disorders. (A) X- linked recessive inheritance, where the dam is carrier of the causal variant. Note that just male offspring are affected. (B) X-linked recessive inheritance, where the sire is hemizygous mutant. Note that the offspring are not affected. (C) X-linked dominant inheritance from the dam. Note that both male and female offspring are affected. (D) X-linked dominant inheritance from the sire. Note that only female offspring are affected.	16
Figure 5: Illustration of an algorithm to diagnose genetic disorders.	17
Figure 6: Illustration of possible methodologies used in the forward genetic approach (FGA) for recessive- and dominantly inherited disorders. The blue row represents population studies, red row represents family studies and yellow row represents the possible identification of the candidate causal variant using whole-genome sequencing. Note that the only method that is exclusively used for recessively inherited disorders is the homozygosity mapping.....	20
Figure 7: Schematic representation of WGS workflow.	23

iii List of tables

Table 1: Overview of cases studied during the PhD study period.....27
Table 2: Total number of genotyped animals per disorder, associated variant and breed.34
Table 3: Results of estimation of allele and carrier frequencies. 190

iv List of additional data in the appendix

Table A1: Genetic congenital skeletal disorders of cattle: brief description of the phenotype, the associated genes and types of variants.	196
Table A2: Genetic neuromuscular disorders of cattle: brief description of the phenotype, the associated genes and types of variants.	202
Table A3: Genetic metabolic disorders of cattle: brief description of the phenotype, the associated genes and types of variants.	207
Table A4: Congenital genodermatosis of cattle: brief description of the phenotype, the associated genes and types of variants.	211
Table A5: Genetic ocular and auricular disorders of cattle: brief description of the phenotype, the associated genes and types of variants.	216
Table A6: Genetic cardiac and diaphragmatic muscle disorders of cattle: brief description of the phenotype, the associated genes and types of variants.	218
Table A7: Genetic congenital renal and genitourinary disorders of cattle: brief description of the phenotype, the associated genes and types of variants.	218

1 Introduction

In humans, genetic disorders are considered to be individually rare; however, they account for approximately 80% of rare disorders, of which there are numerous thousands [1]. There is no overall definition for rare disorders. However, the average prevalence threshold varies between 40 and 50 cases/100,000 people [2]. By similarity the same definition might be applied to cattle.

Genetic disorders might be caused by a complete or partial change in the DNA sequence when compared with the reference sequence [3]. They might be associated with pathogenic variants in one gene (monogenic disorders), in multiple genes (polygenic disorders), or in combination with environmental factors that might render the individual more or less susceptible to develop certain disorders (**Figure 1**) [4]. In addition, genetic disorders might be associated with chromosomal abnormalities such as the trisomy, monosomy or chromosomal translocation [5].

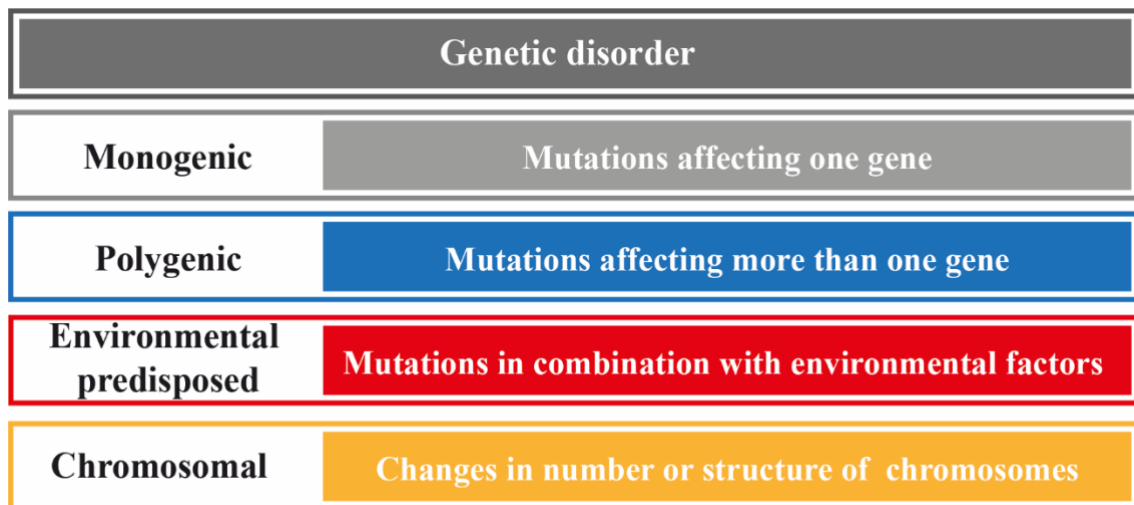


Figure 1: Possible causes of genetic disorders.

The first reports of recessive lethal disorders in cattle were published in 1928, several decades before the structure of DNA had been described [6–8]. In the last decades, the molecular genetics has evolved in a tremendous manner especially with the inventions of second- and third-generation sequencing technologies allowing a rapid and cost-effective whole-genome sequencing (WGS). Unlocking the secrets of the cattle genome in 2009 provided the creation of the first draft of a bovine genomic assembly based on DNA from

the inbred Hereford cow *Dominette* [9]. The availability of the bovine genome sequence represented an important evolutionary step for learning and better understanding genetic disorders in cattle. It can be said, that thanks to the development and continuous improvement of the cattle assembly, the constant advance of molecular genetics methods, as well as the detailed phenotypical descriptions and active participation of stakeholders, all types of genotype-phenotype associations can be potentially investigated.

An extraordinary overview of genetic diseases in cattle can be found in the Online Mendelian Inheritance in Animals (OMIA) database that by January 2022 counted 579 genetic disorders in cattle with potential causal variants described for 402 [10]. Furthermore, 296 of the phenotypes are potential models for human disorders [10].

1.1 Recessively inherited disorders in cattle

During the last six decades, a global improvement on livestock productivity has been observed as a result of e.g., advances in nutrition, disease control and genetics [11]. In particular, genetic improvement occurred through breed substitution, cross-breeding and within-breed selection [12]. Among these strategies, within-breed selection pushes sustained, cumulative progress in comparison with breed substitution and cross-breeding. In fact, extraordinary results have been accomplished in cattle breeding by combining within-breed selection with reproductive techniques such as artificial insemination, ovum pick-up and embryo transfer, to more efficiently spread elite genomes [11]. Nonetheless, within-breed selection has caused a reduction of the effective population size and contemporarily an increased level of inbreeding, with the consequent ineluctable emergence of harmful recessively inherited alleles [13]. Negative effects of inbreeding lead to the so-called inbreeding depression. Doekes *et al.* differentiated between recent and ancient inbreeding, where recent inbreeding is assumed to be more harmful. In fact, man driven breeding pressure may increase the spread of deleterious recessive alleles, differently from natural selection that on the contrary tends to reduce them over time [14]. Traditionally, inbreeding had been estimated based on pedigree relationships. Nowadays, inbreeding is mainly estimated by using genotype-based measurements, such as runs of homozygosity (ROH).

Recessively inherited disorders are genetic conditions that occur when a mutation is present on both alleles of a given gene, meaning that an individual has to be homozygous mutant to express the phenotype, e.g., a disorder.

The majority of recessively inherited disorders in cattle follow a monogenic classical pattern of Mendelian inheritance. Monogenic recessively inherited non-lethal disorders respect the Hardy-Weinberg equilibrium (**Figure 2A**) that on the contrary is not respected by the lethal disorders, due to the absence of homozygous mutant individuals in the population (**Figure 2B**).

More complex disorders with a polygenic or co-dominant inheritance also occur. In these cases, the allele frequencies do not perfectly segregate with the phenotype. Co-dominant disorders are defined as recessively inherited-like: all homozygous animals are affected, but due to a complete or incomplete dominant effects in some animals, also heterozygous animals may present disease (**Figure 2C**). Recessively inherited disorders in cattle encompass a large spectrum of phenotypes and genotypes affecting different systems such as skeletal, neuromuscular, integumentary, ocular, auricular, cardiac, renal, metabolic and reproductive. **Tables A1 to A7** in the Appendix summarize the phenotype, the type of inheritance, the associated genes and causal variants of these disorders.

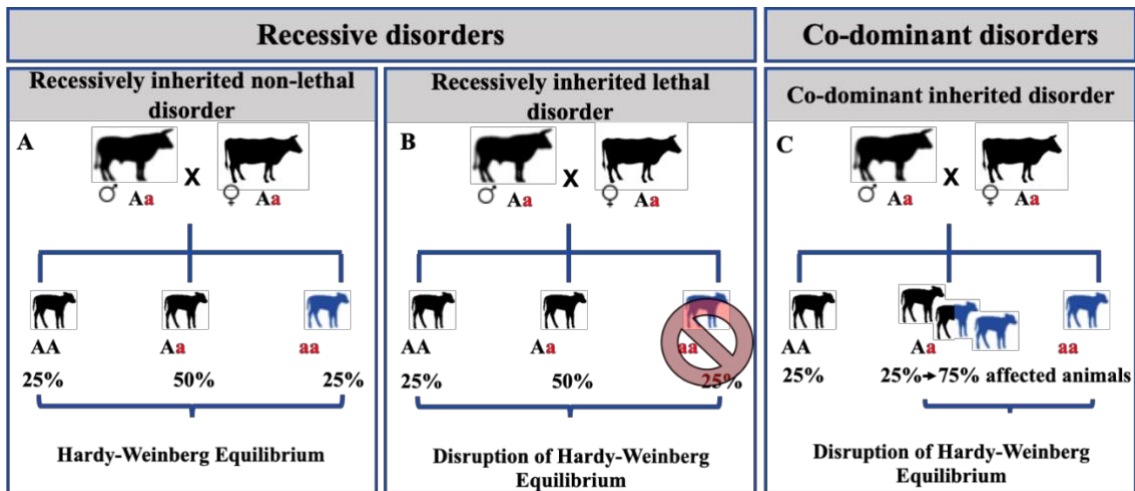


Figure 2: Illustration of the most common modes of recessively inherited disorders. (A) Classical recessive inheritance in non-lethal disorders. **(B)** Classical recessive inheritance in lethal disorders. **(C)** Co-dominant inherited disorders. Note that heterozygous animals of co-dominant disorders might be affected in a completely dominant manner, recessive manner, or any level in between.

1.2 Dominantly inherited disorders in cattle

In the past few years, a rapid accumulation of whole genome-sequences of artificial insemination (AI) sires and parent-offspring trios, industrial scale single-nucleotide polymorphism (SNP) chip genotyping data for routine genomic evaluations, and comprehensive phenotyping have created an exceptional opportunity to study, identify and understand the biology of dominant mutations in cattle.

Dominantly inherited disorders are genetic conditions that develop when a deleterious mutation is present on one only allele of a given gene, meaning that also heterozygous individuals are affected.

The majority of dominantly inherited disorders in cattle are monogenic lethal [15]. However, they might also be caused by chromosomal abnormalities such as trisomy [16]. These disorders may be:

- a) inherited somatically from an affected parent (diseased but still capable of procreate; **Figure 3A, B**),
- b) arise as *de novo* mutations in the germline of an healthy parent (so-called germinal mosaicism; **Figure 3C, D**),
- c) arise post-zygotically in the developing embryo (**Figure 3E**).

In cattle, diseases due to germinal mosaicism are mostly observed in the case the mutation is inherited from the sire. This is due to the fact that breeding sires, especially those used for AI, have an higher effective prolificacy, increasing the possibility of the occurrence, spread and therefore evidence of the phenotype [15].

Dominantly inherited disorders in cattle encompass a large spectrum of congenital phenotypes and genotypes affecting different systems, so far known for the skeletal, neuromuscular and integumentary systems. **Tables A1, A2 and A4** in the Appendix summarize the phenotype, the type of inheritance, the associated genes and the causal variants of these disorders.

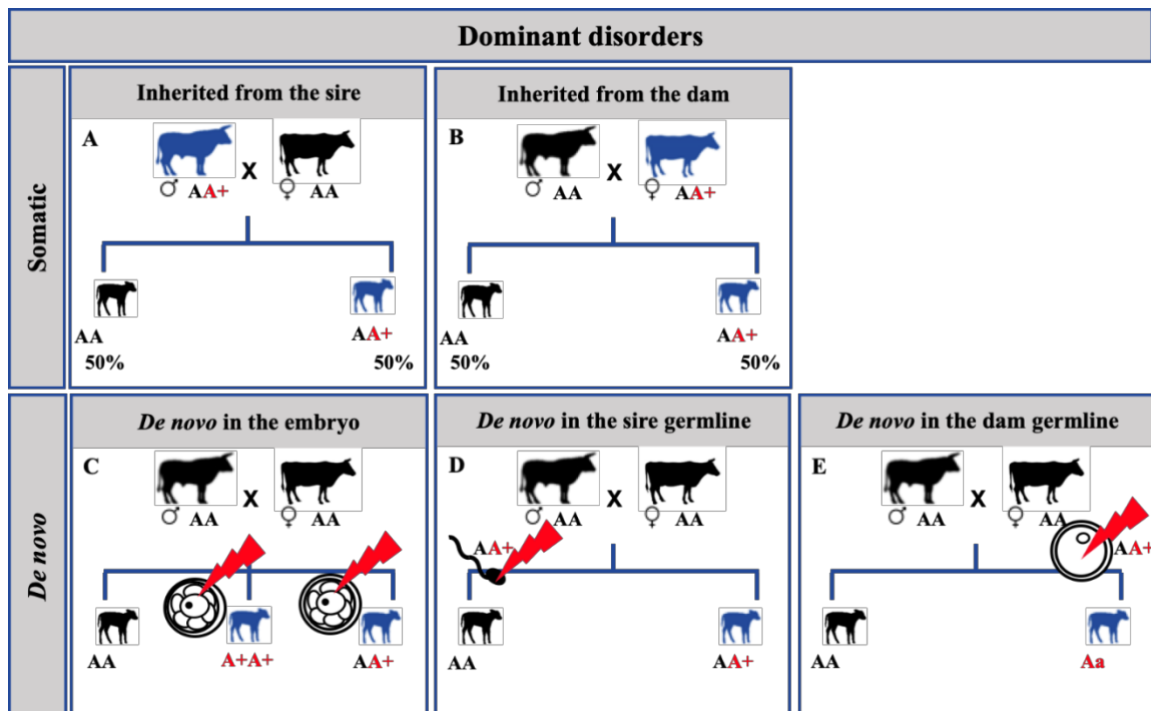


Figure 3: Illustration of the most common modes of dominantly inherited disorders. (A and B) Classical dominant somatic inheritance. (C) De novo post-zygotic mutations during the early embryonic development of the calf. (D) De novo mutations in the germinal line of the sire. (E) De novo mutations in the germinal line of the dam.

1.3 X-linked inherited disorders in cattle

Only a few X-linked disorders have been reported in cattle. X-linked disorders are associated with mutations on the X chromosome and often have a sex bias. Males are hemizygous and therefore are more susceptible to express a X-linked disorder with both recessively and dominantly modes of inheritance (**Figure 4A, C**). In contrast, females have two X chromosomes. In the case of recessively inherited disorders, they are just carriers in the majority of cases and therefore asymptomatic (**Figure 4A, B**). However, females show always the disorder when it is dominantly inherited from the sire. On the contrary, in this situation males are not affected as they always receive a Y chromosome from him (**Figure 4D**).

X-linked inherited disorders in cattle encompass few phenotypes and genotypes including Hemophilia A-*F8*, Anhidrotic ectodermal dysplasia-*EDA* and Streaked hypotrichosis-*TSR2* (**Table A2, Table A4** in the [Appendix](#)).

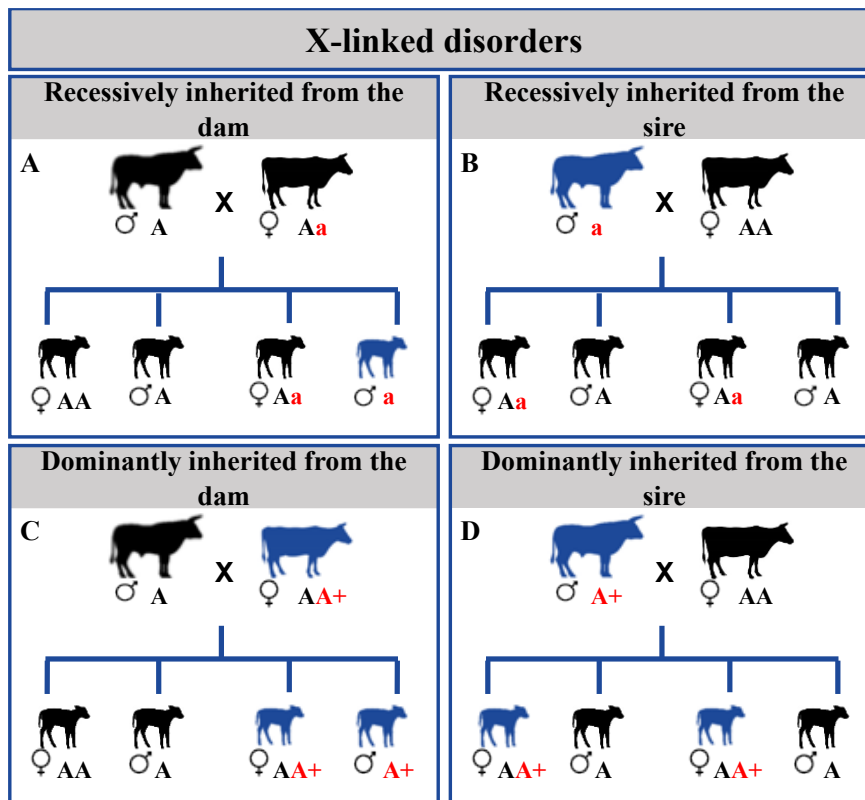


Figure 4: Illustration of the most common modes of X-linked inherited disorders. (A) X-linked recessive inheritance, where the dam is carrier of the causal variant. Note that just male offspring are affected. (B) X-linked recessive inheritance, where the sire is hemizygous mutant. Note that the offspring are not affected. (C) X-linked dominant inheritance from the dam. Note that both male and female offspring are affected. (D) X-linked dominant inheritance from the sire. Note that only female offspring are affected.

1.4 Clinicopathological approach to genetic disorders

It is important to collect a comprehensive anamnesis, perform complete clinical and pathological investigations (eventually integrated by ancillary diagnostics), and carry out genetic testing (when available) to identify genetic disorders (**Figure 5**).

While practitioners and stakeholders might not always be able to make a conclusive diagnosis of a genetic disorder, their role is critical in collecting the anamnestic, clinical and pathological details, considering the possibility of a genetic disease in their differential diagnosis, ordering genetic testing when available, and if not possible, reporting and referring the cases to reference centers.

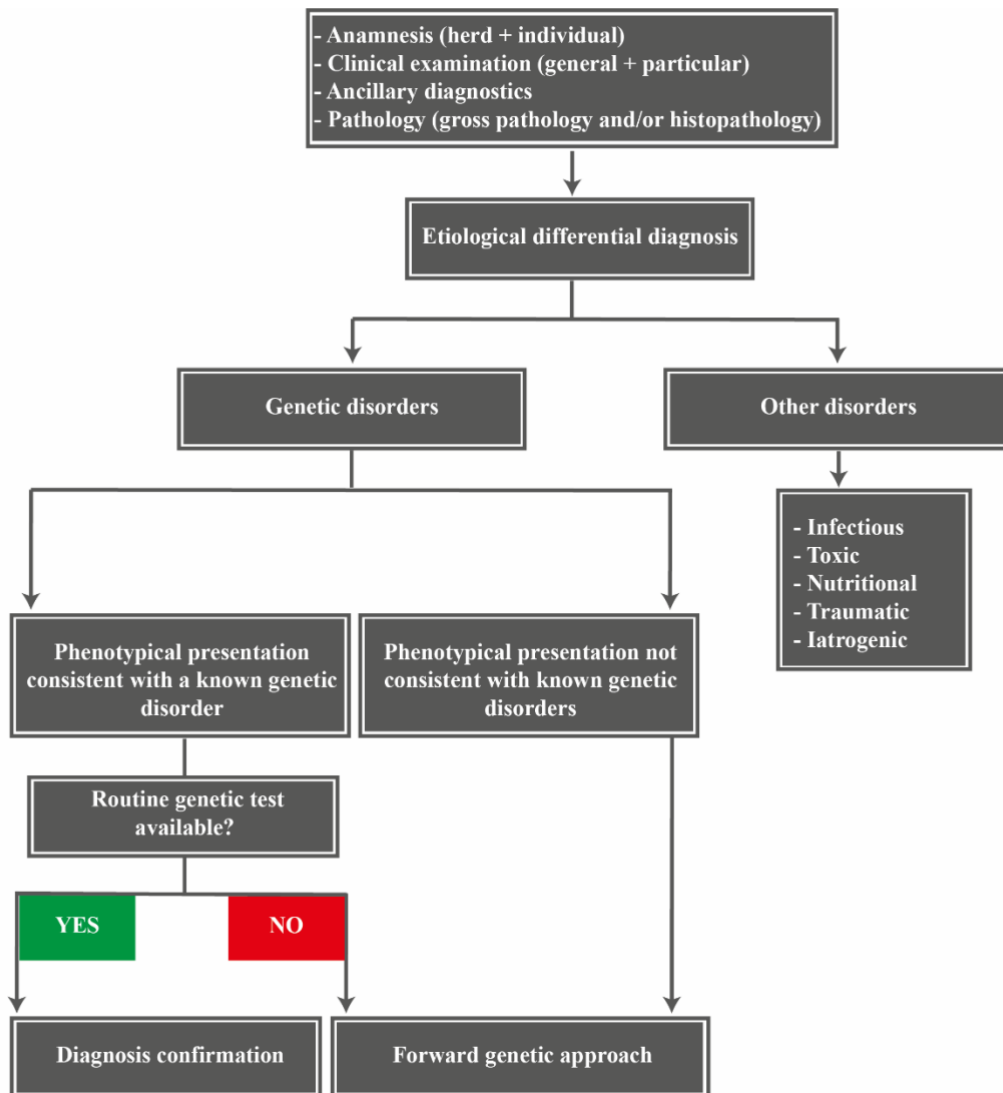


Figure 5: Illustration of an algorithm to diagnose genetic disorders.

1.4.1 Anamnesis

In order to obtain a comprehensive case history, herd anamnestic data must be considered before the individual anamnesis. The herd anamnesis concerns the history of the herd, the relation of the animals with the surrounding environment and the herd management. Among others the following elements should be specifically addressed: type of farm (beef suckler commercial or pedigree, beef fattening, dairy, heifer rearing), type of housing, other enterprises on farm, access or not to pasture, biosecurity status of the herd (open or closed), infectious diseases status of the herd, routine treatments of the herd (e.g. vaccination, anti-parasite treatments), feeding and mineral supplementation.

The individual anamnesis concerns the history of the affected animal(s) where the following elements should be, among others, specifically addressed: breed, date of birth,

ear tag, sex, age of first clinical signs, primary complaint, other presenting signs, previous illness, laboratory tests previously performed if available, previous treatments (in case of previous treatments also the response to treatment), presence of other similarly diseased animals, current feeding and genealogy of the affected animal(s).

In case of congenital defects, special attention should be taken to possible teratogenic agents that act, in most of the cases, via transplacental exposure to the fetus. Teratogenic agents include infectious agents (e.g. bovine viral diarrhea virus, blue tongue virus, Schmallenberg virus, *Neospora caninum* and *Toxoplasma gondii*), plant toxins (e.g. *Veratrum*, *Solanum*, *Nicotiana*, *Astragalus*, *Oxytropis*, *Lupinus*, *Conium maculatum*, *Lathyrus*, *Vicia* and *Leucaena*) [17], chemical agents (e.g. pesticides, herbicides, pharmaceutical agents), nutritional factors (e.g. iodine deficiency, copper deficiency, magnesium deficiency) and physic agents (e.g. irradiation, hyperthermia, uterine positioning). After the exclusion of teratogenic agents, a suspicion of genetic disorder should be strongly considered.

Thereby, a comprehensive anamnesis is extremely useful for better understanding the problem and for guiding when performing the clinical and pathological investigations.

1.4.2 Clinical and pathological investigation

To perform a complete clinical characterization, a general clinical examination followed by a particular examination of the affected system(s) must be carried out and should be recorded using a systematic method. In addition, when possible, ancillary diagnostics (e.g. blood analysis, ultrasonography, radiography, magnetic resonance imaging, etc) should be performed to better understand the disorder.

To perform a complete pathological investigation, biopsies for histopathological should be obtained (if applicable). In case of euthanasia or natural death of the affected animal, gross and histopathology are strongly recommended because they allow a better characterization of the phenotype.

If there is suspicion of a known genetic disorder after assembling the anamnesis, the clinical and pathological investigations, and the ancillary diagnosis, a routine genetic test should be performed to confirm the genetic etiology of that disorder. If the routine genetic test does not confirm the diagnosis or if there is no routine genetic test available or if the

phenotype is not reported in literature, the case should be referred to a reference center where more in depth phenotypical studies as well as a **forward genetic approach** (FGA) (see chapter 1.6.1) can be applied to confirm a genetic cause.

1.5 Genetic approach to disorders in cattle

There are two main genetic approaches that might be used in order to discover the genetic base underlying a certain disorder that appears as single case or population-wide: these are the **forward** and **reverse** genetic approaches.

The **FGA** uses phenotypic information of affected and non-affected individuals to associate the studied phenotype with the variation in the genome [12]. These case-control studies are best applied to monogenic disorders with a dominant or recessive mode of inheritance, where affected individuals (cases) are evidently distinguished from non-affected individuals (controls). In the research forming the foundation for this thesis, FGA was the only applied method. It is in depth detailed in chapter 1.6.1 Methods of the forward genetic approach (FGA).

The **reverse genetic approach** (RGA) uses population-wide massive genomic data that are screened for statistically significant deviations from basic genetic models indicating the segregation of recessive deleterious variants [12, 18]. The basic assumption is that the animals used in a breeding scheme are all healthy and could mate randomly [18]. If a recessive lethal variant is segregating and is in linkage disequilibrium (LD) with one of the single nucleotide variants (SNV), these co-inherited SNV and their associated haplotypes will show a depletion in homozygous carriers. In cattle, this can indicate a broad range of hidden phenotypes, such as early embryonic death, abortion, stillbirth, or birth of weak calves that are non-viable or ill-thriving. For example, several haplotypes have been associated with embryonic death (HH1, HH2, HH6, HH7, JH1), abortion (AH2, HH3, HH4, HH5, MH1, MH2, NH7), increased mortality (AH1) and failure to thrive (BH2, FH2) [19, 20, 29, 30, 21–28].

1.5.1 Methods of the forward genetic approach

Different methods might be used in **FGA** but they are best applied to monogenic disorders with both recessive and dominant inheritance (**Figure 6**). However, they might also be applied for the identification of quantitative trait locus (QTL).

With the FGA it is possible to perform studies applying single SNP and WGS-derived SNV data. For population studies, genome-wide association studies (GWAS) might be applied for recessively and dominantly inherited disorders. For family studies, LD analysis might be applied for recessively and dominantly inherited disorders while homozygosity mapping might be used only in case of recessively inherited disorders. For candidate variant identification, WGS data might be used to perform SNV filtering, investigation of structural variants and chromosomal abnormalities.

	Recessively inherited disorder	Dominantly inherited disorder
Population studies	Genome-wide association studies (single SNP regression)	
Family studies	Linkage disequilibrium analysis	
	Homozygosity mapping	
Candidate variant identification	Whole-genome sequencing	

Figure 6: Illustration of possible methodologies used in the forward genetic approach (FGA) for recessive- and dominantly inherited disorders. The blue row represents population studies, red row represents family studies and yellow row represents the possible identification of the candidate causal variant using whole-genome sequencing. Note that the only method that is exclusively used for recessively inherited disorders is the homozygosity mapping.

1.5.1.1 Genome-wide association study

GWAS is a resourceful and potent genetic approach that allows to discriminate genetic markers related with a phenotype of interest in a population [31, 32]. Traditionally, GWAS is performed based on SNP data; nevertheless, WGS data might also be used [12]. When studying disorders associated with monogenic or quantitative traits, case-control studies might be performed where a certain marker always occurs in cases and only sporadically in controls leading to a significant association. Thus, this association enables the identification of candidate loci [32].

GWAS is a single SNP regression based on a mathematic model and is applied only when there is a collection of several cases showing the same phenotype and healthy controls.

It is important to correct for multiple testing to avoid sporadic associations applying, for example false discovery rates [33] or Bonferroni correction [34]. For the visualization of

the GWAS results, Manhattan plots might be obtained and they might be created using R with the package qqman [35, 36].

1.5.1.2 Linkage disequilibrium analysis

LD analysis is a genetic approach that is applied to map genomic regions that are most likely causing a phenotype of interest in a family [37]. Similarly to GWAS, LD analysis is usually performed on SNP data; nevertheless, WGS data might also be used.

LD analysis is dependent on family information such as pedigree and genome data of closely related individuals. Using the family information it is possible to estimate the co-segregation of loci on the same chromosome as LD and therefore describing the non-random association of loci [37]. In LD analysis, a parameter-based and parameter-free method might be used [38]. For the parameter-based method an assumption of a mode of inheritance to analyze the co-segregation of marker and phenotype is required. For the parameter-free method the assumption of a mode of inheritance to analyze the probability of alleles to be identical by descent is not required [37, 38].

1.5.1.3 Homozygosity mapping

Homozygosity mapping is a powerful genetic approach for the study of recessively inherited disorders that is applied to map homozygous genomic regions that might be associated with a phenotype of interest using family information. Therefore, this genetic approach is effective for the identification of genomic loci that are shared among related individuals showing an identical phenotype allowing to locate alleles that are identical by descent (IBD) [39].

Homozygosity mapping might be performed using the software PLINK v1.9 [40] considering homozygous segments of at least 100 kilo bases for allelic matching between cases resulting in shared ROH indicating chromosomal region of IBD [39]. The length of ROH correlates with the genetic distance, due to recombination events. Therefore, ROH are indicators for recent or ancient inbreeding and can be used to estimate inbreeding [14].

Similarly, to the above-mentioned methods, homozygosity mapping is usually performed based on SNP data. However, WGS data might be also used and in fact is more sensitive for detection of short ROH that are usually missed using SNP data [41].

1.5.1.4 Whole-genome sequencing

WGS is an extremely potent and outstanding method that created the possibility to unravel an individual's entire genomic DNA in a time- and cost-efficient manner.

This genetic approach produces massive quantities of data that require modern bioinformatics methodology to elaborate them. Because creating a *de novo* cattle assembly is a computational highly complex and, a time- and memory-consuming process, a reference sequence and an alignment approach for the sequenced reads are usually performed. Presently, there are four cattle reference sequences registered and with an available annotation in National Center for Biotechnology Information (NCBI), of which three are based on the biological sample of the inbred Hereford cow *Dominette*. The most recent reference sequence and its annotation, the ARS-UCD1.2 genome assembly (GenBank: GCA_002263795.2; RefSeq: GCF_002263795.1), has been publically available in the NCBI database since 2018 [42–44].

The elaboration of the raw data is supported by a wide range of analysis software and pipelines. The elaboration of the raw data is supported by a wide range of analysis software and pipelines. The WGS workflow is briefly illustrated in **Figure 7**.

In the FGA, the identification of candidate pathogenic variants using WGS data is a complex task. In order to increase the success, when analyzing the WGS data with the aim to identify these variants, it is vital to first understand the possible mode of inheritance. The most powerful WGS approach for the identification of candidate pathogenic variants is to perform a WGS trio-approach (case, dam, sire) [45]; however, sequencing data of any additional related individual increases the probability of a successful detection [46].

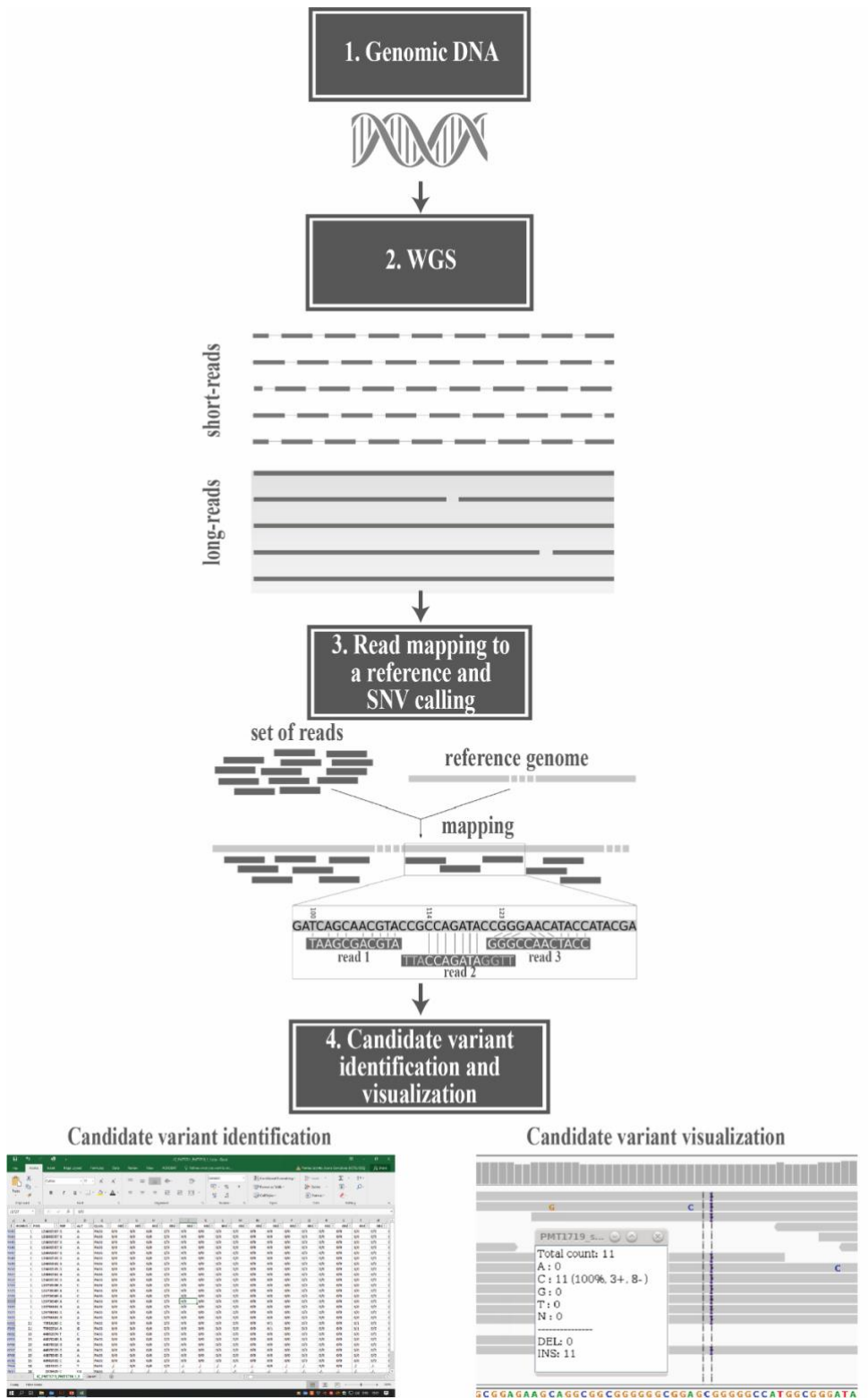


Figure 7: Schematic representation of WGS workflow.

Moreover, for the identification of candidate pathogenic variants, narrowing down the genomic region through GWAS, LD or ROH analyses can be of profound help, particularly if structural variants are involved.

For the identification of candidate pathogenic variants using WGS data, different methods can be applied such as SNV and small indels filtering, coverage analysis across the genome and manual visualization of candidate genes/loci. However, the candidate gene approach is limited because it is only applicable to disorders for which the associated genes have previously been identified in cattle or other species such as dog, cat, sheep, horse, goats, mice, zebra fish and humans.

2 Objectives of thesis work

The objectives of the research forming the base of this thesis were:

- a) **to study genetic disorders** deriving from the past or current caseload available as well as presented or submitted to the Clinic for Ruminants, Department of Veterinary Medical Sciences, University of Bologna, Italy (DIMEVET) and to the Institute for Genetics, Vetsuisse-Faculty, University of Bern, Switzerland (IGVFB). Beside the acquisition of the clinico-morphological aspects as well as – if possible - of the pathological basis of the observed defects, the definitive accomplishment of the research was to identify causal variants;
- b) **to estimate of the frequency of deleterious alleles** responsible for the below listed disorders by means of an evaluation of carrier prevalence in the respective breeds populations:
 - i. Pseudomyotonia congenita *ATP2A1* exon 6-related (Chianina, Romagnola and Marchigiana breeds),
 - ii. Pseudomyotonia congenita *ATP2A1* exon 8-related (Romagnola breed),
 - iii. Paunch calf syndrome *KDM2B*-related (Romagnola and Marchigiana breeds),
 - iv. Hemifacial microsomia *LAMB1*-related (Romagnola breed),
 - v. Congenital bilateral cataract *NIDI*-related (Romagnola breed),
 - vi. Ichthyosis congenita *FA2H*-related (Chianina breed),
 - vii. Ichthyosis fetalis *ABCA12*-related (Chianina breed),
 - viii. Achromatopsia *CNGB3*-related (Braunvieh breed),
 - ix. Hypotrichosis *HEPHL*-related (Belted-Galloway breed),
 - x. Hypotrichosis *KRT71*-related (Hereford breed);
- c) **To enrich the Biobank** for Bovine Genetic Diseases at the DIMEVET and the IGVFB, for further investigations.

3 Materials and Methods

3.1 Study of the genetic disorders

The research was based on clinical cases that were presented or submitted for diagnosis or investigation to the clinic for ruminant of the DIMEVET as well as on clinical cases that were referred to the IGVFB (**Table 8**).

Depending on the situation, type of disorder and clinical/morphological findings, as well as availability of biological materials (live animal admitted to the DIMEVET; live animal examined on farm upon presentation to the DIMEVET and the IGVFB; deceased or stillbirth animal examined or recorded at the DIMEVET or at the IGVFB; blood of investigated animals) each case followed a standardized procedure:

- a) Clinical/laboratory number identification;
- b) Animal data: age, sex, breed, pedigree;
- c) Record of the ear tag of the affected animal (if not stillbirth), dam and sire;
- d) Collection of case history: herd and individual anamnesis;
- e) Storage of biological material from the affected animal (frozen EDTA-blood sample in living animals, ear cartilage or liver in deceased animals or stillbirths);
- f) Request and storage of frozen EDTA-blood samples or semen from related animals (dam, sire and if needed other close relatives);
- g) In depth clinical investigation in living animals;
- h) Ancillary diagnostics (e.g. hemato-biochemistry, radiology, ultrasonography, magnetic resonance imaging, bioptic samples, etc);
- i) Investigation for bovine viral diarrhoea virus, blue tongue virus, Schmallenberg virus, *Neospora caninum*, *Toxoplasma gondii* or antibodies against these; in some cases, also from the dam and sire;
- j) Morphological characterization of deceased or stillbirth animals;
- k) Post mortem gross pathology;
- l) Histopathology;
- m) DNA extraction from the samples obtained in points e) and f);
- n) Storage of the extracted DNA;
- o) Genetic investigation applying the FGA (e.g. GWAS, homozygosity mapping, WGS, etc).

Table 1: Overview of cases studied during the PhD study period.

Disorder	Case ID	Clinical examination	Pathology	FGA	Identification of candidate causal variant
Acephalia	BO089/05 BERM3473	no	yes	yes	UA
	BO051/20 BERM3470	no	yes	yes	UA
Achondrogenesis type II	BO360/09 BERM3476	no	yes	yes	yes
	BO637/21	no	yes	no	no
	BERM2783	no	yes	yes	yes
Acrokeratosis	BO070/10 BEPMT0537	yes	yes	yes	UA
Achromatopsia	BERM3426	yes	yes	yes	yes
	BERM3732	yes	no	yes	yes
	BERM3733	yes	no	yes	yes
	BERM3734	yes	no	yes	yes
Anhidrotic ectodermal dysplasia	BERM3722	yes	yes	yes	UA
Anophthalmia and congenital cardiopathy	BO037/21	yes	yes	no	no
Anophthalmia and perosomus acaudatus	BO072/21	yes	yes	no	no
Anophthalmia and perosomus assacratus	BO031/21	no	yes	no	no
Anophthalmia and splanchnocranium dysplasia	BO155/08 RM0031	yes	yes	yes	UA
	BO147/10 BERM3710	yes	yes	yes	UA
Arnold-Chiari syndrome type II	BO014/19	no	yes	no	no
	BO022/19	yes	yes	no	no
	BO150/19	no	yes	no	UA
	BERM2780	no	yes	yes	UA
	BO278/20 BERM3485	yes	yes	yes	UA
	BERM3594	no	yes	yes	UA
	BERM3595	no	yes	yes	UA
	BERM3596	no	yes	yes	UA
	BERM3597	no	yes	yes	UA
	BERM3598	no	yes	yes	UA
	BERM3599	no	yes	yes	UA
	BERM3600	no	yes	yes	UA
	BERM3601	no	yes	yes	UA
	BERM3602	no	yes	yes	UA
BERM3603	no	yes	yes	UA	

	BERM3604	no	yes	yes	UA
	BERM3605	no	yes	yes	UA
Arthrogryposis and palatoschisis	BERM0971	no	yes	yes	UA
Ataxia Weaver-like, adult onset	BEBV001	yes	no	yes	UA
	BEVV002	yes	no	yes	UA
	BEBV003	yes	no	yes	UA
	BEBV004	yes	no	yes	UA
	BEBV005	yes	no	yes	UA
	BEBV006	yes	no	yes	UA
	BEBV007	yes	no	yes	UA
	BEBV008	yes	no	yes	UA
	BEBV009	yes	no	yes	UA
	BEBV010	yes	no	yes	UA
Atresia ani	BO097/19	no	yes	no	no
	BO064/20	yes	yes	no	no
	BO045/21	yes	yes	no	no
Atresia ani and coli	BO138/21 BEPMT1867	yes	yes	yes	UA
Atresia coli	BO686/20	yes	yes	no	no
	BO138/21	yes	yes	no	no
Atresia coli and amelia	BO060/21	yes	yes	no	no
Bone fragility and inferior brachygnathism	BO632/21 BERM4369	yes	yes	yes	UA
Bovine juvenile angiomas	BE ITPA1507	yes	yes	yes	yes
	BO661/21 BERM3724	yes	yes	yes	UA
Carpus valgus	RM4355	yes	no	no	no
	RM4357	yes	no	no	no
	RM4359	yes	no	no	no
	RM4361	yes	no	no	no
Cheiloschisis	BO192/21	yes	no	no	no
Complex of vertebral malformation-like	BO186/21 BERM4134	yes	yes	yes	UA
	BO305/21	yes	yes	no	no
Congenital cardiopathy, aortic stenosis	BO033/19	yes	yes	no	no
Congenital cardiopathy, atrial and ventricular septal defect	BO630/21	yes	yes	no	no

Congenital cardiopathy, atrial septal defect	BO067/21 BEPMT1865	yes	yes	yes	UA
Congenital cardiopathy, oval foramen defect	BO290/21	yes	yes	no	UA
Congenital cardiopathy, right ventricle double-outlet	BO065/21 BEPMT1863	yes	yes	yes	UA
Congenital cataract	BERM3464	yes	no	yes	UA
	BERM3467	yes	no	yes	UA
	BERM1293	yes	no	yes	UA
	BERM2727	yes	no	yes	UA
Congenital hypotrichosis	BERM3671	yes	yes	yes	yes
	BERM3687	yes	no	yes	yes
	BEBG001	yes	no	yes	yes
Congenital mastocytoma	BO107/18 BERM2881	yes	yes	yes	UA
	BERM2792	yes	yes	yes	UA
Congenital neuromuscular channelopathy	BO514/16 BEPMT1625	yes	yes	yes	yes
Congenital paramyotonia	BERM2835	yes	no	yes	UA
Congenital sarcoma	BO059/19	yes	Yes	no	no
	BO326/21	yes	yes	no	no
Congenital scoliosis and torticollis	BO102/18	yes	yes	no	no
Conjoined twins	BO053/20	no	yes	no	no
Dwarfism	BO123/18	yes	yes	no	no
	BO166/14 BERM0390	yes	no	yes	UA
	BERM0377	yes	no	yes	UA
	BERM3788	yes	no	yes	UA
Ehlers-Danlos syndrome	BO005/20 BERM2884	yes	yes	yes	yes
	BO006/20 BERM2885	yes	yes	yes	yes
	BO676/20 BE1853	no	yes	yes	UA
	BO626/21	yes	yes	no	no
Epidermolysis bullosa, simplex	BERM2777	yes	yes	yes	yes
Fibrinogen storage disease	BERM4105	yes	no	yes	UA
Follicular dysplasia	BO132/13	yes	yes	yes	UA

	BERM3477				
Hemifacial microsomia	BO112/19 BERM2883	yes	yes	yes	yes
Hermaphroditism	BO038/21	no	yes	no	no
Hydrocephalus	BO045/20 BERM3474	yes	yes	yes	no
	BO125/19	no	yes	no	no
Ichthyosis congenita	BO067/20 PMT1719	yes	yes	yes	yes
	BO032/04 BEPMT1860	yes	yes	yes	yes
	BO113/09 BEPMT1711	yes	yes	yes	yes
	BO145/10 BEPMT1713	yes	yes	yes	yes
	BO177/08 BEPMT1714	yes	yes	yes	yes
	BO155/11 BEPMT1715	yes	no	yes	yes
	BO328/08 BE1717	yes	no	yes	yes
	BO070/06 PMT1727	yes	no	yes	yes
	BO184/20 BEPMT1728 7	yes	yes	yes	yes
	BO663/20 BEPMT1851	yes	yes	yes	yes
	BO053/21 BEPMT1861	yes	yes	yes	yes
	Internal ear aplasia	BO024/19 BERM2882	yes	yes	yes
Lethal multi-organ dysplasia	BO57/20 BERM3712	no	yes	yes	UA
	BO159/15 BEPMT1437	no	yes	yes	UA
Malrotation syndrome	BO061/21	yes	no	no	UA
Osteochondrodysplasia	BO516/21 BEPMT1928	no	yes	yes	UA
	BO522/21 BEPMT1930	yes	yes	yes	UA
Osteogenesis imperfecta	BERM2774	no	yes	yes	yes
Paunch calf syndrome	BO314/12 BE PCS663	no	yes	yes	yes

Palatoschisis and amastia	BERM3788	no	yes	yes	UA
Perosomus acaudatus	BO044/21	yes	no	no	no
	BO194/21	yes	no	no	no
	BO313/21	no	yes	no	no
Perosomus assacratus	BO181/21	yes	yes	no	no
Perosomus elumbis	BERM0369	no	yes	yes	UA
	BERM0372	no	yes	yes	UA
	BERM0463	no	yes	yes	UA
	BERM2215	no	yes	yes	UA
	BERM2217	no	yes	yes	UA
	BERM2219	no	yes	yes	UA
Polydactyly	BO139/19	yes	yes	no	no
	BO207/21	yes	yes	no	no
	BO309/21	yes	no	no	no
Polymelia	BO024/21	yes	yes	no	no
Pseudomyotonia congenita	BO016/19	yes	yes	yes	yes
	BEPCS1657				
	BO270/21	yes	yes	yes	yes
Renal dysplasia	BERM4380	yes	no	yes	UA
Schistosoma reflexum	BO329/21	no	yes	no	no
	BERM0974	no	yes	yes	UA
	BERM1214	no	yes	yes	UA
	BERM3735	no	yes	yes	UA
	BERM3739	no	yes	yes	UA
	BERM3742	no	yes	yes	UA
	BERM3745	no	yes	yes	UA
	BERM3747	no	yes	yes	UA
	BERM3749	no	yes	yes	UA
	BERM3751	no	yes	yes	UA
	BERM3753	no	yes	yes	UA
	BERM3756	no	yes	yes	UA
	BERM3759	no	yes	yes	UA
	BERM3762	no	yes	yes	UA
	BERM3764	no	yes	yes	UA
	BERM3767	no	yes	yes	UA
	BERM3769	no	yes	yes	UA
	BERM3770	no	yes	yes	UA
	BERM3771	no	yes	yes	UA
BERM3773	no	yes	yes	UA	
Skeletal-cardio-enteric dysplasia	BO161/10 BEPCS1780	no	yes	yes	yes
Spastic paresis	BO097/06 BEPCS1634	yes	No	yes	UA
	BO116/07	yes	no	yes	UA

	BEPCS1642				
	BO134/10 BEPCS1623	yes	no	yes	UA
	BO037/18	yes	no	no	no
	BO084/19	yes	no	no	no
	BO114/19	yes	yes	no	no
	BO011/20	yes	no	no	no
	BO014/20 BEPCS1777	yes	no	yes	UA
	BO030/20	yes	no	no	no
	BO037/20	yes	no	no	no
	BO050/20 BEPCS1779	yes	no	yes	UA
	BO176/20	yes	no	no	no
	BO334/20 BEPCS2014	yes	no	yes	UA
	BO051/21	yes	no	no	no
	BO169/21	yes	no	no	no
	BETG1975	yes	no	yes	UA
	BETG1976	yes	no	yes	UA
Spastic paresis and congenital monolateral cataract	BO333/20 BEPCS2013	yes	no	yes	UA
	BO679/20 PCS2015	yes	yes	yes	UA
Spastic syndrome	BO104/04 BERM2821	yes	no	yes	UA
	BO47/08 BERM2815	yes	no	yes	UA
	BO204/08 BERM2817	yes	no	yes	UA
	BO232/09 BERM2824	yes	no	yes	UA
	BO486/10 BERM2833	yes	no	yes	UA
	BO026/20	yes	no	no	no
	BO027/20	yes	no	no	no
	BO028/20	yes	no	no	no
	BO031/20	yes	no	no	no
	BO33/21	yes	yes	no	no
Splanchnocranium and forelimbs dysplasia	BO070/20 BERM3714	yes	yes	yes	UA
	BO667/20 BERM3716	yes	yes	yes	UA
Tetraamelia	BO283/21	no	yes	no	no

FGA = forward genetic approach; UA= under analysis

3.2 Estimation of the frequency of deleterious alleles

Frequency estimation for deleterious alleles responsible for the below listed disorders was performed by evaluation of carrier frequency in the respective breed populations. The following diseases were included in the study:

- i. Pseudomyotonia congenita *ATP2A1* exon 6-related (Chianina, Romagnola and Marchigiana),
- ii. Pseudomyotonia congenita *ATP2A1* exon 8-related (Romagnola),
- iii. Paunch calf syndrome *KDM2B*-related (Romagnola and Marchigiana),
- iv. Hemifacial microsomia *LAMB1*-related (Romagnola),
- v. Congenital bilateral cataract *NID1*-related (Romagnola),
- vi. Ichthyosis congenita *FA2H*-related (Chianina),
- vii. Ichthyosis fetalis *ABCA12*-related (Chianina),
- viii. Achromatopsia *CNGB3*-related (Braunvieh),
- ix. Hypotrichosis *HEPHL*-related (Belted-Galloway),
- x. Hypotrichosis *KRT71*-related (Hereford).

Currently, the Pseudomyotonia congenita *ATP2A1* exon 6-related (Chianina, Romagnola and Marchigiana), the Paunch calf syndrome *KDM2B*-related (Romagnola) and the Ichthyosis fetalis *ABCA12*-related (Chianina) are included in the selective program of the Italian Association of Italian Beef Cattle Breeders (ANABIC). The young bulls short-listed for entrance into the performance testing programme are tested and excluded from the programme if they are carriers.

DNA stored in the Biobank for Bovine Genetic Disorders was used. In respect to the Romagnola, Chianina and Marchigiana breeds, the materials were provided by ANABIC. The animals were genotyped using polymerase chain reaction (PCR) and/or commercial SNP chip.

Allele frequency was estimated using the Hardy-Weinberg equation:

$$p^2 + 2pq + q^2 = 1$$

where p is the frequency of the wildtype allele and q is the frequency of the mutant allele.

Table 2 summarizes the information of the total number of genotyped animals per disorder, associated variant and breed.

Table 2: Total number of genotyped animals per each disorders, associated variant and breed.

Disorder	Gene	Variant	Breed	Total number of genotyped animals
Pseudomyotonia congenita	<i>ATP2A1</i> exon 6	Missense g.25940510C>T c.491G>A p.R164H	Chianina	3273
			Marchigiana	2758
			Romagnola	1632
	<i>ATP2A1</i> exon 8	Missense compound heterozygous: g.25939141C>A c.857G>T p.G286V + g.25939366C>A c.632G>T p.G211V	Romagnola	352
Paunch calf syndrome	<i>KDM2B</i>	Missense g.53761149G>A c.2503G>A p.D835N	Marchigiana	368
			Romagnola	1503
Hemifacial microsomia	<i>LAMB1</i>	Missense g.49019693G>A c.2002C>T p.R668C	Romagnola	330
Congenital bilateral cataract	<i>NID1</i>	855 bp deletion c.3579_3604+829 del	Romagnola	689
Ichthyosis congenita	<i>FA2H</i>	2 bp insertion g.2205625_2205626insG c.9dupC p.A4Rfs*142	Chianina	327
Ichthyosis fetalis	<i>ABCA12</i>	Missense g.103025585T>C c.5804A>G p.H1935R	Chianina	7383
Achromatopsia	<i>CNGB3</i>	Missense g.76011964G>A c.751G>A p.D251N	Braunvieh	2940

Hypotrichosis	<i>KRT71</i>	7bp deletion g.27331221_27331228del c.281_288del p.M94Nfs*14	Hereford	352
	<i>HEPHLI</i>	Nonsense g.721234T>A c.1684A>T p.K562*	Belted-Galloway	699

3.3 Enrichment of the biobank for bovine genetic disorders

Regarding improvement of the Biobank for Bovine Genetic Diseases, biological material (EDTA blood, semen, ear cartilage, liver, DNA) of the cases listed in **Table 8** and their available relatives as well as controls used for the allelic frequency estimation listed in **Table 9** were stored at -20°C. DNA was isolated using Promega Maxwell RSC DNA system (Promega, Dübendorf, Switzerland).

4 Results

4.1 Study of the genetic disorders

The results presented in this thesis are limited to the disorders whose study were completed from the clinical to the genetic investigation (applying the FGA) and that were published as original articles in international journals. In particular, FGA allowed the identification of the causative mutation for seven recessive and seven *de novo* dominant disorders, whereas one further disorder revealed to be inconclusive. The observed disorders involved different organ systems, were based on different modes of inheritance, affected different breeds and represented single sporadic cases as well as population issues.

The conditions examined were grouped as:

- **Skeletal disorders** (see chapter 4.1.1)
 - **Achondrogenesis type II**: “*A large deletion in the COL2A1 gene expands the spectrum of pathogenic variants causing bulldog calf syndrome in cattle*”, Acta Veterinaria Scandinavica, 2020, 62, pp. 49 – 49 (see chapter 4.1.1.1)
 - **Achondrogenesis type II associated to Perosomus Elumbis**: “*A 6.7 kb deletion in the COL2A1 gene in a Holstein calf with achondrogenesis type II and perosomus elumbis*”, Animal Genetics, 2021, 52, pp. 244 – 245 (see chapter 4.1.1.2)
 - **Osteogenesis imperfecta**: “*A de novo mutation in COL1A1 in a Holstein calf with osteogenesis imperfecta type II*”, Journal of Veterinary Internal Medicine, 2020, 34, pp. 2800 - 2807 (see chapter 4.1.1.3)
 - **Skeletal-cardio-enteric dysplasia**: “*A heterozygous missense variant in MAP2K2 in a stillborn Romagnola calf with skeletal-cardio-enteric dysplasia*”, Animals, 2021, 11, pp. 1931 – 1931 (see chapter 4.1.1.4)
 - **Paunch calf syndrome**: “*KDM2B-associated paunch calf syndrome in Marchigiana cattle*”, Journal of Veterinary Internal Medicine, 2020, 34, pp. 1657 – 1661 (see chapter 4.1.1.5)

- **Neuromuscular disorders** (see chapter 4.1.2)
 - **Congenital neuromuscular channelopathy:** “*KCNGB1-related syndromic form of congenital neuromuscular channelopathy in a crossbred calf*”, *Genes*, 2021, 12, pp. 1 – 12 (see chapter 4.1.2.1)
- **Metabolic disorders** (see chapter 4.1.3)
 - **Congenital cholesterol deficiency:** “*Autosomal Cholesterol Deficiency in a Holstein Calf*”, *Pakistan Veterinary Journal*, 2020, 40, pp. 274 – 276 (see chapter 4.1.3.1)
- **Genodermatosis** (see chapter 4.1.4)
 - **Epydermolysis bullosa simplex:** “*A de novo mutation in KRT5 in a crossbred calf with epidermolysis bullosa simplex*”, *Journal of Veterinary Internal Medicine*, 2020, 34, pp. 2800 – 2807 (see chapter 4.1.4.1)
 - **Ehlers–Danlos syndrome:** “*A heterozygous missense variant in the COL5A2 in Holstein cattle resembling the classical Ehlers–Danlos syndrome*” *Animals*, 2020, 10, pp. 2002 – 2015 (see chapter 4.1.4.2)
 - **Generalized juvenile angiomas:** “*Clinicopathological and genomic characterization of a Simmental calf with generalized bovine juvenile angiomas*”, *Animals*, 2021, 11, pp. 1 – 11 (see chapter 4.1.4.3)
 - **Ichthyosis congenita:** “*A frameshift insertion in FA2H causes a recessively inherited form of ichthyosis congenita in Chianina cattle*”, *Molecular Genetics and Genomics*, 2021, 296, pp. 1313 – 1322 (see chapter 4.1.4.4)
 - **Hypotrichosis:** “*A KRT71 Loss-of-Function Variant Results in Inner Root Sheath Dysplasia and Recessive Congenital Hypotrichosis of Hereford Cattle*”, *Genes*, 2021, 12, pp. 1038 – 1038 (see chapter 4.1.4.5)
 - **Hypotrichosis:** “*A Nonsense Variant in Hephaestin Like 1 (HEPHL1) is responsible for Congenital Hypotrichosis in Belted Galloway cattle*”, *Genes*, 2021, 12, pp. 1 - 11 (see chapter 4.1.4.6)
- **Ocular and auricular disorders** (see chapter 4.1.5)
 - **Achromatopsia:** “*CNGB3 missense variant causes recessive achromatopsia in Original Braunvieh cattle*”, *International Journal of Molecular Sciences*, 2021, 22, pp. 12440 – 12440 (see chapter 4.1.5.1)

- **Hemifacial microsomia:** “*A homozygous missense variant in laminin subunit beta 1 as candidate causal mutation of hemifacial microsomia in Romagnola cattle*”, *Journal of Veterinary Internal Medicine*, 2021, online, pp. 1 – 8 (see chapter 4.1.5.2).

Each disease will be presented as the published article.

4.1.1 Skeletal disorders

- **Achondrogenesis type II:** “*A large deletion in the COL2A1 gene expands the spectrum of pathogenic variants causing bulldog calf syndrome in cattle*”, *Acta Veterinaria Scandinavica*, 2020, 62, pp. 49 – 49 (see chapter 4.1.1.1)
- **Achondrogenesis type II associated to Perosomus Elumbis:** “*A 6.7 kb deletion in the COL2A1 gene in a Holstein calf with achondrogenesis type II and perosomus elumbis*”, *Animal Genetics*, 2021, 52, pp. 244 – 245 (see chapter 4.1.1.2)
- **Osteogenesis imperfecta:** “*A de novo mutation in COL1A1 in a Holstein calf with osteogenesis imperfecta type II*”, *Journal of Veterinary Internal Medicine*, 2020, 34, pp. 2800 – 2807 (see chapter 4.1.1.3)
- **Skeletal-cardio-enteric dysplasia:** “*A heterozygous missense variant in MAP2K2 in a stillborn Romagnola calf with skeletal-cardio-enteric dysplasia*”, *Animals*, 2021, 11, pp. 1931 – 1931 (see chapter 4.1.1.4)
- **Paunch calf syndrome:** “*KDM2B-associated paunch calf syndrome in Marchigiana cattle*”, *Journal of Veterinary Internal Medicine*, 2020, 34, pp. 1657 – 1661 (see chapter 4.1.1.5)

4.1.1.1 A large deletion in the *COL2A1* gene expands the spectrum of pathogenic variants causing bulldog calf syndrome in cattle

Journal: Acta Veterinaria Scandinavica

Manuscript status: published

Contributions: whole-genome sequencing data analysis, genetic figures, writing original draft and revisions

Displayed version: published version

DOI: [10.1186/s13028-020-00548-w](https://doi.org/10.1186/s13028-020-00548-w)

CASE REPORT

Open Access



A large deletion in the *COL2A1* gene expands the spectrum of pathogenic variants causing bulldog calf syndrome in cattle

Joana Gonçalves Pontes Jacinto^{1,2} , Irene Monika Häfliger² , Anna Letko² , Cord Drögemüller^{2*†}  and Jørgen Steen Agerholm^{3†} 

Abstract

Background: Congenital bovine chondrodysplasia, also known as bulldog calf syndrome, is characterized by disproportionate growth of bones resulting in a shortened and compressed body, mainly due to reduced length of the spine and the long bones of the limbs. In addition, severe facial dysmorphisms including palatoschisis and shortening of the viscerocranium are present. Abnormalities in the gene *collagen type II alpha 1 chain (COL2A1)* have been associated with some cases of the bulldog calf syndrome. Until now, six pathogenic single-nucleotide variants have been found in *COL2A1*. Here we present a novel variant in *COL2A1* of a Holstein calf and provide an overview of the phenotypic and allelic heterogeneity of the *COL2A1*-related bulldog calf syndrome in cattle.

Case presentation: The calf was aborted at gestation day 264 and showed generalized disproportionate dwarfism, with a shortened compressed body and limbs, and dysplasia of the viscerocranium; a phenotype resembling bulldog calf syndrome due to an abnormality in *COL2A1*. Whole-genome sequence (WGS) data was obtained and revealed a heterozygous 3513 base pair deletion encompassing 10 of the 54 coding exons of *COL2A1*. Polymerase chain reaction analysis and Sanger sequencing confirmed the breakpoints of the deletion and its absence in the genomes of both parents.

Conclusions: The pathological and genetic findings were consistent with a case of “bulldog calf syndrome”. The identified variant causing the syndrome was the result of a de novo mutation event that either occurred post-zygotically in the developing embryo or was inherited because of low-level mosaicism in one of the parents. The identified loss-of-function variant is pathogenic due to *COL2A1* haploinsufficiency and represents the first structural variant causing bulldog calf syndrome in cattle. Furthermore, this case report highlights the utility of WGS-based precise diagnostics for understanding congenital disorders in cattle and the need for continued surveillance for genetic disorders in cattle.

Keywords: Chondrodysplasia, Congenital, Malformation, Precision medicine, Rare disease, Type II collagenopathy, Whole-genome sequencing

Background

The bulldog calf syndrome (BDS) is a congenital form of bovine chondrodysplasia affecting bones with endochondral osteogenesis. In its most severe form, this syndrome is lethal [1]. The BDS is often exemplified by the Dexter BDS type [2], which is linked to abnormalities in the *aggrecan (ACAN)* gene [3]. However other BDS types,

*Correspondence: cord.droegemueller@vetsuisse.unibe.ch

†Cord Drögemüller and Jørgen Steen Agerholm contributed equally to this work

² Institute of Genetics, Vetsuisse Faculty, University of Bern, Bremgartenstr. 109a, 3001 Bern, Switzerland

Full list of author information is available at the end of the article



© The Author(s) 2020. This article is licensed under a Creative Commons Attribution 4.0 International License, which permits use, sharing, adaptation, distribution and reproduction in any medium or format, as long as you give appropriate credit to the original author(s) and the source, provide a link to the Creative Commons licence, and indicate if changes were made. The images or other third party material in this article are included in the article's Creative Commons licence, unless indicated otherwise in a credit line to the material. If material is not included in the article's Creative Commons licence and your intended use is not permitted by statutory regulation or exceeds the permitted use, you will need to obtain permission directly from the copyright holder. To view a copy of this licence, visit <http://creativecommons.org/licenses/by/4.0/>. The Creative Commons Public Domain Dedication waiver (<http://creativecommons.org/publicdomain/zero/1.0/>) applies to the data made available in this article, unless otherwise stated in a credit line to the data.

which share gross morphology features with Dexter type, are associated with abnormalities in other genes and occur in different cattle breeds. Abnormalities in the *collagen type II alpha 1 chain (COL2A1)* gene causing BDS have been reported several times during the last 15 years (achondrogenesis/hypochondrogenesis type II in *Bos taurus*; OMIA 001926-9913; <https://omia.org/OMIA01926/9913/>). The purpose of this study was to report a variant in the *COL2A1* gene leading to BDS and provide an overview of the phenotypic and allelic heterogeneity of *COL2A1*-related BDS.

Case presentation

A stillborn Holstein male calf with a body weight of 18.1 kg was aborted at gestation day 264 (normal gestation 281 days (mean)). The pregnancy was the result of insemination with semen of a purebred Holstein sire on a Holstein dam. The parents were not related within at least four generations. The calf had moderate autolysis and was frozen at -20°C before submission for necropsy and was examined after thawing.

The calf had generalized disproportionate dwarfism resembling a case of BDS (Fig. 1). The body appeared shortened and compact. The limbs showed bilateral symmetric shortening, which especially affected the bones proximal to the phalanges, giving the limbs a compact appearance. The phalanges were slightly rotated medially. The limbs were sawed longitudinally, which confirmed the irregular development of diaphysis and the presence

of enlarged chondroid epiphyses without ossification centers (Fig. 2a). Radiological examination prior to sawing revealed normally structured phalangeal bones, but otherwise bones were only seen as irregular diaphyseal segments that could only be identified based on their location (Fig. 2b). Vertebrae had a similar appearance with enlarged chondroid epiphyses and irregular diaphyses. The head had dysplasia of the viscerocranium with shortening of the maxillary bones, palatoschisis, protrusion of the tongue and doming of the calvarium (Fig. 3). Longitudinal sawing of the head through the midline revealed that the direction of the brain axis was elevated due to the abnormally shaped neurocranium (Fig. 3a). Radiological examination highlighted the abnormally shaped bones (Fig. 3b). The thorax was narrow and of reduced volume and was mostly occupied by an enlarged malformed heart. The heart malformation consisted of bilateral ventricular dilation, muscular hypertrophy of the right ventricular wall and dilation of the pulmonary trunk. The lung was hypoplastic and nonaerated. The abdomen was dilated with eversion of intestinal segments and the liver appeared indurated. Due to the level of autolysis and freezing artefacts, histopathology was not performed.

Genetic analysis

Whole-genome sequencing using the NovaSeq 6000 (illumina) was performed at a read depth of $\sim 26\times$ using DNA extracted from skin and cartilage from the ear of



Fig. 1 Calf affected by the OMIA 001926-9913 bulldog calf syndrome. Note the short compact body and limbs and the malformed head. Segments of the intestine protruded through a defect in the ventral abdominal midline, probably as a result of insufficient space within the abdomen due to the short spine. Bar: 5 cm

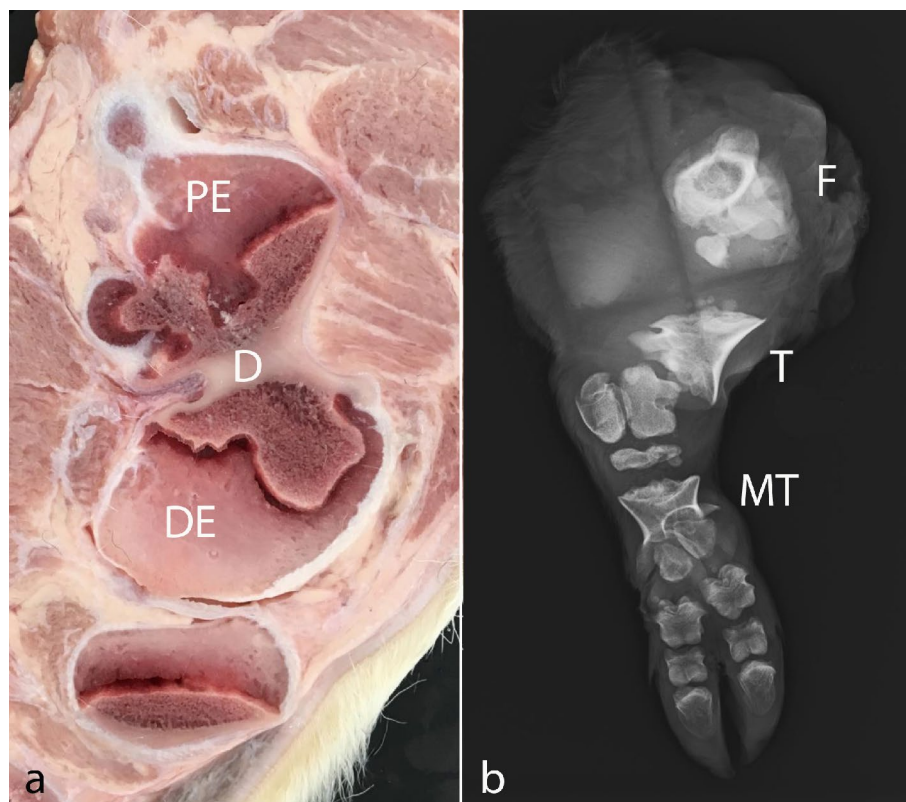
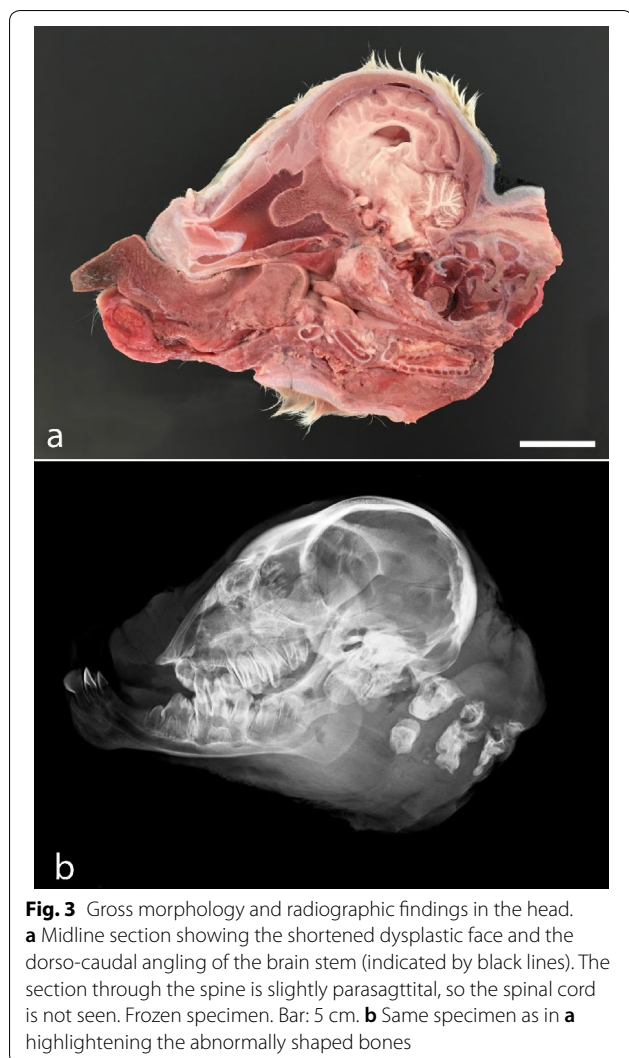


Fig. 2 Lesions in the bones of the limbs. **a** Parasagittal longitudinal section through the femur showing a dysplastic irregular shaped diaphysis (D) bordered by enlarged chondroid proximal and distal epiphyses (PE and DE, respectively). **b** Radiographic image of a hind limb illustrating the severe bone abnormalities of most bones. Of the femur (F), tibia (T) and metatarsal bones (MT), only their irregularly shaped diaphysis are seen and these bones were only identifiable by their location. The phalangeal bones were well developed and of normal shape

the calf. The generated sequences were mapped to the ARS-UCD1.2 reference genome, and single-nucleotide variants (SNVs) and small indel variants were called. The applied software and steps to process fastq files into binary alignment map (BAM) and genomic variant call format (GVCF) files were in accordance with the latest 1000 Bull Genomes Project processing guidelines (www.1000bullgenomes.com) [4]. Furthermore, CombineGVCFs and CatVariants of GATK v3.8 [5] were used to combine the GVCF files and the VariantFiltration tool of GATK was used to give the variants quality labels based on the standard GATK best practices. Lastly, functional impacts were annotated using SNPEFF v4.3 [6] by integrating the information from the NCBI Annotation Release 106 (https://www.ncbi.nlm.nih.gov/genome/annotation_euk/Bos_taurus/106/). With the resulting GVCF, including all individual variants and their functional predictions, filtering for private variants was performed. We compared the genotypes of the calf with 494 cattle genomes of various breeds that had been sequenced in the course of other ongoing studies. The WGS data of the case can be found on ENA under

the sample accession number SAMEA6528902, while a comprehensive list with all ENA accession numbers is shown in Additional file 1. A total of 20 private protein-changing single-nucleotide or short indel variants with a moderate or high predicted impact, located within 19 different genes or loci, were identified (Additional file 2). This list included no variants in *COL2A1*, the most likely candidate gene for the observed BDS phenotype. Therefore, Integrative Genomics Viewer (IGV) [7] software was used for visual inspection of the genome region containing *COL2A1* on chromosome 5. A heterozygous 3513 base pair (bp) sized deletion from position 32,303,127 to 32,306,640 spanning 10 coding exons of the *COL2A1* gene leading to haploinsufficiency of the encoded collagen type II alpha 1 chain protein was observed (Fig. 4). The heterozygous gross deletion variant in *COL2A1* is predicted to lead to a loss-of-function of the encoded collagen type II alpha 1 chain protein and was not observed in any of the 494 cattle genomes used for comparison. Therefore, this variant was further investigated as a potentially causative variant for the observed phenotype.



To evaluate whether the deletion in *COL2A1* occurred de novo, the affected genomic region was amplified by polymerase chain reaction (PCR) and Sanger sequenced using DNA of the calf and both parents. Genomic DNA was extracted from EDTA blood and semen of the dam and sire respectively, and compared to the calf's DNA. PCR products were obtained by using primers flanking the detected *COL2A1* deletion (forward: 5'-CAGGGG ATGGGTCTTCCT-3' and reverse: 5'-GCGTTAGAG AGGGAGACAGG-3') and subsequently sequenced on an ABI3730 capillary sequencer (ThermoFisher, Darmstadt, Germany). Only with the DNA of the affected calf, a PCR product of 128 bp could be amplified, whereas for both parents the amplification failed. Sanger sequencing of the obtained amplicon confirmed the previously identified breakpoints in combination with the insertion of a 10-bp segment fused in-between (chr5:g.32303127_32306640delinsTCTGGGGAGC).

Discussion and conclusions

Based on the morphology of the presented BDS case, a causative genetic variation in the *COL2A1* gene was suspected. As for humans, the morphology of BDS in cattle vary widely both in the overall gross morphology and in bone morphology as exemplified in Fig. 5. It appears that cases of BDS due to abnormalities in the *COL2A1* gene share a common morphology that separates them from at least some other types of bovine BDS, although few types of bovine BDS have been characterised to the molecular level. BDS cases due to abnormalities in the *COL2A1* gene are delivered at term or during the last 3 weeks of gestation. The affected calves have a significantly reduced body weight with a mean of 22.3 kg (variation 16.3–27.5 kg) for 11 Holstein cases [1, 8, 9]. The body and limbs are short and compressed with the digits being almost half of normal size, but normally shaped. The long bones of the limbs and the vertebrae have small irregular diaphyses and enlarged chondroid epiphyses. The viscerocranium is dysplastic with palatoschisis, the neurocranium doomed causing dorso-caudal rotation of the brain, the heart is malformed due to the narrow-spaced thorax, the lungs compressed and the liver with signs of chronic stasis. Cases of BDS that share this morphology, should be suspected of having a defect in the *COL2A1* gene; a suspicion that is helpful when analysing WGS data. However, in this case, filtering for private variants in *COL2A1* did not lead to the detection of a private single-nucleotide or short indel variant. Consequently, the genome data was visually inspected for the presence of structural variants in the gene that allowed the detection of a heterozygous gross deletion. It was assumed that it had occurred either post-zygotically in the developing embryo or was inherited from a parent having low-level mosaicism. The former seems to be more likely as amplification of the mutant allele failed in the examined tissues of both parents, especially because the germline of the sire was analysed by extracting DNA from semen. This means that the *COL2A1* deletion observed in heterozygous state in the affected offspring was most likely absent in the genome of both parents. Therefore, we can assume that the identified mutation arose indeed de novo in the developing embryo explaining this isolated case.

This pathogenic variant is predicted to affect a large portion of the *COL2A1* gene leading to haploinsufficiency. Recent large data from human genome sequencing studies presented in the Genome Aggregation Database (gnomAD) [10] showed that the probability of loss-of-function intolerance score for *COL2A1* was 1 meaning that *COL2A1* falls into the class of loss-of-function haploinsufficient genes. Collagens are normally extracellular structural proteins involved in formation of connective tissue structure. The highly conserved

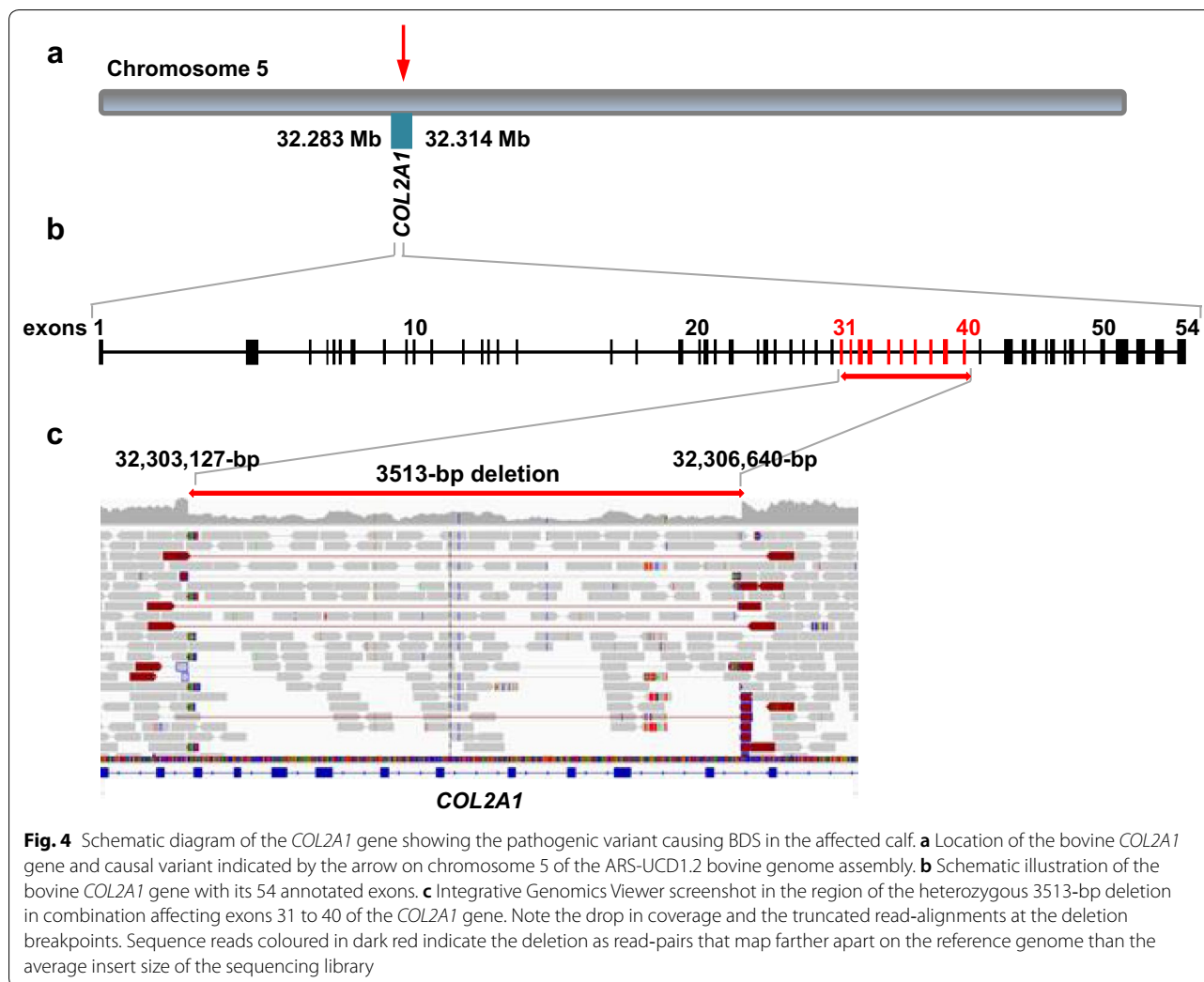


Fig. 4 Schematic diagram of the *COL2A1* gene showing the pathogenic variant causing BDS in the affected calf. **a** Location of the bovine *COL2A1* gene and causal variant indicated by the arrow on chromosome 5 of the ARS-UCD1.2 bovine genome assembly. **b** Schematic illustration of the bovine *COL2A1* gene with its 54 annotated exons. **c** Integrative Genomics Viewer screenshot in the region of the heterozygous 3513-bp deletion in combination affecting exons 31 to 40 of the *COL2A1* gene. Note the drop in coverage and the truncated read-alignments at the deletion breakpoints. Sequence reads coloured in dark red indicate the deletion as read-pairs that map farther apart on the reference genome than the average insert size of the sequencing library

sequence predominantly consists of repeated three amino acids with glycine (Gly) followed by two other amino acids (Gly-x-y, where x and y can be any amino acid) but glycine being mandatory for the tight packing of the polyproline II type helices within the triple helix [11] (Fig. 6). We assume that the pathogenic variant reported in this study disrupted the triple-helical region of alpha 1 (II) chain and caused a dominant-negative effect similar to most of the alterations responsible for achondrogenesis/hypochondrogenesis type II (OMIM 200610; <https://www.omim.org/entry/200610>) in human patients. In man, variants in *COL2A1* are associated with 15 different phenotypes exclusively following dominant inheritance (OMIM 120140).

Interestingly, the OMIA 001926-9913 BDS type occurs either as de novo or inherited from a mosaic parent [12]. Mosaic sires have been found to transmit the dominant genetic abnormality to their offspring at rates ranging from 1 to 21% [12, 13] reflecting at what fetal

developmental stage the gene change occurred. As it cannot be predicted if the abnormality is occurring de novo or if it is transmitted from a parent, cases must be analyzed in detail to prevent the birth of large numbers of defective offspring, in particular if the abnormality is transmitted from breeding sire with high generic merit used for artificial breeding.

A total of six independent pathogenic dominant variants in *COL2A1*, considered to be responsible for BDS, have been previously identified [8, 9, 12–14] (Table 1). All these variants involve a single nucleotide; five out of the six reported variants represent missense variants that cause a change in a glycine residue disrupting the Gly-x-y structural motif essential for the assembly of the collagen triple-helix.

This is the first report of a large deletion in the *COL2A1* gene associated with BDS. The previous reported single nucleotide variants were missense and splicing. The relevance of this case report is to show

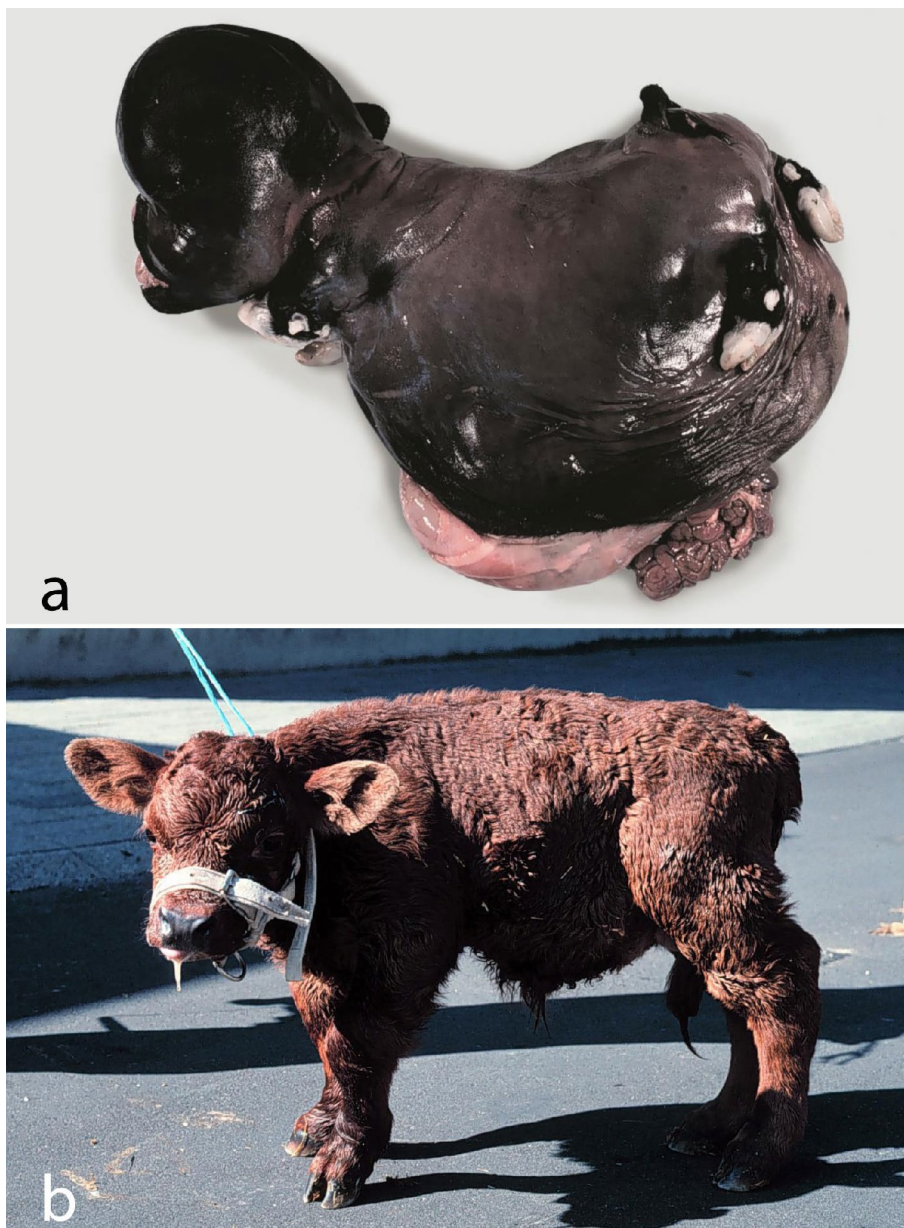


Fig. 5 Examples of the bulldog calf syndrome showing the wide spectrum of phenotypes. **a** The bulldog calf syndrome “prototype” as it occurs in Dexter cattle due to mutations in the *ACAN* gene. Aborted Dexter fetus; **b** Autosomal recessively inherited sublethal form of the bulldog calf syndrome as it occurred in Red Danish cattle [15]. The molecular basis of this phenotype is unknown

that also larger-sized genomic deletions cause a similar congenital phenotype and thereby expanding the knowledge on this condition by emphasizing that different mutations in *COL2A1* cause a uniform phenotype. For many genes it is known that the kind of genetic alteration influence the phenotypic outcome, e.g. the severity of a congenital defect varies or differs totally depending on the individual variant. Interestingly for *COL2A1* in cattle this seems not to be the case

as different kinds of variants always cause an identical phenotype which is of importance for diagnostic pathologists. Furthermore, this report provides an overview of the phenotypic and allelic heterogeneity of the *COL2A1*-related BDS in cattle. This example highlights the utility of WGS-based precise diagnostics for understanding disorders linked to de novo mutations in animals with an available reference genome sequence

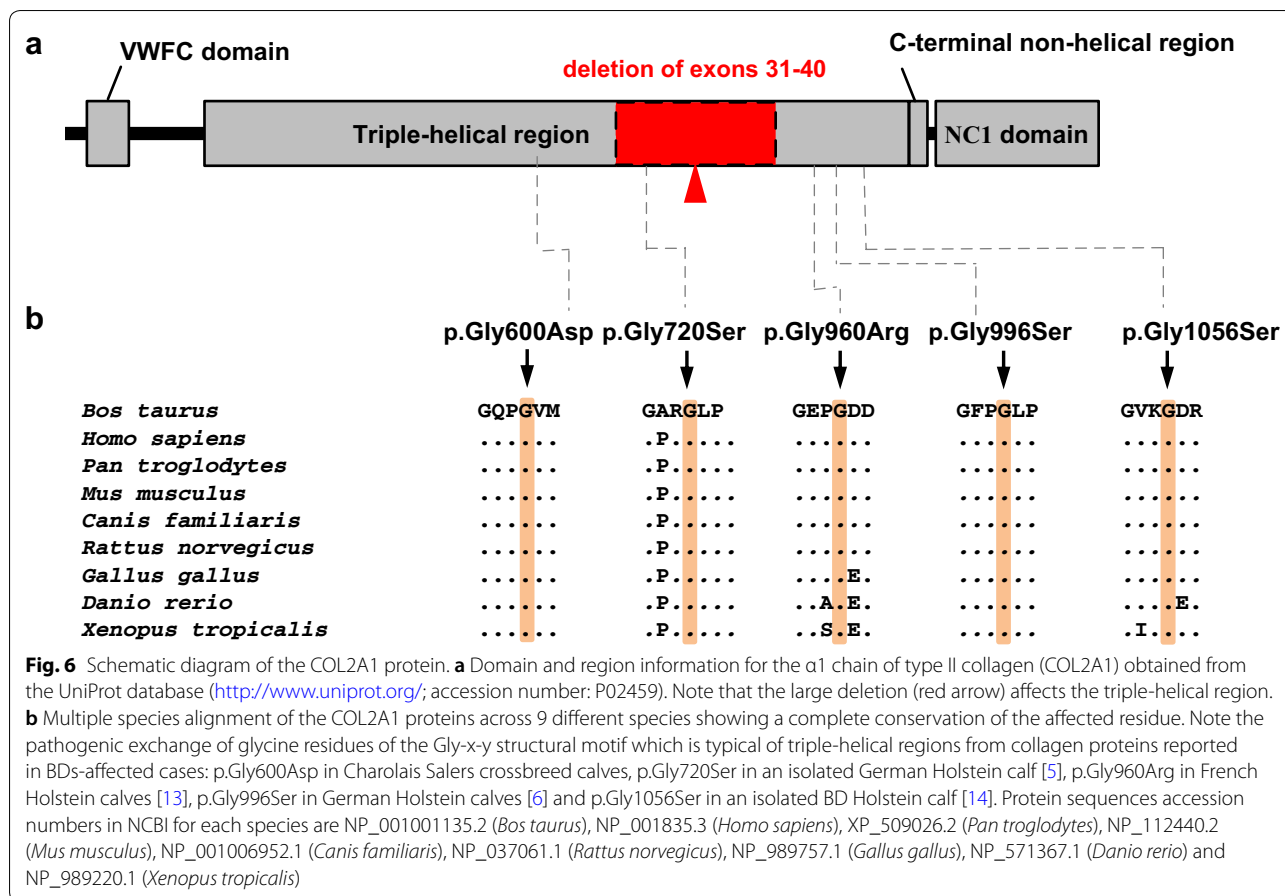


Table 1 Previously reported genetic variants of COL2A1 causing the OMIA 001926-9913 bulldog calf syndrome in cattle

Inheritance	Type of variant	Variant ^a	Breed	References
AD, mosaicism	Missense	g.32307658G > A p.Gly960Arg	Holstein	[13]
AD, mosaicism	Splicing	g.32305226G > A	Holstein	[8]
AD, mosaicism	Missense	g.32301746G > A p.Gly600Asp	Charolais x Salers	[12]
AD, de novo	Missense	g.32303739G > A p.Gly720Ser	Holstein	[12]
AD, mosaicism	Missense	g.32308008G > A p.Gly996Ser	Holstein	[9]
AD, de novo	Missense	g.32308734G > A p.Gly1056Ser	Holstein	[14]

AD autosomal dominant, OMIA Online Mendelian Inheritance in Animals, <https://omia.org/home/>

^a Given positions correspond to chromosome 5 of the ARS-UCD1.2 assembly and NP_001001135.2

and the need for continued surveillance for genetic disorders in cattle breeding. Genome sequencing might improve the precision of the clinicopathological

diagnosis as sometimes unexpected variants in genes that were not known to be associated with a certain disorder could be detected.

Supplementary information

Supplementary information accompanies this paper at <https://doi.org/10.1186/s13028-020-00548-w>.

Additional file 1. EBI Accession numbers of all publicly available genome sequences. We compared the genotypes of the calf with 494 cattle genomes of various breeds that had been sequenced in the course of other ongoing studies and that were publicly available.

Additional file 2. List of the remaining private protein-coding variants after comparison of the genotypes of the calf with 494 cattle genome. A total of 20 private protein-changing single-nucleotide or short indel variants with a moderate or high predicted impact, located within 19 different genes or loci, were identified.

Abbreviations

BAM: Binary alignment map; BDS: Bulldog calf syndrome; Bp: Base pair; *COL2A1*: Collagen type II alpha 1 chain; EDTA: Ethylenediaminetetraacetic acid; Gly: Glycine; gnomAD: Genome Aggregation Database; GVCf: Genomic variant call format; IGV: Integrative Genomics Viewer; OMIA: Online Mendelian Inheritance in Animals, <https://omia.org/home/>; OMIM: Online Mendelian Inheritance in Man, <https://omim.org/>; PCR: Polymerase chain reaction; SNV: Single-nucleotide variant; WGS: Whole-genome sequencing.

Acknowledgements

The veterinary practice Kvægdyrlægerne Midt Aps, Bording, Denmark is thanked for submitting the calf and the owner for donating it. The authors would like to acknowledge the Next Generation Sequencing Platform of the University of Bern for performing the whole-genome sequencing experiments and the Interfaculty Bioinformatics Unit of the University of Bern for providing high-performance computational infrastructure. The authors are grateful to Nathalie Besuchet-Schmutz for expert technical assistance.

Prior publication

Figure 5a has previously been published in Agerholm, JS. Inherited disorders in Danish cattle. *APMIS*. 2007;115 (suppl 122): 1–76.

Authors' contributions

JGPJ, AL and CD performed the genetic analyses. IMH carried out the bioinformatics. JSA performed the post-mortem examination. JGPJ drafted the manuscript and illustrations. JSA and CD designed the study, supervised the project and finalized the manuscript. All authors contributed to the writing of the manuscript. All authors read and approved the final manuscript.

Funding

The study was funded by the Danish Bovine Genetic Disease Programme, internal funds for the University of Copenhagen, and the Swiss National Science Foundation.

Availability of data and materials

Whole-genome sequence data generated from the affected calf is available under study accession PRJEB18113 and sample accession SAMEA6528902 from the European Nucleotide Archive (ENA). In addition, further control genomes are listed in Additional file 1 and can also be accessed on ENA.

Ethics approval and consent to participate

This study did not require official or institutional ethical approval as it was not experimental.

Consent for publication

Not applicable.

Competing interests

JSA is editor-in-chief of *Acta Veterinaria Scandinavica*, but has not in any way been involved in or interacted with the journal's review process or editorial

decision-making. The editor was blinded to the review process. The authors declare that they have no competing interests.

Author details

¹ Department of Veterinary Medical Sciences, University of Bologna, Via Tolara di Sopra 50, Ozzano dell'Emilia, 40064 Bologna, Italy. ² Institute of Genetics, Vetsuisse Faculty, University of Bern, Bremgartenstr. 109a, 3001 Bern, Switzerland. ³ Department of Veterinary Clinical Sciences, University of Copenhagen, Højbakkegaard Allé 5A, 2630 Taastrup, Denmark.

Received: 11 June 2020 Accepted: 30 August 2020

Published online: 07 September 2020

References

1. Agerholm JS, Arnbjerg J, Andersen O. Familial chondrodysplasia in Holstein calves. *J Vet Diagn Invest*. 2004;16:293–8.
2. Seligmann CG. Cretinism in calves. *J Pathol*. 1904;9:311–22.
3. Cavanagh JA, Tammen I, Windsor PA, Bateman JF, Savarirayan R, Nicholas FW, et al. Bulldog dwarfism in Dexter cattle is caused by mutations in *ACAN*. *Mamm Genome*. 2007;18:808–14.
4. Hayes BJ, Daetwyler HD. 1000 Bull Genomes Project to map simple and complex genetic traits in cattle: applications and outcomes. *Annu Rev Anim Biosci*. 2019;7:89–102.
5. DePristo M, Banks E, Poplin R, Garimella KV, Maguire JR, Hartl C, et al. A framework for variation discovery and genotyping using next-generation DNA sequencing data. *Nat Genet*. 2011;43:491–8.
6. Cingolani P, Platts A, Le Wang L, Coon M, Nguyen T, Wang L, et al. A program for annotating and predicting the effects of single nucleotide polymorphisms, SnpEff: sNPs in the genome of *Drosophila melanogaster* strain w1118; iso-2; iso-3. *Fly*. 2012;6:80–92.
7. Robinson JT, Thorvaldsdóttir H, Wenger AM, Zehir A, Mesirov JP. Variant review with the Integrative Genomics Viewer. *Cancer Res*. 2017;77:31–4.
8. Agerholm JS, Menzi F, McEvoy FJ, Jagannathan V, Drögemüller C. Lethal chondrodysplasia in a family of Holstein cattle is associated with a de novo splice site variant of *COL2A1*. *BMC Vet Res*. 2016;12:100.
9. Reinartz S, Mohwinkel H, Sürle C, Hellige M, Feige K, Eikelberg D, et al. Germline mutation within *COL2A1* associated with lethal chondrodysplasia in a polled Holstein family. *BMC Genomics*. 2017;18:762.
10. Karczewski KJ, Francioli LC, Tiao G, Cummings BB, Alföldi J, Wang Q, et al. The mutational constraint spectrum quantified from variation in 141,456 humans. *Nature*. 2020;581:434–43.
11. Shoulders MD, Raines RT. Collagen structure and stability. *Annu Rev Biochem*. 2009;78:929–58.
12. Bourneuf E, Otz P, Pausch H, Jagannathan V, Michot P, Grohs C, et al. Rapid discovery of de novo deleterious mutations in cattle enhances the value of livestock as model species. *Sci Rep*. 2017;7:11466.
13. Daetwyler HD, Capitan A, Pausch H, Stothard P, van Binsbergen R, Brøndum RF, et al. Whole-genome sequencing of 234 bulls facilitates mapping of monogenic and complex traits in cattle. *Nat Genet*. 2014;46:858–65.
14. Häfliger IM, Behn H, Freick M, Jagannathan V, Drögemüller C. A *COL2A1* de novo variant in a Holstein bulldog calf. *Anim Genet*. 2019;50:113–4.
15. Andresen E, Christensen K, Jensen PT, Venge O, Rasmussen PG, Basse A, et al. Dværgvækst hos kvæg af Rød Dansk Malke race (Achondroplasia bovis typus RDM). *Nord VetMed*. 1974;26:681–91.

Publisher's Note

Springer Nature remains neutral with regard to jurisdictional claims in published maps and institutional affiliations.

4.1.1.2 6.7 kb deletion in the *COL2A1* gene in a Holstein calf with achondrogenesis type II and perosomus elumbis

Journal: Animal Genetics

Manuscript status: published

Contributions: phenotype description, whole-genome sequencing data analysis, figures, writing original draft and revisions

Displayed version: published version

DOI: [10.1111/age.13033](https://doi.org/10.1111/age.13033)



doi: 10.1111/age.13033

A 6.7 kb deletion in the *COL2A1* gene in a Holstein calf with achondrogenesis type II and perosomus elumbis

Joana G. P. Jacinto^{*†} , Irene M. Häfliger[†] ,
Arcangelo Gentile^{*} , Cord Drögemüller[†]  and
Marilena Bolcato^{*} 

^{*}Department of Veterinary Medical Sciences, University of Bologna, Ozzano Emilia, Bologna 40064, Italy; [†]Institute of Genetics, Vetsuisse Faculty, University of Bern, Bern 3001, Switzerland

Accepted for publication 02 December 2020

Background

Bovine achondrogenesis type II is also known as bulldog calf (BD) and is caused by a congenital chondrodysplasia characterized by disproportionate growth of bones, resulting in a shortened and compressed body, mostly because of the reduced length of the spine and the long bones of the limbs.¹ Moreover, severe facial dimorphisms, e.g. palathoschisis and shortening of the viscerocranium, are present.¹ Recessively inherited variants in the *ACAN* gene are associated with the so-called lethal Dexter BD type² (OMIA 001271-9913), whereas dominant inherited *COL2A1* variants are related to forms of bovine achondrogenesis type II or BD (OMIA 001926-9913). The latter may be inherited from mosaic parents^{3–6} or due post-zygotic *de novo* mutations.^{5,7,8} So far, a total of seven pathogenic variants in the *COL2A1* have been reported.^{3–8}

Own analysis

A stillborn purebred Holstein male calf was delivered after dystocia. Gross pathology findings revealed a phenotype resembling the bovine chondrodysplasia type II with the additional presence of perosomus elumbis (Fig. S1). WGS was performed using genomic DNA obtained from the ear tissue of the calf as described before.⁷ The sequenced reads were mapped to the ARS-UCD1.2 cattle reference genome,⁹ resulting in an average read depth of approximately 19.8×. The WGS data of the case can be found in the European Nucleotide Archive under the sample accession no. SAMEA7690227. A deleterious variant in the *COL2A1* gene was hypothesized to be causal. Therefore, INTEGRATIVE GENOMICS VIEWER software¹⁰ was used for visual inspection of variants in the region of the *COL2A1* gene on chromosome 5. A single pair of reads indicated the presence of a 6.7 kb-sized deletion, and the sequence coverage within the deleted segment is apparently depleted compared with the flanking regions (Fig. S1). The deletion spanning 19 coding exons of the *COL2A1* gene was subsequently evaluated by performing a multiplex PCR across both breakpoints, revealing an additional PCR product only in the affected calf (Fig. S1).

The two obtained PCR products across the breakpoints represent the wt allele, and thereby we confirmed that the case showing a third PCR product was indeed heterozygous for the suspected structural variant. Sanger sequencing revealed the precise breakpoints of the heterozygous deletion from position 32 301 911 located in intron 25 to 32 308 589 located within exon 45. The 6679 bp deletion includes the entire sequence of 18 exons (26–44) plus the first 36 nucleotides of exon 45 (Fig. S1).

Comments

The heterozygous deletion is predicted to affect a large portion of the *COL2A1* gene. Two possible scenarios could cause the observed phenotype: either haploinsufficiency or co-expression of a significantly truncated protein. The *COL2A1* gene has a probability of loss-of-function intolerance score of 1, meaning that it clearly falls into the class of loss-of-function haploinsufficient genes.¹¹ Consequently, the observed phenotype could be explained by the non-expression of the mutant allele. This has been speculated recently as a cause for a BD case showing a heterozygous 3.5 kb deletion encompassing 10 exons of *COL2A1*.⁸ On the other hand, the variant detected herein is deleting 1413 bp of the coding sequence representing an in-frame deletion that affects 438 residues of the triple helical region of the *COL2A1* protein. Owing to the lack of suitable material, it remains unclear whether this shortened transcript encoding a significantly truncated protein is expressed or not. Nonetheless, the invariant Gly-x-y structural motif is mandatory for perfect triple-helix formation and could thus lead to extensive overmodification. It could be speculated that the variant allele disrupts the triple-helical region of alpha 1 (II) chain causing a dominant-negative effect similar to most of the alterations responsible for achondrogenesis/hypochondrogenesis type II in human patients (OMIM 200610).

Interestingly, so far phenotypically indistinguishable cases of BD calf syndrome in Holstein cattle have shown notable allelic heterogeneity. This report presents another large structural variant affecting the *COL2A1* gene causing a novel form of bovine achondrogenesis type II that occurred in combination with the perosomus elumbis (PE) phenotype (OMIA 000789-9913). Bovine PE has been known as a congenital entity for a long time and shows a certain morphological variation among cases in Holstein cattle, but so far no molecular cause has been reported.¹² Based on our findings, we postulate the *COL2A1* gene as a possible candidate gene for PE in cattle.

Acknowledgements: We thank Nathalie Besuchet Schmutz for expert technical assistance and the Interfaculty Bioinformatics Unit of the University of Bern for providing high-performance computational infrastructure. This study was partially funded by the Swiss National Science Foundation.

References

- 1 Agerholm J.S. *et al.* (2004) *J Vet Diagn Invest* **16**, 293–8.
- 2 Cavanagh J.A. *et al.* (2007) *Mamm Genome* **18**, 808–14.
- 3 Daetwyler H.D. *et al.* (2014) *Nat Genet* **46**, 858–65.
- 4 Agerholm J.S. *et al.* (2016) *BMC Vet Res* **12**, 100.
- 5 Bourneuf E. *et al.* (2017) *Sci Rep* **7**, 11466.
- 6 Reinartz S. *et al.* (2017) *BMC Genomics* **18**, 762.
- 7 Häfliger I.M. *et al.* (2019) *Anim Genet* **50**, 113–4.
- 8 Jacinto J.G.P. *et al.* (2020) *Acta Vet Scand* **62**, 49.
- 9 Rosen B.D. *et al.* (2020) *Gigascience* **9**, 1–9.
- 10 Robinson J.T. *et al.* (2017) *Cancer Res* **77**, e31–4.
- 11 Karczewski K.J. *et al.* (2020) *Nature* **581**, 434–43.
- 12 Agerholm J.S. *et al.* (2014) *BMC Vet Res* **10**, 227.

Correspondence: C. Drögemüller
(cord.droegemueller@vetsuisse.unibe.ch)

Supporting information

Additional supporting information may be found online in the Supporting Information section at the end of the article.

Figure S1. *COL2A1* deletion in a Holstein calf with achondrogenesis type II and persomus elumbis.

4.1.1.3 A *de novo* mutation in *COL1A1* in a Holstein calf with osteogenesis imperfecta type II

Journal: animals

Manuscript status: published

Contributions: whole-genome sequencing data analysis, genetic figures, writing original draft and revisions

Displayed version: published version

DOI: [10.3390/ani11020561](https://doi.org/10.3390/ani11020561)

Article

A De Novo Mutation in *COL1A1* in a Holstein Calf with Osteogenesis Imperfecta Type II

Joana G. P. Jacinto ^{1,2}, Irene M. Häfliger ², Fintan J. McEvoy ³, Cord Drögemüller ^{2,*,†}
and Jørgen S. Agerholm ^{3,†}

¹ Department of Veterinary Medical Sciences, University of Bologna, 40064 Ozzano Emilia, Italy; joana.goncalves2@studio.unibo.it

² Institute of Genetics, Vetsuisse Faculty, University of Bern, 3012 Bern, Switzerland; irene.haefliger@vetsuisse.unibe.ch

³ Department of Veterinary Clinical Sciences, University of Copenhagen, Dyr-lægevej 16, DK 1870 Copenhagen, Denmark; fme@sund.ku.dk (F.J.M.); jager@sund.ku.dk (J.S.A.)

* Correspondence: cord.droegemueller@vetsuisse.unibe.ch; Tel.: +41-31-631-2529

† These authors contributed equally to this work.

Simple Summary: Skeletal connective tissue disorders represent a heterogeneous group of inherited disorders mostly monogenically inherited. Heritable connective tissue disorders such as osteogenesis imperfecta (OI) belong to this group. Herein, an affected calf showing congenital bone lesions such as intrauterine fractures, abnormally shaped long bones and localized arthrogryposis resembling OI type II is reported. Whole-genome sequencing (WGS) identified a most likely disease-causing mutation in the *COL1A1* gene. The *COL1A1* gene is known to be associated with dominant inherited OI type II forms in humans and sporadically in dogs and cattle, but so far, a variant in the fibrillar collagen NC1 domain has not been shown to cause a similar phenotype in domestic animals. We assume that the herein identified most-likely causative variant occurred either within the parental germlines or post-zygotically in the developing embryo. Rare lethal disorders such as OI in livestock are usually not diagnosed to the molecular level, mainly because of the lack of resources and diagnostic tools. WGS-based precision diagnostics allows understanding rare disorders and supports the value of surveillance of cattle breeding populations for harmful genetic disorders.

Abstract: Osteogenesis imperfecta (OI) type II is a genetic connective tissue disorder characterized by bone fragility, severe skeletal deformities and shortened limbs. OI usually causes perinatal death of affected individuals. OI type II diagnosis in humans is established by the identification of heterozygous mutations in genes coding for collagens. The purpose of this study was to characterize the pathological phenotype of an OI type II-affected neonatal Holstein calf and to identify the causative genetic variant by whole-genome sequencing (WGS). The calf had acute as well as intrauterine fractures, abnormally shaped long bones and localized arthrogryposis. Genetic analysis revealed a private heterozygous missense variant in *COL1A1* (c.3917T>A) located in the fibrillar collagen NC1 domain (p.Val1306Glu) that most likely occurred de novo. This confirmed the diagnosis of OI type II and represents the first report of a pathogenic variant in the fibrillar collagen NC domain of *COL1A1* associated to OI type II in domestic animals. Furthermore, this study highlights the utility of WGS-based precise diagnostics for understanding congenital disorders in cattle and the need for continued surveillance for rare lethal genetic disorders in cattle.

Keywords: cattle; *Bos taurus*; collagenopathy; skeletal disorder; bone disease; rare diseases; precision medicine; whole-genome sequencing



check for updates

Citation: Jacinto, J.G.P.; Häfliger, I.M.; McEvoy, F.J.; Drögemüller, C.; Agerholm, J.S. A De Novo Mutation in *COL1A1* in a Holstein Calf with Osteogenesis Imperfecta Type II. *Animals* **2021**, *11*, 561. <https://doi.org/10.3390/ani11020561>

Academic Editors: Francesca Ciotola, Sara Albarella and Vincenzo Peretti

Received: 29 January 2021

Accepted: 19 February 2021

Published: 20 February 2021

Publisher's Note: MDPI stays neutral with regard to jurisdictional claims in published maps and institutional affiliations.



Copyright: © 2021 by the authors. Licensee MDPI, Basel, Switzerland. This article is an open access article distributed under the terms and conditions of the Creative Commons Attribution (CC BY) license (<https://creativecommons.org/licenses/by/4.0/>).

1. Introduction

Osteogenesis imperfecta (OI) encompasses a heterogeneous group of rare genetic connective tissue disorders characterized by skeletal abnormalities, leading to bone fragility,

deformity, low bone mass and growth deficiency [1,2]. Decrease bone strength predisposes to low-trauma fractures or fractures in atypical regions [3]. In humans, extra-skeletal manifestations of OI may include joint hypermobility, dentinogenesis imperfecta, blue sclera, hearing loss, and more rarely pulmonary and cardiovascular complications, and muscle weakness [2].

Currently, OI in humans is classified into as many as 18 types; the classification depends on the genetic causes, severity and clinical observation [4]. OI types I-IV are mainly associated with autosomal dominant variants in *COL1A1* and *COL1A2*; OI type V is a less frequent dominantly inherited form associated with variants in the novel gene *IFTM5*. The remaining types of OI, which usually arise at much lower frequency are autosomal recessive diseases while OI type XVIII has an X-linked inheritance pattern [2,4].

Since the second half of the 20th century several forms of OI have been reported in domestic animal species, including sheep [5], cats [6], dogs [7] and cattle [8]. Until now, one OI-related causative dominant variant in the *COL1A1* is known in dogs (OMIA 002126-9615) [9] and two in cattle (OMIA 002127-9913) [10,11]. In dogs, three OI-related causative dominant variants in the *COL1A2* are also known (OMIA 002112-9615) [12–14] and also in this species, an OI-related recessive form has been associated with a missense variant in *SERPINH1* (OMIA 001483-9615) [15].

In this study, we aimed to characterize an OI-affected Holstein calf, and to identify the causative genetic variant associated with the disorder using whole-genome sequencing (WGS).

2. Materials and Methods

2.1. Pathological Investigation

A male Holstein calf with a weight of 30.6 kg was delivered at gestation day 264 (normal gestation 281 days (mean)). The pregnancy was the result of insemination with semen of a purebred Holstein sire on a Holstein dam. The parents were not related within at least four generations. The calf was immediately humanely euthanized by an intravenous overdose of barbiturate upon delivery due to severe malformations. The carcass was submitted for necropsy during which radiographs were taken of the limbs. Tissue samples were taken during the necropsy and included internal organs, brain, metacarpus, metatarsus, humerus and tibia. These were fixed in 10 % neutral buffered formalin. Bone specimens were thereafter transferred to an aqueous solution containing sodium formate (0.5 mol/L) and formic acid (0.5 mol/L) (Kristensen's decalcifying medium) until suitable for cutting. The tissues were thereafter trimmed, processed by routine methods, paraffin embedded, sectioned at 2 µm and stained with haematoxylin and eosin.

2.2. DNA Samples

Genomic DNA was extracted from skin and cartilage taken from the ear of the calf, from EDTA blood of its dam and from semen of its sire using Promega Maxwell RSC DNA system (Promega, Dübendorf, Switzerland).

2.3. Whole-Genome Sequencing

Using genomic DNA of the affected calf an individual PCR-free fragment library with approximately 400 bp inserts was prepared and sequenced for 150 bp paired-end reads using the NovaSeq6000 system (Illumina, San Diego, CA, USA). The sequenced reads were mapped to the ARS-UCD1.2 reference genome resulting in an average read depth of approximately $18.1 \times$ [16], and single-nucleotide variants (SNVs) and small indel variants were called. The applied software and steps to process fastq files into binary alignment map (BAM) and genomic variant call format (GVCF) files were in accordance with the 1000 Bull Genomes Project processing guidelines of run 7 (www.1000bullgenomes.com (accessed on 31 August 2018)) [17], except for the trimming, which was performed using fastp [18]. Further preparation of the genomic data had been done according to Häfliger et al. 2020 [19]. The impact of the called variants was functionally annotated with snpeff v4.3 [20], using

the NCBI Annotation Release 106 (https://www.ncbi.nlm.nih.gov/genome/annotation_euk/Bos_taurus/106/ (accessed on 31 August 2018)), which resulted in the final VCF file, including all individual variants and their functional annotations. In order to find private variants, we compared the genotypes of the affected calf with 496 cattle genomes of various breeds that had been sequenced in the course of other ongoing studies and that are publicly available (Table S1) in the European Nucleotide Archive (SAMEA6528897 is the sample accession number of the affected calf; <http://www.ebi.ac.uk/en> (accessed on 7 February 2020)). Integrative Genomics Viewer (IGV) [21] software version 2.0 was used for visual inspection of genome regions containing possible candidate genes.

2.4. Targeted Genotyping

Polymerase chain reaction (PCR) and Sanger sequencing were used to validate and genotype the variant identified from WGS. The *COL1A1* missense variant (NM_001034039.2:g.36473359T>A) was genotyped using the following primers: 5'-ATCTTACTTTGCCCCACCCC-3' (forward primer) and 5'-GGCTACAAGGTCCAG CTCAC-3' (reverse primer). The sequence data were analyzed using Sequencher 5.1 software (GeneCodes, Ann Arbor, MI, USA).

2.5. Evaluation of the Molecular Consequences of Amino Acid Substitutions

PROVEAN [22] and DynaMut [23] were used to predict the functional consequences of the discovered variant on protein. For multispecies sequence alignments the following NCBI proteins accessions were used: NP_001029211.1 (*Bos taurus*), NP_000079.2 (*Homo sapiens*), XP_001169409.1 (*Pan troglodytes*), XP_001096194.2 (*Macaca mulatta*), NP_001003090.1 (*Canis lupus*), NP_031768.2 (*Mus musculus*), NP_445756.1 (*Rattus norvegicus*), NP_954684.1 (*Danio rerio*), NP_001011005.1 (*Xenopus tropicalis*).

2.6. Sequence Accessions

All references to bovine *COL1A1* gene correspond to the NCBI accessions NM_001034039.2 (*COL1A1* mRNA) and NP_001029211.1 (*COL1A1* protein). For the protein, structure of *COL1A1* the Uniprot database (<https://www.uniprot.org/> (accessed on 31 August 2018)) accession number P02453 was used.

3. Results

3.1. Pathological Phenotype

The limbs appeared shortened with bilateral symmetric flexion of the fetlock joint and mild lateral rotation of the digits. Flexion of the thoracic limb metacarpo-phalangeal joints was mild (15°) while it was almost 90° in the pelvic limbs. The tibiotarsal joints were extended (Figure 1a). Multiple long bones were abnormal and especially the metacarpal and metatarsal bones were bowed and appeared of reduced diameter (Figure 1b). Several transverse or oblique fractures, some with displaced fracture ends, were present in the long bones and the left hemimandible. Some fractures had fibrous callous formation and cortical bone proliferation. Non-aligned fracture ends showed abnormal healing (Figure 1c,d), while others were acute. Teeth appeared normal as did the color of the sclera.

Histology only revealed lesions in the bones. The epiphyseal trabeculae were reduced in size and number (Figure 2a). Also, ossification was reduced as chondroid matrix was widely present in bone spicules and occasional islets of chondroid matrix were seen. The epiphyseal growth lines were normal, but as for the epiphyses, the metaphyseal and diaphyseal trabecular bone was of reduced amount and quality. The cortical bone appeared thinner (Figure 2b). The bony ends of the fractured left tibia were completely covered by a prominent fibrous callus, while the fracture of the left metacarpus had no signs of repair.

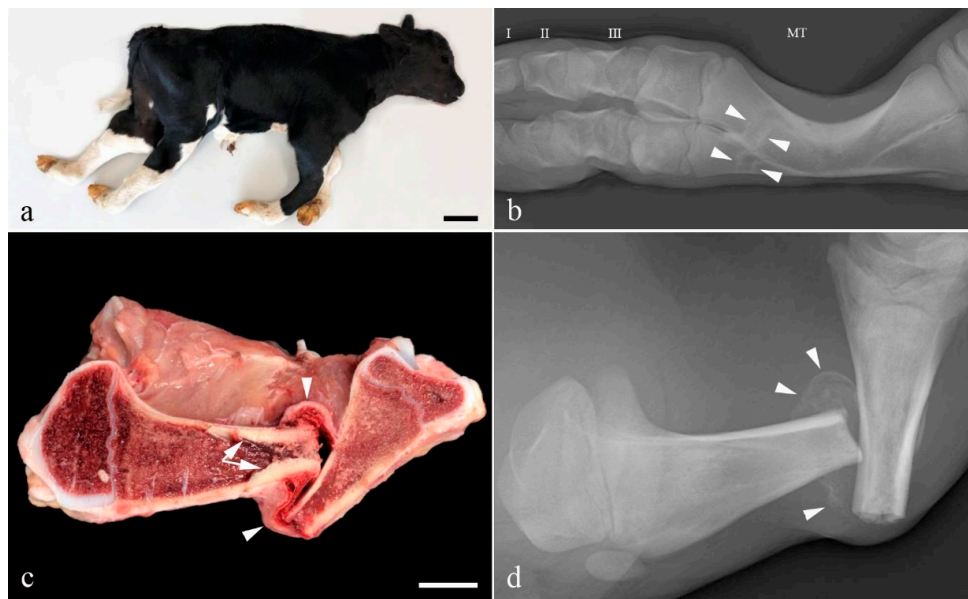


Figure 1. Gross morphology of the OI affected Holstein calf. (a) The limbs appear shortened and the distal joints are flexed. Bar = 10 cm; (b) Radiograph of a metatarsal bone (MT). The diaphysis is curved and transverse lines of sclerosis (arrow heads) are present distally. These may represent sites of healed fracture or growth arrest lines. Phalanx I, II and III are indicated by their respective numbers; (c) Longitudinal section through the left tibia. A transverse fracture with dislocation of the fracture ends is seen. Prominent osseous endosteal proliferation has developed in the proximal part of the fracture (arrows). The fracture is surrounded by fibrosis (arrow heads). The width of the cortex is un-uniform with the caudal part of the proximal diaphysis/metaphysis being thin. Bar = 2.5 cm; (d) Radiograph of the specimen shown in (c) before longitudinal sectioning. The non-aligned fracture ends are surrounded by partly mineralized fibrous callus (arrow heads).

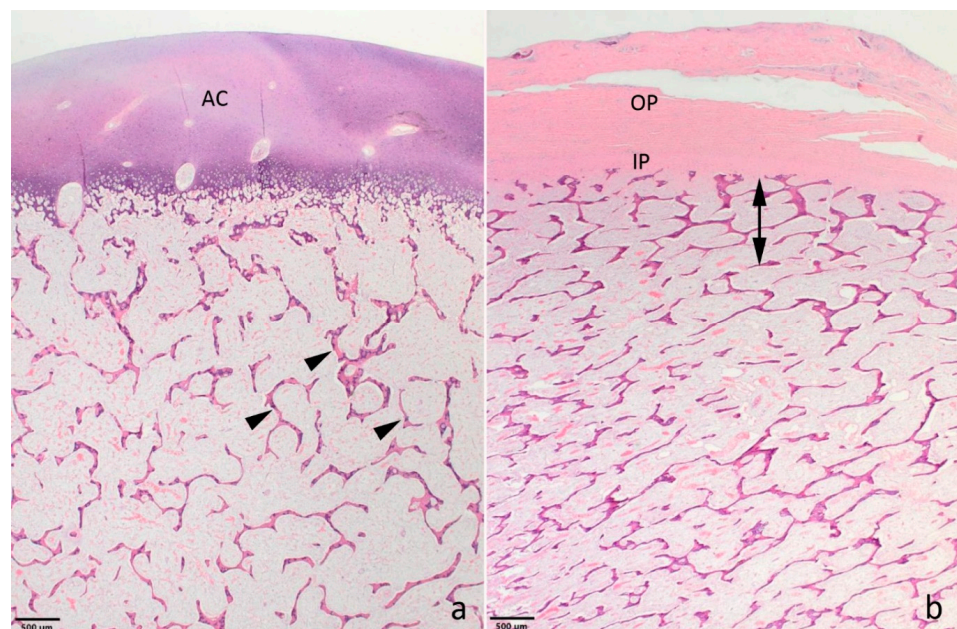


Figure 2. Photomicrographs showing the bone morphology of the OI affected Holstein calf. (a) The epiphyseal spongiosa is characterized by small trabeculae with remnants of chondroid matrix (arrow heads). The amount of spongy bone is reduced resulting in wide spaces between the trabeculae. AC: articular cartilage. Distal epiphysis, metacarpus. (b) The compacta (double headed arrow) is poorly developed and difficult to distinguish from the spongy bone. As for the epiphyses, the trabecular bone is poorly developed. IP and OP: inner and outer layer of the periosteum, respectively. Metaphysis, distal metatarsus. (a,b): Haematoxylin and eosin.

3.2. Genetic Analysis

Filtering of WGS for private variants present in the affected calf and absent in the 496 available control genomes, identified 14 protein-changing variants with a predicted high and moderate impact on the encoded protein. They were found to be heterozygous exclusively in the OI-affected calf and absent in the 496 control genomes that were sequenced in the course of other ongoing projects at the Institute of Genetics. These variants were further investigated for their occurrence in a global control cohort of 3103 genomes of a variety of breeds 1000 Bull Genomes Project run 7 [17], which revealed five protein-changing variants exclusively present heterozygous in the genome of the affected calf (Table S2).

These five variants were subsequently visually inspected using IGV software confirming all as true variants. Of all the remaining private variants, only one occurred in an obvious candidate gene for OI (Figure 3a). The heterozygous variant at chr19:36473359T>A represents a missense variant in COL1A1 (NM_001034039.2: c.3917T>A; Figure 3c). This variant alters the encoded amino acid of COL1A1 residue 1306 (XP_024835395.1: p.Val1306Glu) located in the fibrillar collagen NC1 domain (Figure 3d,e). Furthermore, the valine to glutamine substitution affects an evolutionary conserved amino acid (Figure 3d) and was predicted to be deleterious (PROVEAN score -4.96) and destabilizing (DynaMut, $\Delta\Delta G$: -0.127 kcal/mol). To confirm and evaluate the presence of the COL1A1 variant, the affected genomic region was amplified by PCR and Sanger sequenced in the calf, its sire and dam (Figure 3b). Analyzing the sequencing data, we observed that the calf was indeed heterozygous for the detected COL1A1 variant whereas the sire and dam were both homozygous for the wild type allele (Figure 3b). This showed that the mutation most likely arose spontaneously in the affected calf and finally confirmed the diagnosis of OI type II.

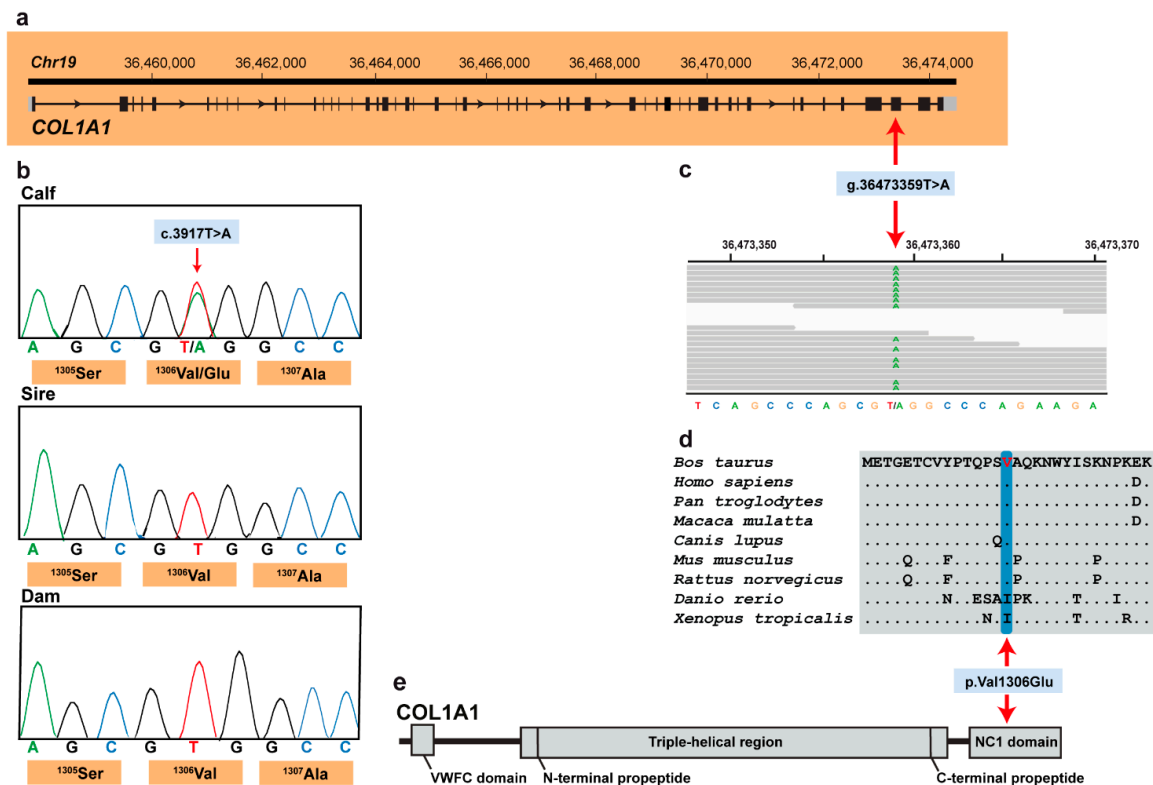


Figure 3. COL1A1 missense variant in an OI type II-affected Holstein calf. (a) COL1A1 gene structure showing the variant location on chromosome 19, exon 49 (red arrow); (b) Electropherograms showing the heterozygous genotype of the calf, and the absence of the variant in its dam genome and in the germline of its sire. (c) IGV screenshot presenting the Chr19: g.36473359T>A variant in the affected calf. (d) Multiple sequence alignment of the collagen alpha-1(I) chain of the COL1A1 protein encompassing the region of the p.Val1306Glu variant demonstrates complete evolutionary conservation across species. (e) Schematic representation of COL1A1 protein and its three functional domains.

4. Discussion

The identified missense variant in *COL1A1* in an obvious candidate gene represents the most likely pathogenic variant associated with the observed OI phenotype. As for humans, OI in cattle is a disorder characterized by bone fragility with perinatal fractures, severe bowing of long bones and reduced mineralization. Furthermore, the OI type II form is frequently lethal in utero or shortly after birth due to severe bone fragility and respiratory insufficiency. In cattle, forms of OI type II (OMIA 002127-9913) have been reported in Fleckvieh and Red Angus cattle associated to dominant acting pathogenic variants in *COL1A1* inherited from mosaic sires [10,11]. In humans, this disorder (OMIM 166210) is linked to pathogenic variants in *COL1A1* and *COL1A2* with a dominant pattern of inheritance. Thus, cases of OI with lesions typical for type II OI could be suspected of having a defect in *COL1A1* or *COL1A2* genes; a suspicion that is helpful when analysing WGS data. In this case, filtering for private variants lead to the identification of a missense variant in *COL1A1*. We assume that this spontaneous mutation most likely occurred either within the parental germlines or post-zygotically in the developing embryo. The mutant allele was detected neither in the dam nor in the sire, given that the variant was not found in the paternal germ line DNA which was analysed. This means that the missense variant was exclusively present in heterozygous state in the affected offspring only. Therefore, it appears more plausible that the identified mutation arose indeed de novo spontaneously in the very early development of the calf. However, a low level mosaicism in the dam cannot be excluded given that the DNA which was analysed was not from the germline.

The identified deleterious variant and the conservation of the affected amino acid residue of COL1A at the position 1306 suggest that this variant is most likely pathogenic. The affected valine residue is conserved across mammals and corresponds to isoleucine in more distant related species such as clawed frogs or zebrafish. As isoleucine and valine are highly similar amino acids having large aliphatic hydrophobic side chains their molecules are rigid, and their mutual hydrophobic interactions are important for the correct folding of proteins, as these chains tend to be located inside of the protein molecule. Because glutamic acid expressed by the mutant allele carries a long hydrophilic acidic group with strong negative charge it most likely impairs proper folding. Type I collagen is a member of group I collagen (fibrillar forming collagen) and is located in the extracellular matrix (ECM). There is a wide range of connective tissue disorders that occur from genetic abnormalities in ECM proteins as for example OI. In contrast to heterozygous null mutations, most of the more severe ECM disorders are caused by heterozygous missense mutations that interrupt the protein structure [24]. Variants in genes coding for collagens provide the perfect scenario for the impact of dominant negative protein structural mutations. In addition to variants in *COL1A1* and *COL1A2* associated with OI, many pathogenic variants in *COL2A1* and *COL10A1* are linked to chondrodysplasias [24].

Interestingly, the identified missense variant in this study occurred in the fibrillar collagen NC1 domain, and by analogy with substitutions in this domain, as in collagen alpha-10(X) in Schmid metaphysical chondrodysplasias (OMIM 156500), it would be expected to disrupt the collagen homotrimer assembly and secretion leading to proteosomal degradation of the unassembled collagen chains [25–28]. To the best of our knowledge, no pathogenic variant in fibrillar collagen NC1 domain of *COL1A1* associated with OI has been reported in domestic animal species and therefore represents the first large animal model for mutations occurring in this domain of *COL1A1*.

5. Conclusions

This is the first report of a most likely pathogenic missense variant in OI type II-affected cattle affecting the fibrillar collagen NC domain of *COL1A1*. So far, disease-causing variants in *COL1A1* in domestic animals were found only in the triple-helical region of the encoded collagen protein. This case demonstrates that pathogenic variants in the other domains of the *COL1A1* protein also cause a similar congenital phenotype. Therefore, this finding expands the spectrum of *COL1A1* mutations that cause a uniform phenotype. Furthermore,

this example highlights the utility of WGS-precise diagnosis for understanding sporadic cases of congenital disorders associated to de novo mutations and the need for continued surveillance of genetic lethal disorders in cattle breeding.

Supplementary Materials: Supplementary materials can be found at <https://www.mdpi.com/2076-2615/11/2/561/s1>. Table S1: EBI Accession numbers of all publicly available genome sequences. We compared the genotypes of the calf with 494 cattle genomes of various breeds that had been sequenced in the course of other ongoing studies and that were publicly available, Table S2: List of the remaining variants after the comparison to the global control cohort of 3103 genomes of other breeds (1000 Bull Genomes Project run 7; www.1000bullgenomes.com (accessed on 31 August 2018)), revealing 5 protein-changing variants only present in the genome of the OI type II-affected calf. These 5 variants with a moderate predicted impact on the encoded protein were located within 5 different genes or loci. Note that the predicted pathogenic variant NM_001034039.2: c.3917T>A is the only one located in a candidate gene for bone diseases.

Author Contributions: Conceptualization, C.D. and J.S.A.; methodology, I.M.H., F.J.M., J.S.A. and C.D.; software, I.M.H.; validation, J.G.P.J.; formal analysis, J.G.P.J., I.M.H., F.J.M., J.S.A. and C.D.; investigation, J.G.P.J. and J.S.A.; resources, C.D. and J.S.A.; data curation, I.M.H.; writing—original draft preparation, J.G.P.J.; writing—review and editing, J.G.P.J., C.D., F.J.M. and J.S.A.; visualization, J.S.A. and J.G.P.J.; supervision, C.D. and J.S.A.; project administration, C.D. and J.S.A.; funding acquisition, C.D. and J.S.A. All authors have read and agreed to the published version of the manuscript.

Funding: The post-mortem investigation was performed as part of the Danish surveillance program for genetic diseases in cattle and funded jointly by SEGES and the University of Copenhagen. This study was partially funded by the Swiss National Science Foundation.

Institutional Review Board Statement: This study did not require official or institutional ethical approval as it was not an experimental study, but part of a clinical and pathological veterinary diagnostic case.

Data Availability Statement: The whole-genome data of the affected calf is freely available at the European Nucleotide Archive (ENA) under sample accession number SAMEA6528897.

Acknowledgments: Tine Skau, Vendsyssel Landdyrlæger is acknowledged for referring the case and the owner for donating the calf for research. We thank Nathalie Besuchet-Schmutz for expert technical assistance and the Interfaculty Bioinformatics Unit of the University of Bern for providing high-performance computational infrastructure.

Conflicts of Interest: The authors declare that they have no conflict of interest.

References

1. Marini, J.C.; Forlino, A.; Cabral, W.A.; Barnes, A.M.; Antonio, J.D.S.; Milgrom, S.; Hyland, J.C.; Körkkö, J.; Prockop, D.J.; De Paepe, A.; et al. Consortium for osteogenesis imperfecta mutations in the helical domain of type I collagen: Regions rich in lethal mutations align with collagen binding sites for integrins and proteoglycans. *Hum. Mutat.* **2007**, *28*, 209–221. [[CrossRef](#)] [[PubMed](#)]
2. Rossi, V.; Lee, B.; Marom, R. Osteogenesis imperfecta: Advancements in genetics and treatment. *Curr. Opin. Pediatr.* **2019**, *31*, 708–715. [[CrossRef](#)] [[PubMed](#)]
3. Peddada, K.V.; Sullivan, B.T.; Margalit, A.; Sponseller, P.D. Fracture Patterns Differ Between Osteogenesis Imperfecta and Routine Pediatric Fractures. *J. Pediatr. Orthop.* **2018**, *38*, e207–e212. [[CrossRef](#)] [[PubMed](#)]
4. Marini, J.C.; Cabral, W.A. *Osteogenesis Imperfecta Genetics of Bone Biology and Skeletal Disease*; Elsevier Inc: Amsterdam, The Netherlands, 2018.
5. Kater, J.C.; Hartley, W.; Dysart, T.; Campbell, A. Osteogenesis imperfecta and bone resorption: Two unusual skeletal abnormalities in young lambs. *New Zealand Veter- J.* **1963**, *11*, 41–46. [[CrossRef](#)]
6. Cohn, L.; Meuten, D.J. Bone fragility in a kitten: An osteogenesis imperfecta-like syndrome. *J. Am. Veter- Med. Assoc.* **1990**, *197*, 98–100.
7. Calkins, E.; Kalm, D.; Diner, W.C. Idiopathic familial osteoporosis in dogs: “Osteogenesis imperfecta”. *Ann. N. Y. Acad. Sci.* **1956**, *64*, 410–423. [[CrossRef](#)]
8. Jensen, P.T.; Rasmussen, P.G.; Basse, A. Congenital osteogenesis imperfecta in Charolais cattle. *Nord. Vet. Med.* **1976**, *28*, 304–308.
9. Campbell, B.G.; Wootton, J.A.; MacLeod, J.N.; Minor, R.R. Sequence of Normal Canine COL1A1 cDNA and Identification of a Heterozygous $\alpha 1(I)$ Collagen Gly208A1a Mutation in a Severe Case of Canine Osteogenesis Imperfecta. *Arch. Biochem. Biophys.* **2000**, *384*, 37–46. [[CrossRef](#)]

10. Petersen, J.L.; Tietze, S.M.; Burrack, R.M.; Steffen, D.J. Evidence for a de novo, dominant germ-line mutation causative of osteogenesis imperfecta in two Red Angus calves. *Mamm. Genome* **2019**, *30*, 81–87. [[CrossRef](#)] [[PubMed](#)]
11. Bourneuf, E.; Otz, P.; Pausch, H.; Jagannathan, V.; Michot, P.; Grohs, C.; Piton, G.; Ammermüller, S.; Deloche, M.C.; Fritz, S.; et al. Rapid Discovery of De Novo Deleterious Mutations in Cattle Enhances the Value of Livestock as Model Species. *Sci. Rep.* **2017**, *7*, 1–19. [[CrossRef](#)] [[PubMed](#)]
12. Letko, A.; Zdora, I.; Hitzler, V.; Jagannathan, V.; Beineke, A.; Möhrke, C.; Drögemüller, C. A de novo in-frame duplication in the COL1A2 gene in a Lagotto Romagnolo dog with osteogenesis imperfecta. *Anim. Genet.* **2019**, *50*, 786–787. [[CrossRef](#)] [[PubMed](#)]
13. Campbell, B.G.; Wootton, J.A.M.; MacLeod, J.N.; Minor, R.R. Canine COL1A2 Mutation Resulting in C-Terminal Truncation of Pro- α 2(I) and Severe Osteogenesis Imperfecta. *J. Bone Miner. Res.* **2001**, *16*, 1147–1153. [[CrossRef](#)] [[PubMed](#)]
14. Quist, E.M.; Doan, R.; Pool, R.R.; Porter, B.F.; Bannasch, D.L.; Dindot, S.V. Identification of a Candidate Mutation in the COL1A2 Gene of a Chow Chow With Osteogenesis Imperfecta. *J. Hered.* **2017**, *109*, 308–314. [[CrossRef](#)] [[PubMed](#)]
15. Drögemüller, C.; Becker, D.; Brunner, A.; Haase, B.; Kircher, P.; Seeliger, F.; Fehr, M.; Baumann, U.; Lindblad-Toh, K.; Leeb, T. A Missense Mutation in the SERPINH1 Gene in Dachshunds with Osteogenesis Imperfecta. *PLoS Genet.* **2009**, *5*, e1000579. [[CrossRef](#)]
16. Rosen, B.D.; Bickhart, D.M.; Schnabel, R.D.; Koren, S.; Elsik, C.G.; Tseng, E.; Rowan, T.N.; Low, W.Y.; Zimin, A.; Couldrey, C.; et al. De novo assembly of the cattle reference genome with single-molecule sequencing. *GigaScience* **2020**, *9*, 1–9. [[CrossRef](#)]
17. Hayes, B.J.; Daetwyler, H.D. 1000 Bull Genomes Project to Map Simple and Complex Genetic Traits in Cattle: Applications and Outcomes. *Annu. Rev. Anim. Biosci.* **2019**, *7*, 89–102. [[CrossRef](#)] [[PubMed](#)]
18. Chen, S.; Zhou, Y.; Chen, Y.; Gu, J. fastp: An ultra-fast all-in-one FASTQ preprocessor. *Bioinform.* **2018**, *34*, i884–i890. [[CrossRef](#)]
19. Häfliger, I.M.; Wiedemar, N.; Švara, T.; Starič, J.; Cociancich, V.; Šest, K.; Gombač, M.; Paller, T.; Agerholm, J.S.; Drögemüller, C. Identification of small and large genomic candidate variants in bovine pulmonary hypoplasia and anasarca syndrome. *Anim. Genet.* **2020**, *51*, 382–390. [[CrossRef](#)] [[PubMed](#)]
20. Cingolani, P.; Platts, A.; Wang, L.L.; Coon, M.; Nguyen, T.; Wang, L.; Land, S.J.; Lu, X.; Ruden, D.M. A program for annotating and predicting the effects of single nucleotide polymorphisms, SnpEff: SNPs in the genome of *Drosophila melanogaster* strain w1118; iso-2; iso-3. *Fly* **2012**, *6*, 80–92. [[CrossRef](#)] [[PubMed](#)]
21. Robinson, J.T.; Thorvaldsdóttir, H.; Wenger, A.M.; Zehir, A.; Mesirov, J.P. Variant Review with the Integrative Genomics Viewer. *Cancer Res.* **2017**, *77*, e31–e34. [[CrossRef](#)] [[PubMed](#)]
22. Choi, Y.; Chan, A.P. PROVEAN web server: A tool to predict the functional effect of amino acid substitutions and indels. *Bioinform.* **2015**, *31*, 2745–2747. [[CrossRef](#)] [[PubMed](#)]
23. Rodrigues, C.H.M.; Pires, D.E.V.; Ascher, D.B. DynaMut: Predicting the impact of mutations on protein conformation, flexibility and stability. *Nucleic Acids Res.* **2018**, *46*, W350–W355. [[CrossRef](#)]
24. Lamandé, S.R.; Bateman, J.F. Genetic Disorders of the Extracellular Matrix. *Anat. Rec. Adv. Integr. Anat. Evol. Biol.* **2019**, *303*, 1527–1542. [[CrossRef](#)] [[PubMed](#)]
25. Kong, L.; Shi, L.; Wang, W.; Zuo, R.; Wang, M.; Kang, Q. Identification of two novel COL10A1 heterozygous mutations in two Chinese pedigrees with Schmid-type metaphyseal chondrodysplasia. *BMC Med. Genet.* **2019**, *20*, 1–9. [[CrossRef](#)]
26. Chan, D.; Cole, W.G.; Rogers, J.; Bateman, J.F. A mutation in the conserved NC1 domain of type X collagen prevents in vitro multimer assembly resulting in a Schmid-type metaphyseal chondrodysplasia. *Matrix Biol.* **1994**, *14*, 396–397. [[CrossRef](#)]
27. Chan, D.; Weng, Y.M.; Golub, S.; Bateman, J.F. Type X collagen NC1 mutations produced by site-directed mutagenesis prevent in vitro assembly. *Ann. N. Y. Acad. Sci.* **1996**, *785*, 231–233. [[CrossRef](#)] [[PubMed](#)]
28. Wilson, R.; Freddi, S.; Bateman, J.F. Collagen X Chains Harboring Schmid Metaphyseal Chondrodysplasia NC1 Domain Mutations Are Selectively Retained and Degraded in Stably Transfected Cells. *J. Biol. Chem.* **2002**, *277*, 12516–12524. [[CrossRef](#)] [[PubMed](#)]

4.1.1.4 A heterozygous missense variant in *MAP2K2* in a stillborn Romagnola calf with skeletal-cardio-enteric dysplasia

Journal: animals
Manuscript status: published
Contributions: phenotype description, whole-genome sequencing data analysis, figures, writing original draft and revisions
Displayed version: published version
DOI: [10.3390/ani11071931](https://doi.org/10.3390/ani11071931)

Article

A Heterozygous Missense Variant in *MAP2K2* in a Stillborn Romagnola Calf with Skeletal-Cardio-Enteric Dysplasia

Joana G. P. Jacinto ^{1,2}, Irene M. Häfliger ², Arcangelo Gentile ¹ and Cord Drögemüller ^{2,*}

¹ Department of Veterinary Medical Sciences, University of Bologna, Ozzano Emilia, 40064 Bologna, Italy; joana.goncalves2@studio.unibo.it (J.G.P.J.); arcangelo.gentile@unibo.it (A.G.)

² Institute of Genetics, Vetsuisse Faculty, University of Bern, 3012 Bern, Switzerland; irene.haeffliger@vetsuisse.unibe.ch

* Correspondence: cord.droegemueller@vetsuisse.unibe.ch

Simple Summary: Skeletal dysplasias encompass a clinical-, pathological- and genetically heterogeneous group of disorders characterized by abnormal cartilage and/or bone formation, growth, and remodeling. They may belong to the so-called RASopathies, congenital conditions caused by heterozygous variants in genes that encode components of the Ras/mitogen-activated protein kinase (MAPK) cell signaling pathway. Herein, an affected calf of the Italian Romagnola breed was reported showing a skeletal-cardio-enteric dysplasia. We identified a most likely disease-causing mutation in the *MAP2K2* gene by whole-genome sequencing (WGS). The *MAP2K2* gene is known to be related with dominant inherited cardio-facio-cutaneous syndrome in humans, but it was so far unknown to cause a similar disease in domestic animals. We assume that the identified missense variant that was predicted to impair the function of the protein, occurred either within the germline of the dam or post-zygotically in the embryo. Rare lethal diseases such as the skeletal-cardio-enteric dysplasia in livestock are usually not characterized to the molecular level, mainly because of the lack of funds and diagnostic opportunities. Precise WGS-based diagnostics enables the understanding of rare diseases and supports the value of monitoring cattle breeding populations for fatal genetic defects.

Abstract: RASopathies are a group of developmental disorders caused by dominant mutations in genes that encode components of the Ras/mitogen-activated protein kinase (MAPK) cell signaling pathway. The goal of this study was to characterize the pathological phenotype of a Romagnola stillborn calf with skeletal-cardio-enteric dysplasia and to identify a genetic cause by whole-genome sequencing (WGS). The calf showed reduced fetal growth, a short-spine, a long and narrow face, cardiac defects and heterotopy of the spiral colon. Genetic analysis revealed a private heterozygous missense variant in *MAP2K2*:p.Arg179Trp, located in the protein kinase domain in the calf, and not found in more than 4500 control genomes including its sire. The identified variant affecting a conserved residue was predicted to be deleterious and most likely occurred de novo. This represents the first example of a dominant acting, and most likely pathogenic, variant in *MAP2K2* in domestic animals, thereby providing the first *MAP2K2*-related large animal model, especially in respect to the enteric malformation. In addition, this study demonstrates the utility of WGS-based precise diagnostics for understanding sporadic congenital syndromic anomalies in cattle and the general utility of continuous surveillance for rare hereditary defects in cattle.

Keywords: cattle; cardiac defect; development; congenital malformations; heterotopy; precision medicine; short spine; RASopathy



Citation: Jacinto, J.G.P.; Häfliger, I.M.; Gentile, A.; Drögemüller, C. A Heterozygous Missense Variant in *MAP2K2* in a Stillborn Romagnola Calf with Skeletal-Cardio-Enteric Dysplasia. *Animals* **2021**, *11*, 1931. <https://doi.org/10.3390/ani11071931>

Academic Editors: Francesca Ciotola, Sara Albarella and Vincenzo Peretti

Received: 5 May 2021
Accepted: 25 June 2021
Published: 29 June 2021

Publisher's Note: MDPI stays neutral with regard to jurisdictional claims in published maps and institutional affiliations.



Copyright: © 2021 by the authors. Licensee MDPI, Basel, Switzerland. This article is an open access article distributed under the terms and conditions of the Creative Commons Attribution (CC BY) license (<https://creativecommons.org/licenses/by/4.0/>).

1. Introduction

Genetic skeletal dysplasias encompass a clinical-, pathological-, and genetically heterogeneous group of rare disorders characterized by abnormal cartilage and/or bone formation, growth, and remodeling [1]. In human medicine, 461 different skeletal disorders

are classified into 42 subtypes [2]. At the present in humans, pathogenic variants affecting more than 437 different genes have been found to be associated with these disorders [2]. In veterinary medicine, genetic skeletal dysplasias are not classified in such detail. Nevertheless, with the progressively widespread availability of molecular tools for genetic mapping, such as single-nucleotide polymorphism (SNP) arrays, and for mutation analysis, such as short-read based whole-genome sequencing (WGS), the recognition of disease-causing pathogenic variants has drastically improved [3,4]. In fact, the 1000 Bull Genomes Project now encompasses a genetic variation from over 4100 genomes providing a comprehensive database for the imputation of genetic polymorphisms for genomic prediction in all cattle breeds, improving the accuracy of genomic prediction in the identification of causal mutations [5]. The OMIA (Online Mendelian Inheritance of Animals) currently lists 22 skeletal disorders in cattle with a known causal mutation, e.g., recessively inherited mostly breed-specific disorders such as the brachyspina syndrome in Holstein (OMIA 000151-9913) [6] and the paunch calf syndrome in Romagnola [7] and Marchigiana [8] (OMIA 001722-9913), or dominantly inherited disorders such as the bovine achondrogenesis type II (OMIA 001926-9913) [9], or cases of facial dysplasia in the progeny of a single bull (OMIA 002090-9913) [10]. The latter two diseases have been shown to result from de novo mutation events in the paternal germline.

This study aimed to characterize in detail the pathological phenotype of a Romagnola calf with skeletal cardio-enteric dysplasia, and to discover a genetic variant causing the abnormality by WGS.

2. Materials and Methods

2.1. Pathological Investigation

A stillborn Romagnola male calf was referred to the Department of Veterinary Medical Sciences, University of Bologna for post-mortem examination. The calf resulted from insemination with semen from a purebred Romagnola bull on a Romagnola cow. The pedigree of both parents showed no common ancestor within four generations. The truncal length was measured from the occipital bone to the tuber coxae. Additionally, radiographic images of the spine were obtained before starting necropsy.

2.2. DNA Samples

Genomic DNA was isolated from skin and cartilage from the ear of the calf and from the semen of the sire using Promega Maxwell RSC DNA system (Promega, Dübendorf, Switzerland). In addition, genomic DNA samples from EDTA-blood samples of 100 apparently normal Romagnola cattle were extracted with the same methodology and used as controls.

2.3. Whole-Genome Sequencing

The genome of the affected calf was sequenced as described before resulting in an average read coverage of approximately $17.4\times$ [11]. Single-nucleotide variants (SNVs) and small indel variants were called subsequently as reported earlier [5], except for the trimming, which was carried out using fastp [12]. Further data processing was carried out according to Häfliger et al., 2020 [13]. The impact of the called sequence variants was evaluated with snpeff v4.3 [14], using NCBI Annotation Release 106 (https://www.ncbi.nlm.nih.gov/genome/annotation_euk/Bos_taurus/106/; accessed on 30 April 2021). In order to search for private variants, we compared the genotypes of the affected calf with 598 bovine genomes of different breeds that have been sequenced in other ongoing studies and are freely available (Table S1) in the European Nucleotide Archive (SAMEA7690195 is the sample accession number of the affected calf; <http://www.ebi.ac.uk/en>; accessed on 30 April 2021). The occurrence of these variants was then investigated in a global control cohort of 4110 genomes of different breeds (1000 Bull Genomes Project run 8; www.1000bullgenomes.com; accessed on 30 April 2021) [5]. Integrative Genomics Viewer

(IGV) [15] software version 2.0 was used to manually look at genomic regions where possible candidate genes map.

2.4. Targeted Genotyping

PCRs were carried out using Amplitaq Gold Master Mix (ThermoFisher, Rotkreuz, Switzerland). The subsequent bi-directional sequencing of PCR products was carried out after shrimp alkaline phosphatase (Roche, Basel, Switzerland) and exonuclease I (NEB, Axon lab, Baden, Switzerland) incubation using the PCR primers with the ABI BigDye Terminator Sequencing Kit 3.1 (Applied Biosystems, Zug, Switzerland) on an ABI 3730 capillary sequencer (Applied Biosystems). The *MAP2K2* missense variant (NM_001038071.2: g.19923991C>T) was genotyped using the following primers: 5'-GGCTTAACAGAGGATGCCCC-3' (forward primer) and 5'-CTGGAAAACCTGGAAA-TCGGG-3' (reverse primer). The evaluation of the sequence data was carried out with Sequencher 5.1 software (GeneCodes, Ann Arbor, MI, USA).

2.5. Evaluation of the Molecular Consequences of Amino Acid Substitutions

PROVEAN [16] and PredictSNP1 [17] were used to predict the biological consequences of the discovered variant on protein. For multispecies sequence alignments the following NCBI proteins accessions were used: NP_001033160.2 (*Bos taurus*), NP_109587.1 (*Homo sapiens*), XP_003318859.1 (*Pan troglodytes*), XP_001118016.2 (*Macaca mulatta*), NP_001041601.1 (*Canis lupus*), NP_075627.2 (*Mus musculus*), NP_579817.1 (*Rattus norvegicus*), NP_990719.1 (*Gallus gallus*), NP_001032468.2 (*Danio rerio*).

2.6. Sequence Accessions

Genomic positions in the cow genome refers to the the ARS-UCD1.2 assembly. All references to the bovine *MAP2K2* gene correspond to the NCBI accessions NC_037334.1 (chromosome 7, ARS-UCD1.2), NM_001038071.2 (*MAP2K2* mRNA), and NP_001033160.2 (*MAP2K2* protein). For the *MAP2K2* protein, the Uniprot database (<https://www.uniprot.org/>) (accessed on 15 March 2021) accession number A0A3S5ZPX3 was used.

3. Results

3.1. Pathological Phenotype

At birth, the calf weighed only 20.3 kg (normal weight of Romagnola calves at birth 40 Kg–mean) and its trunk was disproportionately short for the body size and legs (Figure 1; Figure S1). Shortening of the neck was very pronounced, and it looked as though the head was fixed to the chest. The length of trunk, as measured from the occipital bone to the point of the buttock, was approximately 40 cm. Moreover, it displayed a mild kyphosis at the level of the thoracolumbar region. The limbs were 70 cm long and slender (dolichostenomelia).

Facial deformities were characterized by narrow, longer and laterally deviated splanchnocranium. The lower jaw was slightly longer than normal.

Radiological examination of the axial skeleton showed only a reduced size of the vertebral bodies, but no shape abnormalities (Figure S2).

At gross pathology, the examination of the abdominal cavity showed the absence of the omentum and heterotopy of the spiral colon, the latter characterized by a complete detachment and complete displacement of the spiral loop of the ascending colon from the mesojejunum (Figure 2a,b).

The calf also showed an evident 2 cm diameter persistent patent ductus and pathological cardiac abnormalities, including globous shape, enlarged right ventricle and pulmonary stenosis.

Based on these pathological observations, the animal was considered to present a skeletal-cardio-enteric dysplasia.



Figure 1. Stillborn Romagnola calf with skeletal-cardio-enteric dysplasia: Strikingly, the length of the spine appeared disproportionately short for the height and legs. Mild kyphosis of the thoraco-lumbar vertebral column is also evident. Bar, 30 cm.

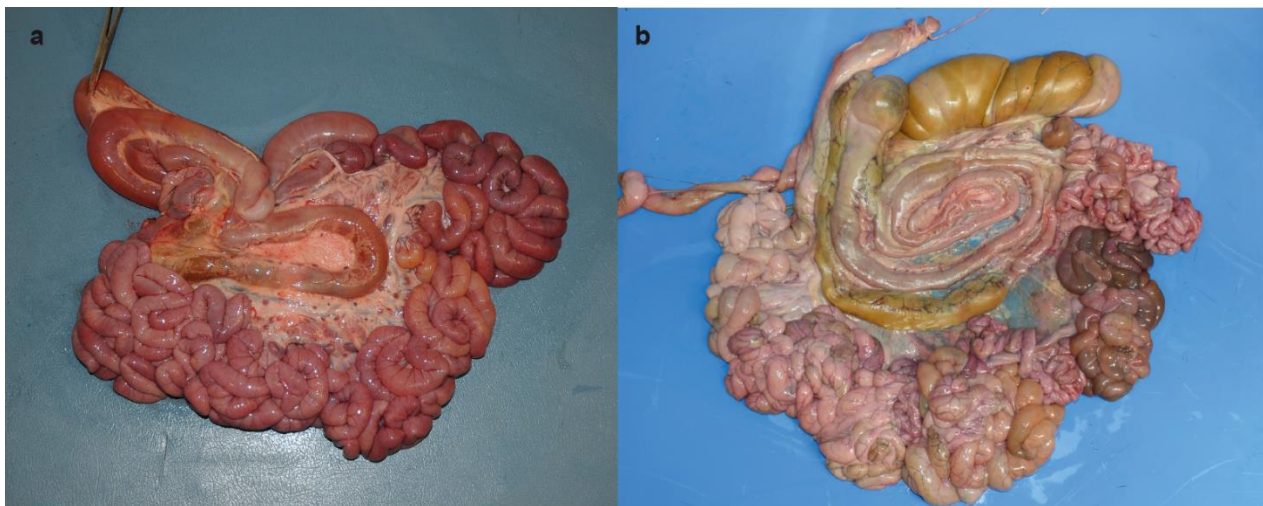


Figure 2. Topography of the spiral loop of the ascending colon. (a) Topography of the spiral loop of the ascending colon in the stillborn Romagnola calf with skeletal-cardio-enteric dysplasia. Note the complete displacement of the spiral loop of the ascending colon from the mesojejunum. (b) Topography of the spiral loop of the ascending colon in a control. Note the spiral loop of the ascending colon located at the middle of the mesojejunum.

3.2. Genetic Analysis

Assuming a spontaneous mutation as the most likely cause for this congenital malformation, the whole genome of the affected calf was sequenced. To evaluate the presence of coding protein-changing variants, filtering of WGS for private variants present in the calf and not present in the 598 control genomes was performed. This approach identified 381 heterozygous private protein-changing variants predicted to have moderate or severe alteration on the encoded proteins. These variants were then tested for their presence

in a global control cohort of 4110 genomes of various breeds collected in run 8 of the 1000 Bull Genomes Project [5], which revealed 66 protein-changing variants only occurring in heterozygous state in the genome of the affected calf. These 66 variants were subsequently evaluated using IGV software, confirming 63 as true variants (Table S2). Of all the remaining private variants, one occurred in a possible candidate gene for observed phenotype (Figure 3a). The heterozygous variant at chr7:19923991C>T represents a missense variant in exon 5 of the *MAP2K2* gene (NM_001038071.2: c.535C>T; Figure 3c). This variant alters the amino acid of the *MAP2K2* protein at site 179 (NP_001033160.2: p.Arg179Trp) located in the protein kinase domain (Figure 3e). Furthermore, the arginine to tryptophan substitution affects an evolutionary conserved residue (Figure 3f) and has been predicted to be harmful (PROVEAN score -4.708 ; Predict SNP score 61%). In order to confirm and finally evaluate the *MAP2K2* variant, the corresponding genome region was amplified by PCR and then analyzed by Sanger sequencing in the calf, its sire, and 100 controls of the same breed. Unfortunately, no biological sample of the dam that was slaughtered in-between was available. When analyzing the sequencing data, we found that the calf was indeed heterozygous for the *MAP2K2* variant detected, while the sire and another 100 controls from the Italian Romagnola population were homozygous for the wild-type allele (Figure 3b,c).

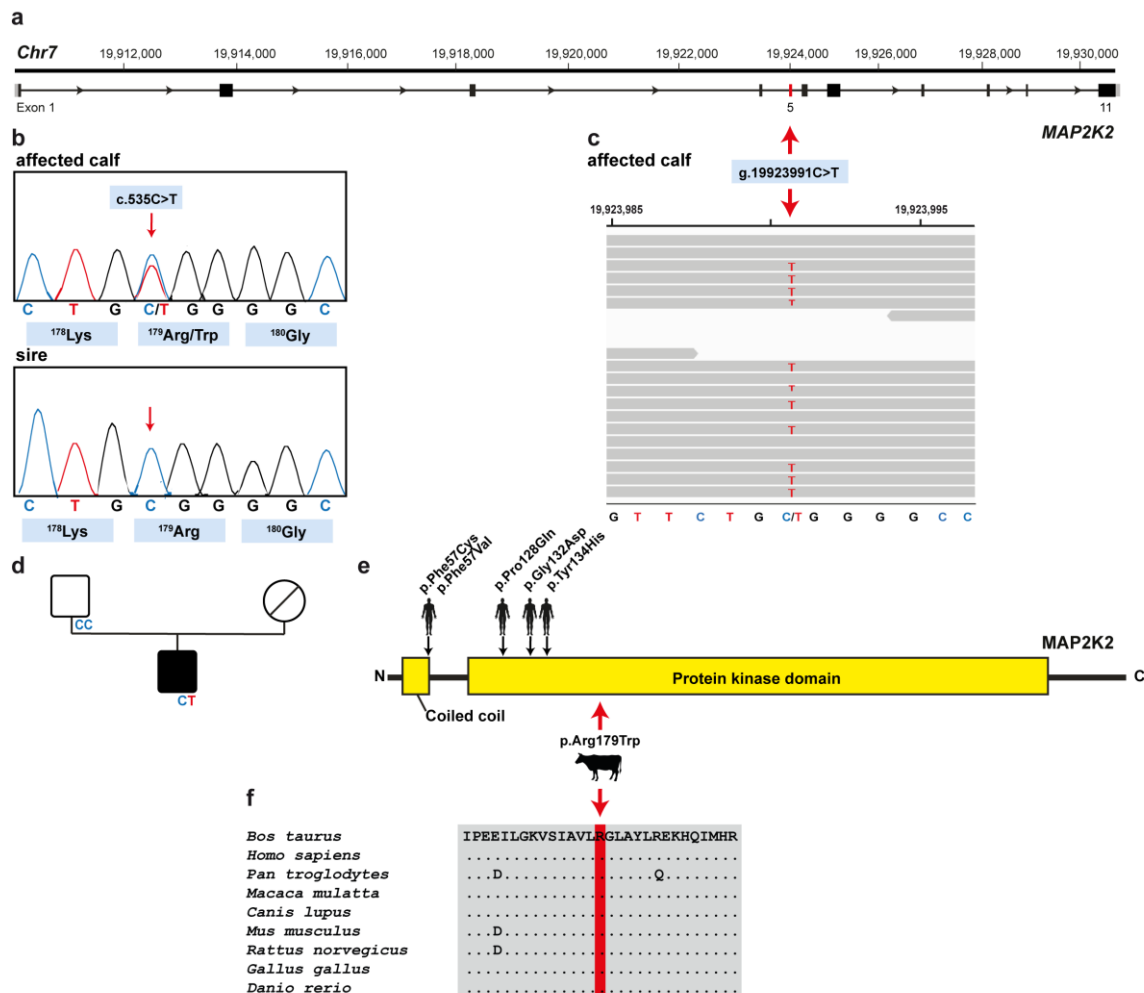


Figure 3. *MAP2K2* missense variant in a Romagnola calf with skeletal-cardio-enteric dysplasia: (a) *MAP2K2* gene structure representation of the exact position of the exon 5 variant on the chromosome 7 (red arrow); (b) Electropherograms confirming heterozygosity in the affected calf and the absence of the variant in the germline of the sire. (c) IGV screenshot presenting

the Chr7: g.19923991C>T variant in the calf. (d) Pedigree of the case. The affected male calf is represented with full black symbol, while both non-affected parents are represented by full white symbols. Unknown genotype is represented by a symbol with a diagonal line. (e) Schematic representation of *MAP2K2* protein and its functional domains and summary of known human *MAP2K2* mutations. The position of the mutation detected in the affected Romagnola calf is indicated by a red arrow, while known human *MAP2K2* mutations associated with cardio-facio-cutaneous syndrome are indicated by black arrows (OMIM601263). (f) Multiple sequence alignment of the protein kinase domain of the *MAP2K2* protein around the position of the p.Arg179Trp variant shows complete evolutionary conservation across all species.

In addition, when looking for homozygous variants, filtering revealed two private protein-changing variants present in the genome of the affected calf (Table S2).

4. Discussion

Non-infectious syndromic congenital malformations of newborns in cattle occur rarely and are most often not further diagnosed in detail. We have carried out a comprehensive pathological and genetic examination in a Romagnola stillborn calf, revealing a skeletal-cardio-enteric dysplasia. We then investigated the hypothesis of a spontaneous mutation as a possible reason for this congenital phenotype. Using state-of-the-art genetic approaches involving WGS, geneticists have only about a 50:50 chance of quickly identifying variants that are causal for developmental anomalies in humans [18]. So far, similar data is missing for veterinary medicine, mostly due to the lack of resources, although the scientific value for biomedical research is widely accepted [4]. Analysis of the genome sequence of the studied case identified a missense variant in a plausible candidate gene affecting the protein kinase domain of *MAP2K2*. In addition, this variant was only present in the genome of the affected calf, and did not occur in a global control cohort of more than 4500 bovine genomes of different breeds. Therefore, considering the rarity of this coding variant and the function of the *MAP2K2*, it was considered to represent the most likely genetic cause for the observed phenotype. To the best of our knowledge, no pathogenic variant in the *MAP2K2* gene has been reported in domestic species. Therefore, this study represents the first large animal model for a *MAP2K2*-related congenital skeletal disorder in cattle.

Furthermore, the PCR to detect the mutant allele in the sire using DNA extracted from semen showed a homozygous wild-type genotype. Therefore, we could exclude the father as a mosaic ancestor. However, to definitively prove that the identified variant in *MAP2K2* indeed occurred *de novo*, genotyping of the dam would be needed. Therefore, we speculate that the mutation either arose post-zygotically during fetal development of the affected calf or represents a maternally derived germline mutation.

The RAS/mitogen activated protein kinase (MAPK) cell signaling pathway plays an important role in the regulation of the cell cycle and differentiation [19]. In particular, during embryonic development, it represents one of the main pathways for the transduction of intracellular signals in response to all types of mitogens (e.g., growth factors), which initiates proliferation, survival, and anti-apoptotic programs [20]. Furthermore, the dysregulation of RAS/MAPK-dependent developmental processes has significant pathophysiological consequences [20].

In humans, somatic mutations leading to hyperactivation of the RAS/MAPK signaling cascade may cause cancers [21], whereas germline or *de novo* mutations in the developing embryo are responsible for several rare genetic conditions, collectively termed RASopathies. These disorders have common phenotypes, such as a short stature, heart defects, facial abnormalities, and cognitive impairments, often associated with abnormal central nervous system development, and include conditions such as neurofibromatosis type 1 (OMIM 162200) [22], Noonan (OMIM 163950) [23], LEOPARD (OMIM 151100) [24], Costello (OMIM 218040) [25], and cardio-facio-cutaneous (CFC; OMIM 115150) [26] syndromes. In humans, RASopathies are a highly heterogeneous group of genetic disorders, being associated to more than 20 causal genes [20]. These genes encode proteins that belong to, or regulate, the RAS/MAPK cell signaling pathway. Their mutations explain the pathophysiological mechanisms, such as the abnormal development of various tissues (e.g., cardiac or craniofacial

defects), as well as the altered hormonal response and consequent endocrine dysfunctions (e.g., growth hormone insensitivity, and growth retardation) [20]. In particular, individuals affected by CFC show characteristic craniofacial dysmorphic features, short stature, cardiac defects, ectodermal anomalies, and developmental delay [26]. Currently, dominantly inherited mutations in four genes have been associated with CFC syndrome: *BRAF* [27], *MAP2K1* [28], *MAP2K2* [26,28], and *KRAS* [27]. Interestingly, the affected calf presented in this study revealed a dominant mutation in *MAP2K2*, and showed retarded growth, skeletal dimorphisms, including a long and narrow face and shortening of the vertebral column, and cardiac defects such as persistent patent ductus and pulmonary stenosis. These findings resemble the phenotype of human CFC syndrome. However, the animal did not show any alteration on the integumentary system.

Moreover, the calf revealed heterotopy of the spiral colon. In cattle, this anatomic anomaly may originate from the loose attachment of the spiral loops to the mesojejunum, abnormal elongation of the mesocolon, overlapping of adjacent loops, abnormal coiling, and finally, complete separation of the spiral loop of the ascending colon from the mesojejunum [29]. This condition can predispose to intestinal injury, such as volvulus and intussusception [29]. Similarly, in human medicine, the so-called intestinal malrotation is a congenital anomaly resulting from incomplete rotation and fixation of the intestine during embryological and fetal development, which may predispose to midgut volvulus and lead to duodenal obstruction and strangulation of the circulation in the superior mesenteric vessels [30]. In humans and mice, *MAP2K2* is known to be highly expressed in the colon and duodenum [31,32]. However, mutations in *MAP2K2* have so far not been associated with enteric congenital defects.

Furthermore, the deleterious nature of the variant and the conservation of the affected arginine amino acid residue of *MAP2K2* at position 179 in protein kinase domain also suggest that this variant is most likely pathogenic. Indeed, mutations of *MAP2K2* affect the negative regulatory region or the core catalytic domain of the kinases, leading to increased kinase activity and gain-of-function effect on the RAS/MAPK pathway [28,33,34].

5. Conclusions

The investigation of this case enabled a pathological and molecular genetic study that, for the first time, allowed the diagnosis of a dominantly inherited skeletal-cardio-enteric dysplasia in a calf associated with a *MAP2K2* missense variant. Thus, we hereby present the first large animal model for similar human diseases. Furthermore, this example highlights the usefulness of genetically precise diagnosis for understanding sporadic cases of congenital disorders caused by de novo mutations, and the need for continuous monitoring of genetic lethal disorders in cattle breeding. Additionally, novel discoveries in large animals such as cattle are useful as biomedical models for human diseases.

Supplementary Materials: The following are available online at <https://www.mdpi.com/article/10.3390/ani11071931/s1>, Table S1: EBI Accession numbers of all publicly available genome sequences. We compared the genotypes of the calf with 598 cattle genomes of various breeds that had been sequenced in the course of other ongoing studies and that were publicly available, Table S2: List of the remaining variants after the comparison to the global control cohort of 4110 genomes of other breeds (1000 Bull Genomes Project run 8; www.1000bullgenomes.com; accessed on 30 April 2021) and after IGV visual inspections, revealing 63 protein-changing variants with a predicted moderate or high impact only present in the affected calf. Figure S1: Newborn Romagnola healthy calf. Figure S2: Radiographic image of the thoraco-lumbar region of the affected calf.

Author Contributions: Conceptualization, C.D. and A.G.; methodology, I.M.H., A.G. and C.D.; validation, J.G.P.J.; formal analysis, J.G.P.J., I.M.H., A.G. and C.D.; investigation, J.G.P.J. and A.G.; resources, C.D.; data curation, I.M.H.; writing—original draft preparation, J.G.P.J.; writing—review and editing, J.G.P.J., I.M.H., A.G. and C.D.; visualization, A.G. and J.G.P.J.; supervision, C.D. and A.G.; project administration, C.D.; funding acquisition, C.D. All authors have read and agreed to the published version of the manuscript.

Funding: This study was partially funded by the Swiss National Science Foundation.

Institutional Review Board Statement: This study did not require official or institutional ethical approval as it was not an experimental study, but part of a clinical and pathological veterinary diagnostic case.

Informed Consent Statement: Not applicable.

Data Availability Statement: The whole-genome data of the affected calf (sample ID PCS1780) is freely available at the European Nucleotide Archive (ENA) under sample accession number SAMEA7690195.

Acknowledgments: We are grateful to Nathalie Besuchet Schmutz for expert technical assistance and the Interfaculty Bioinformatics Unit of the University of Bern for providing high-performance computational infrastructure.

Conflicts of Interest: The authors declare no conflict of interest.

References

1. Song, D.; Maher, C.O. Spinal Disorders Associated with Skeletal Dysplasias and Syndromes. *Neurosurg. Clin. N. Am.* **2007**, *18*, 499–514. [[CrossRef](#)] [[PubMed](#)]
2. Mortier, G.R.; Cohn, D.H.; Cormier-Daire, V.; Hall, C.; Krakow, D.; Mundlos, S.; Nishimura, G.; Robertson, S.; Sangiorgi, L.; Savarirayan, R.; et al. Nosology and classification of genetic skeletal disorders: 2019 revision. *Am. J. Med. Genet. Part A* **2019**, *179*, 2393–2419. [[CrossRef](#)]
3. Dittmer, K.E.; Thompson, K.G. Approach to Investigating Congenital Skeletal Abnormalities in Livestock. *Vet. Pathol.* **2015**, *52*, 851–861. [[CrossRef](#)] [[PubMed](#)]
4. Lyons, L.A. Precision medicine in cats—The right biomedical model may not be the mouse! *PLoS Genet.* **2020**, *16*, 8–11. [[CrossRef](#)] [[PubMed](#)]
5. Hayes, B.J.; Daetwyler, H.D. 1000 Bull Genomes Project to Map Simple and Complex Genetic Traits in Cattle: Applications and Outcomes. *Annu. Rev. Anim. Biosci.* **2019**, *7*, 89–102. [[CrossRef](#)]
6. Charlier, C.; Agerholm, J.S.; Coppieters, W.; Karlskov-Mortensen, P.; Li, W.; de Jong, G.; Fasquelle, C.; Karim, L.; Cirera, S.; Cambisano, N.; et al. A Deletion in the Bovine FANCI Gene Compromises Fertility by Causing Fetal Death and Brachyspina. *PLoS ONE* **2012**, *7*, 2–8. [[CrossRef](#)]
7. Testoni, S.; Bartolone, E.; Rossi, M.; Patrignani, A.; Bruggmann, R.; Lichtner, P.; Tetens, J.; Gentile, A.; Drögemüller, C. KDM2B Is Implicated in Bovine Lethal Multi-Organic Developmental Dysplasia. *PLoS ONE* **2012**, *7*. [[CrossRef](#)]
8. Murgiano, L.; Militerno, G.; Sbarra, F.; Drögemüller, C.; Jacinto, J.G.P.; Gentile, A.; Bolcato, M. KDM2B-associated paunch calf syndrome in Marchigiana cattle. *J. Vet. Intern. Med.* **2020**, *34*, 1657–1661. [[CrossRef](#)]
9. Jacinto, J.G.P.; Häfliger, I.M.; Letko, A.; Drögemüller, C.; Agerholm, J.S. A large deletion in the COL2A1 gene expands the spectrum of pathogenic variants causing bulldog calf syndrome in cattle. *Acta Vet. Scand.* **2020**, *62*, 49. [[CrossRef](#)]
10. Agerholm, J.S.; McEvoy, F.J.; Heegaard, S.; Charlier, C.; Jagannathan, V.; Drögemüller, C. A de novo missense mutation of FGFR2 causes facial dysplasia syndrome in Holstein cattle. *BMC Genet.* **2017**, *18*. [[CrossRef](#)]
11. Rosen, B.D.; Bickhart, D.M.; Schnabel, R.D.; Koren, S.; Elsik, C.G.; Tseng, E.; Rowan, T.N.; Low, W.Y.; Zimin, A.; Couldrey, C.; et al. De novo assembly of the cattle reference genome with single-molecule sequencing. *Gigascience* **2020**, *9*, 1–9. [[CrossRef](#)]
12. Chen, S.; Zhou, Y.; Chen, Y.; Gu, J. Fastp: An ultra-fast all-in-one FASTQ preprocessor. *Bioinformatics* **2018**, *34*, i884–i890. [[CrossRef](#)] [[PubMed](#)]
13. Häfliger, I.M.; Wiedemar, N.; Švara, T.; Starič, J.; Cociancich, V.; Šest, K.; Gombač, M.; Paller, T.; Agerholm, J.S.; Drögemüller, C. Identification of small and large genomic candidate variants in bovine pulmonary hypoplasia and anasarca syndrome. *Anim. Genet.* **2020**, *51*, 382–390. [[CrossRef](#)] [[PubMed](#)]
14. Cingolani, P.; Platts, A.; Wang, L.L.; Coon, M.; Nguyen, T.; Wang, L.; Land, S.J.; Lu, X.; Ruden, D.M. A program for annotating and predicting the effects of single nucleotide polymorphisms, SnpEff: SNPs in the genome of *Drosophila melanogaster* strain w1118; iso-2; iso-3. *Fly* **2012**, *6*, 80–92. [[CrossRef](#)] [[PubMed](#)]
15. Robinson, J.T.; Thorvaldsdóttir, H.; Wenger, A.M.; Zehir, A.; Mesirov, J.P. Variant review with the integrative genomics viewer. *Cancer Res.* **2017**, *77*, e31–e34. [[CrossRef](#)]
16. Choi, Y.; Chan, A.P. PROVEAN web server: A tool to predict the functional effect of amino acid substitutions and indels. *Bioinformatics* **2015**, *31*, 2745–2747. [[CrossRef](#)] [[PubMed](#)]
17. Bendl, J.; Stourac, J.; Salanda, O.; Pavelka, A.; Wieben, E.D.; Zendulka, J.; Brezovsky, J.; Damborsky, J. PredictSNP: Robust and Accurate Consensus Classifier for Prediction of Disease-Related Mutations. *PLoS Comput. Biol.* **2014**, *10*. [[CrossRef](#)] [[PubMed](#)]
18. Kingsmore, S.F.; Cakici, J.A.; Clark, M.M.; Gaughran, M.; Feddock, M.; Batalov, S.; Bainbridge, M.N.; Carroll, J.; Caylor, S.A.; Clarke, C.; et al. A Randomized, Controlled Trial of the Analytic and Diagnostic Performance of Singleton and Trio, Rapid Genome and Exome Sequencing in Ill Infants. *Am. J. Hum. Genet.* **2019**, *105*, 719–733. [[CrossRef](#)] [[PubMed](#)]

19. Takenouchi, T.; Shimizu, A.; Torii, C.; Kosaki, R.; Takahashi, T.; Saya, H.; Kosaki, K. Multiple café au lait spots in familial patients with *MAP2K2* mutation. *Am. J. Med. Genet. Part A* **2014**, *164*, 392–396. [[CrossRef](#)]
20. Tajan, M.; Paccoud, R.; Branka, S.; Edouard, T.; Yart, A. The RASopathy family: Consequences of germline activation of the RAS/MAPK pathway. *Endocr. Rev.* **2018**, *39*, 676–700. [[CrossRef](#)]
21. Santarpia, L.; Lippman, S.M.; El-Naggar, A.K. Targeting the MAPK–RAS–RAF signaling pathway in cancer therapy. *Expert Opin. Ther. Targets* **2012**, *16*, 103–119. [[CrossRef](#)] [[PubMed](#)]
22. Upadhyaya, M.; Majounie, E.; Thompson, P.; Han, S.; Consoli, C.; Krawczak, M.; Cordeiro, I.; Cooper, D.N. Three different pathological lesions in the *NF1* gene originating de novo in a family with neurofibromatosis type 1. *Hum. Genet.* **2003**, *112*, 12–17. [[CrossRef](#)] [[PubMed](#)]
23. Tartaglia, M.; Kalidas, K.; Shaw, A.; Song, X.; Musat, D.L.; Van der Burgt, I.; Brunner, H.G.; Bertola, D.R.; Crosby, A.; Ion, A.; et al. *PTPN11* mutations in noonan syndrome: Molecular spectrum, genotype-phenotype correlation, and phenotypic heterogeneity. *Am. J. Hum. Genet.* **2002**, *70*, 1555–1563. [[CrossRef](#)] [[PubMed](#)]
24. Kalidas, K.; Shaw, A.C.; Crosby, A.H.; Newbury-Ecob, R.; Greenhalgh, L.; Temple, I.K.; Law, C.; Patel, A.; Patton, M.A.; Jeffery, S. Genetic heterogeneity in LEOPARD syndrome: Two families with no mutations in *PTPN11*. *J. Hum. Genet.* **2005**, *50*, 21–25. [[CrossRef](#)] [[PubMed](#)]
25. Kerr, B.; Allanson, J.; Delrue, M.A.; Gripp, K.W.; Lacombe, D.; Lin, A.E.; Rauen, K.A. The diagnosis of Costello syndrome: Nomenclature in Ras/MAPK pathway disorders. *Am. J. Med. Genet. A* **2008**, *146A*, 1218–1220. [[CrossRef](#)]
26. Rauen, K.A.; Tidyman, W.E.; Estep, A.L.; Sampath, S.; Peltier, H.M.; Bale, S.J.; Lacassie, Y. Molecular and functional analysis of a novel *MEK2* mutation in cardio-facio-cutaneous syndrome: Transmission through four generations. *Am. J. Med. Genet. A* **2010**, *152A*, 807–814. [[CrossRef](#)]
27. Niihori, T.; Aoki, Y.; Narumi, Y.; Neri, G.; Cavé, H.; Verloes, A.; Okamoto, N.; Hennekam, R.C.M.; Gillissen-Kaesbach, G.; Wieczorek, D.; et al. Germline *KRAS* and *BRAF* mutations in cardio-facio-cutaneous syndrome. *Nat. Genet.* **2006**, *38*, 294–296. [[CrossRef](#)]
28. Rodriguez-Viciana, P.; Tetsu, O.; Tidyman, W.E.; Estep, A.L.; Conger, B.A.; Cruz, M.S.; McCormick, F.; Rauen, K.A. Germline mutations in genes within the MAPK pathway cause cardio-facio-cutaneous syndrome. *Science* **2006**, *311*, 1287–1290. [[CrossRef](#)]
29. Gentile, A.; Bolcato, M.; Militerno, G.; Rademacher, G.; Desrochers, A.; Grandis, A. Heterotopy (“Error loci”) of the spiral loop of the ascending colon in cattle. *PLoS ONE* **2019**, *14*. [[CrossRef](#)]
30. Salehi Karlslätt, K.; Pettersson, M.; Jäntti, N.; Szafranski, P.; Wester, T.; Husberg, B.; Ullberg, U.; Stankiewicz, P.; Nordgren, A.; Lundin, J.; et al. Rare copy number variants contribute pathogenic alleles in patients with intestinal malrotation. *Mol. Genet. Genomic Med.* **2019**, *7*, 1–9. [[CrossRef](#)]
31. Fagerberg, L.; Hallström, B.M.; Oksvold, P.; Kampf, C.; Djureinovic, D.; Odeberg, J.; Habuka, M.; Tahmasebpoor, S.; Danielsson, A.; Edlund, K.; et al. Analysis of the human tissue-specific expression by genome-wide integration of transcriptomics and antibody-based proteomics. *Mol. Cell. Proteomics* **2014**, *13*, 397–406. [[CrossRef](#)]
32. Yue, F.; Cheng, Y.; Breschi, A.; Vierstra, J.; Wu, W.; Ryba, T.; Sandstrom, R.; Ma, Z.; Davis, C.; Pope, B.D.; et al. A comparative encyclopedia of DNA elements in the mouse genome. *Nature* **2014**, *515*, 355–364. [[CrossRef](#)]
33. Dentici, M.L.; Sarkozy, A.; Pantaleoni, F.; Carta, C.; Lepri, F.; Ferese, R.; Cordeddu, V.; Martinelli, S.; Briuglia, S.; Digilio, M.C.; et al. Spectrum of *MEK1* and *MEK2* gene mutations in cardio-facio-cutaneous syndrome and genotype-phenotype correlations. *Eur. J. Hum. Genet.* **2009**, *17*, 733–740. [[CrossRef](#)] [[PubMed](#)]
34. Anastasaki, C.; Estep, A.L.; Marais, R.; Rauen, K.A.; Patton, E.E. Kinase-activating and kinase-impaired cardio-facio-cutaneous syndrome alleles have activity during zebrafish development and are sensitive to small molecule inhibitors. *Hum. Mol. Genet.* **2009**, *18*, 2543–2554. [[CrossRef](#)] [[PubMed](#)]

4.1.1.5 *KDM2B*-associated paunch calf syndrome in Marchigiana cattle

Journal: Journal of Veterinary Internal Medicine
Manuscript status: published
Contributions: Figures, writing original draft and revisions
Displayed version: Published version
DOI: [10.1111/jvim.15789](https://doi.org/10.1111/jvim.15789)

KDM2B-associated paunch calf syndrome in Marchigiana cattle

Leonardo Murgiano¹ | Gianfranco Militerno² | Fiorella Sbarra³ |
Cord Drögemüller⁴ | Joana G. P. Jacinto² | Arcangelo Gentile²  | Marilena Bolcato²

¹Department of Clinical Sciences & Advanced Medicine, University of Pennsylvania, Philadelphia, Pennsylvania, USA

²Department of Veterinary Medical Sciences, University of Bologna, Bologna, Italy

³National Association of Italian Beef-Cattle Breeders, Perugia, Italy

⁴Institute of Genetics, Vetsuisse Faculty, University of Bern, Bern, Switzerland

Correspondence

Joana G. P. Jacinto, Department of Veterinary Medical Sciences, University of Bologna, Via Tolara di Sopra, 50-40064 Ozzano dell'Emilia (Bologna), Italy.

Email: joana.goncalves2@studio.unibo.it

Abstract

Background: Chianina, Romagnola, and Marchigiana are the 3 most important Italian breeds of cattle raised in the Apennine Mountains. Inherited disorders have been reported in the Chianina and Romagnola breeds but not in the Marchigiana breed. Recently, a case resembling recessively inherited *KDM2B*-associated paunch calf syndrome (PCS) in Romagnola cattle was identified in Marchigiana cattle.

Hypothesis/Objectives: To characterize the features of the observed congenital anomaly, evaluate its possible genetic etiology, and determine the prevalence of the deleterious allele in the Marchigiana population.

Animals: A single stillborn Marchigiana calf was referred for clinicopathological examination because of the presence of PCS-like morphological lesions.

Methods: The animal was necropsied and the calf and its parents were genotyped. A PCR-based direct gene test was applied to determine the *KDM2B* genotype and 114 Marchigiana bulls were genotyped.

Results: The pathological phenotype included facial deformities, enlarged fluid-filled abdomen, and hepatic fibrosis. The affected animal was the offspring of consanguineous mating and homozygous presence of the *KDM2B* missense variant was confirmed. Both parents were heterozygous for *KDM2B* and the prevalence of carriers in a selected population of Marchigiana bulls was <2%.

Conclusions and Clinical Importance: The characteristic malformations and genetic findings were consistent with the diagnosis of PCS and provide evidence that the deleterious *KDM2B* variant initially detected in Romagnola cattle also occurs in the Marchigiana breed.

KEYWORDS

bovine, genetic diseases, introgression, PCS

1 | INTRODUCTION

Chianina, Marchigiana, and Romagnola are the 3 most common Italian cattle breeds in the central part of the Apennine Mountains. Although

used in the past mainly as draft animals, in recent decades they have been included in intensive selective breeding programs to increase their use for beef production.¹⁻³ While pursuing improvement in the performance traits, it also is important to limit the undesirable collateral effects of inbreeding because the accumulation of harmful alleles may lead to emergence of recessively inherited disorders. Many such disorders have been cataloged in the Online Mendelian Inheritance in

Abbreviations: AI, artificial insemination; OMIA, Online Mendelian Inheritance in Animals; PCS, paunch calf syndrome; PMT, congenital pseudomyotonia.

This is an open access article under the terms of the Creative Commons Attribution License, which permits use, distribution and reproduction in any medium, provided the original work is properly cited.

© 2020 The Authors. *Journal of Veterinary Internal Medicine* published by Wiley Periodicals, Inc. on behalf of the American College of Veterinary Internal Medicine.

Animals (OMIA) database,⁴ and identification of recessive pathogenic variants allows targeted genotyping and the avoidance of high-risk matings of carrier animals.⁵ Although many are unknown and routine screenings are not performed, recessive variants can quickly spread through a population by widespread use of popular carrier bulls in artificial insemination (AI). This practice led to the appearance of worrisome pathogenic variants in the Chianina and Romagnola breeds.⁶⁻¹⁰

In Chianina cattle, the c.491G>A missense variant in the *ATP2A1* gene, encoding the SERCA1 pump, was reported to cause autosomal recessive pseudomyotonia (PMT), a congenital muscle function disorder (OMIA 001464-9913).⁹ Among the ranked Chianina sires in the years 2007 to 2011, the prevalence of heterozygous PMT carriers was 13.6%, illustrating the scale of the problem.¹¹ Subsequently, *ATP2A1*-associated PMT also was reported in the Romagnola breed associated with allelic heterogeneity of the *ATP2A1* gene.¹⁰ In addition to the previously reported c.491G>A missense variant originating from accidental introgression of a Chianina PMT carrier, 2 additional rare *ATP2A1* missense variants (c.632G>T and c.857G>T) also were found to be causative for the disorder.¹⁰

Ichthyosis fetalis caused by a missense variant in the *ABCA12* gene (harlequin ichthyosis; OMIA 002238-9913) is another lethal recessively inherited disorder that occurs in the Chianina breed.¹² A less severe form of congenital ichthyosis also was reported in Chianina cattle, but no causative genetic variant thus far has been found.¹³ More recently, rare recessively inherited congenital bilateral immature nuclear cataracts have been found in Romagnola cattle (OMIA 001936-9913) and are associated with a large deletion affecting the coding region of the *NID1* gene.¹⁴ Previously, an outbreak of a lethal multiorgan developmental dysplasia was described in 65 Romagnola cattle (OMIA 001722-9913) and determined to be caused by a c.2503G>A missense variant in the *KDM2B* gene.^{6,7} On the basis of the phenotype, this disorder was named "paunch calf syndrome" (PCS). Affected calves usually are stillborn or die within hours of delivery.^{6,7} The *KDM2B* gene encodes a histone demethylase that acts as an important transcription regulator affecting organ development and cell differentiation. The disease-associated variant leads to an amino acid exchange in a highly conserved domain, thus explaining the phenotypic effect of the genetic variant.⁷ The PCS phenotype mainly is characterized by facial dysplasia, an enlarged and pendulous abdomen ("paunch") with considerable abdominal effusion and hepatic fibrosis.^{6,7} Additional lesions, such as cleft palate, lack of the medial dew claws of ≥ 1 limbs, SC edema, perihepatic cysts, and cardiac malformations are found in some cases.^{6,7} Moreover, after identifying its molecular cause, results of a subsequent survey on the prevalence of carriers for PCS in the Romagnola breed were concerning. The prevalence of PCS carriers among top-ranked Romagnola sires over the years 2007 to 2012 was 29.3%, and even higher (30.9%) among young males selected for performance testing.¹⁵

Recently, a Marchigiana calf with a complex congenital malformation phenotype resembling PCS of Romagnola cattle was presented for examination. Our aim was to describe the clinicopathological phenotype associated with the inherited disorder of *KDM2B* causing this disease entity in Marchigiana cattle.

2 | MATERIALS AND METHODS

A full-term stillborn, 55 kg, male Marchigiana calf delivered after dystocia was referred to the teaching hospital of the Department of Veterinary Medical Sciences of the University of Bologna for evaluation of multiple congenital malformations.

A complete phenotype study was performed. Representative samples from the liver were collected, fixed in 10% buffered formalin, embedded in paraffin, and processed for histological examination. Five-micron histological sections of the liver were stained with hematoxylin and eosin, Masson's trichrome and rhodanine, and specific immunohistochemical methods, using the streptavidin-biotin peroxidase technique, including vimentin (VIM; dilution 1:100; Dako, Glostrup, Denmark) and α -smooth muscle actin (α -SMA; dilution 1:100; Dako) were applied to formalin-fixed liver samples.

Additionally, a pedigree analysis of the affected calf was performed. We harvested cutaneous tissue from the calf, as well as EDTA blood from its parents. Desoxyribonucleic acid was extracted and the 3 subjects were genotyped for the c.2503G>A variant in the *KDM2B* gene, as previously described⁷ and implicated in PCS in Romagnola cattle.⁷ Furthermore, 114 samples were collected for *KDM2B* genotyping, including semen samples from 87 Marchigiana adult bulls that were classified as suitable for reproduction and an additional 27 EDTA blood samples from young males selected for performance testing.

3 | RESULTS

3.1 | Clinical phenotype

The affected calf had an enlarged head caused by a SC swelling that was especially evident in the periocular and the submandibular regions. The splanchnocranium was shortened and the frontal region asymmetric. The tongue was swollen and protruded from the mouth. The eyes were enlarged with evident scleral injection and conjunctival



FIGURE 1 Stillborn Marchigiana calf showing multiple congenital anomalies. Note the shortened face and distended ventral abdomen resembling paunch calf syndrome reported in Romagnola cattle. Note the swollen hind legs and the right fetlock externally rotated

edema. The ventro-abdominal region was enlarged and pendulous and generalized swelling was noticed. The hind legs also were swollen and the right fetlock was externally rotated (Figure 1).

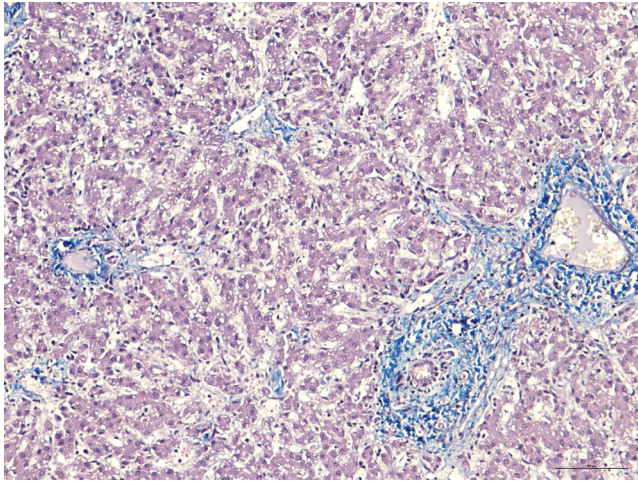


FIGURE 2 Histological section from the liver of the stillborn Marchigiana calf. Note the slight to moderate fibrosis in the portal fields and, in some cases, around the central space of the liver lobule. The fibrosis, characterized by the formation of thin portal-portal and portal-central fibrotic septa, extends, in some lobules, to the perisinusoidal spaces. There are many enlarged sinusoids and cellular hepatic degeneration, possibly due to autolysis phenomena. Masson's trichrome, bar = 100 μ m

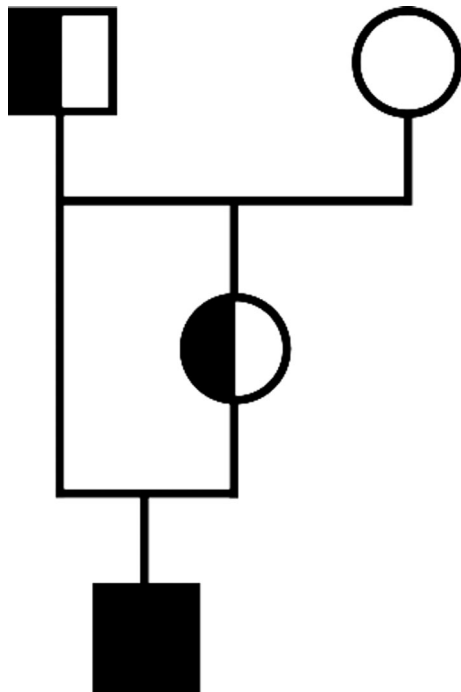


FIGURE 3 Pedigree of the stillborn Marchigiana calf. Note the inbreeding loop and the homozygous genotype of the case related to the pathogenic *KDM2B* variant (black symbol) and the half-filled symbols showing the parents as carriers

3.2 | Pathological phenotype

The swellings were caused by generalized SC infiltration of sero-anguineous fluid, as evidenced at necropsy. Similar fluid collection also was present in the peritoneal, pleural, and pericardial cavities.

The liver was larger than normal, with an irregular surface and firm consistency. Upon sectioning, the cut surface of the liver had numerous bands of whitish, collagenous connective tissue, and a lobular structure partitioned by fibrous septa, which also were visible inside the lobules. Two round 5-mm diameter cysts, containing reddish fluid, were present on the peritoneal surface of the left lobe of the liver.

Histopathology identified extensive distortion of the lobular architecture by slight to moderate fibrosis in the portal fields and, in some cases, around the central space of the liver lobule (hematoxylin and eosin staining). The fibrosis was more evident in sections stained with Masson's trichrome, and was characterized by the formation of thin portal-portal and portal-central fibrotic septa. In some lobules, fibrosis extended to the perisinusoidal spaces. Fusiform cells were observed in the inner wall of the sinusoids. Enlarged sinusoids, cellular hepatic degeneration or atrophy, and capsular fibrotic thickening were detected. No copper deposits responsible for fibrogenesis were detected on rhodanine staining. Immunohistochemical examination (vimentin and α -smooth muscle actin) identified slight immunoreactivity for laminin intermediate filaments. The fusiform cells, positive using antivimentin and anti- α -smooth muscle actin antibodies and observed within the sinusoids in fibrotic areas, were considered myofibroblasts actively involved in fibrogenesis (Figure 2). Histopathologically, cysts had an inner wall lined by a single layer of cuboidal biliary epithelium and were considered to represent bile duct dilatation associated with fibrosis.

3.3 | Genetic analysis

Pedigree analysis of the stillborn Marchigiana calf disclosed the presence of a consanguineous mating, because the sire of the affected calf was also the sire of its dam (Figure 3). In light of this inbreeding, autosomal recessive inheritance seemed a likely explanation for the occurrence of the congenital anomaly. The homozygous presence of the *KDM2B* variant subsequently was confirmed in the affected animal, and both parents were confirmed as heterozygous carriers of this deleterious allele. Evaluation of the prevalence of this pathogenic variant in Marchigiana cattle identified a frequency of 1.75% (2 of the 114 tested bulls were heterozygous carriers).

4 | DISCUSSION

The clinical and pathological findings described in the calf of our study completely overlapped with the phenotype reported for PCS of the Romagnola breed. Therefore, our report constitutes the first description of a *KDM2B* homozygous mutant case of PCS in Marchigiana

cattle, confirming an identical genetic etiology for a disorder that has been known to exist for many years in Romagnola cattle. It is possible that the origin of this rare disease-causing *KDM2B* variant in Marchigiana breed is based on either accidental crossbreeding or targeted introgression of Romagnola cattle. In the available pedigree data for the presented case, no indication of cattle other than the Marchigiana breed was found. Present day Marchigiana cattle are derived from Podolian cattle, a stock typical of the Italian Marche region that originated in the region of Podolia in present day Ukraine. The breed was introduced to Italy after the fall of the Roman Empire and in the past was used for draft work. In the late 19th and early 20th centuries, the Marchigiana breed was improved first by crossing with the Chianina breed and successively by further crossing with the Romagnola breed (also deriving from Podolian cattle). Since the 1930s, the breed has undergone appropriate breeding strategy that has directed it toward beef production, resulting in 1 of the most competitive beef breeds in Italy that also is exported throughout the world.¹

Unfortunately, no information is available to determine when the PCS-associated *KDM2B* variant was introduced into the Marchigiana breed. In fact, it cannot be excluded that the variant already was present before the Marchigiana breed was established as distinct breed, and therefore it may represent the identical variant as in the Romagnola breed. To the best of our knowledge, no other cases have been reported, and it is possible that the frequency of the deleterious allele is very low.

This speculation was confirmed by the genotyping of 114 bulls used for AI. Nevertheless, additional data might be useful to make a more precise estimate. For this purpose, DNA isolated from skin biopsy samples or semen should be used to determine the individual's genotype without concern about cattle-specific leukochimerism possibly causing a false genotype.¹⁶ The occurrence of the PCS-causing variant in another historically related breed is similar to what we have observed before in PMT-affected Romagnola cattle, carrying the same disease-causing allele previously detected in the Chianina breed.¹⁰

Compared to the substantial allele frequencies of the PCS variants in Romagnola cattle (14.6% in top-ranked sires and 15.4% in young bull calves),¹⁵ the low prevalence (<2%) suggests that the variant is not widespread within the Marchigiana population. The observed phenotype in the affected stillborn Marchigiana calf differs somewhat from the PCS cases in Romagnola cattle reported previously,^{6,7} specially the swollen hind limbs and rotated right fetlock. Nonetheless, the most striking features of the disorder such as the short face, pendulous abdomen, serosanguineous fluid in the abdominal cavity, and hepatic fibrosis strongly resemble the previously described PCS phenotype. The observed differences may have reflected the different genetic background of Marchigiana breed.

Our report serves to alert breeders of Marchigiana cattle about the possible emergence of PCS in the future and will permit the avoidance of carrier matings by systematic genetic testing of potential sires.

ACKNOWLEDGMENTS

The data reported in this work are classified and stored in the tissue bank of the Institute of Genetics, Vetsuisse Faculty, University of

Bern. Data concerning the genotyping of the specific bulls are property of the breeding association.

CONFLICTS OF INTERESTS DECLARATION

Authors declare no conflict of interests.

OFF-LABEL ANTIMICROBIAL DECLARATION

Authors declare no off-label use of antimicrobials.

INSTITUTIONAL ANIMAL CARE AND USE COMMITTEE (IACUC) OR OTHER APPROVAL DECLARATION

This study was not based on an invasive animal experiment and used a naturally occurring case, therefore there are no associated permit numbers. The blood used for the genetic analysis derives from samples obtained for sanitary controls or for other reasons not related to this investigation. The investigation cannot be considered including "animal experiment" according to the exemptions contemplated by the Italian legislative decree n. 26/2014 (Dir. 2010/63/UE on the protection of animals used for scientific purposes).

HUMAN ETHICS APPROVAL DECLARATION

Authors declare human ethics approval was not needed for this study.

ORCID

Arcangelo Gentile  <https://orcid.org/0000-0002-6091-8978>

REFERENCES

1. ANABIC, Associazione Nazionale Allevatori Bovini Italiani da Carne. <http://www.anabic.it/index1.htm>. Accessed December 11, 2019.
2. Dalvit C, De Marchi M, Dal Zotto R, Gervaso M, Meuwissen T, Cassandro M. Breed assignment test in four Italian beef cattle breeds. *Meat Sci.* 2008;80(2):389-395.
3. Sbarra F, Mantovani R, Quaglia A, Bittante G. Genetics of slaughter precocity, carcass weight, and carcass weight gain in Chianina, Marchigiana, and Romagnola young bulls under protected geographical indication. *J Anim Sci.* 2013;91(6):2596-2604.
4. Nicholas FW, Hobbs M. Mutation discovery for Mendelian traits in non-laboratory animals: a review of achievements up to 2012. *Anim Genet.* 2014;45:157-170.
5. Cole JB. A simple strategy for managing many recessive disorders in a dairy cattle breeding program. *Genet Sel Evol.* 2015;47:94.
6. Testoni S, Militerno G, Rossi M, Gentile A. Congenital facial deformities, ascites and hepatic fibrosis in Romagnola calves. *Vet Rec.* 2009;164(22):693-694.
7. Testoni S, Bartolone E, Rossi M, et al. *KDM2B* is implicated in bovine lethal multi-organic developmental dysplasia. *PLoS One.* 2012;7(9):e45634.
8. Yoshikawa H, Fukuda T, Oyama T, Yoshikawa T. Congenital hepatic fibrosis in a newborn calf. *Vet Pathol.* 2002;39:143-145.
9. Drögemüller C, Drögemüller M, Leeb T, et al. Identification of a missense mutation in the bovine *ATP2A1* gene in congenital pseudomyotonia of Chianina cattle: an animal model of human Brody disease. *Genomics.* 2008;92(6):474-477.
10. Murgiano L, Sacchetto R, Testoni S, et al. Pseudomyotonia in Romagnola cattle caused by novel *ATP2A1* mutations. *BMC Vet Res.* 2012;8:186.
11. Murgiano L, Testoni S, Drögemüller C, Bolcato M, Gentile A. Frequency of bovine congenital pseudomyotonia carriers in selected Italian Chianina sires. *Vet J.* 2013;195(2):238-240.

12. Charlier C, Coppieters W, Rollin F, et al. Highly effective SNP-based association mapping and management of recessive defects in livestock. *Nat Genet.* 2008;40(4):449-454.
13. Testoni S, Zappulli V, Gentile A. Ichthyosis in two Chianina calves. *Dtsch Tierarztl Wochenschr.* 2006;113(9):351-354.
14. Murgiano L, Jagannathan V, Calderoni V, Joechler M, Gentile A, Drögemüller C. Looking the cow in the eye: deletion in the NID1 gene is associated with recessive inherited cataract in Romagnola cattle. *PLoS One.* 2014;27(10):9.
15. Murgiano L, Drögemüller C, Sbarra F, Bolcato M, Gentile A. Prevalence of paunch calf syndrome carriers in Italian Romagnola cattle. *Vet J.* 2013;200(3):459-461.
16. Ryncarz RE, Dietz AB, Kehrl ME Jr. Recognition of leukochimerism during genotyping for bovine leukocyte adhesion deficiency (BLAD) by polymerase-chain-reaction-amplified DNA extracted from blood. *J Vet Diagn Invest.* 1995;7(4):569-572.

How to cite this article: Murgiano L, Militerno G, Sbarra F, et al. *KDM2B-associated paunch calf syndrome in Marchigiana cattle.* *J Vet Intern Med.* 2020;34:1657-1661. <https://doi.org/10.1111/jvim.15789>

4.1.2 Neuromuscular disorders

- **Congenital neuromuscular channelopathy:** *“KCNG1-related syndromic form of congenital neuromuscular channelopathy in a crossbred calf”*, Genes, 2021, 12, pp. 1 – 12 ([see chapter 4.1.2.1](#))

4.1.2.1 *KCNQ1*-related syndromic form of congenital neuromuscular channelopathy in a crossbred calf

Journal: genes

Manuscript status: published

Contributions: phenotype description, whole-genome sequencing data analysis, figures, writing original draft and revisions

Displayed version: published version

DOI: [10.3390/genes12111792](https://doi.org/10.3390/genes12111792)

Article

KCNQ1-Related Syndromic Form of Congenital Neuromuscular Channelopathy in a Crossbred Calf

Joana G. P. Jacinto ^{1,2} , Irene M. Häfliger ² , Eylem Emek Akyürek ³, Roberta Sacchetto ³, Cinzia Benazzi ¹ , Arcangelo Gentile ¹  and Cord Drögemüller ^{2,*} 

- ¹ Department of Veterinary Medical Sciences, University of Bologna, 40064 Ozzano Emilia, Italy; joana.goncalves2@studio.unibo.it (J.G.P.J.); cinzia.benazzi@unibo.it (C.B.); arcangelo.gentile@unibo.it (A.G.)
- ² Institute of Genetics, Vetsuisse Faculty, University of Bern, 3012 Bern, Switzerland; irene.haefliger@vetsuisse.unibe.ch
- ³ Department of Comparative Biomedicine and Food Science, University of Padova, 35020 Legnaro, Italy; eylememek.akyurek@phd.unipd.it (E.E.A.); roberta.sacchetto@unipd.it (R.S.)
- * Correspondence: cord.droegemueller@vetsuisse.unibe.ch

Abstract: Inherited channelopathies are a clinically and heritably heterogeneous group of disorders that result from ion channel dysfunction. The aim of this study was to characterize the clinico-pathologic features of a Belgian Blue x Holstein crossbred calf with paradoxical myotonia congenita, craniofacial dysmorphism, and myelodysplasia, and to identify the most likely genetic etiology. The calf displayed episodes of exercise-induced generalized myotonic muscle stiffness accompanied by increase in serum potassium. It also showed slight flattening of the splanchnocranium with deviation to the right side. On gross pathology, myelodysplasia (hydrosyringomyelia and segmental hypoplasia) in the lumbosacral intumescence region was noticed. Histopathology of the muscle profile revealed loss of the main shape in 5.3% of muscle fibers. Whole-genome sequencing revealed a heterozygous missense variant in *KCNQ1* affecting an evolutionary conserved residue (p.Trp416Cys). The mutation was predicted to be deleterious and to alter the pore helix of the ion transport domain of the transmembrane protein. The identified variant was present only in the affected calf and not seen in more than 5200 other sequenced bovine genomes. We speculate that the mutation occurred either as a parental germline mutation or post-zygotically in the developing embryo. This study implicates an important role for *KCNQ1* as a member of the potassium voltage-gated channel group in neurodegeneration. Providing the first possible *KCNQ1*-related disease model, we have, therefore, identified a new potential candidate for related conditions both in animals and in humans. This study illustrates the enormous potential of phenotypically well-studied spontaneous mutants in domestic animals to provide new insights into the function of individual genes.

Keywords: cattle; channelopathy; skeletal muscle; neuromuscular disorder; paradoxical myotonia congenita; potassium voltage-gated channel; precision medicine; hydrosyringomyelia; craniofacial dysmorphism



Citation: Jacinto, J.G.P.; Häfliger, I.M.; Akyürek, E.E.; Sacchetto, R.; Benazzi, C.; Gentile, A.; Drögemüller, C. *KCNQ1*-Related Syndromic Form of Congenital Neuromuscular Channelopathy in a Crossbred Calf. *Genes* **2021**, *12*, 1792. <https://doi.org/10.3390/genes12111792>

Academic Editor: Emilia Bagnicka

Received: 18 October 2021

Accepted: 10 November 2021

Published: 12 November 2021

Publisher's Note: MDPI stays neutral with regard to jurisdictional claims in published maps and institutional affiliations.



Copyright: © 2021 by the authors. Licensee MDPI, Basel, Switzerland. This article is an open access article distributed under the terms and conditions of the Creative Commons Attribution (CC BY) license (<https://creativecommons.org/licenses/by/4.0/>).

1. Introduction

Inherited channelopathies represent a clinically and heritably heterogeneous group of genetic disorders that result from a ion channel dysfunction of all cellular plasma membranes and/or of cell organelles [1]. They usually follow a dominant inheritance [1].

Neuromuscular channelopathies can cause different diseases affecting the brain, spinal cord, peripheral nerve, and/or muscle [2]. In particular, those that lead to primary skeletal muscle diseases, the so-called skeletal muscle channelopathies, exhibit a clinical spectrum ranging from flaccid paralysis to myotonia, the latter defined as delayed relaxation of a muscle that has been voluntarily or reflexively contracted [3].

In human medicine, skeletal muscle channelopathies are associated with pathogenic variants in genes coding for ion channels that influence muscle excitability [1,4]. They

are subdivided into two types, periodic paralysis (PPs) and non-dystrophic myotonias (NDMs) [5].

Various forms of PPs are due to abnormal depolarization that inactivates sodium channels, causing decreased muscle excitability of the muscle membrane, often accompanied by changes in extracellular potassium. The main finding is the susceptibility to episodes of focal or generalized weakness and paralysis [1]. This group of channelopathies includes three conditions: (a) hypokalemic periodic paralysis (HypoPP); (b) hyperkalemic periodic paralysis (HyperPP); and (c) Andersen-Tawil syndrome. HypoPP is the most common PP in humans, characterized by episodes of flaccid muscle weakness associated with low serum potassium levels, lasting hours to days [6]. The attacks of flaccid paralysis typically occur after waking during the night or early morning. It is due to a dysfunction of calcium channels associated with heterozygous variants in *CACNA1S* [7] or to a dysfunction of sodium channels associated with heterozygous variants in *SCN4A* [8]. HyperPP is characterized by episodes of flaccid muscle weakness associated with elevated serum potassium levels and occasional myotonia lasting minutes to hours [2]. It is due to dysfunction of sodium channels also associated with mutations in *SCN4A* [9]. The Andersen-Tawil syndrome is characterized by the following clinical triad: periodic paralysis, cardiac manifestations, and abnormal physical features. It is due to dysfunction of potassium channels associated with variants in *KCNJ2* [2,10]. In veterinary medicine, a *SCN4A*-related equine form of HyperPP has been reported (OMIA 000785-9796) [11].

Various forms of NDMs are due to defects in the muscle fiber repolarization, resulting in muscle hyperexcitability and myotonic discharges [10]. The main findings are muscular stiffness, in the absence of severe fixed weakness or muscle wasting, and muscle hypertrophy [4]. NDMs encompasses three different disorders, defined as following: (a) myotonia congenita (MC); (b) paramyotonia congenita (PMC); and (c) Na channel myotonias [6]. MC is the most common skeletal muscle channelopathy in humans, characterized by stiffness especially during rapid movements after a period of rest (action myotonia), and improving with exercise (“warm-up phenomenon”) [3]. It is due to a dysfunction of chloride channels associated with dominant (Thomsen’s disease) or recessively (Becker’s disease) inherited mutations in *CLCN1* [12]. PMC is characterized by stiffness that, unlike MC, worsens with sustained exercise (exercise-induced or paradoxical myotonia) [6]. The symptoms last for seconds to minutes following the exercise. It is due to a dysfunction of sodium channels [13] also associated with heterozygous pathogenic variants in *SCN4A* [14]. There are several subtypes of sodium channel myotonia, such as acetazolamide-responsive myotonia, myotonia that develops approximately 10–20 min after exercise (*myotonia fluctans*) [15], and severe persistent myotonia associated with unique electromyographic pattern (*myotonia permanens*) [16]. Common to these subtypes is exacerbation by K (potassium-aggravated myotonias). Similarly to the PMC, they are all also associated with heterozygous pathogenic variants in *SCN4A* [14].

In veterinary medicine, forms of MC have been reported in horses (OMIA 000698-9796) [17], dogs (OMIA 000698-9615) [18], cats (OMIA 000698-9685) [19], sheep (OMIA 000698-9940) [20], and goats (OMIA 000698-9925) [21], associated with pathogenic variants in the orthologue *CLCN1* genes.

Altogether, it can be said that many clinicopathological similarities to *CLCN1*- and *SCN4A*-related human genetic diseases can be evidenced in veterinary pathology, highlighting the usefulness of translational research in the field of the congenital neuromuscular channelopathies. To our knowledge, no neuromuscular channelopathies have been reported in cattle. Therefore, with the present study we intended to characterize the clinical and pathological phenotype of a crossbred calf affected by congenital paradoxical myotonia, craniofacial dysmorphism, and myelodysplasia, and to find a possible genetic explanation after whole-genome sequencing (WGS).

2. Materials and Methods

2.1. Clinical and Pathological Investigation

A five-day-old male Belgian Blue x Holstein crossbred calf, weighting 47 kg, was admitted to the University of Bologna due to difficulty on quadrupedal stance and locomotion due to generalized muscle stiffness present since birth. The affected calf was clinically examined and a complete blood count (CBC), serum biochemical analysis, and venous blood gas analysis were obtained. Blood gas and serum biochemical analysis were performed at rest and after stimulation. Stimulation was the term used when the calf was in quadrupedal stance.

Nineteen days after hospitalization the calf showed a worsening of the general condition related to neuromuscular disease and was euthanized for welfare reasons. The calf was subsequently submitted for necropsy and histologic examination. Semimembranosus muscle was fixed in buffered neutral paraformaldehyde at 4 °C, washed in phosphate-buffered saline and de-hydrated through a graded series of ethanol. Samples embedded in paraffin were cut at 5 µm and stained with hematoxylin and eosin (H&E), or Azan–Mallory method, specific for detection of collagen fibers. Muscle sections were scanned with a semiautomatic microscope equipped (D-Sight v2, Menarini Diagnostics, Florence, Italy) with a computer. The average percentage of pathological muscle fibers was determined as the ratio of muscle fibers that lost their main shape and/or took a round shape to the total muscle fibers in the region. The spinal cord was fixed in 10% buffered formalin, embedded in paraffin, cut at 4 µm, and stained with hematoxylin and eosin (H&E), Periodic acid-Schiff (PAS), and Luxol-Fast-Blue for histological evaluation.

2.2. DNA Extraction, Whole-Genome Sequencing and Variant Calling

Genomic DNA was isolated from EDTA blood of the affected calf using a Promega Maxwell RSC DNA system (Promega, Dübendorf, Switzerland). Using genomic DNA from the affected calf, an individual PCR-free fragment library with approximately 400 bp inserts was created and sequenced on a NovaSeq6000 for 150 bp paired-end reads (Illumina, San Diego, CA, USA). The sequenced reads were aligned to the ARS-UCD1.2 reference genome, resulting in an average coverage of approximately 17.4× [22], and single-nucleotide variants (SNVs) and small indel variants were called. The applied software and steps to process fastq files into binary alignment map (BAM) and genomic variant call format (GVCF) files were in accordance with the processing guidelines of the 1000 Bull Genomes Project (run 7) [23], with the exception of trimming, which was performed with fastp [24]. Further processing of the genomic data was performed according to Häfliger et al. 2020 [25]. The effects of the above variants were functionally evaluated with snpeff v4.3 [26], using the NCBI Annotation Release 106 (https://www.ncbi.nlm.nih.gov/genome/annotation_euk/Bos_taurus/106/; accessed on 17 July 2021). This resulted in the final VCF file, containing individual variants and their functional annotations. To find private variants, we compared the genotypes of the case with 691 cattle genomes of different breeds sequenced as part of the ongoing Swiss Comparative Bovine Resequencing project. All of its data are available (Table S1; <https://www.ebi.ac.uk/ena/browser/view/PRJEB18113> accessed on 17 July 2021) in the European Nucleotide Archive (SAMEA7690196 is the sample accession number of the affected calf). Integrative Genomics Viewer (IGV) [27] software version 2.0 was used for visual evaluation of genome regions containing potential candidate genes.

2.3. Validation and Selection of Potential Candidate Variants

2.3.1. Occurrence of Variants in a Global Control Cohort

The comprehensive variant catalogue of run 9 of the 1000 Bull Genomes Project was available to investigate the allele distribution of variants within a global control cohort (www.1000bullgenomes.com; accessed on 17 July 2021) [23]. The whole data set includes 5116 cattle genomes including 576 from the Swiss Comparative Bovine Resequencing project, from a variety of breeds (>130 breeds indicated). Within the dataset, there are 9

purebred Belgian Blue and 1209 purebred Holstein cattle, allowing for the exclusion of common variants.

2.3.2. In Silico Assessment of the Molecular Consequences of Amino Acid Exchanges

Mutpred2 [28], PROVEAN [29] and PredictSNP1 [30] were used to predict the biological consequences of the detected missense variant. For cross-species sequence alignments, the following NCBI protein accessions were considered: NP_001192648.1 (*Bos taurus*), NP_002228.2 (*Homo sapiens*), XP_001168521.2 (*Pan troglodytes*), XP_543053.2 (*Canis lupus*), NP_001074603.1 (*Mus musculus*), NP_001100015.1 (*Rattus norvegicus*), XP_004947317.1 (*Gallus gallus*), and NP_001103880.1 (*Danio rerio*), NP_001096675.1 (*Xenopus tropicalis*).

2.4. Sequence Accessions

All references to the bovine *KCNG1* gene correspond to the NCBI accessions NC_037340.1 (chromosome 13, ARS-UCD1.2), NM_001205719.1 (*KCNG1* mRNA), and NP_001192648.1 (*KCNG1* protein). For the protein structure of *KCNG1* the Uniprot database (<https://www.uniprot.org/>; accessed on 17 July 2021) with accession number Q9UIX4 was used.

3. Results

3.1. Clinical Phenotype

On clinical examination at the time of admission, the calf was bright and alert but with generalized muscle stiffness that prevented it from spontaneously assuming and maintaining the quadrupedal stance.

At rest, the animal preferred the sternal recumbency, with the forelimbs folded under its chest while the hindlimbs were rigid and hyperextended (Figure 1a). It was not possible to flex the hindlimbs due to the muscle stiffness. If stimulated to stand the muscle stiffness increased inducing a rigid posture accompanied by spastic contractions that prevented him to acquire a definitive quadrupedal stance. On the contrary, if gently passively positioned, the calf was able to acquire and maintain the quadrupedal stance. In standing, the hind limbs were contracted and hyperextended, especially the right hindlimb that showed caudal stretching (Video S1). Additionally, the back was slightly arched, and the tail head elevated (Figure 1b). The thoracic girdle was also involved but less severely. On hooping and hoof replacement, the calf was unable to re-acquire the physiological position of the limbs/hoof. Unless supported, the calf was unable to walk or maintain the quadrupedal stance for long time. In fact, uncontrolled hypertonic postural reactions and muscular contractions resulted in loss of stance, with a fall in lateral recumbency. If not further stimulated and stressed, the stiffness slowly tended to decrease, enabling the calf to acquire the sternal recumbency. However, the hypertonia never disappeared completely. The cutaneous trunci reflex was increased in intensity as well as the withdrawal reflex of the forelimbs while in the hindlimbs the latter was absent. No abnormalities in the cranial nerves' reflexes, threat response, and pain perception were noticed.

The calf showed a slight flattening of the splanchnocranium with deviation to the right side. It displayed carpal and tarsal skin lesions due to permanent recumbency. Moreover, the animal presented diarrhea.

CBC revealed moderate leukocytosis ($23,650/\text{mm}^3$) with neutrophilia ($14,280/\text{mm}^3$) and monocytosis ($2400/\text{mm}^3$). Serum biochemical profile after stimulation showed increase in: creatinine kinase, lactate dehydrogenase (LDH), L-lactate, potassium (K^+), and calcium (Ca^{2+}) (Table 1).

Based on the clinical findings, the calf was suspected of suffering from a form of paradoxical myotonia congenita and/or from a spinal cord lesion associated with craniofacial dysmorphism.



Figure 1. Crossbred calf with a congenital neuromuscular disorder characterized by paradoxical myotonia congenita and myelodysplasia. (a) Sternal recumbency at rest. Note that the calf sustains the forelimbs folded underneath its chest while the hindlimbs are hyperextended. (b) Quadrupedal stance after passive positioning. Note that the pelvic girdle appears to be more affected with a marked hyperextension of the hindlimbs, the back is slightly arched, and the tail head is elevated. The thoracic girdle was affected with the forelimbs' hooves resting on tip.

Table 1. Results of altered parameters of serum biochemical profiles of the affected calf at rest and after stimulation.

Parameter	At Rest	After Stimulation	Unit of Measure
Creatinine kinase (CK)	147	329	IU/L
Lactate dehydrogenase (LDH)	1975	2556	IU/L
L-lactate	1	3.8	mmol/L
Potassium (K ⁺)	3.6	4.3	mmol/L
Calcium (Ca ²⁺)	0.99	1.14	mmol/L

3.2. Pathological Phenotype

At gross pathology, the examination of central nervous system revealed narrowing of the spinal cord (myelodysplasia) between lumbar spinal nerves IV and VI associated with hydrosyringomyelia between lumbar spinal nerves III and V with the larger cavity at the level of lumbar spinal nerve IV (Figure 2a,b). Macroscopically, the muscles were normal.

Microscopically, at lumbar spinal nerves III to V there were two cavities with only the larger partially lined by ependymal cells (hydrosyringomyelia) (Figure 2c). Vasogenic and intramyelinic edemas were present in the areas around the cavities, characterized as multiple fluid-filled clear extracellular spaces in the gray matter. Around the capillaries near the smaller channel, there was neutrophilic and lymphoid inflammatory cells. The astrocytes in the white matter showed foci of chromatin margination.

Routinely morphological (hematoxylin-eosin) analysis was used for histopathological evaluation on semimembranosus muscle biopsy sections. Muscle parenchyma showed normal fibers distribution. (Figure 3a). Nevertheless, some fibers appeared round shaped (Figure 3c) and most of them exhibited an enlarged cross-sectional area (Figure 3d). It was determined that the average percentage of pathological muscle fibers was 5.3%. A possible presence of fibrosis was determined by Azan–Mallory staining (Figure 3b). No signs of fibrosis were found in the sections obtained from the tissue. Infiltrated inflammatory mononuclear cells were not revealed by histological analysis of the muscle.

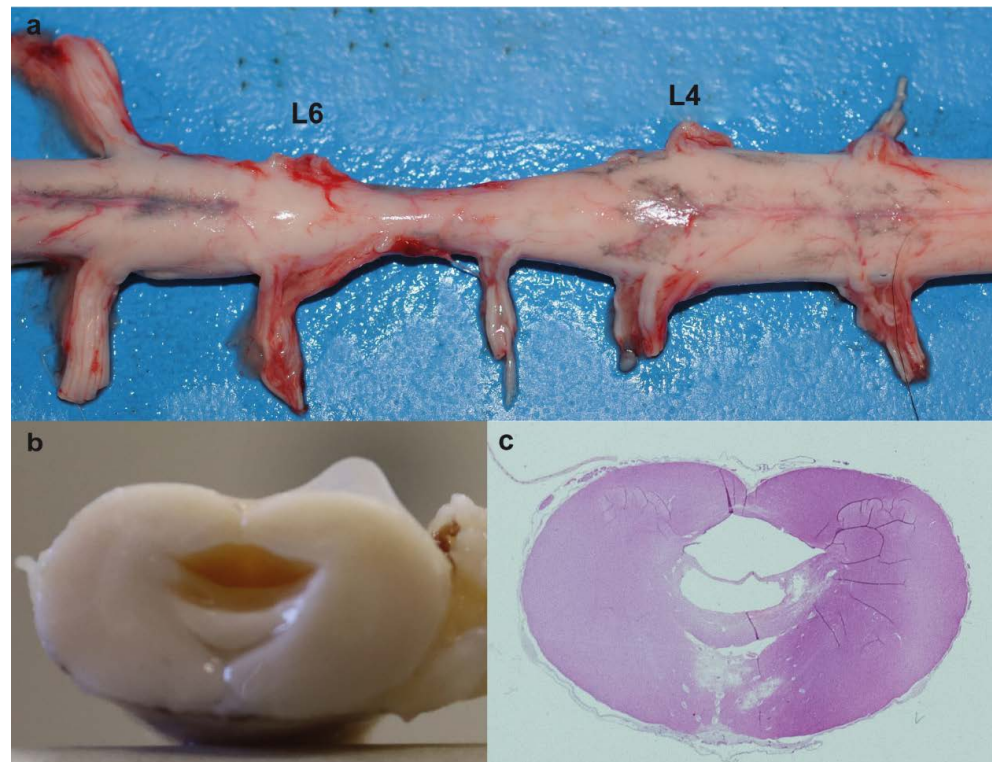


Figure 2. Myelodysplasia associated with hydrosyringomyelia in the affected calf. (a) Note the narrowing of the spinal cord between lumbar spinal nerves IV (L4) and VI (L6) (myelodysplasia). (b) Transversal section of the spinal cord between lumbar spinal nerve V (L5) and VI (L6). Note the cavity formed within the spinal cord. (c) Histological section of (b). Note that there are two cavities with only the larger partially lined by ependymal cells (hydrosyringomyelia). hematoxylin and eosin (H&E) staining.

3.3. Genetic Analysis

Assuming spontaneous mutation as the cause of this congenital neuromuscular condition, the WGS data were filtered for heterozygous coding variants that were present in the calf and were absent in the 691 available cattle genomes of different breeds. Thereby, 151 variants with a predicted high or moderate impact were identified (Table 2). In a second step, these variants were analyzed for their occurrence in a global cohort of 4540 genomes from a variety of breeds. This revealed 27 remaining protein-changing variants that are exclusively heterozygous in the affected calf and absent in all controls. These 27 variants were then visually inspected using the IGV software (Broad institute, Cambridge, MA, USA), which confirmed 25 as true variants (Tables 2 and S2).

Table 2. Results of whole-genome sequencing variant filtering of the calf affected by paramyotonia congenita and myelodysplasia.

Filtering Step	Homozygous Variants	Heterozygous Variants
All variants	2,562,043	5,168,233
Private variants	3580	21,104
Protein-changing private variants using 691 cattle genome controls	12	115
Remaining protein-changing private variants using a global control cohort of 4540 cattle genomes and subsequent IGV inspection	0	25

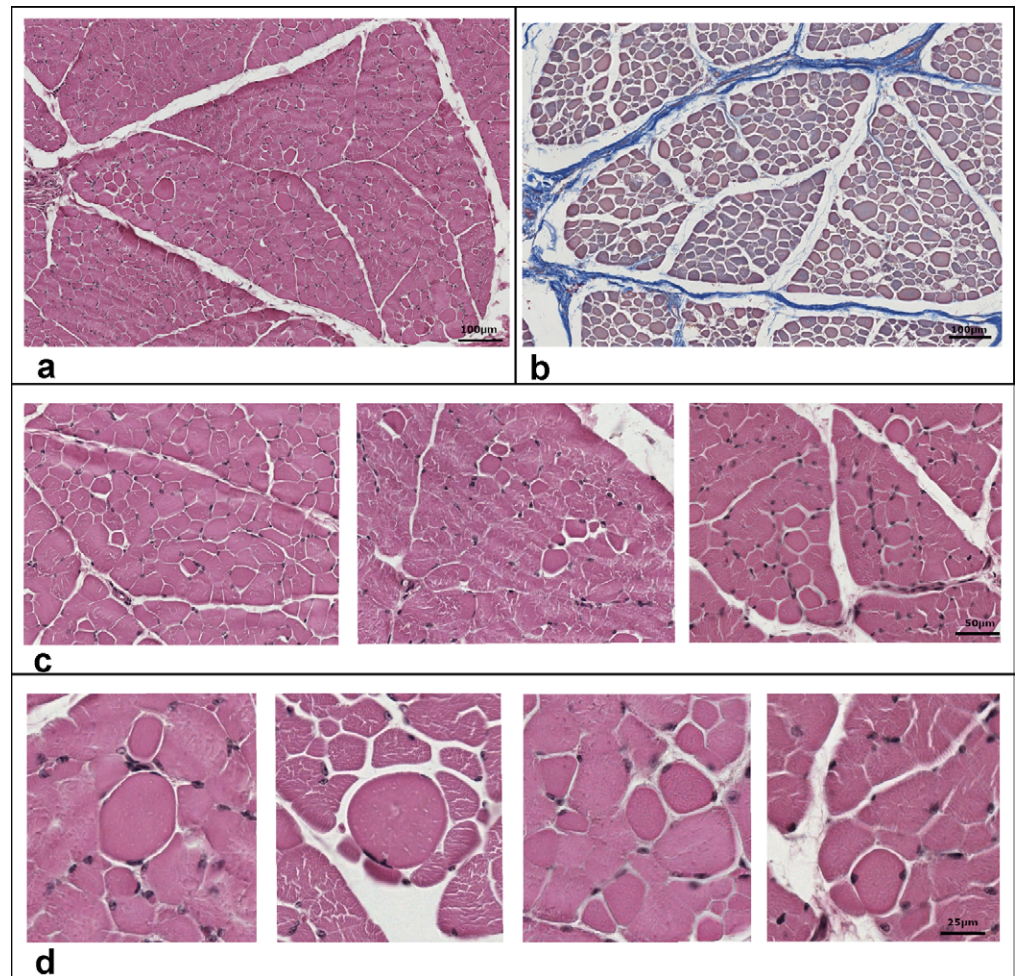


Figure 3. Histological features of semimembranosus muscle of the studied case. Transversal sections from muscle biopsies were stained with hematoxylin and eosin (**a,c,d**) or with Azan–Mallory method (**b**) to identify collagen fibers. Enlarged round shaped fibers are highlighted in panels (**c,d**). The percentage value of round shaped fibers (5.3%) was determined as the ratio of muscle fibers that lost their main shape and/or took a round shape to the total muscle fibers in the region. Scale bars correspond to 100 μ m in panels (**a,b**), and 50 and 25 μ m in panels **c** and **d**, respectively.

Among these 25 remaining private variants, one single variant affects an interesting functional candidate gene for the studied phenotype (Figure 4a). This heterozygous variant at chr13:78918850C>A is a missense variant in exon 2 of the *potassium voltage-gated channel modifier subfamily G member 1* (*KCNG1*) gene (NM_001205719.1: c.1248G>T; Figure 4b). It exchanges the encoded amino acid of *KCNG1* at position 416 (NP_001192648.1: p.Trp416Cys), located in the pore helix of the ion transport domain (Figure 4c). Furthermore, the tryptophan-to-cysteine substitution affects a highly conserved residue (4d), and was predicted to be deleterious by three different tools (Mutpred2 score 0.951; PROVEAN score -12.212; PredictSNP1 score 0.869) and to alter the transmembrane protein and ordered interface. Unfortunately, biological samples of the dam and sire that were slaughtered in the meantime, were not available. Analysis of the other 24 identified variants, taking into account the known function of the gene, the reported association with Mendelian diseases, and/or the in silico assessment of the molecular consequences of the variants in the protein, did not reveal any other plausible cause for the observed phenotype (Table S2).

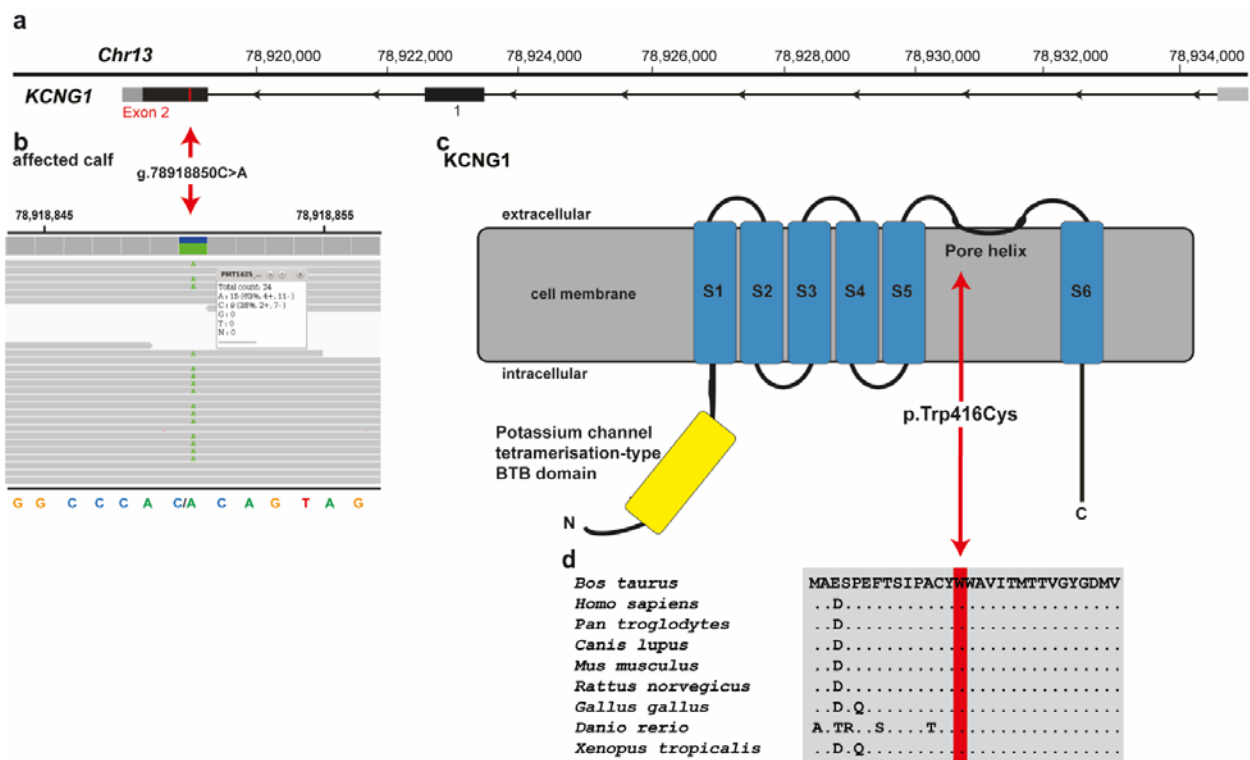


Figure 4. *KCNG1* missense variant in a crossbred calf with paradoxical myotonia congenita and myelodysplasia. (a) Structure of *KCNG1* showing the exon 2 variant located on chromosome 13. (b) IGV screenshot presenting the Chr13: 78918850C>A variant in the affected calf. (c) Schematic representation of *KCNG1* protein and its functional domains with the position of the identified pathogenic variant (red arrow). The six transmembrane domains are shown in blue (S1–S6). (d) Cross-species sequence comparison of the ion transport domain of the *KCNG1* protein with the region around the p.Trp416Cys variant shows complete evolutionary conservation.

Assuming recessive inheritance, filtering of WGS data for homozygous coding variants present in the calf and missing in the 691 control genomes of different breeds identified 12 variants with likely moderate impact. These 12 variants were further investigated for their occurrence in a diverse cohort of additional 4540 bovine genomes, which revealed the absence of variants only present homozygous in the affected calf (Table 2).

4. Discussion

This study aimed to investigate the clinicopathological phenotype and the underlying genetic cause in a crossbred calf displaying paradoxical myotonia congenita, craniofacial dysmorphism and myelodysplasia. The phenotype of this syndromic form of congenital neuromuscular disorder displays striking similarities with *SCN4A*-related forms of human PMC because it presents with episodes of exercise-induced generalized myotonic muscle stiffness. Clinical diagnosis of PMC in humans is based on consistent history, and typical clinical and electromyographic findings [6].

In PMC patients, changes in muscle fiber diameters and internal nuclei are also among the nonspecific histologic features suggestive of mild myopathic changes [31]. The muscle profile in this study revealed that 5.3% of muscle fibers lost their main shape and/or took a round shape to the total muscle fibers in the region, findings that are consistent with the human PMC features. However, the lack of an electromyography prevented a definite categorization of this paradoxical myotonia as PMC.

Moreover, some further phenotypical differences from the typical form of human PMC were noticed, such as: (1) increase in serum K^+ after stimulation; (2) inability to relax muscle immediately after the stimulation; (3) craniofacial dysmorphism; and (4) permanent extension of the hindlimbs, the latter explained by the retrieved myelodysplasia associated

with hydrosyringomyelia in the lumbosacral intumescence region. Taken together, the muscle stiffness episodes and the findings of points (1) and (2) more resembled *CACNA1S*-related forms of HyperPP. Human patients with this genetic disease show an increase in serum potassium during an attack [4]. Moreover, approximately half of the patients display muscle stiffness arising from myotonia or paramyotonia [32]. On the other side, considering the clinical muscle findings and point (3)—craniofacial dysmorphism—the observed phenotype shows similarities to the human *KCNJ2*-related Andersen–Tawil syndrome.

Hence, to the best of our understanding, our patient showed a previously unreported combination of paradoxical myotonia congenita, hyperkalemia during episodes, craniofacial dysmorphism, and myelodysplasia associated with hydrosyringomyelia, representing a novel clinicopathological presentation.

In humans, genetic confirmation of known pathogenic variants in *SCN4A*-related PMC and HyperPP, and *KCNJ2*-related Andersen–Tawil syndrome-related, is included in the diagnosis of these disorders [6]. In the studied calf, no candidate causal variant in *CACNA1S*, *SCN4A*, or *KCNJ2* were found by genome re-sequencing. Likewise, in human medicine, patients with phenotypical characteristics of PMC, HyperPP, and Andersen–Tawil syndrome were found not to present pathogenic variants in the *SCN4A* or in *KCNJ2*, suggesting further genetic heterogeneity [33]. Therefore, we evaluated the possible genetic cause for this novel congenital phenotype systematically, assuming both recessively inherited and de novo mutations. Our results from the analysis of WGS data showed that there was not a single homozygous protein-changing variant present in the affected calf, ruling out a possible recessive inheritance as the most likely cause. Furthermore, as our case was an offspring of a crossbred mating it seems to be highly unlikely that a monogenic recessive variant was causal. Especially since no bovine simple genetic disease is known that segregates in such diverse dairy and beef breeds as Holstein and Belgian-Blue, respectively. Therefore, the more plausible explanation would be to search for allelic heterogeneity, meaning two different (breed-specific) coding variants affecting the same gene. Our results from the WGS identified 25 heterozygous private protein-changing variants present in the genome of the affected calf which were absent in a cohort of more than 5200 cattle genomes. Considering the known function of the affected gene, the rarity of the variant, and the outcome of the in silico effect prediction, the identified heterozygous *KCNNG1* missense variant was assumed to represent the most likely genetic cause for the observed phenotype. We could only speculate that the mutation either occurred post-zygotically in the developing embryo or it represents a germline mutation in the dam or sire. To confirm that the identified mutation in the *KCNNG1* gene occurred indeed de novo, genotyping of the parents would be needed. Unfortunately, no genetic material of both parents was available. To the best of our knowledge, no pathogenic variant in *KCNNG1* gene has been reported in animals and humans. Therefore, this study represents the first example of a *KCNNG1*-related neuromuscular disorder as a conserved residue in the pore helix of the ion transport domain of the potassium voltage-gated channel subfamily G member 1 protein is altered.

Voltage-gated potassium channels represent a family of transmembrane proteins that are highly expressed in the central nervous system of the mammalian species, playing a major role in the control of neuronal excitability [34]. Additionally, they regulate a variety of electrophysiological properties, including the interspike membrane, the wave-form of the action potential and the firing frequency [35]. In particular, *KCNNG1* is a potassium channel subunit that cannot form functional channels by itself [36]. However, it forms functional channels with the *KCNB1* (one of the most important voltage-gated potassium channels) and modulates the delayer rectifier voltage-gated potassium channel activation and deactivation rate of this protein [34,37]. Specifically, *KCNNG1* in co-expression with *KCNB1* results in potassium channels that have slower kinetics of deactivation, due to a negative shift of the steady-state activation curve, and marked slowing of deactivation tail currents [34,37]. The performed in silico evaluations of the identified p.Trp416Cys mutation predicted that this mutation altered the transmembrane protein and ordered

interface. Therefore, we hypothesize that our mutant protein leads to a malfunction of the encoded channels allowing an additional release of intracellular potassium from the skeletal muscle. Subsequently, this change in ion transport impairs the ability of the muscle to contract, leading to the observed stiffness.

Moreover, in human medicine, there are several potassium channelopathies whose presentations are suggestive of developmental disorders, with findings including intellectual disability, craniofacial dysmorphism or other physical abnormalities [38]. Physiological functions of *KCNG1* are largely unknown, by similarity, therefore, it is plausible that the identified mutation in our study is also the underlying cause for the craniofacial dysmorphism and myelodysplasia associated with hydrosyringomyelia.

5. Conclusions

We have uncovered a novel phenotype of a most likely dominantly inherited neuromuscular channelopathy in cattle related to a potentially pathogenic variant in the bovine *KCNG1* gene. Targeted expression of affected potassium channels in transfected cell lines, in combination with recently developed gene editing tools such as CRISPR/Cas9 to mimic the consequences of the exchanged residue, may be suitable to functionally prove our claims in the future. Nevertheless, we propose here the first *KCNG1* mutation present with a disorder in a mammalian species. Our study highlights that the genetics of inherited disorders in well-phenotyped large animals, such as cattle, is a valuable model system for studying fundamental aspects of gene function.

Supplementary Materials: The following are available online at <https://www.mdpi.com/article/10.3390/genes12111792/s1>, Table S1: EBI Accession numbers of all publicly available genome sequences. We compared the genotypes of the calf with 691 cattle genomes of various breeds that had been sequenced in the course of other ongoing studies and that were publicly available; Table S2: List of the remaining variants after the comparison to the global control cohort of 5116 genomes of other breeds (1000 Bull Genomes Project run 9; www.1000bullgenomes.com; accessed on 17 July 2021) and after IGV visual inspection, revealing 25 protein-changing variants with a predicted moderate or high impact only present in the affected calf; Video S1: After passively positioned, the calf was able to acquire and maintain the quadrupedal stance. In standing the hind limbs were contracted and hyperextended, and tail head elevated.

Author Contributions: Conceptualization, C.D. and A.G.; methodology, I.M.H., E.E.A., R.S., C.B., A.G. and C.D.; validation, J.G.P.J.; formal analysis, J.G.P.J., I.M.H., E.E.A., R.S., C.B., A.G. and C.D.; investigation, J.G.P.J. and A.G.; resources, C.D.; data curation, I.M.H.; writing—original draft preparation, J.G.P.J.; writing—review and editing, J.G.P.J., I.M.H., E.E.A., R.S., C.B., A.G. and C.D.; visualization, R.S., A.G. and J.G.P.J.; supervision, C.D. and A.G.; project administration, C.D.; funding acquisition, C.D. All authors have read and agreed to the published version of the manuscript.

Funding: This study was partially funded by the Swiss National Science Foundation, grant number 172911.

Institutional Review Board Statement: This study did not require official or institutional ethical approval as it was not an experimental study, but part of a clinical and pathological veterinary diagnostic case.

Informed Consent Statement: Not applicable.

Data Availability Statement: The whole-genome data of the affected calf (sample ID PMT1625) is freely available at the European Nucleotide Archive (ENA) under sample accession number SAMEA7690196.

Acknowledgments: We acknowledge the Interfaculty Bioinformatics Unit of the University of Bern for providing high-performance computational infrastructure.

Conflicts of Interest: The authors declare no conflict of interest.

References

1. Kim, J.-B. Channelopathies. *Korean J. Pediatr.* **2014**, *57*, 1–18. [[CrossRef](#)] [[PubMed](#)]
2. Spillane, J.; Kullmann, D.M.; Hanna, M.G. Genetic neurological channelopathies: Molecular genetics and clinical phenotypes. *J. Neurol. Neurosurg. Psychiatry* **2016**, *87*, 37–48. [[CrossRef](#)] [[PubMed](#)]

3. Colding-Jørgensen, E. Phenotypic variability in myotonia congenita. *Muscle Nerve* **2005**, *32*, 19–34. [[CrossRef](#)]
4. Phillips, L.; Trivedi, J.R. Skeletal Muscle Channelopathies. *Neurother. J. Am. Soc. Exp. Neurother.* **2018**, *15*, 954–965. [[CrossRef](#)]
5. Montagnese, F.; Schoser, B. Dystrophic and non-dystrophic myotonias. *Fortschr. Neurol. Psychiatr.* **2018**, *86*, 575–583. [[CrossRef](#)] [[PubMed](#)]
6. Stunnenberg, B.C.; LoRusso, S.; Arnold, W.D.; Barohn, R.J.; Cannon, S.C.; Fontaine, B.; Griggs, R.C.; Hanna, M.G.; Matthews, E.; Meola, G.; et al. Guidelines on clinical presentation and management of nondystrophic myotonias. *Muscle Nerve* **2020**, *62*, 430–444. [[CrossRef](#)] [[PubMed](#)]
7. Fontaine, B.; Vale-Santos, J.; Jurkat-Rott, K.; Reboul, J.; Plassart, E.; Rime, C.S.; Elbaz, A.; Heine, R.; Guimarães, J.; Weissenbach, J. Mapping of the hypokalaemic periodic paralysis (HypoPP) locus to chromosome 1q31-32 in three European families. *Nat. Genet.* **1994**, *6*, 267–272. [[CrossRef](#)] [[PubMed](#)]
8. Bulman, D.E.; Scoggan, K.A.; van Oene, M.D.; Nicolle, M.W.; Hahn, A.F.; Tollar, L.L.; Ebers, G.C. A novel sodium channel mutation in a family with hypokalemic periodic paralysis. *Neurology* **1999**, *53*, 1932–1936. [[CrossRef](#)]
9. Ptacek, L.J.; Trimmer, J.S.; Agnew, W.S.; Roberts, J.W.; Petajan, J.H.; Leppert, M. Paramyotonia congenita and hyperkalemic periodic paralysis map to the same sodium-channel gene locus. *Am. J. Hum. Genet.* **1991**, *49*, 851–854. [[PubMed](#)]
10. Raja Rayan, D.L.; Hanna, M.G. Skeletal muscle channelopathies: Nondystrophic myotonias and periodic paralysis. *Curr. Opin. Neurol.* **2010**, *23*, 466–476. [[CrossRef](#)] [[PubMed](#)]
11. Koch, M.C.; Steinmeyer, K.; Lorenz, C.; Ricker, K.; Wolf, F.; Otto, M.; Zoll, B.; Lehmann-Horn, F.; Grzeschik, K.H.; Jentsch, T.J. The skeletal muscle chloride channel in dominant and recessive human myotonia. *Science* **1992**, *257*, 797–800. [[CrossRef](#)] [[PubMed](#)]
12. Cannon, S.C. Channelopathies of skeletal muscle excitability. *Compr. Physiol.* **2015**, *5*, 761–790. [[CrossRef](#)] [[PubMed](#)]
13. Ptáček, L.J.; George, A.L.J.; Barchi, R.L.; Griggs, R.C.; Riggs, J.E.; Robertson, M.; Leppert, M.F. Mutations in an S4 segment of the adult skeletal muscle sodium channel cause paramyotonia congenita. *Neuron* **1992**, *8*, 891–897. [[CrossRef](#)]
14. Ricker, K.; Moxley, R.T., 3rd; Heine, R.; Lehmann-Horn, F. *Myotonia fluctuans*. A third type of muscle sodium channel disease. *Arch. Neurol.* **1994**, *51*, 1095–1102. [[CrossRef](#)] [[PubMed](#)]
15. Colding-Jørgensen, E.; Duno, M.; Vissing, J. Autosomal dominant monosymptomatic myotonia permanens. *Neurology* **2006**, *67*, 153–155. [[CrossRef](#)]
16. Wijnberg, I.D.; Owczarek-Lipska, M.; Sacchetto, R.; Mascarello, F.; Pascoli, F.; Grünberg, W.; van der Kolk, J.H.; Drögemüller, C. A missense mutation in the skeletal muscle chloride channel 1 (CLCN1) as candidate causal mutation for congenital myotonia in a New Forest pony. *Neuromuscul. Disord.* **2012**, *22*, 361–367. [[CrossRef](#)]
17. Rhodes, T.H.; Vite, C.H.; Giger, U.; Patterson, D.F.; Fahlke, C.; George, A.L.J. A missense mutation in canine ClC-1 causes recessive myotonia congenita in the dog. *FEBS Lett.* **1999**, *456*, 54–58. [[CrossRef](#)]
18. Gandolfi, B.; Daniel, R.J.; O'Brien, D.P.; Guo, L.T.; Youngs, M.D.; Leach, S.B.; Jones, B.R.; Shelton, G.D.; Lyons, L.A. A novel mutation in CLCN1 associated with feline myotonia congenita. *PLoS ONE* **2014**, *9*, e109926. [[CrossRef](#)]
19. Monteagudo, L.V.; Tejedor, M.T.; Ramos, J.J.; Lacasta, D.; Ferrer, L.M. Ovine congenital myotonia associated with a mutation in the muscle chloride channel gene. *Vet. J.* **2015**, *204*, 128–129. [[CrossRef](#)] [[PubMed](#)]
20. Beck, C.L.; Fahlke, C.; George, A.L.J. Molecular basis for decreased muscle chloride conductance in the myotonic goat. *Proc. Natl. Acad. Sci. USA* **1996**, *93*, 11248–11252. [[CrossRef](#)] [[PubMed](#)]
21. Rudolph, J.A.; Spier, S.J.; Byrns, G.; Rojas, C.V.; Bernoco, D.; Hoffman, E.P. Periodic paralysis in quarter horses: A sodium channel mutation disseminated by selective breeding. *Nat. Genet.* **1992**, *2*, 144–147. [[CrossRef](#)] [[PubMed](#)]
22. Rosen, B.D.; Bickhart, D.M.; Schnabel, R.D.; Koren, S.; Elsik, C.G.; Tseng, E.; Rowan, T.N.; Low, W.Y.; Zimin, A.; Couldrey, C.; et al. De novo assembly of the cattle reference genome with single-molecule sequencing. *Gigascience* **2020**, *9*, g1aa021. [[CrossRef](#)] [[PubMed](#)]
23. Hayes, B.J.; Daetwyler, H.D. 1000 Bull Genomes Project to Map Simple and Complex Genetic Traits in Cattle: Applications and Outcomes. *Annu. Rev. Anim. Biosci.* **2019**, *7*, 89–102. [[CrossRef](#)] [[PubMed](#)]
24. Chen, S.; Zhou, Y.; Chen, Y.; Gu, J. Fastp: An ultra-fast all-in-one FASTQ preprocessor. *Bioinformatics* **2018**, *34*, i884–i890. [[CrossRef](#)]
25. Häfliger, I.M.; Wiedemar, N.; Švara, T.; Starič, J.; Cociancich, V.; Šest, K.; Gombač, M.; Paller, T.; Agerholm, J.S.; Drögemüller, C. Identification of small and large genomic candidate variants in bovine pulmonary hypoplasia and anasarca syndrome. *Anim. Genet.* **2020**, *51*, 382–390. [[CrossRef](#)]
26. Cingolani, P.; Platts, A.; Wang, L.L.; Coon, M.; Nguyen, T.; Wang, L.; Land, S.J.; Lu, X.; Ruden, D.M. A program for annotating and predicting the effects of single nucleotide polymorphisms, SnpEff: SNPs in the genome of *Drosophila melanogaster* strain w1118; iso-2; iso-3. *Fly* **2012**, *6*, 80–92. [[CrossRef](#)]
27. Robinson, J.T.; Thorvaldsdóttir, H.; Wenger, A.M.; Zehir, A.; Mesirov, J.P. Variant review with the integrative genomics viewer. *Cancer Res.* **2017**, *77*, e31–e34. [[CrossRef](#)] [[PubMed](#)]
28. Pejaver, V.; Urresti, J.; Lugo-Martinez, J.; Pagel, K.; Lin, G.N.; Nam, H.-J.; Mort, M.; Cooper, D.; Sebat, J.; Iakoucheva, L.; et al. MutPred2: Inferring the molecular and phenotypic impact of amino acid variants. *bioRxiv* **2017**. [[CrossRef](#)]
29. Choi, Y.; Chan, A.P. PROVEAN web server: A tool to predict the functional effect of amino acid substitutions and indels. *Bioinformatics* **2015**, *31*, 2745–2747. [[CrossRef](#)] [[PubMed](#)]
30. Bendl, J.; Stourac, J.; Salanda, O.; Pavelka, A.; Wieben, E.D.; Zendulka, J.; Brezovsky, J.; Damborsky, J. PredictSNP: Robust and accurate consensus classifier for prediction of disease-related mutations. *PLoS Comput. Biol.* **2014**, *10*, e1003440. [[CrossRef](#)] [[PubMed](#)]

31. Izumi, Y.; Fukuuchi, Y.; Koto, A.; Nakajima, S. Paramyotonia congenita without cold paralysis: A case report. *Keio J. Med.* **1994**, *43*, 94–97. [[CrossRef](#)] [[PubMed](#)]
32. Statland, J.M.; Fontaine, B.; Hanna, M.G.; Johnson, N.E.; Kissel, J.T.; Sansone, V.A.; Shieh, P.B.; Tawil, R.N.; Trivedi, J.; Cannon, S.C.; et al. Review of the Diagnosis and Treatment of Periodic Paralysis. *Muscle Nerve* **2018**, *57*, 522–530. [[CrossRef](#)] [[PubMed](#)]
33. Miller, T.M.; Dias da Silva, M.R.; Miller, H.A.; Kwiecinski, H.; Mendell, J.R.; Tawil, R.; McManis, P.; Griggs, R.C.; Angelini, C.; Servidei, S.; et al. Correlating phenotype and genotype in the periodic paralyses. *Neurology* **2004**, *63*, 1647–1655. [[CrossRef](#)] [[PubMed](#)]
34. Schnitzler, M.M.; Rinné, S.; Skrobek, L.; Renigunta, V.; Schlichthörl, G.; Derst, C.; Gudermann, T.; Daut, J.; Preisig-Müller, R. Mutation of histidine 105 in the T1 domain of the potassium channel Kv2.1 disrupts heteromerization with Kv6.3 and Kv6.4. *J. Biol. Chem.* **2009**, *284*, 4695–4704. [[CrossRef](#)]
35. Hille, B. *Ion. Channels of Excitable Membranes*, 3rd ed.; Sinauer Associates Institute, Ed.; Sinauer: Sunderland, MA, USA, 2001.
36. Post, M.A.; Kirsch, G.E.; Brown, A.M. Kv2.1 and electrically silent Kv6.1 potassium channel subunits combine and express a novel current. *FEBS Lett.* **1996**, *399*, 177–182. [[CrossRef](#)]
37. Kramer, J.W.; Post, M.A.; Brown, A.M.; Kirsch, G.E. Modulation of potassium channel gating by coexpression of Kv2.1 with regulatory Kv5.1 or Kv6.1 α -subunits. *Am. J. Physiol. Physiol.* **1998**, *274*, C1501–C1510. [[CrossRef](#)] [[PubMed](#)]
38. Hamilton, M.J.; Suri, M. *Chapter Four—“Electrifying Dysmorphology”: Potassium Channelopathies Causing Dysmorphic Syndromes*; Kumar, B.T.-A., Dionis, G., Eds.; Academic Press: New York, NY, USA, 2020; Volume 105, pp. 137–174. ISBN 0065-2660.

4.1.3 Metabolic disorders

- **Congenital cholesterol deficiency:** “*Autosomal Cholesterol Deficiency in a Holstein Calf*”, Pakistan Veterinary Journal, 2020, 40, pp. 274 – 276 (see [chapter 4.1.3.1](#))

4.1.3.1 Autosomal Cholesterol Deficiency in a Holstein Calf

Journal: Pakistan Veterinary Journal

Manuscript status: published

Contributions: phenotype description, figures, writing original draft and revisions

Displayed version: published version

DOI: [10.29261/pakvetj/2019.120](https://doi.org/10.29261/pakvetj/2019.120)



CASE REPORT

Autosomal Cholesterol Deficiency in a Holstein Calf

Joana Gonçalves Pontes Jacinto¹, Marilena Bolcato^{1*}, Cord Drögemüller², Arcangelo Gentile¹ and Gianfranco Militerno¹

¹Department of Veterinary Medical Sciences, University of Bologna, Via Tolara di Sopra, 50-40064 Ozzano dell'Emilia (Bologna), Italy; ²Institute of Genetics, Vetsuisse Faculty, University of Bern, Bremgartenstr. 109a-3001 Bern, Switzerland

*Corresponding author: marilena.bolcato2@unibo.it

ARTICLE HISTORY (19-266)

Received: June 23, 2019
Revised: November 06, 2019
Accepted: November 07, 2019
Published online: November 28, 2019

Key words:

Apolipoprotein B
Cattle
Cholesterol deficiency
Diarrhea
Holstein

ABSTRACT

Cholesterol deficiency (CD) is an autosomal recessive defect in Holstein cattle caused by a mutation in the apolipoprotein B gene (*APOB*). This paper reports the clinical and pathological phenotype of a case of CD in a 5-months-old Holstein calf. Retarded growth, chronic, intermittent diarrhea, stomatitis, hypocholesterolemia and low blood triglycerides concentrations were the most important clinical and ancillary findings. Histopathologically, inflammation of the digestive organs was the most evident sign. Blood from the patient, the dam, sister1, sister2 and semen of the sire were tested for *APOB* mutation: the calf resulted homozygous, whereas the dam and the sire resulted heterozygous carriers. Both sisters were *APOB* mutation free. Cholesterol deficiency should be considered in the differential diagnosis of chronic diarrhea and failure to thrive in Holstein calves.

©2019 PVJ. All rights reserved

To Cite This Article: Jacinto JGP, Bolcato M, Drögemüller C, Gentile A and Militerno G, 2020. Autosomal cholesterol deficiency in a Holstein calf. Pak Vet J, 40(2): 274-276. <http://dx.doi.org/10.29261/pakvetj/2019.120>

INTRODUCTION

Cholesterol deficiency (CD) is an autosomal recessive genetic defect in Holstein cattle (Menzi *et al.*, 2016). The affected animals show unresponsive diarrhea, buccal lesions and retarded growth of unknown etiology and suffer hypocholesterolemia indicating a fat metabolism disorder (Mock *et al.*, 2016). Calves do not respond to symptomatic treatment and usually die within the first 6 months of their life (Kipp *et al.*, 2016). The causative mutation has been identified in exon 5 of the apolipoprotein B gene (*APOB*) (Charlier, 2016). The lack of *APOB* in homozygous mutant animals provokes a malabsorption of dietary fat and fat-soluble vitamins in the intestine and is assumed to impair cholesterol metabolism and transport in blood circulation and liver (Gross *et al.*, 2016). The genetic test allows the detection of animals with CD without pedigree information (Menzi *et al.*, 2016).

In humans, truncating mutations in *APOB* give rise to Human Familial Hypobetalipoproteinemia (FHBL) and homozygous show: steatorrhea, neurological dysfunction, vision problems, and non-alcoholic fatty liver (Welty, 2014).

CLINICAL CASE

History: A 5-months-old female Holstein calf was admitted to teaching hospital of the Department of Veterinary Medical Sciences of the University of Bologna

for in-depth clinical study due to a history of failure to thrive, intermittent diarrhea and progressive emaciation.

Clinical examination: The calf presented a reduced skeletal development if compared to cohort animals, was cachectic and showed muscular hypotonia. Difficulty with mastication was accompanied by sialorrhea and signs of buccal pain. The calf revealed gingival, sub-lingual and palatine lesions compatible with fibrinous-ulcerative stomatitis (Fig. 1). Body temperature was within the normal limits, whereas pulse and respiratory rates were slightly increased (100 bpm and 48 rpm, respectively). In addition, pulmonary auscultation revealed a moderate increase of the vesicular lung sound. A profuse foamy diarrhea increased in quantity and frequency; undigested material remained constantly present for the entire period of observation at the teaching hospital. Despite supportive treatment, the animal died 33 days after admission.

Ancillary diagnostic: Blood samples for cells count and clinical biochemistry were collected from the calf, the dam and two maternal half-sisters. Severe hypocholesterolemia (2.0 mg/dl; reference range: 80-120 mg/dl) and hypotriglyceridemia (1.0 mg/dl; reference range: 12-31 mg/dl) were the most important findings in the calf. Although not so extreme, also the dam showed hypocholesterolemia (62 mg/dl; reference range: 80-120 mg/dl), whereas the two half-sisters had blood cholesterol values within the normal range.



Fig. 1: Fibrinous-ulcerative gingivitis. Note the hemorrhagic background partially covered by an adherent and detachable yellowish to pink membrane. *Candida albicans* was isolated from the buccal swab.



Fig. 2: Esophagitis. Note the ulceration of the cranial third of the esophageal mucosa with exposing of the submucosa and a marked tissue retraction.



Fig. 3: Segmental enteritis of the small intestine. Note the generalized congestion and hyperemia.

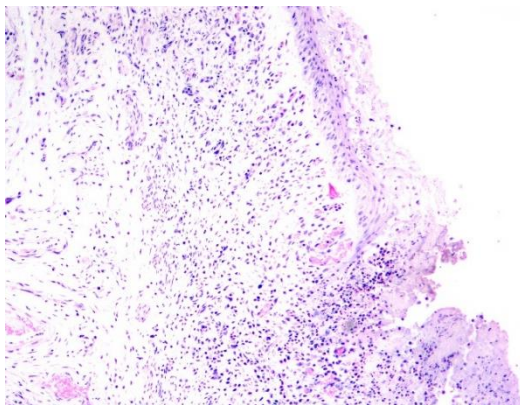


Fig. 4: Severe subacute lymphoplasmacytic esophagitis. Note the lack of the epithelium (ulcer). H&E 10X.

The calf showed also a slight anemia (hemoglobin 7.2 gr/dl) and hypoproteinemia (total protein 5.61 g/dl, with albumin corresponding to 1.96 g/dl). Calf's blood resulted negative for BVDV antigens and antibodies. In addition, calf's fecal sample resulted negative to *Eimeria* spp., *Cryptosporidium* spp. and to BVDV (RT-PCR). Diarrhea caused by dietetic management was excluded by clinical history.

Furthermore, a buccal swab and an endoscopy of the nasal cavity and larynx were performed in the patient: swab samples were positive to *Candida albicans*, whereas the endoscopy revealed a slight rhinolaryngitis associated to a severe tracheitis.

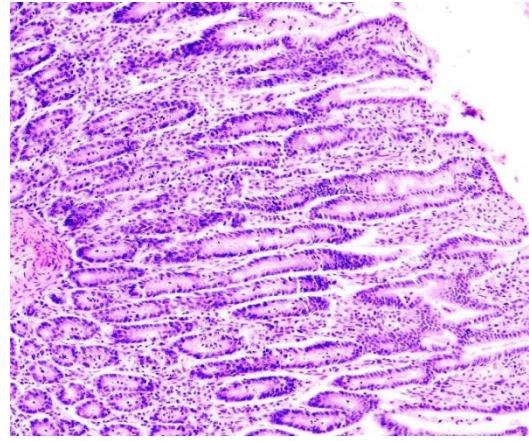


Fig. 5: Moderate acute duodenal enteritis. Note the cellular infiltration constituted mainly by lymphoplasmacytic cells but also by some neutrophil granulocytes. H&E 10X.

Postmortem findings: At gross examination, the animal showed a poor corporal condition (1.5/5), exhibiting scarce subcutaneous adipose tissue. The perineal region and the pelvic limbs were defiled with feces. The buccal cavity showed a fibrinous-ulcerative stomatitis. A profound segmental ulceration of the cranial third of the esophageal mucosa with exposed submucosa and a marked tissue retraction was present (Fig. 2). The ulcerative areas were covered by fibrin. Furthermore, the intestine revealed a moderate amount of bright yellow, partially foamy to fatty content and presented a segmental enteritis (Fig. 3). A congestion of the serosa covering the colon was also present, as well as a slight perihepatitis. A laryngitis and a presence of slight deposits of greenish exudate at the level of the first rings of the trachea were observed. The brain presented hyperemia of meningeal vessels (arachnoid and pia mater). A slight cerebral edema was also noticed. Samples of the esophagus and intestine were fixed and processed for histology. In both organs the most remarkable findings indicated a lymphoplasmacytic inflammation of different grade of severity (Fig. 4 and 5).

Genetic analysis: Genomic DNA extracted from the blood samples of the affected calf, the dam, the two half-sisters, as well as from semen straw of the sire obtained by retail dealer was screened for the mutation of the *APOB*. The calf resulted homozygous for the *APOB* mutation, the dam and the sire heterozygous carrier, the half-sister homozygous wild type.

DISCUSSION

Although diarrheic syndrome may be considered quite a common condition in calves, the same cannot be said when it acquires a chronic course in the absence of evidence of parasitic infestations or inappropriate nutritional management. In these cases, CD, at least in the Holstein breed, should be included in the differential diagnosis. Moreover, the suspect does increase if the patient additionally presents stomatitis and failure to thrive.

Although of moderate intensity, the intermittent diarrhea, the retarded growth, the progressive emaciation and the buccal lesions presented by the calf of this paper, were in compliance with what described in patients affected by CD by Mock *et al.* (2016). Cachexia, muscular atrophy,

signs of diarrhea, intestine diffusely filled with a moderate amount of bright yellow, partially foamy to fatty content and enteritis were also described in other cases of CD by Kipp *et al.* (2016). The latter author reported also respiratory findings as in the here described animal.

Enteritis, failure to thrive, hypocholesterolemia and low TG concentration, are the characteristic signs of the human FHBL (Welty, 2014). In FHBL the malabsorption of lipid-soluble vitamins (A, D, E, K), leads to retinal degeneration, neuropathy, and coagulopathy (Lee and Hegele, 2014). Neurologic disorders are therefore consequences of cerebellar dysfunction and demyelination of the central and peripheral nervous systems (Lee and Hegele, 2014; Welty, 2014). Although the reported calf did not show any neurological signs, hyperemia of meningeal vessels and a slight cerebral edema were present supporting similar mechanisms.

In addition, also the presence of esophagitis and perihepatitis of the calf reminds of the FHBL (Lee and Hegele, 2014). Despite the absence of histological signs of fatty liver, the calf showed increased alkaline phosphatase and total bilirubin (both components, direct and indirect).

Kipp *et al.* (2016) reported that homozygous CD calves had markedly decreased concentrations of LDL-C consisting of cholesterol bound to APOB. Apolipoproteins form the structural proteins of lipoproteins allowing to transport lipophilic cholesterol and triacylglycerol in hydrophilic blood (Kipp *et al.*, 2016). APOB is the protein that binds cholesterol to form LDL-C and VLDL-C (Kipp *et al.*, 2016). In general, APOB-containing lipoproteins carry lipids from site of synthesis and site of absorption to various sites of utilization for energy production, storage, membrane assembly, or steroid hormone production (Marcovina and Packard, 2006). Unfortunately, in the described patient no data are available in respect to the values of LDL-C and VLDL-C.

In this study, total cholesterol was below reference values also in the dam: nevertheless, she did not present any clinical signs of malabsorption. Also Gross *et al.* (2016) observed no clinical signs of maldigestion in heterozygous carriers of the APOB mutation, both in calves and adult animals. This may conclude that despite lower plasma concentrations of TG and total cholesterol, heterozygous animals are apparently able to maintain cholesterol and lipoprotein homeostasis adequate for, e.g., steroid hormone biosynthesis and cell membrane function (Gross *et al.*, 2016). However, it might also be speculated that these effects might not be fully overt resulting in possible unspecific signs of reduced fertility, growth, and health (Gross *et al.*, 2016).

As cholesterol is an essential component of the reticulocyte membrane, red blood cells of affected animals might be more fragile than normal, explaining the low RBC, Hb, and Ht observed in the described case as well as by Inokuma *et al.* (2017) and Mock *et al.* (2016).

A protein-losing enteropathy might be the explanation for the observed hypoproteinemia and hypoalbuminemia, as also reported by Kipp *et al.* (2016).

In respect to the isolation of *Candida albicans* from the buccal swab and the slight rhino-laryngitis associated to the severe tracheitis, a secondary infection as a consequence of vitamins induced increased susceptibility may be postulated. Hypovitaminosis was shown to

decrease the resistance to infections in cattle (Xiuyuan *et al.*, 2012).

Unspecific clinical signs of diarrhea and failure to thrive in young calves are the main challenges for the diagnosis of CD in cattle. However, CD must be considered in the differential diagnosis in all case of unresponsiveness chronic course. The total cholesterol and TG evaluation is the first step for the diagnosis of CD that, however, can be definitely confirmed as inherited disease only by the genetic test. An early diagnosis of CD may prevent an ineffective utilization of antibiotics and eventually also an unnecessary and hopeless suffering of the diseased animal.

Conclusions: Despite the generality of the single clinical findings, a clinical picture including unresponsive chronic diarrhea, retarded growth and buccal lesions in Holstein calves should always address the clinical suspect also to the CD. The determination of blood cholesterol is decisive for the diagnosis, that may be etiologically confirmed by the genetic test for APOB mutation. If CD will be considered in the differential diagnosis of such clinical pictures further cases of the defect may be expected in the future. Therefore, awareness of this fact is urged among breeders and veterinarians in order to identify possible carriers, thus preventing unnoticed spread of the anomaly in the Holstein populations.

Authors contribution: Conceptualization: AG, JJ. Formal analysis: AG, GM. Investigation: MB, GM, JJ, CD. Project administration: AG. Supervision: CD, AG. Validation: CD, AG. Writing – original draft: AG, JJ. Writing – review & editing: AG, GM. All authors critically revised the manuscript for important intellectual contents and approved the final version.

REFERENCES

- Charlier C, 2016. The role of mobile genetic elements in the bovine genome. Proc "Plant and Animal Genome Conference XXIV", San Diego, USA, January 9-13, 2016, Abstract W636.
- Gross JJ, Schwinn A, Schmitz-Hsu F, *et al.*, 2016. Rapid communication: Cholesterol deficiency-associated APOB mutation impacts lipid metabolism in Holstein calves and breeding bulls. *J Anim Sci* 94:1761-6.
- Inokuma H, Horiuchi N, Watanabe K, *et al.*, 2017. Retrospective study of clinical and laboratory findings of autosomal recessive cholesterol deficiency in Holstein calves in Japan. *Jpn J Vet Res* 65:107-12.
- Kipp S, Segelke D, Schierenbeck S, *et al.*, 2016. Identification of a haplotype associated with cholesterol deficiency and increased juvenile mortality in Holstein cattle. *J Dairy Sci* 99:8915-31.
- Lee J and Hegele RA, 2014. Abetalipoproteinemia and homozygous hypobetalipoproteinemia: a framework for diagnosis and management. *J Inher Metab Dis* 37:333-9.
- Marcovina S and Packard CJ, 2006. Measurement and meaning of apolipoprotein AI and apolipoprotein B plasma levels. *J Intern Med* 259:437-46.
- Menzi F, Besuchet-Schmutz N, Fagnière M, *et al.*, 2016. A transposable element insertion in APOB causes cholesterol deficiency in Holstein cattle. *Anim Genet* 47:253-7.
- Mock T, Mehinagic K, Menzi F, *et al.*, 2016. Clinicopathological Phenotype of autosomal recessive cholesterol deficiency in holstein cattle. *J Vet Intern Med* 30:1369-75.
- Welty FK, 2014. Hypobetalipoproteinemia and abetalipoproteinemia. *Curr Opin Lipidol* 25:161-8.
- Xiuyuan H, Yongtao L, Meng L, *et al.*, 2012. Hypovitaminosis A coupled to secondary bacterial infection in beef cattle. *BMC Vet Res* 8:222.

4.1.4 Genodermatosis

- **Epydermolysis bullosa simplex:** “*A de novo mutation in KRT5 in a crossbred calf with epidermolysis bullosa simplex*”, *Journal of Veterinary Internal Medicine*, 2020, 34, pp. 2800 – 2807 ([see chapter 4.1.4.1](#))
- **Ehlers–Danlos syndrome:** “*A heterozygous missense variant in the COL5A2 in Holstein cattle resembling the classical Ehlers–Danlos syndrome*” *Animals*, 2020, 10, pp. 2002 – 2015 ([see chapter 4.1.4.2](#))
- **Generalized juvenile angiomatosis:** “*Clinicopathological and genomic characterization of a Simmental calf with generalized bovine juvenile angiomatosis*”, *Animals*, 2021, 11, pp. 1 – 11 ([see chapter 4.1.4.3](#))
- **Ichthyosis congenita:** “*A frameshift insertion in FA2H causes a recessively inherited form of ichthyosis congenita in Chianina cattle*”, *Molecular Genetics and Genomics*, 2021, 296, pp. 1313-1322 – 1322 ([see chapter 4.1.4.4](#))
- **Hypotrichosis:** “*A KRT71 Loss-of-Function Variant Results in Inner Root Sheath Dysplasia and Recessive Congenital Hypotrichosis of Hereford Cattle*”, *Genes*, 2021, 12, pp. 1038 – 1038 ([see chapter 4.1.4.5](#))
- **Hypotrichosis:** “*A Nonsense Variant in Hephaestin Like 1 (HEPHL1) is responsible for Congenital Hypotrichosis in Belted Galloway cattle*”, *Genes*, 2021, 12, pp. 1 – 11 ([see chapter 4.1.4.6](#))

4.1.4.1 A *de novo* mutation in *KRT5* in a crossbred calf with epidermolysis bullosa simplex

Journal: Journal of Veterinary Internal Medicine

Manuscript status: published

Contributions: whole-genome sequencing data analysis, genetic figures, writing original draft and revisions

Displayed version: published version

DOI: [10.1111/jvim.15943](https://doi.org/10.1111/jvim.15943)

CASE REPORT

A de novo mutation in *KRT5* in a crossbred calf with epidermolysis bullosa simplex

Joana G. P. Jacinto^{1,2}  | Irene M. Häfliger²  | Inês M. B. Veiga³  |
 Cord Drögemüller²  | Jørgen S. Agerholm⁴ 

¹Department of Veterinary Medical Sciences, University of Bologna, Bologna, Italy

²Institute of Genetics, Vetsuisse Faculty, University of Bern, Bern, Switzerland

³Institute of Animal Pathology, Vetsuisse Faculty, University of Bern, Bern, Switzerland

⁴Department of Veterinary Clinical Sciences, University of Copenhagen, Copenhagen, Denmark

Correspondence

Cord Drögemüller, Institute of Genetics, Vetsuisse Faculty, University of Bern, Bremgartenstr. 109a, 3001 Bern, Switzerland. Email: cord.droegemueller@vetsuisse.unibe.ch

Abstract

A 6-day-old Belgian Blue-Holstein calf was referred because of a syndrome resembling epidermolysis bullosa simplex (EBS). The clinical phenotype included irregular and differently sized erosions and ulcerations spread over the body, in particular on the limbs and over bone prominences, as well as in the nasal planum and oral mucosa. Blisters were easily induced by rubbing the skin. The skin lesions displayed a clear dermal-epidermal separation at the level of the basal cell layer. Post mortem examination revealed erosions in the pharynx, proximal esophagus, and rumen. Whole-genome sequencing revealed a heterozygous disruptive in-frame deletion variant in *KRT5* (c.534_536delCAA). Genotyping of both parents confirmed the variant as de novo mutation. Clinicopathological and genetic findings were consistent with the diagnosis of *KRT5*-related EBS providing the second example of a spontaneous mutation causing epidermolysis bullosa in cattle.

KEYWORDS

cattle, *KRT5*, precision medicine, skin fragility, WGS

1 | INTRODUCTION

Epidermolysis bullosa (EB) encompasses a heterogeneous group of genetic mechanobullous disorders characterized by blistering from even minor mechanical trauma with disruption at the dermal-epidermal junction.¹ Epidermolysis bullosa disorders are characterized by clinical heterogeneity, both in their appearance and severity. The disease might be congenital or develop later in life. In congenital cases, the lesions are more severe, accompanied by mucosal fragility, and might involve other organs than the skin.² In noncongenital cases, the

skin fragility is less severe and the lesions are usually localized to the extremities of the limbs, occasionally only expressed as nail/hof dystrophy.³ Based on the ultrastructural level of skin cleavage, there are 4 major classical types: EB simplex (EBS), junctional EB (JEB), dystrophic EB (DEB), and Kindler EB (KEB).⁴ In EBS, the skin cleavage occurs within the epidermis, in JEB within the lamina lucida and in DEB within the superficial dermis. Kindler EB might present with all 3 cleavage levels.³ The same classification might be used in veterinary medicine; however, cases of KEB are not reported in domestic animals. In human, these phenotypical classifications are complicated by the fact that, depending on the variant, the same gene might be associated with different modes of inheritance, thus resulting in distinct clinical phenotypes.⁵ Dystrophic EB and EBS phenotypes might be inherited either dominantly or recessively, and might be caused by pathogenic

Abbreviations: DEB, dystrophic EB; EBS, EB simplex; EDTA, ethylenediaminetetraacetic acid; EB, epidermolysis bullosa; HE, hematoxylin and eosin; HIM, helix initiation peptide motif; HTM, helix termination peptide motif; IGV, Integrative Genomics Viewer; JEB, junctional EB; *KRT5*, keratin 5; KEB, Kindler EB; WGS, whole-genome sequencing.

This is an open access article under the terms of the Creative Commons Attribution License, which permits use, distribution and reproduction in any medium, provided the original work is properly cited.

© 2020 The Authors. *Journal of Veterinary Internal Medicine* published by Wiley Periodicals LLC on behalf of American College of Veterinary Internal Medicine.

variants in different genes.⁴ In human medicine, EB is associated with more than 1000 variants in at least 18 genes encoding structural proteins.^{1,5}

Four EB-related causative recessive variants are known in cattle,⁶⁻⁹ 3 in dogs,¹⁰⁻¹³ 2 in sheep,^{14,15} and 2 in horses,¹⁶⁻¹⁹ and 1 dominant variant is known in cattle²⁰ (Table S1). For cattle, a dominant form of EBS is associated with a keratin 5 (*KRT5*) missense variant (OMIA 002081-9913),²⁰ and recessive forms of JEB are associated with deleterious variants in *ITGB4* (OMIA 001948-9913), *LAMA3* (OMIA 001677-9913), and *LAMC2* (OMIA 001678-9913).⁶⁻⁸ In addition, a form of recessive DEB is associated with a nonsense variant in *COL7A1* (OMIA 000341-991).⁹

Older reports of familial occurrence of EB,²¹ outbreaks of several inherited-related cases in single herds²¹⁻²³ and sporadic cases of EB²⁴⁻²⁷ in cattle exist. In the abovementioned cases,²¹⁻²³ the diagnosis was based only on the clinical and histopathological findings.

The majority of the previous reports focused on disorders with a recessive inheritance. However, single cases because of dominant acting de novo variants might occur sporadically without impact on breeding. At present, this obvious genetic heterogeneity could be analyzed in cattle using whole-genome sequencing (WGS)-based precision diagnostics.²⁸ Therefore, the purpose of this study was to characterize the clinical and pathological phenotype of an EBS-affected calf, and to evaluate its possible genetic etiology using WGS.

2 | CASE DESCRIPTION

A 6-day-old (46 kg) male Belgian Blue-Holstein crossbred calf was submitted for clinical investigation because of ulcerations of the skin and nasal planum since short time after birth. The animal was delivered after a gestation period of 287 days.

The cutaneous lesions were characterized by widespread irregular erosions and ulcerations of various sizes on most parts of the body (Figure 1A), but in particular on the limbs (Figure 1B) and over bony prominences. Upon handling, the epidermis easily separated leaving a blister with a black colored, nonhemorrhagic base indicating a separation superficial to the stratum basale. Peracute blister were easily induced by rubbing the skin by an eraser after having cut the hair locally. Older lesions consisted of ulcerations covered by crusts and occasional acute hemorrhage. On the nasal platum, lips and nares extensive ulcerations were present; the calf also showed a purulent nasal discharge (Figure 1C). Moreover, the animal seemed to be in pain when walking on a hard surface. The aspect resembled EB and therefore was further referred to the Danish surveillance program for genetic diseases in cattle for further examination. Because of the poor prognosis and the painful situation, the calf was euthanized for welfare reasons by IV administration of an overdose of pentobarbital. In addition to the skin lesions, gross pathologic examination revealed erosions in the oral cavity, pharynx, proximal esophagus, and rumen.

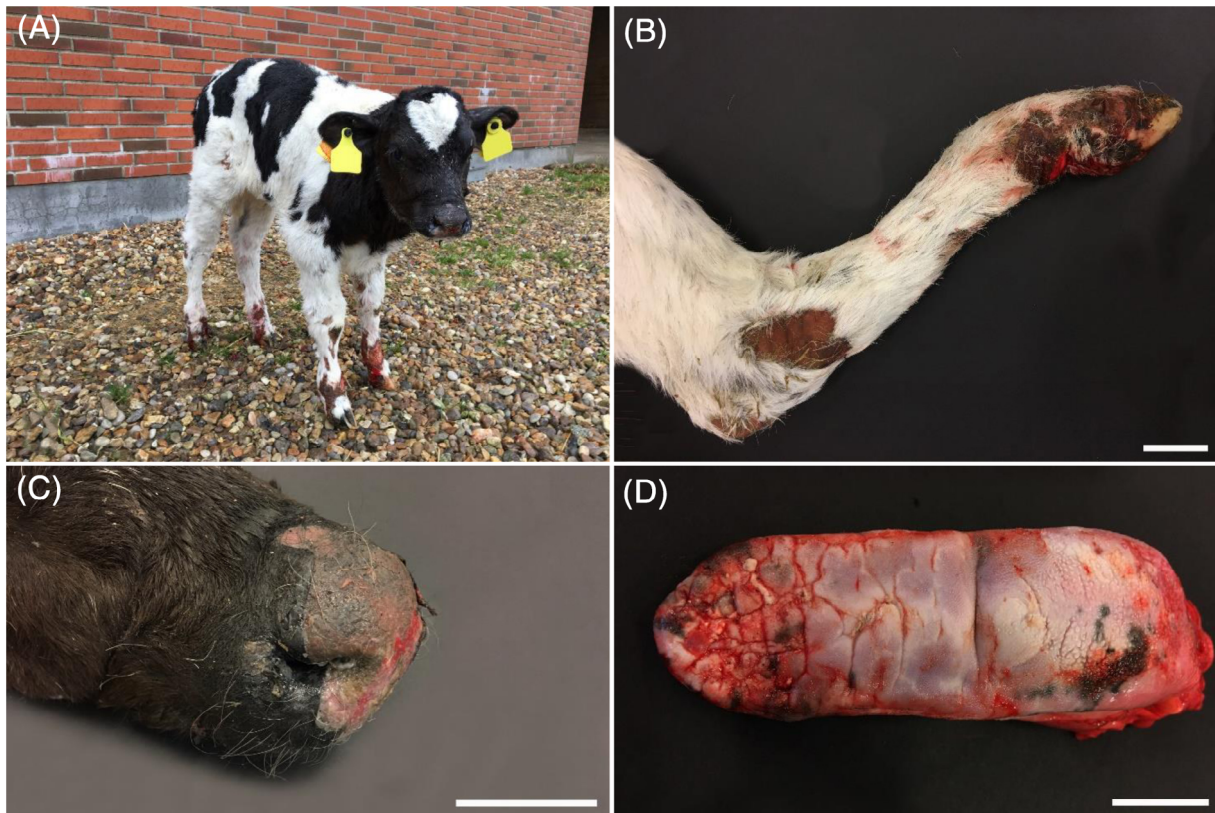


FIGURE 1 Lesions in the affected calf. A, Widespread irregular ulcerations of various sizes on most parts of the body. B, Irregular ulceration on the hindlimb. Scale bar = 5 cm. C, Extensive ulcerations on the nasal planum, lips and nares; also, purulent nasal discharge was present. Scale bar = 2.5 cm. D, Thickened and the furrows of the epithelium on the dorsal surface of the tongue. Scale bar = 5 cm

The epithelium on the dorsal surface of the tongue was thickened and with furrows (Figure 1D). The incisor teeth were disorganized and not completely erupted and the surrounding parts of the mandibles appeared thickened and cystic. The hoofs seemed intact, yet when sawed longitudinally, the capsule was partly separated from the dermal lamella with hemorrhage in the interface.

Immediately before euthanasia, the skin covering the dorsal part of the pelvis was gently scrubbed with an eraser with blister formation. Skin biopsies from this area and from other representative cutaneous lesions were taken immediately after euthanasia for histological analysis, whereas the necropsy was completed at the university a few hours later. Additional specimens for histological analysis were then collected, including the oral mucosa, pharynx, rumen, reticulum, and major internal organs. All collected samples were fixed in 10% neutral buffered formalin, trimmed, processed, embedded in paraffin wax, sectioned at 4 to 5 μm , and stained by hematoxylin and eosin (HE). Histologically, the peracute lesions induced by rubbing before euthanasia displayed a very striking, multifocal to coalescing dermal-epidermal separation at the level of the basal layer, which extended into the wall of the hair follicle infundibula (Figure 2). The spontaneously occurring,

chronic lesions present in the nasal planum and in the distal limbs displayed a multifocal to coalescing epithelial loss with consequent severe ulceration and underlying neutrophilic infiltration, replacement of the papillary dermis by granulation tissue, and re-epithelialization. A multifocal dermal-epidermal separation at the level of the basal cell layer with multifocal underlying accumulation of free erythrocytes and fibrin exudation was occasionally visible at the border of the ulcerated areas.

In the tongue, the mucosa of the dorsal surface showed a marked parakeratotic hyperkeratosis. At the lateral borders, where the epithelium had a normal thickness, areas with complete loss of mucosa were observed. The superficial layer of the submucosal connective tissue had a necrotic surface, intense hyperemia, and infiltration with neutrophils. Mucosa cleavage in the adjacent areas was not observed, but the height of the epithelium gradually decreased. The stratum spinosum showed ballooning degeneration and in these areas, the stratum corneum was not present. In the pharyngeal lining, multiple intensely inflamed ulcers covered by a debris of fibrin, degenerated neutrophils, erythrocytes, bacterial colonies were present.

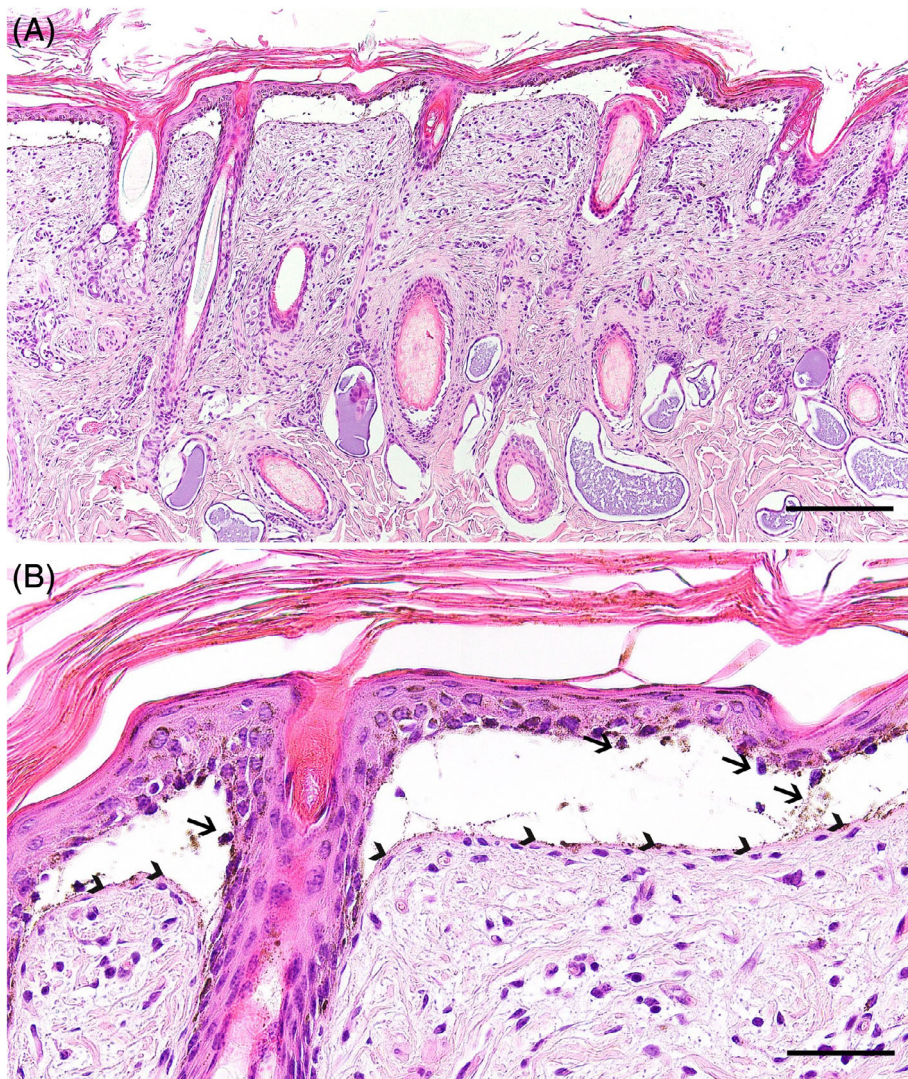


FIGURE 2 Histopathological findings of the affected calf. A, The peracute cutaneous lesions displayed an extensive dermal-epidermal separation at the level of the basal layer, which also affected the wall of the hair follicle infundibula. HE staining, scale bar = 200 μm . B, Higher magnification of the dermal-epidermal detachment at the basal cell layer level, where it is possible to observe the presence of occasional basal cell remains within the cleft (arrows) and the basement membrane overlying the dermis (arrowheads). HE staining, scale bar = 50 μm

The epithelium of the rumen and reticulum was normally developed but an acute suppurative multifocal rumenitis was present. Separation of the epithelium from the underlying submucosa was seen in some areas but considered as a post mortem artifact. Additional findings included suppurative periportal hepatitis and multifocal intense pulmonary hyperemia associated with fibrin in the alveoli. Other tissues were unremarkable. The histopathological findings in the skin and pharyngeal linings resembled EBS.

Additionally, WGS using the Illumina NovaSeq6000 was performed on DNA extracted from ethylenediaminetetraacetic acid (EDTA) blood of the calf. The sequenced reads were mapped to the ARS-UCD1.2 reference genome resulting in an average read depth of approximately 19x,²⁹ and single-nucleotide variants and small indel variants were called. The applied software and steps to process fastq files into binary alignment map and genomic variant call format files were in accordance with the 1000 Bull Genomes Project processing guidelines of run 7 (www.1000bullgenomes.com),³⁰ except for the trimming, which was performed using fastp.³¹ Further preparation of the genomic data had been done according to Häfliger et al.³² In order to find private variants, we compared the genotypes of the affected calf with 493 cattle genomes of various breeds that had been sequenced in the course of other ongoing studies and that are publicly available (Table S2) in the European Nucleotide Archive (SAMEA6528898 is the sample accession number of the case; <http://www.ebi.ac.uk/en>). Integrative Genomics Viewer (IGV)³³ software was used for visual inspection of candidate variants. A total of 115 private protein-changing variants with a moderate or high predicted impact on the encoded protein, located within 108 different genes or loci, were identified. These variants were further checked for their occurrence in a global control cohort of 3103 genomes of a variety of breeds (1000 Bull Genomes Project run 7; www.1000bullgenomes.com), which revealed 26 protein-changing variants exclusively present heterozygous in the genome of the EBS-affected calf. These 26 variants located within 25 different genes or loci (Table S3) were subsequently visually inspected using IGV software confirming all as true variants. Of all these 26 remaining private variants, only 1 occurred in a candidate for EB: keratin 5 (*KRT5*). The variant was a heterozygous disruptive in-frame deletion variant on chromosome 5: 27367604delCAA (NM_001008663.1:c.534_536delCAA), leading to a loss of an asparagine amino acid at residue 178 of the encoded *KRT5* protein (NP_001008663.1:p.Asn178del). This variant affecting an EB candidate gene was further investigated as likely causal mutation for the observed phenotype.

To confirm that the c.534_536delCAA variant in *KRT5* was a de novo mutation, the affected genomic region was amplified by polymerase chain reaction (PCR) and Sanger sequenced in the affected calf, its Belgian Blue sire and Holstein dam based on DNA extracted from EDTA blood of the dam, and from both EDTA blood and semen of the sire. PCR products were amplified using flanking primers for the *KRT5* exon 1 deletion with 5'-AGGCATCCAAGAGGTCACCG-3' (forward primer) and 5'-TAGCACATATCCCACACTCATGG-3' (reverse primer). Sequence data were analyzed using Sequencher 5.1 (GeneCodes). Analyzing the sequencing data, we concluded that only the EBS-affected calf was heterozygous for the *KRT5* variant and the dam and sire were

both homozygous for the wild type allele in all analyzed samples including both semen and blood of the sire (Figure 3).

3 | DISCUSSION

The clinical and pathological findings in the calf were consistent with EB. Although most lesions had the appearance of unspecific inflamed ulcerations, which usually develop shortly after dermal-epidermal separation, blistering could be easily induced in intact skin by rubbing the skin surface. Histopathological analysis of these lesions showed that the dermal-epidermal separation occurred at the level of the basal cell layer, which is suggestive for EBS.

The predicted deleterious protein effect c.534_536delCAA variant and the conservation of the affected asparagine amino acid residue at position 178 in the helix initiation motif (HIM) of the highly conserved 1A rod domain of *KRT5* suggest that this de novo mutation variant is certainly pathogenic (Figure 4). The mutation most likely occurred post-zygotically during the calf's fetal development as it was absent in both parents. In cattle, a de novo missense variant in *KRT5* is reported in an asymptomatic Friesian-Jersey crossbred mosaic sire and EBS-affected offspring. That mutation results in an amino acid exchange (p.Glu478Lys) in the final glutamic acid of the KLEGE motif of the highly conserved 2B rod domain of *KRT5* (Figure 4).²⁰

The early onset combined with multifocal to widespread lesions in the skin and mucosal membranes classifies this condition as a severe form of EB. The reported bovine *KRT5* associated EB case also had such lesions²⁰; this indicates that mutations in the *KRT5* in cattle might cause severe EBS when present. Histologically the present case showed suppurative rumenitis and rumen epithelial detachment. Because of the delayed necropsy, the latter might have been a post mortem artifact. However, no ulcerations were observed in the forestomach and inflamed areas were covered by an epithelium, therefore a possible association with EB remains hypothetical.

The case of EB presented in this study can be classified as EBS. In humans, among the several subtypes reported in the literature, the most common EBS subtypes might be considered the so-called localized, severe, and intermediate form. In the localized EBS, the blisters are present only on the extremities of the limbs. Rare phenotypical subtypes of localized EBS are associated with nephropathy.³⁴ In severe forms of EBS the lesions are present from birth, are more diffuse on the body, with main severity on the extremities and over bone prominences, and deep ulceration might be observed. After some time, large tense blisters might arise spontaneously or secondary to minor trauma. The blisters characteristically have an arciform pattern and eventuate with crusts to necrosis with a visual similarity to inflammatory plaques.¹ Also, the oral mucosa might be affected. Some phenotypical subtypes of the severe EBS are accompanied by other systemic complications with subsequent growth retardation, nutritional deficiency or even lethal outcome because of secondary infections or respiratory failure.³⁵ In intermediate EBS the skin lesions are diffuse on the body, however they are not so serious as in the severe

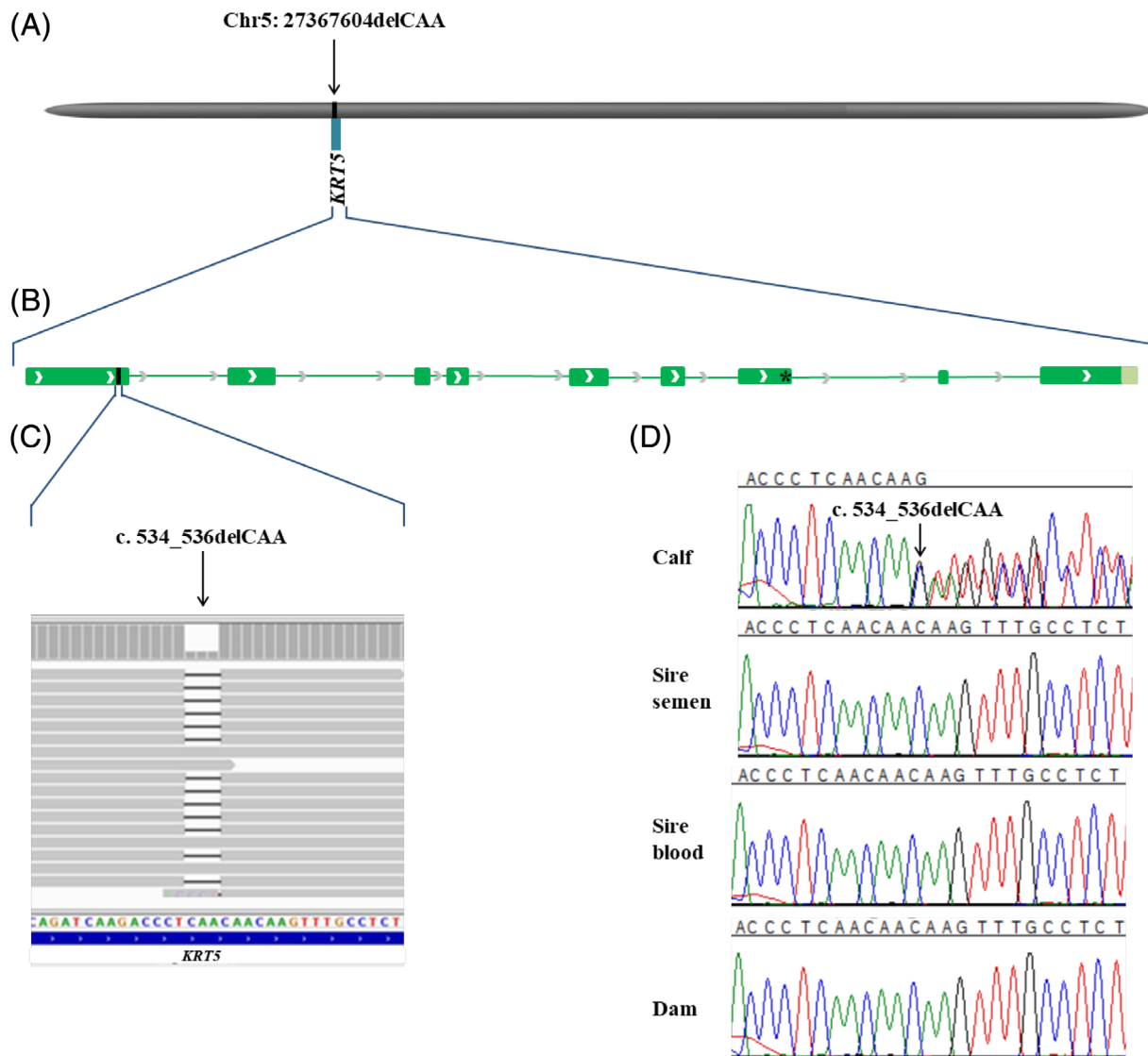


FIGURE 3 Schematic diagram of the *KRT5* gene showing the location of the candidate causal variant NM_001008663.1:c.534_536delCAA of the affected calf. A, Location of the bovine *KRT5* gene, Chr5:27 367 078-27 372 929 and causal variant, Chr5:27 367 604 on the ARS-UCD1.2 bovine genome assembly. B, Genomic structure of *KRT5* gene. Green boxes represent the exons. The c.534_536delCAA is located in the 1st exon of *KRT5* gene. The previous reported g.27371128G>A missense variant is located in the 7th exon of *KRT5* gene. C, Integrative Genomics Viewer (IGV) screenshot presenting the *KRT5* variant. D, Sanger sequencing results confirmed that the variant occurred de novo as sequencing of PCR products from DNA of both parents (for the sire both semen and blood) showed that the variant was absent

EBS. Rare phenotypical subtypes of intermediate EBS are accompanied by cardiomyopathy^{36,37} and muscular dystrophy.^{38,39}

In human, intermediate EBS with muscular dystrophy is often associated with enamel hypoplasia.³⁹ Furthermore, beyond the characteristic skin lesions, it might include diffuse alopecia, short stature, slow weight gain, punctate keratitis, urethral strictures, muscular dystrophy, and degenerative changes with increased connective tissue.³⁵ Such findings were not observed in the studied calf.

In human medicine, a de novo missense variant in *KRT5* resulting in an amino acid exchange (p.Asn177Ser) in the HIM has been reported in a patient with localized EBS.⁴⁰ This human *KRT5* protein position corresponds to the position of the p.Asn178del variant

present in this case. In human medicine, the localized, severe, and intermediate subtypes of the EBS are mostly linked to an autosomal dominant pattern and are associated to a high rate of de novo mutations. The mutation in the present case was in that aspect similar to the human cases, in that it was autosomal dominant and of de novo origin. The most common mutations are caused by monoallelic pathogenic missense, nonsense, frameshift, or splice site variants or in frame deletions in *KRT5* and *KRT14*.⁴¹ However, rare EBS subtypes might be associated with pathogenic variants in other genes, such as *EXPH5*,⁴² *KLHL24*,⁴³ *DST*,⁴⁴ *PLEC*,⁴⁵⁻⁴⁸ and *CD151*.³⁴

Epidermolysis bullosa simplex is a rare disorder known in man and animals. Rare disorders such as EBS in livestock are usually not

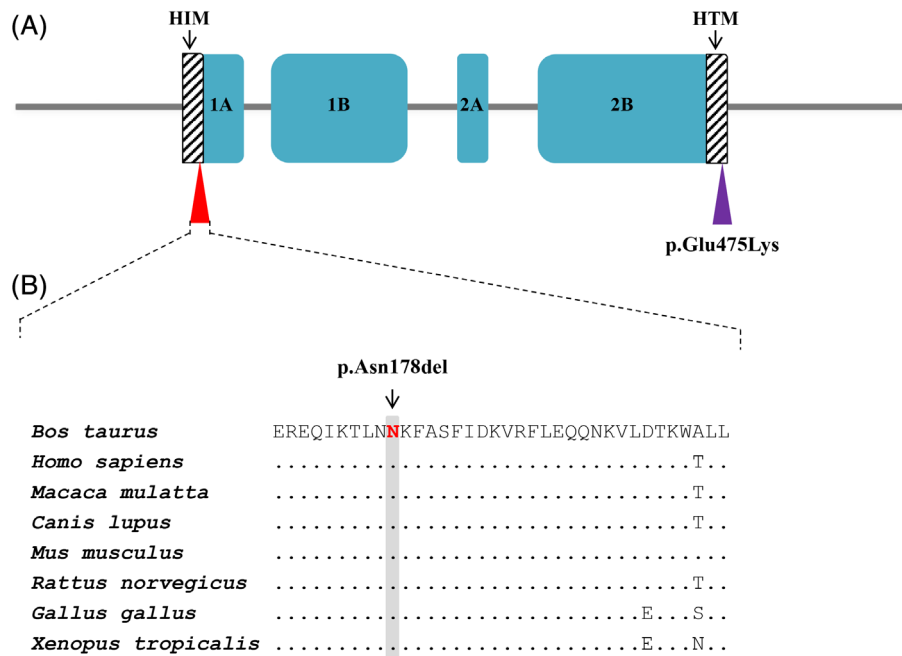


FIGURE 4 Schematic diagram of the KRT5 protein. A, Domain and region information of KRT5 protein obtained from the UniProt database (<http://www.uniprot.org/>; accession number: Q5XQN5). The p.Asn178del variant in the helix initiation peptide motif (HIM) is indicated by the red triangle. The EBS-causing p.Glu475Lys variant previously reported²⁰ in the helix termination peptide motif (HTM) is indicated by a violet triangle. The arrows indicate the HIM and the HTM. B, Multiple sequence alignment of 1A rod domain of the KRT5 protein encompassing the region of the p.Asn178del variant demonstrates a complete evolutionary conservation across species. The observed variant is indicated by an arrow and the respective position highlighted in gray. Protein sequences accession numbers in NCBI for each species are NP_001008663.1 (*Bos taurus*), NP_000415.2 (*Homo sapiens*), XP_002798641.1 (*Macaca mulatta*), XP_005636850.1 (*Canis familiaris*), NP_081287.1 (*Mus musculus*), NP_899162.1 (*Rattus norvegicus*), NP_001001195.1 (*Gallus gallus*), and NP_001072377.1 (*Xenopus tropicalis*)

diagnosed to the molecular level, mainly because of lack of resources and diagnostic tools as well as low value and often-short lifespan of the animals. The report of this case allowed the performance of a complete clinical, pathological, and molecular genetic study enabling the diagnosis of a severe form of EBS. Furthermore, this example highlights the utility of WGS-based precision diagnostics for understanding rare disorders in animals with an available reference genome sequence and the value of surveillance of cattle breeding populations for harmful genetic disorders.

ACKNOWLEDGMENTS

No funding was received for this study. The authors acknowledge the Next Generation Sequencing Platform of the University of Bern for performing the whole-genome sequencing and the Interfaculty Bioinformatics Unit of the University of Bern for providing computational infrastructure. The whole-genome sequencing data are available under the study accession no. PRJEB18113 at the European Nucleotide Archive (www.ebi.ac.uk/ena; sample accessions SAMEA6528898). Monika Welle from the Institute of Veterinary Pathology of the University of Bern is acknowledged for the fruitful case discussion.

CONFLICT OF INTEREST DECLARATION

Authors declare no conflicts of interests.

OFF-LABEL ANTIMICROBIAL DECLARATION

Authors declare no off-label use of antimicrobials.

INSTITUTIONAL ANIMAL CARE AND USE COMMITTEE (IACUC)

This study was not based on an invasive animal experiment but was based on a spontaneously occurring case; therefore, there are no associated permit numbers.

HUMAN ETHICS APPROVAL DECLARATION

Authors declare human ethics approval was not needed for this study.

ORCID

Joana G. P. Jacinto <https://orcid.org/0000-0002-6438-7975>

Irene M. Häfliger <https://orcid.org/0000-0002-5648-963X>

Inês M. B. Veiga <https://orcid.org/0000-0001-8554-790X>

Cord Drögemüller <https://orcid.org/0000-0001-9773-522X>

Jørgen S. Agerholm <https://orcid.org/0000-0003-1653-4552>

REFERENCES

1. Fine JD, Bruckner-Tuderman L, Eady RAJ, et al. Inherited epidermolysis bullosa: updated recommendations on diagnosis and classification. *J Am Acad Dermatol.* 2014;70(6):1103-1126. <https://doi.org/10.1016/j.jaad.2014.01.903>.

2. Has C, Liu L, Bolling MC, et al. Clinical practice guidelines for laboratory diagnosis of epidermolysis bullosa. *Br J Dermatol*. 2020;182(3):574-592.
3. Has C, Fischer J. Inherited epidermolysis bullosa: new diagnostics and new clinical phenotypes. *Exp Dermatol*. 2019;28(10):1146-1152.
4. Has C, Bauer JW, Bodemer C, et al. Consensus reclassification of inherited epidermolysis bullosa and other disorders with skin fragility. *Br J Dermatol*. 2020;183(4):1-14. <https://doi.org/10.1111/bjd.18921>.
5. Has C, Bruckner-Tuderman L. The genetics of skin fragility. *Annu Rev Genomics Hum Genet*. 2014;15:245-268.
6. Peters M, Reber I, Jagannathan V, Raddatz B, Wohlsein P, Drögemüller C. DNA-based diagnosis of rare diseases in veterinary medicine: a 4.4 kb deletion of ITGB4 is associated with epidermolysis bullosa in Charolais cattle. *BMC Vet Res*. 2015;11(1):1-8.
7. Sartelet A, Harland C, Tamma N, et al. A stop-gain in the laminin, alpha 3 gene causes recessive junctional epidermolysis bullosa in Belgian Blue cattle. *Anim Genet*. 2015;46(5):566-570.
8. Murgiano L, Wiedemar N, Jagannathan V, Isling LK, Drögemüller C, Agerholm JS. Epidermolysis bullosa in Danish Hereford calves is caused by a deletion in LAMC2 gene. *BMC Vet Res*. 2015;11(1):23.
9. Menoud A, Welle M, Tetens J, Lichtner P, Drögemüller C. A COL7A1 Mutation Causes Dystrophic Epidermolysis Bullosa in Rotes Höhenvieh Cattle. *PLoS ONE*. 2012;7(6):e38823. <http://dx.doi.org/10.1371/journal.pone.0038823>.
10. Mauldin EA, Wang P, Olivry T, Henthorn PS, Casal ML. Epidermolysis bullosa simplex in sibling Eurasier dogs is caused by a PLEC non-sense variant. *Vet Dermatol*. 2017;28(1):10-e3.
11. Capt A, Spirito F, Guaguere E, Spadafora A, Ortonne JP, Meneguzzi G. Inherited junctional epidermolysis bullosa in the German pointer: establishment of a large animal model. *J Invest Dermatol*. 2005;124(3):530-535. <https://doi.org/10.1111/j.0022-202X.2004.23584.x>.
12. Niskanen J, Dillard K, Arumilli M, et al. Nonsense variant in COL7A1 causes recessive dystrophic epidermolysis bullosa in Central Asian Shepherd dogs. *PLoS One*. 2017;12(5):1-10.
13. Baldeschi C, Gache Y, Rattenholl A, et al. Genetic correction of canine dystrophic epidermolysis bullosa mediated by retroviral vectors. *Hum Mol Genet*. 2003;12(15):1897-1905.
14. Suárez-Vega A, Gutiérrez-Gil B, Benavides J, et al. Combining GWAS and RNA-Seq approaches for detection of the causal mutation for hereditary junctional epidermolysis bullosa in sheep. *PLoS One*. 2015;10(5):e0126416.
15. Mönke S, Kerkmann A, Wöhleke A, et al. A frameshift mutation within LAMC2 is responsible for herlitz type junctional epidermolysis bullosa (HJEB) in black headed mutton sheep. *PLoS One*. 2011;6(5):e18943.
16. Graves KT, Henney PJ, Ennis RB. Partial deletion of the LAMA3 gene is responsible for hereditary junctional epidermolysis bullosa in the American Saddlebred Horse. *Anim Genet*. 2009;40(1):35-41.
17. Cappelli K, Brachelente C, Passamonti F, Flati A, Silvestrelli M, Capomaccio S. First report of junctional epidermolysis bullosa (JEB) in the Italian draft horse. *BMC Vet Res*. 2015;11(1):2-5.
18. Milenkovic D, Chaffaux S, Taourit S, Guérin G. A mutation in the LAMC2 gene causes the Herlitz junctional epidermolysis bullosa (H-JEB) in two French draft horse breeds. *Genet Sel Evol*. 2003;35:249-256.
19. Spirito F, Charlesworth A, Linder K, Ortonne JP, Baird J, Meneguzzi G. Animal models for skin blistering conditions: absence of laminin 5 causes hereditary junctional mechanobullous disease in the Belgian horse. *J Invest Dermatol*. 2002;119(3):684-691. <https://doi.org/10.1046/j.1523-1747.2002.01852.x>.
20. Ford CA, Stanfield AM, Spelman RJ, et al. A mutation in bovine keratin 5 causing epidermolysis bullosa simplex, transmitted by a mosaic sire. *J Invest Dermatol*. 2005;124(6):1170-1176. <https://doi.org/10.1111/j.0022-202X.2005.23610.x>.
21. Bassett H. A congenital bovine epidermolysis resembling epidermolysis bullosa simplex of man. *Vet Rec*. 1987;121:8-11.
22. Thompson KG, Crandell RA, Rugeley WW, Sutherland RJ. A mechanobullous disease with sub-basilar separation in Brangus calves. *Vet Pathol*. 1985;22:283-285.
23. Foster AP, Skuse AM, Higgins RJ, et al. Epidermolysis Bullosa in calves in the United Kingdom. *J Comp Pathol*. 2010;142(4):336-340. <https://doi.org/10.1016/j.jcpa.2009.10.001>.
24. Deprez P, Maenhout T, De Cock H, et al. Epidermolysis bullosa in a calf: a case report [in Dutch]. *Vlaams Diergeneesk Tijdschr*. 1993;62:155-159.
25. Agerholm JS. Congenital generalized epidermolysis bullosa in a calf. *Zentralbl Veterinarmed A*. 1994;41:139-142.
26. Stocker H, Lott G, Straumann U, Rüschi P. Epidermolysis bullosa in a calf [in German]. *Tierarztl Prax*. 1995;23:123-126.
27. Medeiros GX, Riet-Correa F, Armien AG, Dantas AFM, de Galiza GJN, Simões SVD. Junctional epidermolysis bullosa in a calf. *J Vet Diagnostic Investig*. 2012;24(1):231-234.
28. Bourneuf E, Otz P, Pausch H, et al. Rapid discovery of de novo deleterious mutations in cattle enhances the value of livestock as model species. *Sci Rep*. 2017;7(1):1-19.
29. Rosen BD, Bickhart DM, Schnabel RD, et al. De novo assembly of the cattle reference genome with single-molecule sequencing. *Gigascience*. 2020;9(3):1-9.
30. Hayes BJ, Daetwyler HD. 1000 bull genomes project to map simple and complex genetic traits in cattle: applications and outcomes. *Annu Rev Anim Biosci*. 2019;7:89-102.
31. Chen S, Zhou Y, Chen Y, Gu J. Fastp: an ultra-fast all-in-one FASTQ preprocessor. *Bioinformatics*. 2018;34(17):i884-i890.
32. Häfliger IM, Wiedemar N, Švara T, et al. Identification of small and large genomic candidate variants in bovine pulmonary hypoplasia and anasarca syndrome. *Anim Genet*. 2020;51(3):382-390.
33. Robinson JT, Thorvaldsdóttir H, Wenger AM, Zehir A, Mesirov JP. Variant review with the integrative genomics viewer. *Cancer Res*. 2017;77(21):e31-e34.
34. Crew VK, Burton N, Kagan A, et al. CD151, the first member of the tetraspanin (TM4) superfamily detected on erythrocytes, is essential for the correct assembly of human basement membranes in kidney and skin. *Blood*. 2004;104(8):2217-2223.
35. Fine JD, Johnson LB, Weiner M, Suchindran C. Cause-specific risks of childhood death in inherited epidermolysis bullosa. *J Pediatr*. 2008;152(2):276-280.e2.
36. Schwieger-Briel A, Fuentes I, Castiglia D, et al. Epidermolysis bullosa simplex with KLHL24 mutations is associated with dilated cardiomyopathy. *J Invest Dermatol*. 2019;139(1):244-249.
37. Bolling MC, Pas HH, De Visser M, et al. PLEC1 mutations underlie adult-onset dilated cardiomyopathy in epidermolysis bullosa simplex with muscular dystrophy. *J Invest Dermatol*. 2010;130(4):1178-1181.
38. Kyrova J, Kopeckova L, Buckova H, et al. Epidermolysis bullosa simplex with muscular dystrophy. Review of the literature and a case report. *J Dermatol Case Rep*. 2016;10(3):39-48.
39. OMIM. Online Mendelian Inheritance in Man: phenotype 226670 Epidermolysis bullosa simplex with muscular dystrophy; EBSMD [Internet]. [https://omim.org/entry/226670?search=epidermolysis bullosa simplex with teeth alterations&highlight=alteration bullosa epidermolysi simplex tooth with](https://omim.org/entry/226670?search=epidermolysis%20bullosa%20simplex%20with%20teeth%20alterations&highlight=alteration%20bullosa%20epidermolysi%20simplex%20tooth%20with). Accessed March 30, 2020.
40. Liovic M, Bowden PE, Marks R, Komel R. A mutation (N177S) in the structurally conserved helix initiation peptide motif of keratin 5 causes a mild EBS phenotype. *Exp Dermatol*. 2004;13(5):332-334.
41. Szeverenyi I, Cassidy AJ, Cheuk WC, et al. The human intermediate filament database: comprehensive information on a gene family involved in many human diseases. *Hum Mutat*. 2008;29(3):351-360.
42. Turcan I, Pasmooij AMG, Van Den Akker PC, Lemmink H, Sinke RJ, Jonkman MF. Association of epidermolysis bullosa simplex with mottled pigmentation and EXPH5 mutations. *JAMA Dermatol*. 2016;152(10):1137-1141.

43. Lee JYW, Liu L, Hsu CK, et al. Mutations in KLHL24 add to the molecular heterogeneity of epidermolysis bullosa simplex. *J Invest Dermatol.* 2017;137(6):1378-1380.
44. Groves RW, Liu L, Dopping-Hepenstal PJ, et al. A homozygous nonsense mutation within the dystonin gene coding for the coiled-coil domain of the epithelial isoform of BPAG1 underlies a new subtype of autosomal recessive epidermolysis bullosa simplex. *J Invest Dermatol.* 2010;130(6):1551-1557. <https://doi.org/10.1038/jid.2010.19>.
45. Koss-Harnes D, Høyheim B, Anton-Lamprecht I, et al. A site-specific plectin mutation causes dominant epidermolysis bullosa simplex Onga: two identical de novo mutations. *J Invest Dermatol.* 2002;118(1):87-93.
46. Smith FJ, Eady RA, Leigh IM, et al. Plectin deficiency results in muscular dystrophy with epidermolysis bullosa. *Nat Genet.* 1996;13(4):450-457. <https://doi.org/10.1038/ng0896-450>.
47. Pfindner E, Uitto J. Plectin gene mutations can cause epidermolysis bullosa with pyloric atresia. *J Invest Dermatol.* 2005;124(1):111-115. <https://doi.org/10.1111/j.0022-202X.2004.23564.x>.
48. Argyropoulou Z, Liu L, Ozoemena L, et al. A novel PLEC nonsense homozygous mutation (c.7159G>T; p.Glu2387*) causes epidermolysis bullosa simplex with muscular dystrophy and diffuse alopecia: a case report. *BMC Dermatol.* 2018;18(1):1-5.

SUPPORTING INFORMATION

Additional supporting information may be found online in the Supporting Information section at the end of this article.

How to cite this article: Jacinto JGP, Häfliger IM, Veiga IMB, Drögemüller C, Agerholm JS. A de novo mutation in KRT5 in a crossbred calf with epidermolysis bullosa simplex. *J Vet Intern Med.* 2020;34:2800–2807. <https://doi.org/10.1111/jvim.15943>

4.1.4.2 A heterozygous missense variant in the *COL5A2* in Holstein cattle resembling the classical Ehlers–Danlos syndrome

Journal: animals

Manuscript status: published

Contributions: phenotype description, whole-genome sequencing data analysis, figures, writing original draft and revisions

Displayed version: published version

DOI: [10.3390/ani10112002](https://doi.org/10.3390/ani10112002)

Article

A Heterozygous Missense Variant in the *COL5A2* in Holstein Cattle Resembling the Classical Ehlers–Danlos Syndrome

Joana G. P. Jacinto ^{1,2,†}, Irene M. Häfliger ^{2,†}, Inês M. B. Veiga ^{3,†}, Anna Letko ²,
Cinzia Benazzi ¹, Marilena Bolcato ¹ and Cord Drögemüller ^{2,*}

¹ Department of Veterinary Medical Sciences, University of Bologna, 40064 Ozzano Emilia (Bologna), Italy; joana.goncalves2@studio.unibo.it (J.G.P.J.); cinzia.benazzi@unibo.it (C.B.); marilena.bolcato2@unibo.it (M.B.)

² Institute of Genetics, Vetsuisse Faculty, University of Bern, 3012 Bern, Switzerland; irene.haefliger@vetsuisse.unibe.ch (I.M.H.); anna.letko@vetsuisse.unibe.ch (A.L.)

³ Institute of Animal Pathology, Vetsuisse Faculty, University of Bern, 3012 Bern, Switzerland; ines.veiga@vetsuisse.unibe.ch

* Correspondence: cord.droegemueller@vetsuisse.unibe.ch

† These authors contributed equally to the work.

Received: 13 October 2020; Accepted: 28 October 2020; Published: 30 October 2020



Simple Summary: Genodermatoses represent inherited disorders of the skin that mostly follow a monogenic mode of inheritance. Heritable connective tissue disorders such as classical Ehlers–Danlos syndrome (cEDS) belong to this group of human rare diseases that sporadically occur in other species. Herein, affected cattle are reported showing skin lesions including cutis laxa clinically and pathologically resembling cEDS in humans. Microscopic findings in the deeper dermis were consistent with collagen dysplasia. Whole-genome sequencing (WGS) identified a most likely disease-causing mutation in the *COL5A2* gene. The *COL5A2* gene is known to be associated with dominant inherited cEDS forms in mice and humans, but so far, it was not shown to cause a similar phenotype in domestic animals. The disease phenotype examined herein showed co-segregation with the identified missense variant within the maternal line across two generations and is most likely due to a spontaneous mutation event. Rare non-lethal disorders such as cEDS in livestock are mostly not diagnosed, but might affect animal welfare and thus lower the value of affected animals. WGS-based precision diagnostics allows understanding rare disorders and supports the value of surveillance of cattle breeding populations for harmful genetic disorders.

Abstract: Classical Ehlers–Danlos syndrome (cEDS) is a heritable connective tissue disorder characterized by variable degrees of skin hyperextensibility and fragility, atrophic scarring, and generalized joint hypermobility. The purpose of this study was to characterize the clinicopathological phenotype of a cEDS-affected Holstein calf and to identify the causative genetic variant associated with the disorder by whole-genome sequencing (WGS). A 3-day-old female Holstein calf was referred because of easily induced skin detachment and hyperextensibility in the neck. A complete clinical investigation was performed in the calf, dam, and maternal-grandmother. The calf and dam showed hyperextensibility of the neck skin and atrophic scarring; additionally, the calf presented skin fragility. Moreover, the histopathology of biopsies from the calf and its dam showed that the collagen bundles in affected skin areas were wavy, short, thin, and surrounded by edema and moderate to severe acute hemorrhages. Genetic analysis revealed a private heterozygous missense variant in *COL5A2* (c.2366G>T; p.Gly789Val) that was present only in the calf and dam. This confirmed the diagnosis of cEDS and represents the first report of a causal variant for cEDS in cattle and the first *COL5A2*-related large animal model.

Keywords: *Bos taurus*; collagen dysplasia; collagen V; connective tissue; precision medicine; skin fragility; whole-genome sequencing

1. Introduction

Sporadically occurring, genodermatoses represent inherited disorders of the skin that mostly follow a monogenic mode of inheritance in livestock animals such as cattle [1]. Heritable connective tissue disorders, e.g., Ehlers–Danlos syndrome (EDS), belong to this group of human rare diseases. EDS encompasses a clinically- and heritably-heterogeneous group of connective tissue disorders (Online Mendelian Inheritance in Man (OMIM PS130000)) (<https://www.omim.org/phenotypicSeries/PS130000>) characterized by a variable degree of skin hyperextensibility, joint hypermobility, and tissue fragility. Currently, human EDS classification distinguishes 13 subtypes and 19 different associated genes mainly involved in collagen and extracellular matrix synthesis and maintenance reflecting the clinical and genetic heterogeneity [2]. Human EDS forms are grouped based on the underlying pathogenetic mechanisms related to primary structure and processing of collagen (*COL1A1*, *COL1A2*, *COL3A1*, *COL5A1*, *COL5A2*, *ADAMTS2*), collagen folding and cross-linking (*PLOD1*, *FKBP14*), structure and function of the myomatrix (*TNXB*, *COL12A1*), glycosaminoglycan biosynthesis (*B4GALT7*, *B3GALT6*, *CHST14*, *DSE*), complement pathway (*C1S*, *C1R*), and intracellular processes (*SLC39A13*, *ZNF469*, *PRDM5*) [3]. Classical EDS (cEDS) in humans is a rare autosomal dominant disorder predominantly associated with a deficiency of type V collagen (COLLV) encoded by the *COL5A1* and *COL5A2* genes, which is a quantitatively minor fibrillar collagen that presents a nearly ubiquitous distribution in a variety of connective tissues [4].

Various forms of EDS have been identified in many animal species (OMIA000327), including horses [5,6], dogs [7–9], cats [10], mink [11], rabbits [12], sheep [13–15], and cattle (OMIA000328-9913 (<https://www.omia.org/OMIA000328/9913/>); OMIA001716-9913 (<https://www.omia.org/OMIA001716/9913/>)) [16–18]. Pathogenic variants causing forms of EDS in animals have been identified in known candidate genes for EDS (*COL5A1*, *ADAMTS2*, *PLOD1*) [5,7,8,10,13,15,18], or novel genes (*EPYC*, *TNBX*, *PPIB*) discovered in EDS-affected domestic animals [6,9,17]. This highlights the potential of studying inherited conditions in such species to assign a role or function to previously uncharacterized genes or to add additional functions to known genes in regard to skin development [1].

In this study, we aimed to characterize the clinical and pathological phenotypes of a cEDS-affected Holstein calf and its dam, and to identify the causative genetic variant associated with the disorder using whole-genome sequencing (WGS).

2. Materials and Methods

2.1. Ethics Statement

This study did not require official or institutional ethical approval as it was not experimental, but rather part of clinical and pathological veterinary diagnostics. All animals in this study were examined with the consent of their owners and handled according to good ethical standards.

2.2. Clinicopathological Investigation

A 3-day-old female Holstein calf was referred by the farm veterinarian because of easily induced skin detachment in the neck and skin hyperextensibility shortly after birth. Upon specific request, the owner informed that its 3-year-old dam and its 6-year-old maternal-grandmother had also been presenting skin alterations for a long time, but was not able to specify since when. All three animals, the calf, its dam, and its maternal-grandmother, were clinically examined and a complete blood count (CBC) and blood chemistry profile were obtained. Blood samples from the calf and its dam were sent for routine viral and parasitological analysis (bovine viral diarrhea, bovine Schmallenberg virus,

bluetongue virus, *Neospora* spp., *Toxoplasma* spp.) using antigen-enzyme-linked immunosorbent assay (ELISA) and antibody-polymerase chain reaction (PCR). Three weeks later (calf's age = 29 days), skin biopsies using an 8 mm punch were obtained from the ulcerated cervical skin, from the skin surrounding the cervical ulceration, and from normal skin from the neck from the calf, as well as from the altered cervical skin from its dam. The collected samples were fixed in 10% neutral buffered formalin, trimmed, processed, embedded in paraffin wax, sectioned at 4 µm, and stained with haematoxylin and eosin (H&E) for further histological evaluation. Further clinical control was carried out after six months (calf's age = 7 months). All animals were housed in a freestall system.

2.3. DNA Samples

Genomic DNA was isolated from ethylenediaminetetraacetic acid (EDTA) blood samples from the calf and its dam; from EDTA blood sample, normal skin, and lesioned skin of the maternal-grandmother; and from the semen of the sire using Promega Maxwell RSC DNA system (Promega, Dübendorf, Switzerland).

2.4. Whole-Genome Sequencing

WGS using the Illumina NovaSeq6000 (Illumina Inc., San Diego, CA, USA) was performed on the genomic DNA of the calf. The sequenced reads were mapped to the ARS-UCD1.2 reference genome, resulting in an average read depth of approximately 17× [19], and single-nucleotide variants (SNVs) and small indel variants were called. The applied software and steps to process fastq files into binary alignment map (BAM) and genomic variant call format files were in accordance with the 1000 Bull Genomes Project processing guidelines of run 7 (www.1000bullgenomes.com) [20], except for the trimming, which was performed using fastp [21]. Further preparation of the genomic data was done according to Häfliger et al., 2020 [22]. In order to find private variants, we compared the genotypes of the affected calf with 496 cattle genomes of various breeds that had been sequenced in the course of other ongoing studies and that are publicly available (Table S1) in the European Nucleotide Archive (SAMEA7015115 is the sample accession number of the affected calf; <http://www.ebi.ac.uk/en>). Integrative Genomics Viewer (IGV) [23] software was used for visual inspection of genome regions containing possible candidate genes.

2.5. Targeted Genotyping

Polymerase chain reaction (PCR) and Sanger sequencing were used to validate and genotype the variant identified from WGS. PCR products from genomic DNA were amplified using AmpliTaq Gold 360 Master Mix (Thermo Fisher Scientific, Waltham, MA, USA) and the PCR amplicons were directly sequenced on an ABI3730 capillary sequencer (Thermo Fisher Scientific, Darmstadt, Germany). The *COL5A2* missense variant (XM_024979774.1:g.7331916G>T) was genotyped using the following primers: 5'- ACCAGGGCTTCAAGGTATGC-3' (forward primer) and 5'-CACCATGGGAACATGAGGCT-3' (reverse primer). The sequence data were analyzed using Sequencher 5.1 software (GeneCodes, Ann Arbor, MI, USA).

2.6. Protein Predictions

PROVEAN [24], MutPred2 [25], and PredictSNP1 [26] were used to predict the biological consequences of the discovered variant on protein. For multispecies sequence alignments, the following National Center for Biotechnology Information (NCBI) proteins accessions were used: XP_024835542.1 (*Bos taurus*), NP_000384.2 (*Homo sapiens*), XP_001164152.1 (*Pan troglodytes*), XP_002799008.1 (*Macaca mulatta*), XP_005640450.1 (*Canis lupus*), NP_031763.2 (*Mus musculus*), NP_445940.1 (*Rattus norvegicus*), XP_004942453.1 (*Gallus gallus*), NP_001139254.1 (*Danio rerio*), and XP_002931546.2 (*Xenopus tropicalis*).

2.7. Sequence Accessions

All references to the bovine *COL5A2* gene correspond to the NCBI accessions NC_037329.1 (chromosome 2, ARS-UCD1.2), XM_024979774 (*COL5A2* mRNA), and XP_024835542.1 (*COL5A2* protein). For the protein structure of *COL5A2*, the Uniprot database (<https://www.uniprot.org/>) accession number A0A3Q1MDT9 was used.

3. Results

3.1. Clinical Phenotype

On clinical investigation, the calf, its dam, and its maternal-grandmother were found to be clinically healthy with the exception of the skin alterations. Particular clinical examination of the cardiovascular, respiratory, urinary, musculoskeletal, and nervous systems showed no abnormalities. Moreover, no joint hypermobility was observed. The blood investigation of the calf showed a moderate monocytosis ($1760/\text{mm}^3$), a mild neutrophilia ($4650/\text{mm}^3$), a mild hypocholesterolemia (47 mg/dL), and a mild hypoproteinemia (6.10 g/dL) with hypoalbuminemia (2.82 g/dL). No abnormalities were detected in the CBC and chemistry profiles of the dam and maternal-grandmother. Blood viral analysis revealed positivity for bovine Schmallenberg virus using antigen-ELISA in the calf, and positivity for bovine viral diarrhoea using antigen-ELISA in the calf and its dam. The animals tested negative for all the remaining viral and parasitological analyses.

The integumentary system examination at 3 days of age of the calf revealed a symmetrical, bilateral ulceration secondary to minor trauma, delimited cranially by the occipital region, caudally by the cranial margin of the scapula, and ventrally by the sternocephalic muscles (Figure 1a). The ulcerated surface was dry, non-painful, non-bleeding, and pinkish with the presence of purulent material at the edges. During palpation, at the wound edges, a spontaneous detachment of the skin from the subcutaneous tissue was noticed. Furthermore, the animal presented hyperextensibility of the skin mostly in the neck. At 29 days of age, the previously observed neck wound was dry, scabby, and crustose with the edges of the lesion firmly embedded in the subcutaneous tissue; atrophic scarring was also present (Figure 1b). At seven months, the calf's lesions were similar to its dam, and characterized by multiple wrinkles, folds, papyraceous scars, cutis laxa, and hyperextensibility of the neck skin (Figure 1c).

Examination of the dam revealed multiple wrinkles, folds, papyraceous scars, cutis laxa, and hyperextensibility of the neck skin (Figure 2a,b). Moreover, its maternal-grandmother showed milder skin lesions in the ventral part of the neck at the level of the larynx, characterized by the presence of bald areas and scabs (Figure S1).

Based on these clinical observations, the calf and its dam were consequently suspected to suffer from cEDS, while the skin lesions observed in the maternal-grandmother were suspected to be acquired as the skin has been traumatised by recurring long-term mechanical stress of the feed fence.

3.2. Histopathological Phenotype

Histologically, the epidermis at the level of the cervical lesion of the calf displayed a severe, diffuse ulceration, with underlying proliferation of mature granulation tissue associated with neovascularisation, abundant neutrophilic superficial infiltrates, and adnexal structure loss (Figure 3a). The epidermis at the border of the ulcerated area displayed abundant serocellular crusts associated with serum lake formation, spongiosis, and ballooning degeneration of the stratum granulosum. Multifocal perivascular, moderate lymphoplasmacytic infiltrates could be observed in the dermis underlying the ulcerated area. The deeper dermis displayed interlacing, wavy, short, thin collagen bundles, which were surrounded by a moderate interstitial edema, as well as moderate to severe acute hemorrhages (Figure 3a).



Figure 1. Neck skin lesions of the classical Ehlers–Danlos syndrome (cEDS)-affected Holstein calf. (a) Calf age = 3 days: severe, extensive ulceration secondary to minor trauma; note the spontaneous detachment of the skin from the subcutaneous tissue. (b) Calf age = 29 days: atrophic scarring; note the scabby and crustose wound with the edges firmly embedded in the subcutaneous tissue. (c) Calf age = 7 months: papyraceous scars and cutis laxa.



Figure 2. Neck skin lesions of the cEDS-affected Holstein dam. (a) Note the multiple wrinkles, folds, papyraceous scars and cutis laxa. (b) Details of the neck skin lesion.

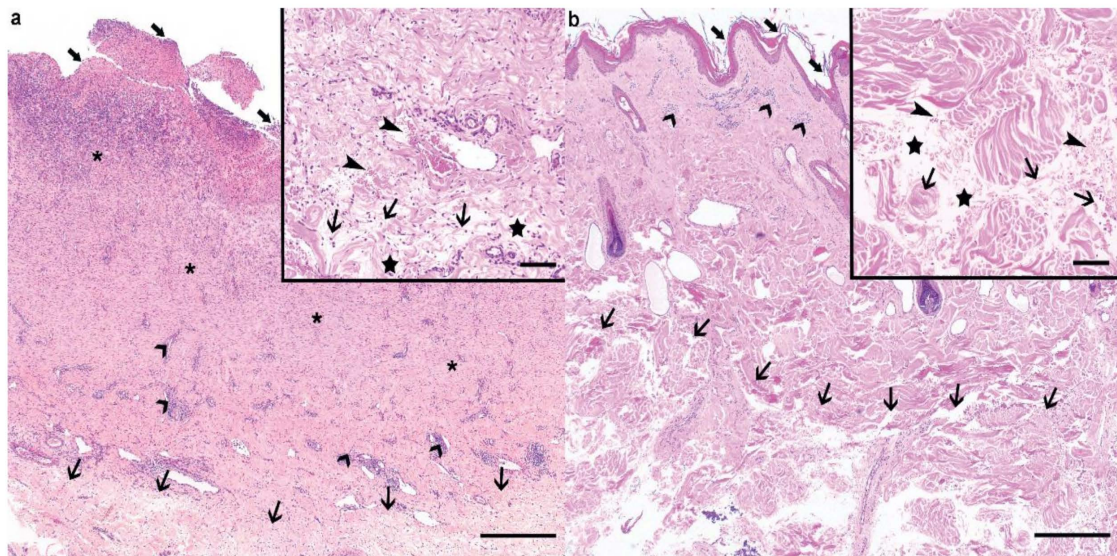


Figure 3. Histological findings of the cEDS-affected Holstein calf and its dam. (a) The ulcerated (large arrows) cervical lesion from the calf displayed a prominent granulation tissue proliferation (asterisks) associated with neovascularization and severe neutrophilic infiltration. Moderate, lymphoplasmacytic perivascular infiltrates were visible in the superficial dermis (large arrowheads). Within the deeper dermis, the collagen bundles were loose and irregular (thin arrows). Haematoxylin and eosin (H&E), bar 500 μm . Inset: higher magnification of the affected connective tissue within the deeper dermis. The collagen bundles were wavy, short, and thin (thin arrows), and surrounded by edema (stars) and acute hemorrhage (thin arrowheads) in the absence of vascular changes. Haematoxylin and eosin (H&E), bar 100 μm . (b) In the dam, the epidermis was irregular, mildly hyperplastic, and layered by large amount of lamellar to compact, orthokeratotic keratin (large arrows). Mild to moderate, perivascular lymphocytic and plasmacellular infiltrates were visible in the superficial dermis (large arrowheads), while similar changes to the ones described in the calf could be observed in the deeper dermis (thin arrows). Haematoxylin and eosin (H&E), bar 500 μm . Inset: Higher magnification of the affected connective tissue within the deeper dermis. Similar changes to the ones observed in the calf could be observed, namely, wavy, short, and thin collagen bundles (thin arrows), interstitial edema (stars), and acute hemorrhage (thin arrowheads). Haematoxylin and eosin (H&E), bar 100 μm .

In the punch biopsy taken from the normal skin from the neck, the epidermis displayed a normal thickness and was covered by a large amount of fairly compact, orthokeratotic keratin. Mild to severe, interstitial eosinophilic and neutrophilic infiltrates of unknown origin were present mostly within the deeper dermis and did not allow the identification of the dermal changes observed at the site of the ulceration.

The cutaneous punch biopsy taken from the neck of the dam displayed a mildly hyperplastic and irregular epidermis, and was covered by a large amount of lamellar to compact, orthokeratotic keratin (Figure 3b). The superficial dermis displayed mild to moderate perivascular infiltrates composed of lymphocytes, plasma cells, and occasionally eosinophils. The deeper dermis displayed similar changes to the ones observed in the biopsies from the calf (Figure 3b).

The histological findings in the deeper dermis from both the calf and its dam were compatible with collagen dysplasia within the deeper dermis, and thus with the clinical suspicion of cEDS.

3.3. Genetic Analysis

Filtering of WGS for private variants present in the affected calf and absent in the 496 available control genomes identified a single protein-changing variant in COL5A2 with a predicted moderate impact on the encoded protein. The heterozygous variant in COL5A2 exon 35 on chromosome 2 (chr2:g.7331916G>T) was confirmed using IGV software (Figure 3a,c). The detected COL5A2 variant

(XM_024979774.1: c.2366G>T) alters the encoded amino acid of COL5A2 residue 789 of the collagen triple-helical region (XP_024835542.1: p.Gly789Val) included in the collagen alpha-2(V) chain (Figure 4e). Furthermore, the glycine to valine substitution affects an evolutionary conserved residue (Figure 4f) and was predicted to be deleterious (PROVEAN score: -8.294 ; MutPred2 score: 0.917 ; PredictSNP1 score: 0.869). To confirm and evaluate the presence of the COL5A2 variant, the affected genomic region was amplified by PCR and Sanger sequenced in the calf, its dam, its maternal-grandmother, and its sire (Figure 4b). Analyzing the sequencing data, we observed that the calf and its dam were heterozygous for the detected COL5A2 variant, whereas the sire and the maternal-grandmother were homozygous for the wild type allele (Figure 4b,d). Unfortunately, no samples from other closely related animals such as the maternal-grandfather were available.

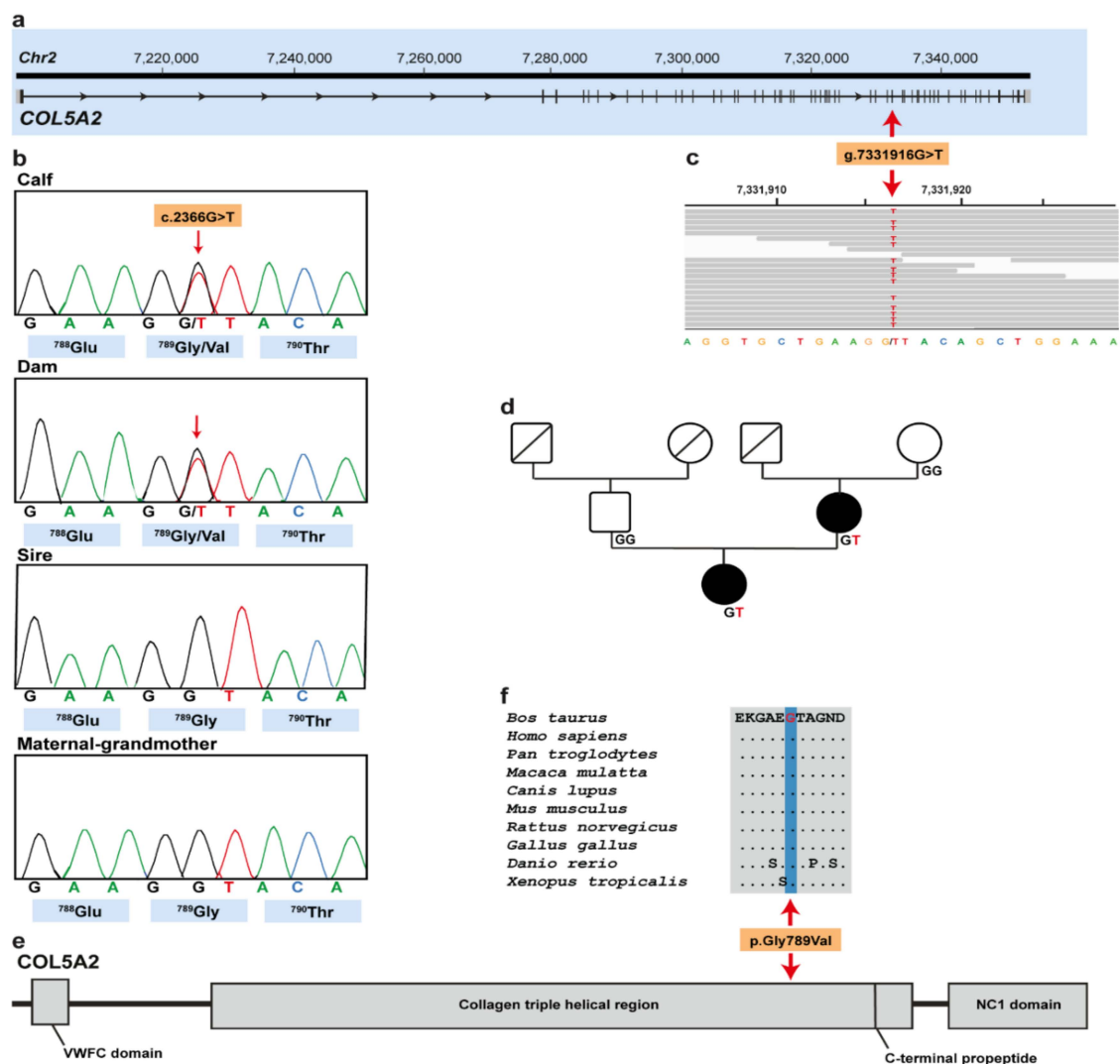


Figure 4. cEDS-associated COL5A2 missense variant in Holstein cattle. (a) COL5A2 gene structure showing the variant location on chromosome 2, exon 35 (red arrow). (b) Electropherograms of the calf, dam, sire, and maternal-grandmother. (c) Integrative Genomics Viewer (IGV) screenshot presenting the g.7331916G>T variant in the affected calf. (d) Pedigree of the cEDS-affected Holstein family. Males are represented by squares and females by circles. Affected animals are represented with full black symbols, while non-affected animals are represented by full white symbols. Unknown genotypes are represented by symbols with a diagonal line. COL5A2 genotypes are shown for all available animals. (e) Schematic representation of COL5A2 protein and its three functional domains. (f) Multiple sequence alignment of the collagen alpha-2(V) chain of the COL5A2 protein encompassing the region of the p.Gly789Val variant demonstrates complete evolutionary conservation across species.

4. Discussion

The identified missense *COL5A2* variant affects a functionally important site of an obvious candidate gene and thus represents the most likely pathogenic variant associated with the observed cEDS phenotype of two examined Holstein cattle family members. In veterinary medicine, so far, two distinct pathogenic variants in *COL5A1* associated with cEDS have been reported in dogs [8] and cats [10]. To the best of our knowledge, no pathogenic variant in the *COL5A2* associated with cEDS has been reported in domestic animal species. Therefore, this study in cattle provides the first example of a *COL5A2*-related congenital skin disorder in domestic animals.

In human medicine, mutations in *COL5A2* are associated with autosomal dominantly inherited cEDS type 2 (OMIM 130010) (<https://omim.org/entry/130010>). The most recent update of the Leiden Open Variation Database (LOVD) lists 312 different pathogenic variants that affect *COL5A2* [27]. In particular, 220 distinct *COL5A1* and 92 *COL5A2* pathogenic variants are described [28]. Diagnosis of cEDS in humans relies on fulfilling minimal criteria that encompass skin hyperextensibility and atrophic scarring plus either another major criterion, generalized joint hypermobility, and/or at least three minor criteria (Table 1), as well as mandatory molecular test confirmation [2].

Table 1. Classification of human classical Ehlers–Danlos syndrome (cEDS).

Inheritance	Autosomal dominant
Molecular Basis	<i>COL5A1</i> ; <i>COL5A2</i> ; <i>COL1A1</i> ; <i>COL3A1</i>
Major Criteria	<ol style="list-style-type: none"> 1. Skin hyperextensibility and atrophic scarring 2. Generalized joint hypermobility
Minor Criteria	<ol style="list-style-type: none"> 1. Easy bruising 2. Soft, doughy skin 3. Skin fragility (or traumatic splitting) 4. Molluscoid pseudotumors 5. Subcutaneous spheroids 6. Hernia 7. Epicanthal folds 8. Complications of joint hypermobility 9. Family history of first-degree relative who meets clinical criteria

Adapted from Malfait et al. 2017 [2].

As described before, the calf and its dam carry a deleterious heterozygous missense variant in the *COL5A2* gene. More than 90% of cEDS human patients harbor a heterozygous mutation in one of the genes encoding *COL5A1* [4,29,30], such as, for example, the missense variant p.Gly934Arg in *COL5A2*, where there is a substitution of a glycine residue within the triple helical domain (Gly-X-Y) [31].

The clinical and pathological phenotype in both cases of this study resembled a form of cEDS. The affected Holstein calf and its dam met one major criterion (skin hyperextensibility and atrophic scarring) of the human classification system (Table 1). Furthermore, one minor criterion was met in the calf (skin fragility/traumatic splitting). Even though the two presented cases do not completely fulfill the clinical criteria for human cEDS classification, the diagnosis of cEDS has been assumed. It is worth noting that, in veterinary medicine, just a few cases have been reported in the literature, rendering it difficult to develop such a classification system adapted for domestic animal species. In addition, the cases presented herein show lesions restricted to the neck region. Therefore, this may be a specific characteristic of bovine cEDS. Furthermore, it is assumed that the skin lesions observed in the maternal-grandmother were linked to trauma. In fact, the prevalence of neck skin lesions related to the infrastructure of freestall farms is around 9% [32]. Environmental factors cause phenocopies, which are incidents in which non-genetic conditions simulate a genetic disorder. On the farm where the three animals were housed, there were more cows showing neck skin lesions similar to the maternal-grandmother's that may represent phenocopies due to recurring long-term mechanical stress of the feed fence. However, the calf's owner did not recall having any similarly affected animals in the past as the cEDS-affected calf and its dam.

We speculate that the mutation either occurred post-zygotically during the fetal development of the affected dam or represents a germline mutation that occurred in the maternal-grandfather. Nonetheless, this *de novo* mutation was then transmitted to the cEDS-affected calf. The amplification of the mutated allele in the maternal-grandmother using DNA extracted from EDTA blood, skin from the neck lesions area, and normal skin resulted in homozygous wild-type status. Therefore, the maternal-grandmother has been excluded as a mosaic ancestor. However, to prove that the identified mutation in *COL5A2* indeed occurred *de novo*, genotyping of the maternal-grandsire would be needed.

Moreover, the identified deleterious variant and the conservation of the affected glycine amino acid residue of *COL5A2* at position 789 in the highly conserved triple-helical domain also suggest that this variant is most likely pathogenic. The predicted amino acid exchange occurs in the protein triple-helical domain, and by analogy with helix glycine substitutions; for example, in collagen alpha-1(I) in osteogenesis imperfecta (OMIM 120150) (<https://www.omim.org/entry/120150>), in collagen alpha-2(II) in chondrodysplasias (OMIM 120160) (<https://www.omim.org/entry/120160>), and in collagen alpha-3(III) and -4(IV) in Alport syndrome II (OMIM 203780) (<https://www.omim.org/entry/203780>), it would be expected to disrupt the propagation of collagen triple helix, resulting in abnormal molecules linked to the disorder [33]. Collagen triple helix folding and stability is critically dependent on having a glycine as every third amino acid in the triplet repeat sequence (Gly-x-y). Therefore, replacing glycine with a bulky amino acid (in this case, a valine) has the potential to disrupt helix folding and lead to increased posttranslational lysine hydroxylation and glycosylation, compromising the triple helix structural integrity and retention of the mutant trimers in the endoplasmic reticulum, which can have an impact in the cellular function [34]. In addition, cellular quality control mechanisms that bring about endoplasmic reticulum-retention and degradation of misfolded collagens are leaky and collagen hetero- or homotrimers containing one or several mutant pro-alpha-chains are often secreted, having an important predicted impact on collagen fibril formation and stability, and altered interactions with other extracellular matrix components [34]. The major variant of COLLV is a heterotrimer composed of two pro-alpha-1 chains and a single pro-alpha-2 chain, which are encoded by the *COL5A1* and *COL5A2* genes, respectively [35]. COLLV plays a central role in the assembly of tissue-specific matrices. Several COLLV isoforms have been reported, however, the most widely accepted form is the $[\alpha 1(V)]_2\alpha 2(V)$ heterotrimer that co-assembles with type I collagen into heterotypic type I/V collagen fibrils in the extracellular matrix. COLLV is thought to regulate the diameter of these fibrils by retention of its large N-propeptide domain, which projects above the surface of the collagen fibril [35].

5. Conclusions

Rare non-lethal disorders such as cEDS in livestock are usually not reported or diagnosed when the animals show mild to moderate phenotype, but they affect animal welfare through secondary wounds and thus lower the value of the affected animals. Additionally, molecular diagnosis is often not performed because of a lack of resources and diagnostic tools, and/or low value of the animals.

Investigation of these cases allowed a complete clinical, pathological, and molecular genetic study, enabling for the first time the diagnosis of a dominantly inherited cEDS form in a family of Holstein cattle associated with a *COL5A2* variant. Furthermore, this example highlights the utility of WGS-based precision diagnostics for understanding rare disorders in animals with an available reference genome sequence and the value of surveillance of cattle breeding populations for harmful genetic disorders.

Supplementary Materials: The following are available online at <http://www.mdpi.com/2076-2615/10/11/2002/s1>, Table S1: Project and Sample ID for public access of the whole genome sequenced genomes used in this study. EBI Accession numbers of all publicly available genome sequences. We compared the genotypes of the calf with 496 cattle genomes of various breeds that had been sequenced in the course of other ongoing studies and that were publicly available. Figure S1: Neck skin lesions of the maternal-grandmother. Note the presence of bald areas and scabs.

Author Contributions: Conceptualization, M.B. and C.D.; methodology, J.G.P.J.; software, I.M.H. and A.L.; validation, C.B., I.M.B.V., and C.D.; formal analysis, I.M.H. and A.L.; investigation, J.G.P.J., I.M.B.V., A.L., and M.B.; resources, I.M.B.V., C.B., and C.D.; data curation, I.M.H.; writing—original draft preparation, J.G.P.J., I.M.H., and I.M.B.V.; writing—review and editing, J.G.P.J., I.M.H., I.M.B.V., A.L., C.B., M.B., and C.D.; visualization, J.G.P.J.

and I.M.B.V.; supervision, M.B. and C.D.; project administration, C.D. All authors have read and agreed to the published version of the manuscript.

Funding: This study was partially funded by the Swiss National Science Foundation.

Acknowledgments: We acknowledge Stefano Allodi for referring the clinical cases. We thank Nathalie Besuchet Schmutz, Manuela Bozzo, Erika Bürgi, and Francesca Caravello for expert technical assistance and the Interfaculty Bioinformatics Unit of the University of Bern for providing high-performance computational infrastructure. Monika Welle is acknowledged for the case discussion.

Conflicts of Interest: C.B. is an editorial board member of *Animals*, but has not in any way been involved in or interacted with the journal's review process or editorial decision-making. The authors declare no conflict of interest.

References

1. Leeb, T.; Müller, E.J.; Roosje, P.; Welle, M. Genetic testing in veterinary dermatology. *Vet. Dermatol.* **2017**, *28*, e1. [[CrossRef](#)] [[PubMed](#)]
2. Malfait, F.; Francomano, C.; Byers, P.; Belmont, J.; Berglund, B.; Black, J.; Bloom, L.; Bowen, J.M.; Brady, A.F.; Burrows, N.P.; et al. The 2017 international classification of the Ehlers–Danlos syndromes. *Am. J. Med. Genet. Part C Semin. Med. Genet.* **2017**, *175*, 8–26. [[CrossRef](#)] [[PubMed](#)]
3. Chiarelli, N.; Ritelli, M.; Zoppi, N.; Colombi, M. Cellular and molecular mechanisms in the pathogenesis of classical, vascular, and hypermobile ehlers-danlos syndromes. *Genes* **2019**, *10*, 609. [[CrossRef](#)] [[PubMed](#)]
4. Ritelli, M.; Dordoni, C.; Venturini, M.; Chiarelli, N.; Quinzani, S.; Traversa, M.; Zoppi, N.; Vascellaro, A.; Wischmeijer, A.; Manfredini, E.; et al. Clinical and molecular characterization of 40 patients with classic Ehlers–Danlos syndrome: Identification of 18 COL5A1 and 2 COL5A2 novel mutations. *Orphanet J. Rare Dis.* **2013**, *8*, 1–19. [[CrossRef](#)] [[PubMed](#)]
5. Monthoux, C.; de Brot, S.; Jackson, M.; Bleul, U.; Walter, J. Skin malformations in a neonatal foal tested homozygous positive for Warmblood Fragile Foal Syndrome. *BMC Vet. Res.* **2015**, *11*, 1–8. [[CrossRef](#)] [[PubMed](#)]
6. Tryon, R.C.; White, S.D.; Bannasch, D.L. Homozygosity mapping approach identifies a missense mutation in equine cyclophilin B (PPIB) associated with HERDA in the American Quarter Horse. *Genomics* **2007**, *90*, 93–102. [[CrossRef](#)]
7. Jaffey, J.A.; Bullock, G.; Teplin, E.; Guo, J.; Villani, N.A.; Mhlanga-Mutangadura, T.; Schnabel, R.D.; Cohn, L.A.; Johnson, G.S. A homozygous ADAMTS2 nonsense mutation in a Doberman Pinscher dog with Ehlers Danlos syndrome and extreme skin fragility. *Anim. Genet.* **2019**, *50*, 543–545. [[CrossRef](#)]
8. Bauer, A.; Bateman, J.F.; Lamandé, S.R.; Hanssen, E.; Kirejczyk, S.G.M.; Yee, M.; Ramiche, A.; Jagannathan, V.; Welle, M.; Leeb, T.; et al. Identification of two independent COL5A1 variants in dogs with ehlers-danlos syndrome. *Genes* **2019**, *10*, 731. [[CrossRef](#)]
9. Bauer, A.; de Lucia, M.; Leuthard, F.; Jagannathan, V.; Leeb, T. Compound heterozygosity for TNXB genetic variants in a mixed-breed dog with Ehlers–Danlos syndrome. *Anim. Genet.* **2019**, *50*, 546–549. [[CrossRef](#)]
10. Spycher, M.; Bauer, A.; Jagannathan, V.; Frizzi, M.; De Lucia, M.; Leeb, T. A frameshift variant in the COL5A1 gene in a cat with Ehlers–Danlos syndrome. *Anim. Genet.* **2018**, *49*, 641–644. [[CrossRef](#)]
11. Hegreberg, G.A.; Padgett, G.A.; Gorham, J.R.; Henson, J.B. A heritable connective tissue disease of dogs and Mink Resembling the Ehlers–Danlos. *J. Investig. Dermatol.* **1970**, *54*, 377–380. [[CrossRef](#)] [[PubMed](#)]
12. Harvey, R.; Brown, P.; Young, R.; Whitbread, T. A connective tissue defect in two rabbits similar to the Ehlers–Danlos syndrome. *Vet. Rec.* **1990**, *126*, 130–132. [[PubMed](#)]
13. Joller, S.; Berenguer Veiga, I.; Drögemüller, C. Dermatosparaxis in White Dorper sheep: Confirmation of a causative nonsense mutation in ADAMTS2. *Anim. Genet.* **2017**, *48*, 729–730. [[CrossRef](#)]
14. Zhou, H.; Hickford, J.G.H.; Fang, Q. A premature stop codon in the ADAMTS2 gene is likely to be responsible for dermatosparaxis in Dorper sheep. *Anim. Genet.* **2012**, *43*, 471–473. [[CrossRef](#)] [[PubMed](#)]
15. Monteagudo, L.V.; Ferrer, L.M.; Catalan-Insa, E.; Savva, D.; Mcguffin, L.J.; Tejedor, M.T. In silico identification and three-dimensional modelling of the missense mutation in ADAMTS2 in a sheep flock with dermatosparaxis. *Vet. Dermatol.* **2015**, *26*, 49–52. [[CrossRef](#)]
16. Carty, C.I.; Lee, A.M.; Wienandt, N.A.E.; Stevens, E.L.; Alves, D.A.; Browne, J.A.; Bryan, J.; Ryan, E.G.; Cassidy, J.P. Dermatosparaxis in two Limousin calves. *Ir. Vet. J.* **2016**, *69*, 1–5. [[CrossRef](#)]

17. Tajima, M.; Miyake, S.; Takehana, K.; Kobayashi, A.; Yamato, O.; Maede, Y. Gene defect of dermatan sulfate proteoglycan of cattle affected with a variant form of Ehlers-Danlos syndrome. *J. Vet. Intern. Med.* **1999**, *13*, 202–205. [[CrossRef](#)]
18. Colige, A.; Sieron, A.L.; Li, S.W.; Schwarze, U.; Petty, E.; Wertelecki, W.; Wilcox, W.; Krakow, D.; Cohn, D.H.; Reardon, W.; et al. Human ehlers-danlos syndrome type VII C and bovine dermatosparaxis are caused by mutations in the procollagen I N-proteinase gene. *Am. J. Hum. Genet.* **1999**, *65*, 308–317. [[CrossRef](#)]
19. Rosen, B.D.; Bickhart, D.M.; Schnabel, R.D.; Koren, S.; Elsik, C.G.; Tseng, E.; Rowan, T.N.; Low, W.Y.; Zimin, A.; Couldrey, C.; et al. De novo assembly of the cattle reference genome with single-molecule sequencing. *Gigascience* **2020**, *9*, 1–9. [[CrossRef](#)]
20. Hayes, B.J.; Daetwyler, H.D. 1000 Bull Genomes Project to Map Simple and Complex Genetic Traits in Cattle: Applications and Outcomes. *Annu. Rev. Anim. Biosci.* **2019**, *7*, 89–102. [[CrossRef](#)]
21. Chen, S.; Zhou, Y.; Chen, Y.; Gu, J. Fastp: An ultra-fast all-in-one FASTQ preprocessor. *Bioinformatics* **2018**, *34*, i884–i890. [[CrossRef](#)] [[PubMed](#)]
22. Häfliger, I.M.; Wiedemar, N.; Švara, T.; Starič, J.; Cociancich, V.; Šest, K.; Gombač, M.; Paller, T.; Agerholm, J.S.; Drögemüller, C. Identification of small and large genomic candidate variants in bovine pulmonary hypoplasia and anasarca syndrome. *Anim. Genet.* **2020**, *51*, 382–390. [[CrossRef](#)] [[PubMed](#)]
23. Robinson, J.T.; Thorvaldsdóttir, H.; Wenger, A.M.; Zehir, A.; Mesirov, J.P. Variant review with the integrative genomics viewer. *Cancer Res.* **2017**, *77*, e31–e34. [[CrossRef](#)]
24. Choi, Y.; Chan, A.P. PROVEAN web server: A tool to predict the functional effect of amino acid substitutions and indels. *Bioinformatics* **2015**, *31*, 2745–2747. [[CrossRef](#)]
25. Pejaver, V.; Urresti, J.; Lugo-Martinez, J.; Pagel, K.; Lin, G.N.; Nam, H.-J.; Mort, M.; Cooper, D.; Sebat, J.; Iakoucheva, L.; et al. MutPred2: Inferring the molecular and phenotypic impact of amino acid variants. *bioRxiv* **2017**, 134981. [[CrossRef](#)]
26. Bendl, J.; Stourac, J.; Salanda, O.; Pavelka, A.; Wieben, E.D.; Zendulka, J.; Brezovsky, J.; Damborsky, J. PredictSNP: Robust and Accurate Consensus Classifier for Prediction of Disease-Related Mutations. *PLoS Comput. Biol.* **2014**, *10*, 1–11. [[CrossRef](#)] [[PubMed](#)]
27. Dalgleish, R. The Human Collagen Mutation Database 1998. *Nucleic Acids Res.* **1998**, *26*, 253–255. [[CrossRef](#)] [[PubMed](#)]
28. Dalgleish, R.; Teh, W.K. Ehlers Danlos Syndrome Variant Database. Available online: https://eds.gene.je.ac.uk/home.php?select_db=COL5A1 (accessed on 29 September 2020).
29. Symoens, S.; Syx, D.; Malfait, F.; Callewaert, B.; de Backer, J.; Vanakker, O.; Coucke, P.; de Paepe, A. Comprehensive molecular analysis demonstrates type V collagen mutations in over 90% of patients with classic EDS and allows to refine diagnostic criteria. *Hum. Mutat.* **2012**, *33*, 1485–1493. [[CrossRef](#)]
30. Zoppi, N.; Chiarelli, N.; Cinquina, V.; Ritelli, M.; Colombi, M. GLUT10 deficiency leads to oxidative stress and non-canonical $\alpha\beta3$ integrin-mediated TGF β signalling associated with extracellular matrix disarray in arterial tortuosity syndrome skin fibroblasts. *Hum. Mol. Genet.* **2015**, *24*, 6769–6787. [[CrossRef](#)]
31. Richards, A.J.; Martin, S.; Nicholls, A.C.; Harrison, J.B.; Pope, F.M.; Burrows, N.P. A single base mutation in COL5A2 causes Ehlers-Danlos syndrome type II. *J. Med. Genet.* **1998**, *35*, 846–848. [[CrossRef](#)]
32. Zaffino Heyerhoff, J.C.; LeBlanc, S.J.; DeVries, T.J.; Nash, C.G.R.; Gibbons, J.; Orsel, K.; Barkema, H.W.; Solano, L.; Rushen, J.; de Passillé, A.M.; et al. Prevalence of and factors associated with hock, knee, and neck injuries on dairy cows in freestall housing in Canada. *J. Dairy Sci.* **2014**, *97*, 173–184. [[CrossRef](#)] [[PubMed](#)]
33. Mitchell, A.L.; Schwarze, U.; Jennings, J.F.; Byers, P.H. Molecular Mechanisms of Classical Ehlers-Danlos Syndrome. *Hum. Mutat.* **2009**, *30*, 995–1002. [[CrossRef](#)]
34. Lamandé, S.R.; Bateman, J.F. Genetic Disorders of the Extracellular Matrix. *Anat. Rec.* **2020**, *303*, 1527–1542. [[CrossRef](#)] [[PubMed](#)]
35. DE, B. Type V collagen: Heterotypic type I/V collagen interactions in the regulation of fibril assembly. *Micron* **2001**, *32*, 223–237.

Publisher’s Note: MDPI stays neutral with regard to jurisdictional claims in published maps and institutional affiliations.



© 2020 by the authors. Licensee MDPI, Basel, Switzerland. This article is an open access article distributed under the terms and conditions of the Creative Commons Attribution (CC BY) license (<http://creativecommons.org/licenses/by/4.0/>).

4.1.4.3 Clinicopathological and genomic characterization of a Simmental calf with generalized bovine juvenile angiomas

Journal: animals

Manuscript status: published

Contributions: whole-genome sequencing data analysis, genetic figures, writing original draft and revisions

Displayed version: published version

DOI: [10.3390/ani11030624](https://doi.org/10.3390/ani11030624)

Article

Clinicopathological and Genomic Characterization of a Simmental Calf with Generalized Bovine Juvenile Angiomas

Joana G. P. Jacinto ^{1,2}, Irene M. Häfliger ², Nicole Borel ³, Patrik Zanolari ⁴, Cord Drögemüller ^{2,*}
and Inês M. B. Veiga ⁵

- ¹ Department of Veterinary Medical Sciences, University of Bologna, 40064 Ozzano Emilia (BO), Italy; joana.goncalves2@studio.unibo.it
- ² Institute of Genetics, Vetsuisse Faculty, University of Bern, 3012 Bern, Switzerland; irene.haefliger@vetsuisse.unibe.ch
- ³ Institute of Veterinary Pathology, Vetsuisse Faculty, University of Zurich, 8057 Zurich, Switzerland; n.borel@access.uzh.ch
- ⁴ Clinic for Ruminants, Vetsuisse Faculty, University of Bern, 3012 Bern, Switzerland; patrik.zanolari@vetsuisse.unibe.ch
- ⁵ Institute of Animal Pathology, Vetsuisse Faculty, University of Bern, 3012 Bern, Switzerland; ines.veiga@vetsuisse.unibe.ch
- * Correspondence: cord.droegemueller@vetsuisse.unibe.ch; Tel.: +41-31-631-2529



Citation: Jacinto, J.G.P.; Häfliger, I.M.; Borel, N.; Zanolari, P.; Drögemüller, C.; Veiga, I.M.B. Clinicopathological and Genomic Characterization of a Simmental Calf with Generalized Bovine Juvenile Angiomas. *Animals* **2021**, *11*, 624. <https://doi.org/10.3390/ani11030624>

Academic Editors: Francesca Ciotola, Sara Albarella and Vincenzo Peretti

Received: 28 January 2021

Accepted: 22 February 2021

Published: 26 February 2021

Publisher's Note: MDPI stays neutral with regard to jurisdictional claims in published maps and institutional affiliations.



Copyright: © 2021 by the authors. Licensee MDPI, Basel, Switzerland. This article is an open access article distributed under the terms and conditions of the Creative Commons Attribution (CC BY) license (<https://creativecommons.org/licenses/by/4.0/>).

Simple Summary: Vascular anomalies represent a heterogeneous group of rare disorders encompassing both vascular malformations and tumors, which can be congenital or arise shortly after birth. They often pose a diagnostic challenge in human and veterinary medicine, and the referring nomenclature is equivocal. Bovine juvenile angiomas (BJA), a clinical condition belonging to this group of disorders, encompasses vascular malformations and tumors arising in calves. Usually, such vascular anomalies are not further investigated on a molecular genetic level, mainly because of a lack of resources and diagnostic tools, as well as the low value and short lifespan of the affected animals. Here we report the clinical, pathological, immunohistochemical, and genetic features of a Simmental calf that displayed multiple cutaneous, subcutaneous, and visceral vascular hamartomas compatible with a generalized form of BJA. Whole-genome sequencing identified six coding variants, including four heterozygous variants in the *PREX1*, *UBE3B*, *PCDHGA2*, and *ZSWIM6* genes, which occurred only in the BJA-affected calf and were absent in the global control cohort of more than 4500 cattle. Assuming a germline mutation as etiology, one of these variants might be responsible for the vascular malformations identified in this calf.

Abstract: Bovine juvenile angiomas (BJA) comprises a group of single or multiple proliferative vascular anomalies in the skin and viscera of affected calves. The purpose of this study was to characterize the clinicopathological phenotype of a 1.5-month-old Simmental calf with multiple cutaneous, subcutaneous, and visceral vascular hamartomas, which were compatible with a generalized form of BJA, and to identify genetic cause for this phenotype by whole-genome sequencing (WGS). The calf was referred to the clinics as a result of its failure to thrive and the presence of multiple cutaneous and subcutaneous nodules, some of which bled abundantly following spontaneous rupture. Gross pathology revealed similar lesions at the inner thoracic wall, diaphragm, mediastinum, pericardium, inner abdominal wall, and mesentery. Histologically, variably sized cavities lined by a single layer of plump cells and supported by a loose stroma with occasional acute hemorrhage were observed. Determined by immunochemistry, the plump cells lining the cavities displayed a strong cytoplasmic signal for PECAM-1, von Willebrand factor, and vimentin. WGS revealed six private protein-changing variants affecting different genes present in the calf and absent in more than 4500 control genomes. Assuming a spontaneous de novo mutation event, one of the identified variants found in the *PREX1*, *UBE3B*, *PCDHGA2*, and *ZSWIM6* genes may represent a possible candidate pathogenic variant for this rare form of vascular malformation.

Keywords: cattle; bovine juvenile angiomatosis; vascular hamartoma; precision medicine; vascular malformation; rare diseases; whole-genome sequencing

1. Introduction

Congenital vascular tumors and malformations are rare anomalies that develop during pregnancy or within the first three months of life [1]. The International Society for the Study of Vascular Anomalies (ISSVA) published an updated classification of these lesions in 2020 that includes genetic and extended histologic findings that came to light since the original ISSVA classification was created in 1996 [2,3]. However, the differentiation between vascular tumors and malformations is not always straightforward [4], and the terminology of vascular anomalies often remains a challenge [2], not only in human, but also in veterinary medicine [5–7]. Specifically, calves are known to display several types of vascular anomalies, some of which are congenital [6]. Vascular hamartomas are relatively common and might be found in the mandibular gingiva [7–11], skin [12], heart [13], and lung [14]. Hemangioma is the most frequently reported benign vascular neoplasm in calves [15] and might be localized in the gingiva [15,16], skin [5,17,18], heart [6], or multifocally [17]. In addition, although malignant vascular tumors are rarely described in cattle [18,19], a multifocal hemangiosarcoma was diagnosed in a stillborn calf [20]. In 1990, Watson and Thompson [6] proposed that these different manifestations of single and multiple vascular anomalies in calves should be grouped under the term bovine juvenile angiomatosis (BJA). This condition differs from the so-called bovine cutaneous angiomatosis, which is mostly identified in adult dairy cattle with a mean age of 5.5 years and is characterized by the appearance of mostly single, proliferative cutaneous vascular anomalies that range from hamartomas to hemangiomas [21–25]. It was postulated that bovine cutaneous angiomatosis may be a consequence of exuberant granulation tissue formation, especially due to histologic similarities to lobular capillary hemangioma or granulation tissue-type hemangioma of man [6,21]. Some authors mentioned chromosomal abnormalities as a putative cause for the bovine juvenile angiomatosis in comparison to what has been described in humans with similar vascular lesions [6,26]. However, chromosomal abnormalities or other types of genetic mutations have not been identified in calves affected by BJA [6,26].

Herein, we aimed to characterize the clinical and pathological phenotype of multiple cutaneous, subcutaneous, and visceral vascular hamartomas compatible with a generalized form of BJA in a Simmental calf. In addition, whole-genome sequencing (WGS) was carried out to identify putatively pathogenic variants.

2. Materials and Methods

2.1. Clinical and Pathological Investigation

A 1.5-month-old female Simmental calf with a body weight of 64 kg was referred to the Clinic for Ruminants at the Vetsuisse Faculty, University of Bern, as a result of poor weight gain and skin lesions. Previous treatment by the referring veterinarian included anthelmintics (Ivermectin 0.2 mg/kg, sc, Ivomec, Biokema SA, Crissier, Switzerland) and antibiotics (Benzylpenicillinum procainum, 30,000 IU/kg, iv, Cobiotic, Virbac AG, Glatburg, Switzerland). The calf was euthanized with an intravenous injection of pentobarbital (pentobarbitalum natricum, 150 mg/kg, iv, Streuli Pharma AG, Uznach, Switzerland) and was subsequently submitted to the Institute of Animal Pathology at the Vetsuisse Faculty, University of Bern, for necropsy and histologic examination. Tissue samples from the subcutaneous and internal nodules, as well as from several inner organs, were immediately collected, fixed in 4% buffered formalin, embedded in paraffin, cut at 4 µm, and stained with haematoxylin and eosin (H&E) for further histologic evaluation. Immunohistochemical (IHC) analysis for platelet endothelial cell adhesion molecule (PECAM-1), von Willebrand factor, smooth muscle actin (SMA), vimentin, and a broad-spectrum cytokeratin

marker (MNF116) were performed from one subcutaneous and one mediastinal nodule. For the PECAM-1 IHC, antigen retrieval using pressure cooking (98 °C, 20 min) in basic EDTA buffer (pH 9.0) was performed, and the primary antibody (sc1506, Santa Cruz Biotechnology, Dallas, TX, USA) was incubated for 1 h at room temperature (RT) (1:1000 dilution). For the von Willebrand factor IHC, pressure cooking in citate buffer (pH 6.0, S2031 Agilent Technologies, Santa Clara, CA, USA) was performed for antigen retrieval, and the primary antibody (A0082, Agilent Technologies) was incubated for 40 min (1:100 dilution) at RT. Peroxidase blocking (S2023, Agilent Technologies) was performed prior to primary antibody incubation for 10 min in both cases, followed by incubation with Envision+system HRP rabbit (K4003, Agilent Technologies) for 30 min at RT, labeling with 3,3'-diaminobenzidine (DAB) (K3468, Agilent Technologies) for 10 min, counterstaining with hematoxylin, and mounting. For the SMA IHC, no antigen retrieval was performed, primary antibody incubation (M085, Agilent Technologies) took place for 1 h at RT (1:400 dilution), and the Mach 4 Universal HRP Polymer kit (BRR 4012L, Medite, Dietikon, Switzerland) was used as secondary antibody at RT. Peroxidase blocking and DAB labeling were performed as previously described. For the vimentin IHC, antigen retrieval was performed with Bond Epitope Retrieval Buffer Type 2 (Tris-EDTA pH 9, AR9640 Leica Biosystems, Wetzlar, Germany) for 10 min at 95 °C, and was followed by primary antibody incubation (V9, M0725, Agilent Technologies) for 15 min at RT (1:1000 dilution). For the MNF116 IHC, antigen retrieval was performed with Bond Enzyme 1 (AR9551 Leica Biosystems) for 5 min at 37 °C, followed by primary antibody incubation (M0821, Agilent Technologies) for 15 min at RT (1:400 dilution). In both cases, all further steps were performed using reagents of the Bond Polymer Refine Detection Kit (DS9800, Leica Biosystems), namely peroxidase blocking for 5 min, incubation with rabbit anti-mouse secondary antibody for 8 min at RT, and peroxidase-labelled polymer incubation for 8 min. Finally, slides were developed in DAB/H₂O₂ for 10 min, counterstained with hematoxylin, and mounted. Tissue sections from normal haired skin from a cow were used as positive control for the PECAM-1, von Willenbrand, vimentin, and MNF116 IHCs, while a tissue section from the small intestine from a cow was used as positive control for the SMA IHC. Tissue sections from the nodules from the affected calf without primary antibody incubation were used as negative controls.

2.2. DNA Sample and Whole-Genome Sequencing

Genomic DNA was isolated from the liver of the calf using the Promega Maxwell RSC DNA system (Promega, Dübendorf, Switzerland). WGS using the Illumina NovaSeq6000 was performed on the genomic DNA of the calf. The sequenced reads were mapped to the ARS-UCD1.2 reference genome, resulting in an average read depth of approximately 17.5× [27], and single-nucleotide variants (SNVs) and small indel variants were called. The applied software and steps to process fastq files into binary alignment map (BAM) and genomic variant call format files were in accordance with the 1000 Bull Genomes Project processing guidelines of run 8 (www.1000bullgenomes.com) [28], except for the trimming, which was performed using fastp [29]. Further preparation of the genomic data had been done according to Häfliger et al. 2020 [30]. In order to find private variants, we compared the genotypes of the affected calf with 496 cattle genomes of various breeds that had been sequenced in the course of other ongoing studies at the Institute of Genetics at the Vetsuisse Faculty, University of Bern, and that are publicly available in the European Nucleotide Archive (SAMEA6528880 is the sample accession number of the affected calf; <http://www.ebi.ac.uk/en>) (Table S1). The filtered list of remaining variants were further checked for their occurrence in a global control cohort of 4110 genomes of a variety of breeds (1000 Bull Genomes Project run 8; www.1000bullgenomes.com accessed on 15 November 2020) [28]. Integrative Genomics Viewer (IGV) [31] software was used for visual inspection of genome regions containing possible candidate genes.

In order to evaluate possible chromosomal abnormalities, the read depth along all chromosomes was calculated. A sliding window approach was used where 3 different window sizes were executed (10 kb, 200 kb, 500 kb). Using the function bedcov of the

program Samtools [32], the output generated was the number of reads within each specified window. Furthermore, coverage plots were produced using the function Manhattan of the package “qqman” in R [33].

2.3. Evaluation of the Molecular Consequences of Amino Acid Substitutions

PROVEAN [34], MutPred2 [35], and PredictSNP1 [36] were used to predict the functional consequences of the identified variants on protein.

3. Results

3.1. Clinical Phenotype

At clinical examination, the calf was alert but moderately reduced in its general body condition. The rectal body temperature was 39.0 °C, the heart rate was 80 beats per minute, and the respiratory rate was 40 beats per minute. Examination of the cardiovascular, respiratory, digestive, and urinary systems did not reveal any abnormalities.

The integumentary system of the calf revealed multiple, cutaneous and subcutaneous, soft, movable nodules, which measured up to 5 cm in diameter. These were predominantly present in the caudal aspect of the back, the pelvis, and the hind limbs (Figure 1a). The cutaneous nodules were occasionally covered by sanguineous crusts, and some nodules bled abundantly following spontaneous rupture (Figure 1b). No hematological and biochemical analyses were performed due to cost restrictions. Based on these findings and considering that no other calves in the herd showed similar skin lesions, a presumptive diagnosis of multifocal vascular anomalies was made. The animal was then euthanized due to a lack of response to treatment and poor prognosis.



Figure 1. Cutaneous and subcutaneous nodules (arrows) located at the back, flank, and hindlimbs

of the Simmental calf (a), some of which were covered by abundant serosanguineous crusts (b). At necropsy, similar looking nodules (arrows) were identified, namely in the inner thoracic wall (c) and in the mediastinum (d). All nodules measured up to 5 cm in diameter, were well demarcated from the adjacent tissue, and displayed a white to reddish cut surface. Bar 5 cm (b), 3 cm (c), and 4 cm (d).

3.2. Pathological Phenotype

At necropsy, the cutaneous and subcutaneous nodules displayed either a white or reddish cut surface. Additionally, mostly pedunculated but similar looking nodules were occasionally present at the inner thoracic wall and diaphragm (Figure 1c), the mediastinum (Figure 1d), the pericardium, the inner abdominal wall, and the mesentery adjacent to the duodenum. The remaining organs were macroscopically unremarkable.

Histologically, all analyzed nodules consisted of encapsulated (with the exception of the nodule present in the mesentery adjacent to the duodenum), well demarcated, expansively growing, moderately cellular masses. These consisted of abundant, variably sized, mostly empty cavities, which were lined by a single layer of plump cells and supported by a loose, partially edematous fibrovascular stroma (Figure 2a,b), with occasionally intermingled foci of mature connective tissue. The plump cells displayed a moderate amount of eosinophilic, homogeneous cytoplasm, an oval nucleus with finely stippled chromatin, and up to two basophilic, round nucleoli. The anisocytosis and anisokaryosis were low to moderate, and there were very few mitotic figures visible. Moderate to high numbers of free erythrocytes (compatible with acute hemorrhage), as well as occasional neutrophils and lymphocytes, were visible within the stroma.

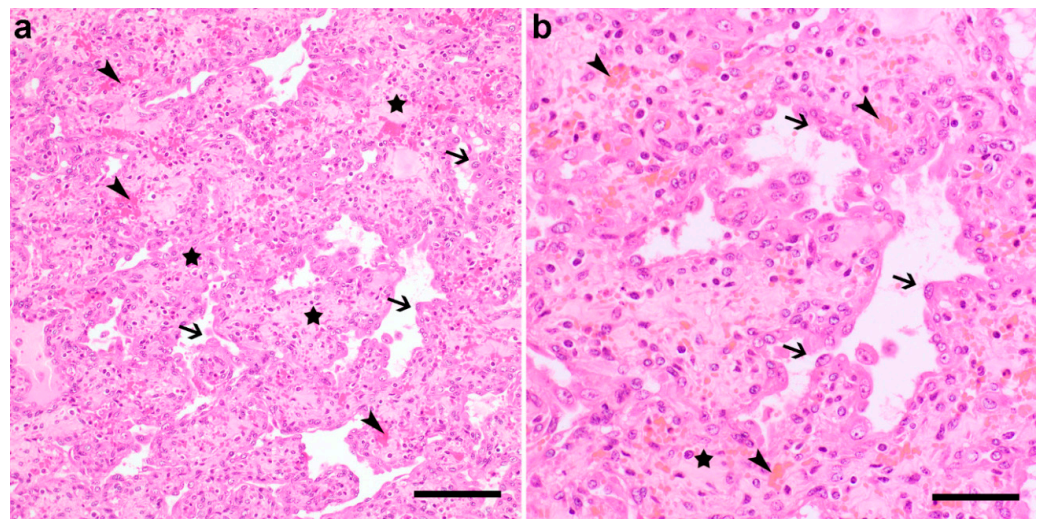


Figure 2. Histology of one of the subcutaneous nodules from the Bovine juvenile angiomas (BJA)-affected Simmental calf. Note the variably sized, mostly empty cavities lined by a single layer of plump cells (arrows) and supported by a loose fibrovascular stroma (stars) with occasional acute hemorrhage (arrowheads). Hematoxylin and eosin (H&E) staining, Bar 100 μ m (a) and 50 μ m (b).

To determine the cellular origin of these nodules, IHC was performed. In both nodules, the plump cells lining the cavities displayed a strong cytoplasmic signal for PECAM-1 (Figure 3a), von Willebrand factor (Figure 3b), and vimentin (Figure 3c) but not for SMA (Figure 3d). In addition, the supporting stromal cells displayed a strong cytoplasmic signal for vimentin (Figure 3c) and SMA (Figure 3d), as well as a rather strong background staining in the von Willebrand factor IHC (Figure 3b). Cells lining the cavities and stromal cells were negative for the pan cytokeratin marker MNF116 (not shown).

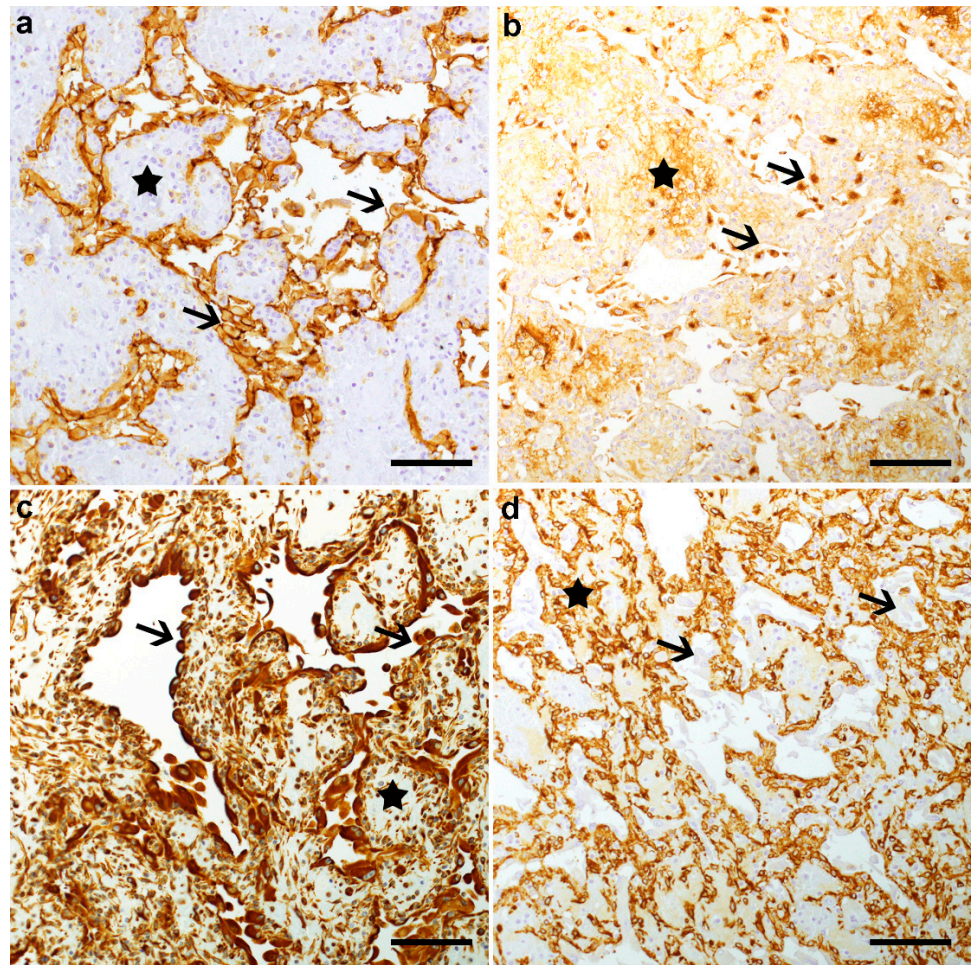


Figure 3. Immunohistochemical (IHC) analysis of a subcutaneous nodule from the BJA-affected Simmental calf with platelet endothelial cell adhesion molecule (PECAM-1) (a), von Willebrand factor (b), vimentin (c), and smooth muscle actin (SMA) (d). Note that the plump cells lining the cavities (arrows) displayed a strong positive signal in the PECAM-1, von Willebrand factor, and vimentin IHC but were negative in the SMA IHC. The stromal cells (stars) displayed a positive cytoplasmic signal in the vimentin and SMA IHC staining, while the signal seen in the von Willebrand factor IHC was considered to represent background staining. IHC staining, Hematoxylin counterstain, Bar 100 μ m.

The above described histologic and immunohistochemical features resemble previously described vascular anomalies in calves [7,8]. In spite of the often conflicting nomenclature terminology [6,7], a final diagnosis of multiple cutaneous, subcutaneous, and visceral vascular hamartomas compatible with a generalized form of BJA as described by Watson and Thompson [6] was made in this case.

3.3. Genetic Analysis

Assuming a spontaneous mutation as etiology for this most likely congenital condition, the sequencing of the whole genome of the affected calf was carried out. Filtering of the obtained variant catalogue for private variants exclusively present in the BJA-affected calf and absent in 496 available control genomes identified 31 private protein-changing variants, and subsequent visual inspection using IGV software confirmed 29 as real variants. Analyzing the occurrence of these variants in the global control cohort of 4110 genomes of a variety of breeds [28], six heterozygous protein-changing variants exclusively present in the genome of the affected calf were identified (Table S2). A total of 137 sequenced genomes from Simmental cattle were considered during variant filtering. Results of the functional impact prediction of these six heterozygous protein-changing variants are presented in Table 1.

Table 1. Pathogenicity prediction results for the six heterozygous protein-changing variants exclusively present in the genome of the BJA-affected calf and absent in global control cohort of more than 4500 genomes of a variety of breeds.

Gene	Effect	Protein-Changing	pLI ¹	PROVEAN Score	PROVEAN Impact	MutPred2 Score	MutPred2 Impact	PredictSNP1 Score	PredictSNP1 Impact
<i>PREX1</i>	missense	p.Arg401Cys	1	−5.149	deleterious	0.387	neutral	0.719	deleterious
<i>UBE3B</i>	missense	p.Ala32Val	0	−1.946	neutral	0.583	neutral	0.510	deleterious
<i>PCDHGA2</i>	in-frame deletion disruptive	p.Lys141_Val142del	0	−11.366	deleterious	0.338	neutral	NA	NA
<i>ZSWIM6</i>	in-frame deletion	p.Ala146_Gly148del	1	1.280	neutral	0.366	neutral	NA	NA
<i>NR1H3</i>	missense	p.Thr46Met	0.9	−0.371	neutral	0.086	neutral	0.653	neutral
<i>C23H6orf132</i>	missense	p.Gly692Glu	NA	−0.907	neutral	0.035	neutral	0.826	neutral

¹ probability of loss-of-function intolerance score (pLI) provided by the Genome Aggregation Database (gnomAD) [37]. NA, not available.

Based on the function of the identified genes and in the predicted impact on the protein, the variants identified in *PREX1*, *UBE3B*, *ZSWIM6*, and *PCDHGA2* were considered the most likely candidate pathogenic variants for the observed phenotype. Unfortunately, no biological samples of the sire and dam were available to evaluate if one of these variants has occurred de novo in the calf.

No evidence for chromosomal abnormalities were detected by analyzing the obtained read depth or coverage along all chromosomes.

4. Discussion

We performed a comprehensive clinical, pathological, and genetic investigation in a Simmental calf displaying multifocal subcutaneous and visceral vascular hamartomas compatible with a generalized form of BJA.

We evaluated the hypothesis of a spontaneous mutation as the possible cause for this most likely congenital phenotype. Analysis of the genome sequence revealed six heterozygous protein-changing variants in the *PREX1*, *UBE3B*, *PCDHGA2*, *ZSWIM6*, *NR1H3*, and *C23H6orf132* genes that were exclusively present in the genome of the affected calf and absent in a global control cohort of more than 4500 cattle genomes of a variety of breeds. Therefore, we considered these apparently rare coding variants as possible candidates for the observed BJA phenotype. In the following, literature and in silico effect predictions are used to discuss a conceivable causal role. The missense variants identified in the *NR1H3* and *C23H6orf132* genes were not considered as putative causes for these vascular malformations because they were predicted to have a neutral or benign effect.

However, the missense variant found in *PREX1* was predicted to be deleterious by different tools such as PROVEAN and PredictSNP1 [34,36]. This gene belongs to the family of Rac guanine nucleotide exchange factors (Rac-GEF) and is activated by phosphatidylinositol 3,4,5-trisphosphate (PI (3,4,5) P3), which is generated by class I phosphoinositide 3-kinase (*PI3K*) and the β -gamma subunits of the heterotrimeric-G proteins ($G\beta\gamma$) [38]. Furthermore, *PREX1* has an important role in the control of many fundamental cellular functions, including cell migration, actin cytoskeletal rearrangement, adhesion, and the production of reactive oxygen species (ROS) [39]. Additionally, the major effector of *PREX1* protein activity is related to the induction of actin-mediated membrane ruffling and lamellipodia production at the leading edge of cell migration, and abnormally activated Rac is involved in the metastasis and invasion of tumor cells [40]. Evidence suggested that Rac and *PREX1* protein are increased in cell proliferation and migration in several human cancers such as melanoma [41], breast cancer [42], prostate cancer [43], and oral squamous cell carcinoma [44]. However, no association between *PREX1* and the occurrence of vascular tumors has been reported to date.

The missense variant in *UBE3B* was predicted to be deleterious by PredictSNP1 [36]. An independent splice site variant in bovine *UBE3B* is associated with an autosomal-recessive inherited disorder called PIRM syndrome in Finnish Ayrshire cattle, which causes

intellectual disability, retarded growth, and mortality (OMIA 001934-9913) [45], and which resembles the human autosomal-recessive Kaufman oculocerebrofacial syndrome (OMIM 244450) [46]. In addition, a recent study demonstrated that suppression of the E3 ubiquitin ligase UBE3B-mediated MYC ubiquitination and degradation caused by the integration of *TRIB3* with *MYC* is associated with high proliferation and self-renewal of lymphoma cells [47]. However, in the case presented in this study, the identified variant in *UBE3B* was heterozygous, and the calf did not show a phenotype compatible with these disorders.

Moreover, a disruptive in-frame deletion in *PCDHGA2* was predicted to have a deleterious impact in the protein using PROVEAN [34]. This gene presents a probability of loss-of-function intolerance score (pLI) of zero according to Genome Aggregation Database (gnomAD) [37]. Considering that transcripts with a pLI superior or equal to 0.9 are predicted to be loss-of-function (LoF) intolerant due to haploinsufficiency of the gene [48], *PCDHGA2* most likely does not belong to the group of LoF haploinsufficient genes. In addition, *PCDHGA2* protein is a potential calcium-dependent cell-adhesion protein that might be involved in the establishment and maintenance of specific neuronal connections in the brain [49,50]. In humans, somatic mutations in *PCDHGA2* have been associated with cell and biological adhesion in aggressive papillary thyroid microcarcinomas [51]. However, and similarly to *PREX1*, no association between this gene and the occurrence of vascular tumors has been reported to date.

To date, no pathogenic variants of *ZSWIM6* have been reported in domestic animals. Interestingly, recent data obtained from human genome sequencing studies presented in the gnomAD [37] showed that the pLI for this gene was 1, meaning that *ZSWIM6* falls into the class of LoF haploinsufficient genes. The encoded protein, so-called Zinc finger SWIM domain-containing protein 6, is a protein of unknown function that is involved in the nervous system development and regulation [52]. Moreover, *ZSWIM6* enables the zinc ion binding [53] and is part of the Cul2-RING ubiquitin ligase complex [49]. In humans, pathogenic variants in the *ZSWIM6* gene (OMIM 615951) are associated to acromelic frontonasal dysostosis [54] and neurodevelopmental disorder with movement abnormalities, abnormal gait, and autistic features [52,55]. Additionally, the *ZSWIM6* protein, according to the Biological General Repository for Interaction Datasets (BioGRID), is predicted to interact physically with *ARIH1* [56], *GLMN* [57], *HECW2* [58], *HNRNPH1* [59] and *HNRNPL* [60]. Similarly to *ZSWIM6*, the *GLMN* is part of the Cul2-RING ubiquitin ligase complex [61] and known to be involved in numerous different processes, namely the normal development of the vasculature [62]. Particularly, autosomal dominant pathogenic variants in the *GLMN* gene (OMIM 138000) are associated with the development of glomuvenous malformations (GVMs) [63] and Blue rubber bleb nevus syndrome (BRBNS) (OMIM 112200) [64] in humans.

Based on these findings, we speculate whether the above-described vascular lesions in this calf could be due to an impaired interaction between *ZSWIM6* and *GLMN*. However, it cannot be excluded that the phenotype displayed by this calf is due to one of the other remaining variants found exclusively in the sequenced case, or even to a combination of these. Either way, we hypothesize that one of these variants either occurred post-zygotically during the fetal development of the affected calf or represent a germline mutation that occurred in one of the parents. To prove that the private variants occurred was indeed de novo, genotyping of the sire and dam would be needed. Unfortunately, no samples from these animals were available at the time the genetic analysis was performed, therefore this hypothesis cannot be confirmed.

We hope that these findings may contribute to a better knowledge and characterization of BJA. However, it is highly unlikely that the candidate causal variants identified in the genome of the studied calf are responsible for other BJA cases since this condition encompasses several kinds of vascular anomalies, including both vascular malformations and tumors [6].

5. Conclusions

This report highlights the utility of WGS-based precision diagnostics for understanding the underlying genetics of rare disorders in animals with an available reference genome sequence and the value of surveillance for harmful genetic disorders in cattle breeding populations.

Supplementary Materials: The following are available online at <https://www.mdpi.com/2076-2615/11/3/624/s1>, Table S1: Project and Sample ID for public access of the whole genome sequenced genomes used in this study. EBI Accession numbers of all publicly available genome sequences. We compared the genotypes of the calf with 496 cattle genomes of various breeds that had been sequenced in the course of other ongoing studies and that were publicly available, Table S2: List of the remaining variants after the comparison to the global control cohort of 4110 genomes of other breeds (1000 Bull Genomes Project run 8; www.1000bullgenomes.com), revealing 6 protein-changing variants with a predicted moderate impact only present in the affected calf.

Author Contributions: Conceptualization, C.D. and I.M.B.V.; methodology, I.M.H., N.B., P.Z. and I.M.B.V.; software, I.M.H.; validation, J.G.P.J., N.B. and C.D.; formal analysis, J.G.P.J. and I.M.H.; investigation, J.G.P.J., N.B. and I.M.B.V.; resources, N.B., P.Z., C.D. and I.M.B.V.; data curation, C.D.; writing—original draft preparation, J.G.P.J. and I.M.B.V.; writing—review and editing, J.G.P.J., C.D., N.B. and I.M.B.V.; visualization, J.G.P.J., N.B. and I.M.B.V.; supervision, C.D.; project administration, I.M.B.V. and C.D.; funding acquisition, C.D. All authors have read and agreed to the published version of the manuscript.

Funding: This study was partially funded by the Swiss National Science Foundation.

Institutional Review Board Statement: This study did not require official or institutional ethical approval as it was not an experimental study, but part of a clinical and pathological veterinary diagnostic case. The animal in this study was examined and euthanized with the consent of its owner.

Data Availability Statement: The whole-genome data of the affected calf is freely available at the European Nucleotide Archive (ENA) under sample accession number SAMEA6528880.

Acknowledgments: We thank Nathalie Besuchet Schmutz, Hans Gantenbein, Manuela Bozzo, Erika Bürgi, and Bettina de Breuyn for expert technical assistance. The Next Generation Sequencing Platform and the Interfaculty Bioinformatics Unit of the University of Bern for providing high-performance computational infrastructure.

Conflicts of Interest: The authors declare no conflict of interest.

References

1. Alamo, L.; Beck-Popovic, M.; Gudinchet, F.; Meuli, R. Congenital tumors: Imaging when life just begins. *Insights Imaging* **2011**, *2*, 297–308. [[CrossRef](#)]
2. Wassef, M.; Blei, F.; Adams, D.; Alomari, A.; Baselga, E. Vascular Anomalies Classification: Recommendations From the International Society for the Study of Vascular Anomalies. *Pediatrics* **2015**, *136*, 203–214. [[CrossRef](#)] [[PubMed](#)]
3. ISSVA Classification of Vascular Anomalies. Available online: issva.org/classification (accessed on 23 November 2020).
4. Mansfield, S.A.; Williams, R.F.; Jacobas, I. Vascular tumors. *Semin. Pediatr. Surg.* **2020**, *29*. [[CrossRef](#)]
5. Priestnall, S.L.; De Bellis, F.; Bond, R.; Alony-Gilboa, Y.; Summers, B.A. Spontaneous regression of congenital cutaneous hemangiomas in a calf. *Vet. Pathol.* **2010**, *47*, 343–345. [[CrossRef](#)]
6. Watson, T.D.; Thompson, H. Juvenile bovine angiomas: A syndrome of young cattle. *Vet. Rec.* **1990**, *127*, 279–282.
7. Rösti, L.; Lauper, J.; Merhof, K.; Gorgas, D.; Ross, S.; Grest, P.; Welle, M. Angeborene Gefässanomalien in der Maulhöhle bei zwei Kälbern. *Schweiz Arch Tierheilkd* **2013**, *627*–632. [[CrossRef](#)]
8. Sheahan, B.J.; Donnelly, W. Vascular hamartoma in the gingiva of two neonatal calves. *J. Am. Vet. Med. Assoc.* **1981**, *184*, 205–206.
9. Yeruham, I.; Abramovitch, I.; Perl, S. Gingival vascular hamartoma in two calves. *Aust. Vet. J.* **2004**, *82*, 152–153. [[CrossRef](#)]
10. Stanton, M.; Meunier, P.; Smith, D. Vascular hamartoma in the gingiva of two neonatal calves. *J. Am. Vet. Med. Assoc.* **1984**, *184*, 205–206.
11. Wilson, R.B. Gingival vascular hamartoma in three calves. *J. Vet. Diagnostic Investig.* **1990**, *2*, 338–339. [[CrossRef](#)]
12. Yeruham, I.; Perl, S.; Orgad, U. Congenital skin neoplasia in cattle. *Vet. Dermatol.* **1999**, *10*, 149–156. [[CrossRef](#)]
13. Brisville, A.C.; Buczinski, S.; Chénier, S.; Francoz, D. A cardiac vascular hamartoma in a calf: Ultrasonographic and pathologic images. *J. Vet. Cardiol.* **2012**, *14*, 377–380. [[CrossRef](#)]
14. Roth, L.; Bradley, G.A. Pulmonary hamartoma in a calf. *J. Comp. Pathol.* **1991**, *105*, 471–474. [[CrossRef](#)]
15. Misdorp, W. Tumours in calves: Comparative aspects. *J. Comp. Pathol.* **2002**, *127*, 96–105. [[CrossRef](#)] [[PubMed](#)]

16. Tontis, A. Kongenitales kavernoöses Hämangiom beim Brown-Swiss-Kalb, ein seletenes orales Blastom. *Tierarztl. Prax.* **1994**, *22*, 137–139.
17. Baker, J.C.; Hultgren, B.D.; Larson, V.L. Disseminated cavernous hemangioma in a calf. *J. Am. Vet. Med. Assoc.* **1982**, *181*, 172–173.
18. Poulsen, K.; McSloy, A.; Perrier, M.; Prichard, M.; Steinberg, H.; Semrad, S. Primary mandibular hemangiosarcoma in a bull. *Can. Vet. J.* **2008**, *49*, 901–903. [[PubMed](#)]
19. Stock, M.L.; Smith, B.I.; Engiles, J.B. Disseminated hemangiosarcoma in a cow. *Can. Vet. J.* **2011**, *52*, 409–413.
20. Badylak, S.F. Congenital Multifocal Hemangiosarcoma in a Stillborn Calf. *Vet. Pathol.* **1983**, *20*, 245–247. [[CrossRef](#)]
21. Hendrick, M.J. Mesenchymal Tumors of the Skin and Soft Tissues. *Tumors Domest. Anim.* **2016**, 142–175. [[CrossRef](#)]
22. Cotchin, E.; Swarbrick, O. Bovine cutaneous angiomas: A lesion resembling human pyogenic granuloma (granuloma telangiecticum). *Vet. Rec.* **1963**, *75*, 437–444.
23. Lombard, C.; Levesque, L. H'émangiomatose hyperplasique cutan'ee de vaches Normandes. *Ann. Anat. Pathol. (Paris)* **1964**, *9*, 453–462. [[PubMed](#)]
24. Moulton, J.E. *Tumors in Domestic Animals*, 2nd ed.; University of California Press: Berkeley, CA, USA, 1978.
25. Waldvogel, A.; Hauser, B. "Bovine kutane Angiomatose" in der Schweiz. *Schweiz. Arch. Tierheilkd.* **1983**, *125*, 329–333. [[PubMed](#)]
26. Schilcher, F.; Gasteiner, J.; Palmethofer, G.; Baumgartner, W. Generalisierte juvenile Angiomatose bei einem Kalb. *Wien. Tierarztl. Monatsschr.* **2000**, *87*, 10–13.
27. Rosen, B.D.; Bickhart, D.M.; Schnabel, R.D.; Koren, S.; Elisk, C.G.; Tseng, E.; Rowan, T.N.; Low, W.Y.; Zimin, A.; Couldrey, C.; et al. De novo assembly of the cattle reference genome with single-molecule sequencing. *Gigascience* **2020**, *9*, 1–9. [[CrossRef](#)]
28. Hayes, B.J.; Daetwyler, H.D. 1000 Bull Genomes Project to Map Simple and Complex Genetic Traits in Cattle: Applications and Outcomes. *Annu. Rev. Anim. Biosci.* **2019**, *7*, 89–102. [[CrossRef](#)] [[PubMed](#)]
29. Chen, S.; Zhou, Y.; Chen, Y.; Gu, J. Fastp: An ultra-fast all-in-one FASTQ preprocessor. *Bioinformatics* **2018**, *34*, i884–i890. [[CrossRef](#)] [[PubMed](#)]
30. Häfliger, I.M.; Wiedemar, N.; Švara, T.; Starič, J.; Cociancich, V.; Šest, K.; Gombač, M.; Paller, T.; Agerholm, J.S.; Drögemüller, C. Identification of small and large genomic candidate variants in bovine pulmonary hypoplasia and anasarca syndrome. *Anim. Genet.* **2020**, *51*, 382–390. [[CrossRef](#)] [[PubMed](#)]
31. Robinson, J.T.; Thorvaldsdóttir, H.; Wenger, A.M.; Zehir, A.; Mesirov, J.P. Variant review with the integrative genomics viewer. *Cancer Res.* **2017**, *77*, e31–e34. [[CrossRef](#)]
32. Li, H. A statistical framework for SNP calling, mutation discovery, association mapping and population genetical parameter estimation from sequencing data. *Bioinformatics* **2011**, *27*, 2987–2993. [[CrossRef](#)]
33. R Core Team. *R: A Language and Environment for Statistical Computing*; R Core Team: Vienna, Austria, 2013.
34. Choi, Y.; Chan, A.P. PROVEAN web server: A tool to predict the functional effect of amino acid substitutions and indels. *Bioinformatics* **2015**, *31*, 2745–2747. [[CrossRef](#)] [[PubMed](#)]
35. Pejaver, V.; Urresti, J.; Lugo-Martinez, J.; Pagel, K.; Lin, G.N.; Nam, H.-J.; Mort, M.; Cooper, D.; Sebat, J.; Iakoucheva, L.; et al. MutPred2: Inferring the molecular and phenotypic impact of amino acid variants. *Nat. Commun.* **2017**, 134981. [[CrossRef](#)]
36. Bendl, J.; Stourac, J.; Salanda, O.; Pavelka, A.; Wieben, E.D.; Zendulka, J.; Brezovsky, J.; Damborsky, J. PredictSNP: Robust and Accurate Consensus Classifier for Prediction of Disease-Related Mutations. *PLoS Comput. Biol.* **2014**, *10*, 1–11. [[CrossRef](#)] [[PubMed](#)]
37. Karczewski, K.J.; Francioli, L.C.; Tiao, G.; Cummings, B.B.; Alfoldi, J.; Wang, Q.; Collins, R.L.; Laricchia, K.M.; Ganna, A.; Birnbaum, D.P.; et al. The mutational constraint spectrum quantified from variation in 141,456 humans. *Nature* **2020**, *581*, 434–443. [[CrossRef](#)]
38. Welch, H.C.E.; Coadwell, W.J.; Ellson, C.D.; Ferguson, G.J.; Andrews, S.R.; Erdjument-Bromage, H.; Tempst, P.; Hawkins, P.T.; Stephens, L.R. P-Rex1, a PtdIns(3,4,5)P3- and gβγ-regulated guanine-nucleotide exchange factor for Rac. *Cell* **2002**, *108*, 809–821. [[CrossRef](#)]
39. Jaffe, A.B.; Hall, A. Rho GTPases: Biochemistry and biology. *Annu. Rev. Cell Dev. Biol.* **2005**, *21*, 247–269. [[CrossRef](#)] [[PubMed](#)]
40. Vigil, D.; Cherfils, J.; Rossman, K.L.; Der, C.J. Ras superfamily GEFs and GAPs: Validated and tractable targets for cancer therapy? *Nat. Rev. Cancer* **2010**, *10*, 842–857. [[CrossRef](#)] [[PubMed](#)]
41. Ryan, M.B.; Finn, A.J.; Pedone, K.H.; Thomas, N.E.; Der, C.J.; Cox, A.D. ERK/MAPK signaling drives overexpression of the rac-GEF, PREX1, in BRAF- and NRAS-mutant melanoma. *Mol. Cancer Res.* **2016**, *14*, 1009–1018. [[CrossRef](#)] [[PubMed](#)]
42. Sosa, M.S.; Lopez-Haber, C.; Yang, C.; Wang, H.B.; Lemmon, M.A.; Busillo, J.M.; Luo, J.; Benovic, J.L.; Klein-Szanto, A.; Yagi, H.; et al. Identification of the Rac-GEF P-Rex1 as an Essential Mediator of ErbB Signaling in Breast Cancer. *Mol. Cell* **2010**, *40*, 877–892. [[CrossRef](#)]
43. Goel, H.L.; Pursell, B.; Shultz, L.D.; Greiner, D.L.; Brekken, R.A.; Vander Kooi, C.W.; Mercurio, A.M. P-Rex1 Promotes Resistance to VEGF/VEGFR-Targeted Therapy in Prostate Cancer. *Cell Rep.* **2016**, *14*, 2193–2208. [[CrossRef](#)] [[PubMed](#)]
44. Wan, S.C.; Wu, H.; Li, H.; Deng, W.W.; Xiao, Y.; Wu, C.C.; Yang, L.L.; Zhang, W.F.; Sun, Z.J. Overexpression of PREX1 in oral squamous cell carcinoma indicates poor prognosis. *J. Mol. Histol.* **2020**, *51*, 531–540. [[CrossRef](#)]
45. Venhoranta, H.; Pausch, H.; Flisikowski, K.; Wurmser, C.; Taponen, J.; Rautala, H.; Kind, A.; Schnieke, A.; Fries, R.; Lohi, H.; et al. In frame exon skipping in UBE3B is associated with developmental disorders and increased mortality in cattle. *BMC Genom.* **2014**, *15*, 1–9. [[CrossRef](#)]

46. Flex, E.; Ciolfi, A.; Caputo, V.; Fodale, V.; Leoni, C.; Melis, D.; Bedeschi, M.F.; Mazzanti, L.; Pizzuti, A.; Tartaglia, M.; et al. Loss of function of the E3 ubiquitin-protein ligase UBE3B causes kaufman oculocerebrofacial syndrome. *J. Med. Genet.* **2013**, *50*, 493–499. [[CrossRef](#)] [[PubMed](#)]
47. Li, K.; Wang, F.; Yang, Z.N.; Zhang, T.T.; Yuan, Y.F.; Zhao, C.X.; Yeerjiang, Z.; Cui, B.; Hua, F.; Lv, X.X.; et al. TRIB3 promotes MYC-associated lymphoma development through suppression of UBE3B-mediated MYC degradation. *Nat. Commun.* **2020**, *11*. [[CrossRef](#)] [[PubMed](#)]
48. Lek, M.; Karczewski, K.J.; Minikel, E.V.; Samocha, K.E.; Banks, E.; Fennell, T.; O'Donnell-Luria, A.H.; Ware, J.S.; Hill, A.J.; Cummings, B.B.; et al. Analysis of protein-coding genetic variation in 60,706 humans. *Nature* **2016**, *536*, 285–291. [[CrossRef](#)]
49. Gaudet, P.; Livstone, M.S.; Lewis, S.E.; Thomas, P.D. Phylogenetic-based propagation of functional annotations within the Gene Ontology consortium. *Brief. Bioinform.* **2011**, *12*, 449–462. [[CrossRef](#)] [[PubMed](#)]
50. Uniprot UniProtKB - Q9Y5H1. Available online: <https://www.uniprot.org/uniprot/Q9Y5H1> (accessed on 16 December 2020).
51. Song, J.; Wu, S.; Xia, X.; Wang, Y.; Fan, Y.; Yang, Z. Cell adhesion-related gene somatic mutations are enriched in aggressive papillary thyroid microcarcinomas. *J. Transl. Med.* **2018**, *16*, 1–9. [[CrossRef](#)]
52. Tischfield, D.J.; Saraswat, D.K.; Furash, A.; Fowler, S.C.; Fuccillo, M.V.; Anderson, S.A. Loss of the neurodevelopmental gene Zswim6 alters striatal morphology and motor regulation. *Neurobiol. Dis.* **2017**, *103*, 174–183. [[CrossRef](#)]
53. InterPro Zinc finger, SWIM-type (IPR007527). Available online: <http://www.ebi.ac.uk/interpro/entry/InterPro/IPR007527/> (accessed on 24 November 2020).
54. Twigg, S.R.F.; Ousager, L.B.; Miller, K.A.; Zhou, Y.; Elaloui, S.C.; Sefiani, A.; Bak, G.S.; Hove, H.; Hansen, L.K.; Fagerberg, C.R.; et al. Acromelic frontonasal dysostosis and ZSWIM6 mutation: Phenotypic spectrum and mosaicism. *Clin. Genet.* **2016**, *90*, 270–275. [[CrossRef](#)]
55. Palmer, E.E.; Kumar, R.; Gordon, C.T.; Shaw, M.; Hubert, L.; Carroll, R.; Rio, M.; Murray, L.; Leffler, M.; Dudding-Byth, T.; et al. A Recurrent De Novo Nonsense Variant in ZSWIM6 Results in Severe Intellectual Disability without Frontonasal or Limb Malformations. *Am. J. Hum. Genet.* **2017**, *101*, 995–1005. [[CrossRef](#)]
56. Scott, D.C.; Rhee, D.Y.; Duda, D.M.; Kelsall, I.R.; Olszewski, J.L.; Paulo, J.A.; de Jong, A.; Ova, H.; Alpi, A.F.; Harper, J.W.; et al. Two Distinct Types of E3 Ligases Work in Unison to Regulate Substrate Ubiquitylation. *Cell* **2016**, *166*, 1198–1214. [[CrossRef](#)]
57. Huttlin, E.L.; Bruckner, R.J.; Paulo, J.A.; Cannon, J.R.; Ting, L.; Baltier, K.; Colby, G.; Gebreab, F.; Gygi, M.P.; Parzen, H.; et al. Architecture of the human interactome defines protein communities and disease networks. *Nature* **2017**, *545*, 505–509. [[CrossRef](#)] [[PubMed](#)]
58. Lu, L.; Hu, S.; Wei, R.; Qiu, X.; Lu, K.; Fu, Y.; Li, H.; Xing, G.; Li, D.; Peng, R.; et al. The HECT type ubiquitin ligase NEDL2 is degraded by anaphase-promoting complex/cyclosome (APC/C)-Cdh1, and its tight regulation maintains the metaphase to anaphase transition. *J. Biol. Chem.* **2013**, *288*, 35637–35650. [[CrossRef](#)]
59. Uren, P.J.; Bahrami-Samani, E.; de Araujo, P.R.; Vogel, C.; Qiao, M.; Burns, S.C.; Smith, A.D.; Penalva, L.O.F. High-throughput analyses of hnRNP H1 dissects its multi-functional aspect. *RNA Biol.* **2016**, *13*, 400–411. [[CrossRef](#)] [[PubMed](#)]
60. Fei, T.; Chen, Y.; Xiao, T.; Li, W.; Cato, L.; Zhang, P.; Cotter, M.B.; Bowden, M.; Lis, R.T.; Zhao, S.G.; et al. Genome-wide CRISPR screen identifies HNRNPL as a prostate cancer dependency regulating RNA splicing. *Proc. Natl. Acad. Sci. USA* **2017**, *114*, E5207–E5215. [[CrossRef](#)]
61. Tron, A.E.; Arai, T.; Duda, D.M.; Kuwabara, H.; Olszewski, J.L.; Fujiwara, Y.; Bahamon, B.N.; Signoretti, S.; Schulman, B.A.; DeCaprio, J.A. The Glomuvenous Malformation Protein Glomulin Binds Rbx1 and Regulates Cullin RING Ligase-Mediated Turnover of Fbw7. *Mol. Cell* **2012**, *46*, 67–78. [[CrossRef](#)]
62. Brouillard, P.; Boon, L.M.; Mulliken, J.B.; Enjolras, O.; Ghassibé, M.; Warman, M.L.; Tan, O.T.; Olsen, B.R.; Vikkula, M. Mutations in a novel factor, glomulin, are responsible for glomuvenous malformations (“glomangiomas”). *Am. J. Hum. Genet.* **2002**, *70*, 866–874. [[CrossRef](#)] [[PubMed](#)]
63. Irrthum, A.; Brouillard, P.; Enjolras, O.; Gibbs, N.F.; Eichenfield, L.F.; Olsen, B.R.; Mulliken, J.B.; Boon, L.M.; Vikkula, M. Linkage disequilibrium narrows locus for venous malformation with glomus cells (VMGLOM) to a single 1.48 Mbp YAC. *Eur. J. Hum. Genet.* **2001**, *9*, 34–38. [[CrossRef](#)] [[PubMed](#)]
64. Yin, J.; Qin, Z.; Wu, K.; Zhu, Y.; Hu, L.; Kong, X. Rare Germline GLMN Variants Identified from Blue Rubber Bleb Nevus Syndrome Might Impact mTOR Signaling. *Comb. Chem. High Throughput Screen.* **2019**, *22*, 675–682. [[CrossRef](#)]

4.1.4.4 A frameshift insertion in *FA2H* causes a recessively inherited form of ichthyosis congenita in Chianina cattle

Journal: Molecular Genetics and Genomics

Manuscript status: published

Contributions: phenotype description, whole-genome sequencing data analysis, figures, writing original draft and revisions

Displayed version: published version

DOI: [10.1007/s00438-021-01824-8](https://doi.org/10.1007/s00438-021-01824-8)



A frameshift insertion in *FA2H* causes a recessively inherited form of ichthyosis congenita in Chianina cattle

Joana G. P. Jacinto^{1,2} · Irene M. Häfliger² · Inês M. B. Veiga³ · Anna Letko² · Arcangelo Gentile¹ · Cord Drögemüller²

Received: 14 July 2021 / Accepted: 23 September 2021 / Published online: 2 October 2021
© The Author(s) 2021

Abstract

The aim of this study was to characterize the phenotype and to identify the genetic etiology of a syndromic form of ichthyosis congenita (IC) observed in Italian Chianina cattle and to estimate the prevalence of the deleterious allele in the population. Sporadic occurrence of different forms of ichthyosis including IC have been previously reported in cattle. However, so far, no causative genetic variant has been found for bovine IC. Nine affected cattle presenting congenital xerosis, hyperkeratosis and scaling of the skin as well as urolithiasis and cystitis associated with retarded growth were examined. Skin histopathology revealed a severe, diffuse orthokeratotic hyperkeratosis with mild to moderate epidermal hyperplasia. The pedigree records indicated a monogenic recessive trait. Homozygosity mapping and whole-genome sequencing allowed the identification of a homozygous frameshift 1 bp insertion in the *FA2H* gene (c.9dupC; p.Ala4ArgfsTer142) located in a 1.92 Mb shared identical-by-descent region on chromosome 18 present in all cases, while the parents were heterozygous as expected for obligate carriers. These findings enable the selection against this sub-lethal allele showing an estimated frequency of ~7.5% in Chianina top sires. A sporadic incidence of mild clinical signs in the skin of heterozygous carriers was observed. So far, pathogenic variants affecting the encoded fatty acid 2-hydroxylase catalyzing the synthesis of 2-hydroxysphingolipids have been associated with myelin disorders. In conclusion, this study represents the first report of an *FA2H*-related autosomal recessive inherited skin disorder in a mammalian species and adds *FA2H* to the list of candidate genes for ichthyosis in humans and animals. Furthermore, this study provides a DNA-based diagnostic test that enables selection against the identified pathogenic variant in the Chianina cattle population. However, functional studies are needed to better understand the expression of *FA2H* in IC-affected Chianina cattle.

Keywords Bovine · Genodermatoses · Fatty acid 2-hydroxylase · Precision medicine · Skin · Urolithiasis

Introduction

The aim of this study was to report a series of nine cases of IC in Chianina cattle, to characterize the clinicopathological phenotype and finally to present the results of the genetic

Communicated by Joan Cerdá.

✉ Cord Drögemüller
cord.droegemueller@vetsuisse.unibe.ch

Joana G. P. Jacinto
joana.goncalves2@studio.unibo.it

Irene M. Häfliger
irene.haeffliger@vetsuisse.unibe.ch

Inês M. B. Veiga
ines.veiga@vetsuisse.unibe.ch

Anna Letko
anna.letko@vetsuisse.unibe.ch

Arcangelo Gentile
arcangelo.gentile@unibo.it

¹ Department of Veterinary Medical Sciences, University of Bologna, Ozzano Emilia, 40064 Bologna, Italy

² Institute of Genetics, Vetsuisse Faculty, University of Bern, 3001 Bern, Switzerland

³ Institute of Animal Pathology, Vetsuisse Faculty, University of Bern, 3012 Bern, Switzerland

analysis that evidenced a homozygous frameshift variant in bovine *FA2H* gene. Moreover, the prevalence of the deleterious allele in a selected population of Chianina sires is also estimated.

Genodermatoses are sporadic inherited disorders of the skin that both in humans and in livestock animals mostly follow a monogenic mode of inheritance (Leeb et al. 2017; Jacinto et al. 2020; Pope 2020).

In human medicine, the concept of ‘genodermatosis with skin fragility’ was recently introduced by adding other genetic disorders with skin fragility such erosive or hyperkeratotic disorders (Pope 2020). Inherited ichthyosis characterized by an abnormal terminal keratinocyte differentiation belongs to this group of skin fragility disorders encompassing a clinically, pathologically and heritably heterogeneous presentation with a thickened stratum corneum resulting in localized or generalized scaling (Marukian and Choate 2016).

In human medicine, the classification of the different forms of ichthyosis is based on clinicopathological manifestations and mode of inheritance, being divided in two main types: non-syndromic forms when clinical findings are limited to the skin, and syndromic forms in case additional organs are involved (Oji et al. 2010). In this respect, ichthyosis has been associated to pathogenic variants in more than 30 genes that are involved in several cellular functions, such as DNA repair, lipid biosynthesis, adhesion and desquamation (Oji et al. 2010). In particular, recent advances have reinforced the causative role of mutations in genes encoding proteins essential to the formation of the hydrophobic barrier (Marukian and Choate 2016).

In domestic animals, ichthyosis has been described in dogs (Credille et al. 2009; Grall et al. 2012; Metzger et al. 2015; Bauer et al. 2017; Casal et al. 2017), pigs (Wang et al. 2019), sheep (Câmara et al. 2017) and cattle (Charlier et al. 2008; Woolley et al. 2019; Eager et al. 2020). Furthermore, it has also been reported in greater kudu calves (Chittick et al. 2002). While in sheep, pigs and greater kudu the underlying genetic cause of this condition has not been determined, in dogs pathogenic variants have been identified in five different candidate genes associated with the phenotype, four breed specific recessive inherited forms (*TGM1*, *SLC27A4*, *PNPLA1*, *NIPAL4*) (OMIA 000546-9615; OMIA 001973-9615; OMIA 001588-9615; OMIA 001980-9615) as well as a single dominant inherited form in a single affected dog (*ASPRV1*) (OMIA 002099-9615).

In Chianina, Shorthorn and Polled Hereford cattle, a form of ichthyosis named ichthyosis fetalis, which resembles the Harlequin-type ichthyosis described in human medicine, has been associated with recessively inherited mutations in *ABCA12* (OMIA 002238-9913) (Charlier et al. 2008; Woolley et al. 2019; Eager et al. 2020). Affected calves are still-born or die within the first days after birth and the skin is

diffusely covered with large horny plates separated by deep fissures and resembling a ‘leather cuirass’. Furthermore, eversion at mucocutaneous junctions provokes eclabium and ectropion (Chittick et al. 2002; Molteni et al. 2006).

In Chianina cattle, a second less severe form of ichthyosis, named ichthyosis congenita (IC), has also been described (Testoni et al. 2006) and in subsequent time repeatedly presented to the authors. Animals with IC show milder but comparable lesions to those of ichthyosis fetalis. It is clinically characterized by a more or less extended scale-like hyperkeratosis and multifocal alopecic areas, and histopathologically by a diffuse lamellar orthokeratotic hyperkeratosis. The underlying genetic cause of this form of syndromic form of ichthyosis associated with retarded growth is unknown.

Methods

Animals

This study did not require official or institutional ethical approval as it was not experimental, but rather part of clinical and pathological veterinary diagnostics. All animals in this study were examined with the consent of their owners and handled according to good ethical standards. It deals with a total of 129 Chianina cattle, including 9 IC-affected animals, 4 dams, 6 sires and 110 artificial insemination (AI) top sires. The tenth affected animal included in the study (case 10) was the one previously reported by Testoni et al. (2006), whose blood had at that time been frozen and therefore had remained available for genetic studies.

Clinical and pathological investigations

Eight calves (cases 1–8) and one heifer (case 9) presenting cutaneous hyperkeratosis and retarded growth were recorded by the teaching hospital of the Department of Veterinary Medical Sciences, University of Bologna between 2005 and 2020 (Online Resource 1). The mean age of record of the calves was 2.6 months (minimum–maximum: 2 days–7 months), whereas the heifer was 18 months. The mean age at death was 11.2 months (natural death, euthanasia or slaughtering). All affected animals and one dam (case 8’s dam) were thoroughly clinically examined. Information related to the skin condition of the other dams as well as of the sires were obtained by interviewing the owners or the breeders’ association, respectively.

A parasitological test for detection of ectoparasites and fungi infection was performed on case 8’s dam.

Skin biopsies using an 8 mm punch were obtained from seven affected animals (cases 1–3 and cases 6, 8, 9) and from case 8’s dam. The collected samples were fixed in 10% neutral buffered formalin, trimmed, processed, embedded in

paraffin wax, sectioned at 4 μm , and stained with hematoxylin and eosin (H&E) for further histological evaluation. Two affected animals (cases 2 and 8) were submitted to necropsy.

Pedigree design

Pedigree analysis was performed using Pedigraph version 2.4 software (Department of Animal Science, University of Minnesota, USA).

DNA extractions

Genomic DNA was extracted from the IC-affected animals (EDTA blood samples), four related dams (EDTA blood samples) and six related sires (semen) using Promega Maxwell RSC DNA system (Promega, Dübendorf, Switzerland). Furthermore, genomic DNA was also obtained from semen of 110 Chianina AI top sires with the same methodology.

SNP array genotyping and homozygosity mapping

High-density SNP genotyping was carried out for seven cases (cases 1–7) and eight obligate carriers (three dams and five sires) (Online Resource 1) on the Illumina BovineHD BeadChip array including 777,962 SNPs. All given SNP positions correspond to the bovine ARS-UCD1.2 genome assembly. The PLINK v1.9 software (Chang et al. 2015) was used to perform basic quality filtering of the dataset. Even though no sample was excluded, a total of 146,440 variants were removed owing to minor allele thresholds. The total genotyping rate was approximately 0.98. With a total of 631,522 remaining markers, homozygosity mapping was performed for the 7 IC-affected animals using the software PLINK v1.9 (Purcell et al. 2007) with the commands `--homozyg-kb 100` (considering homozygous segments of at least 100 kb), `--homozyg-match 0.95` (for allelic matching between both cases) and `--homozyg-group` (for generating an overlap-file), resulting in shared runs of homozygosity (ROH) indicating chromosomal region of identity-by-descent (IBD).

Whole-genome sequencing and variant calling

WGS using the Illumina NovaSeq6000 (Illumina Inc., San Diego, CA, USA) was performed on the genomic DNA of two affected calves (cases 1 and 6). The sequenced reads were mapped to the ARS-UCD1.2 reference genome, resulting in an average read depth of approximately 18.2 \times in case 1 and 17.9 \times in case 6, and single-nucleotide variants (SNVs) and small indel variants were called (Rosen et al. 2020). The applied software and steps to process fastq files into binary alignment map (BAM) and genomic variant call format files were in accordance with the 1000 Bull Genomes Project

processing guidelines of run 7 (Hayes and Daetwyler 2019), except for the trimming, which was performed using fastp (Chen et al. 2018). Further preparation of the genomic data was done according to Häfliger et al. 2020 (Häfliger et al. 2020). To find private variants, we compared the genotypes of the two calves with 597 cattle genomes of various breeds that had been sequenced in the course of other ongoing studies and that are publicly available (Online Resource 2) in the European Nucleotide Archive (SAMEA7690197 and SAMEA7690198 are the samples accession number of case 1 and case 6, respectively; <http://www.ebi.ac.uk/en>). The filtered list of remaining variants were further checked for their occurrence in a global control cohort of 4110 genomes of a variety of breeds (Hayes and Daetwyler 2019). Integrative Genomics Viewer (IGV) (Robinson et al. 2017) software was used for visual inspection of genome regions containing possible candidate genes.

Variant validation and genotyping via Sanger sequencing

PCR and Sanger sequencing were used to confirm the WGS results and to perform targeted genotyping for the identified *FA2H* frameshift insertion variant (18:2205625C>CG). All IC-affected animals, four available dams and six sires, as well as 113 AI top sires that included three fathers of the studied cases, were genotyped for the identified variant. Also the case reported by Testoni in 2006 (case 10) (Testoni et al. 2006) was genotyped. Primers were designed using the Primer-BLAST tool (Ye et al. 2012). After amplification with AmpliTaqGold360Mastermix (Thermo Fisher Scientific) the purified PCR products were directly sequenced on an ABI3730 capillary sequencer (Thermo Fisher Scientific). The primer sequences used were the following: 5'-AAATTCCTGGTT-GGGGAGCC-3' (forward primer) and 5'-CTCGACAACGAGACGCACC-3' (reverse primer). The sequence data were analyzed using Sequencher 5.1 software (GeneCodes).

Results

Clinical phenotype

All patients (case 1–9) showed a more or less extended skin xerosis, hyperkeratosis and scaling besides a retarded growth. In the affected area the skin was dry and greyish with scale-like hyper-keratosis, and the most severe lesions were present at the level of trunk and neck (Fig. 1a). The coat was dull and bristly. Moreover, multifocal alopecic lesions were noticed, mostly affecting the muzzle, eyelids, ears, and inner region of limbs. The youngest calves displayed multiple wrinkles and folds (≤ 1 month of age)

Fig. 1 Clinical characterization of Chianina cattle affected by ichthyosis congenita. **a** Note the dry, greyish skin with scale-like hyperkeratosis over most of the body surface (case 1). **b** Note the multiple wrinkles, folds and wounds secondary to the hyperkeratosis (case 8). **c** Higher magnification of **b** from the skin of the thoracic region. Note the pyoderma. **d** Note the urolithiasis characterized by the presence of small stones and crystals (arrows) on the perigenital region (case 7)



(Fig. 1b). No abnormalities were observed at the level of the mucocutaneous junctions. One of the animals (case 8) also showed secondary wounds and pyodermatitis (Fig. 1c). Urolithiasis evidenced by the presence of small stones and crystals in the perigenital region (Fig. 1d) accompanied the cutaneous disease in cases 1, 7, 8 and 10. A hypoglycemic and hypothermic crisis that provoked the death of case 8 during the winter season was interpreted as a secondary phenomenon of imbalanced thermoregulation capacity. No abnormalities were registered at the level of the cardiovascular, respiratory, musculoskeletal, and nervous systems in any animals.

Interestingly, case 8's dam showed mild localized xerosis, hyperkeratosis and scaling in the region of the rump. Unfortunately, since in most cases the parents of the affected animals had already been slaughtered, we could not evaluate the phenotype in more of these obligate carriers. However, we did see a total of three other confirmed *FA2H* heterozygous Chianina cattle and they were clinically normal.

Based on the clinical observations, the affected animals were consequently suspected to suffer from IC as described in this breed in 2006 (Testoni et al. 2006). A similar diagnosis was advanced also for the dam of case 8, although in a very mild form. For this animal the differential diagnosis of ectoparasitosis and fungi infection were excluded on the base of a parasitological test.

Pathological phenotype

Histological analysis of the biopsies from the cutaneous lesions revealed a severe, diffuse orthokeratotic

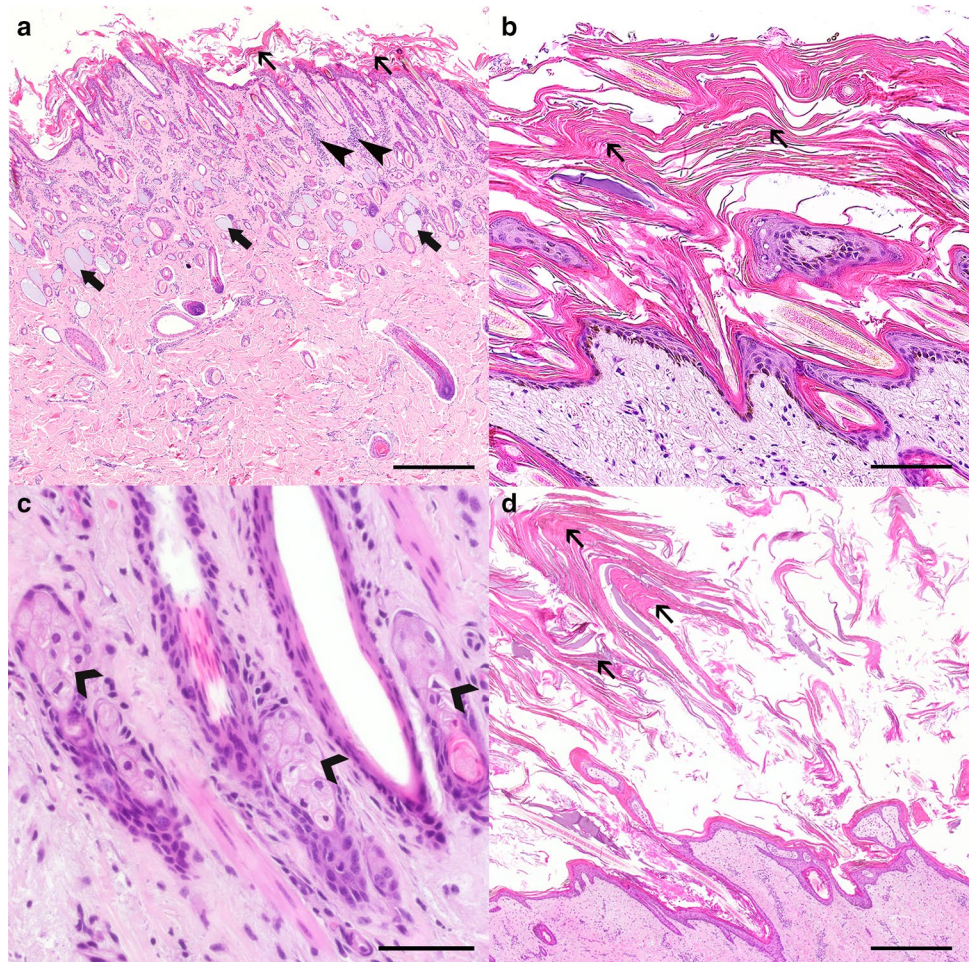
hyperkeratosis with mild to moderate epidermal hyperplasia (Fig. 2a, b). Serocellular crusts, serum lakes, and plant material were occasionally present among the abundant keratin scales. The superficial dermis displayed multifocal, moderate eosinophilic infiltrates, as well as a mostly perivascular, moderate infiltration with plasma cells and lymphocytes (Fig. 2a). Also, it was possible to observe the presence of intracytoplasmic, spindle-shaped, optically empty clefts within the sebocytes (Fig. 2c) in several of the affected animals, while the remaining adnexal structures were unremarkable. Similar findings were observed histologically in the punch biopsies taken from the dam of case 8 (Fig. 2d). These findings were consistent with the clinical diagnosis of IC.

Moreover, post-mortem examination of three cases (cases 1, 8 and 10) revealed inflammation of the urinary bladder (cystitis).

Genetic analysis

Pedigree records allowed the identification of a common ancestor as all IC-affected Chianina cattle were inbred from a sire born in 1976 (Online Resource 3). Pedigree analysis was consistent with monogenic autosomal recessive inheritance, and therefore carried out homozygosity mapping as all cases would likely be homozygous for a common chromosome segment flanking the causal mutation. This revealed a total of two identical-by-descent (IBD) segments shared by all seven cases with available SNP data (case 1–7): one 548 kb-sized region on

Fig. 2 Histology of the skin lesions displayed by a IC-affected Chianina calf (**a–c**) and its dam (**d**). **a** The epidermis of the calf (case 8) is irregular and mildly hyperplastic, with a thick overlying stratum corneum composed of abundant orthokeratotic, lamellar keratin scales (thin arrows). The sebaceous glands are not noticeable at this magnification, and the sweat glands are often dilated and filled with basophilic, homogeneous material (large arrows). Occasional interstitial inflammatory infiltrates can be observed in the superficial dermis (thin arrowheads). H&E staining, 500 μ m. **b** Detail of the abundant orthokeratotic, lamellar keratin scales (thin arrows) (case 8). H&E staining, 100 μ m. **c** Detail of the sebaceous glands. Some sebocytes display intracytoplasmic, spindle-shaped, optically empty clefts (large arrowheads) (case 8). H&E staining, 50 μ m. **d** A severe orthokeratotic hyperkeratosis (thin arrows) could also be observed in the dam from case 8. H&E staining, 500 μ m



chromosome 5 from 21.75 to 22.298 Mb and a second 1.92 Mb-sized region on chromosome 18 from 1.37 to 3.29 Mb (Fig. 3a).

Filtering of WGS for private shared homozygous variants present in sequenced genomes of cases 1 and 6 and absent in 597 available control genomes identified ten private protein-changing variants with a predicted moderate or high impact. Analyzing the occurrence of these variants in the global control cohort of 4110 genomes of a variety of breeds (Hayes and Daetwyler 2019), a single frameshift variant in *FA2H* with a predicted high impact on the encoded protein exclusively present in the genome of the case 1 and 6 remained. The homozygous variant in *FA2H* exon 1 on chromosome 18 (chr18:g.2205625C>CG; c.9dupC) was confirmed using IGV software (Fig. 3b, d). The deleterious *FA2H* variant (NM_001192455.1: c.9dupC) was predicted to result in a frameshift in the beginning of the protein after alanine 4 with a stop codon after aspartate 142 (NP_001179384.1: p.Ala4ArgfsTer142) resulting in a completely different

amino acid sequence, if expressed, when compared with the wild type protein (Fig. 3e, f).

FA2H genotyping

To confirm and evaluate the presence of the *FA2H* variant, the affected genomic region was amplified by PCR and Sanger sequenced (Fig. 3c) in a total of ten cases, and presumable dams and sires when available. Analyzing the sequencing data, we observed that all cases were homozygous for the variants, whereas the available parents were heterozygous as expected for obligate carriers (Table 1). Furthermore, genotyping of 113 Chianina sires representing the active breeding population revealed a carrier ratio of 15% whereas the variant was absent in a global cohort of more than 4700 cattle of various breeds (Table 1).

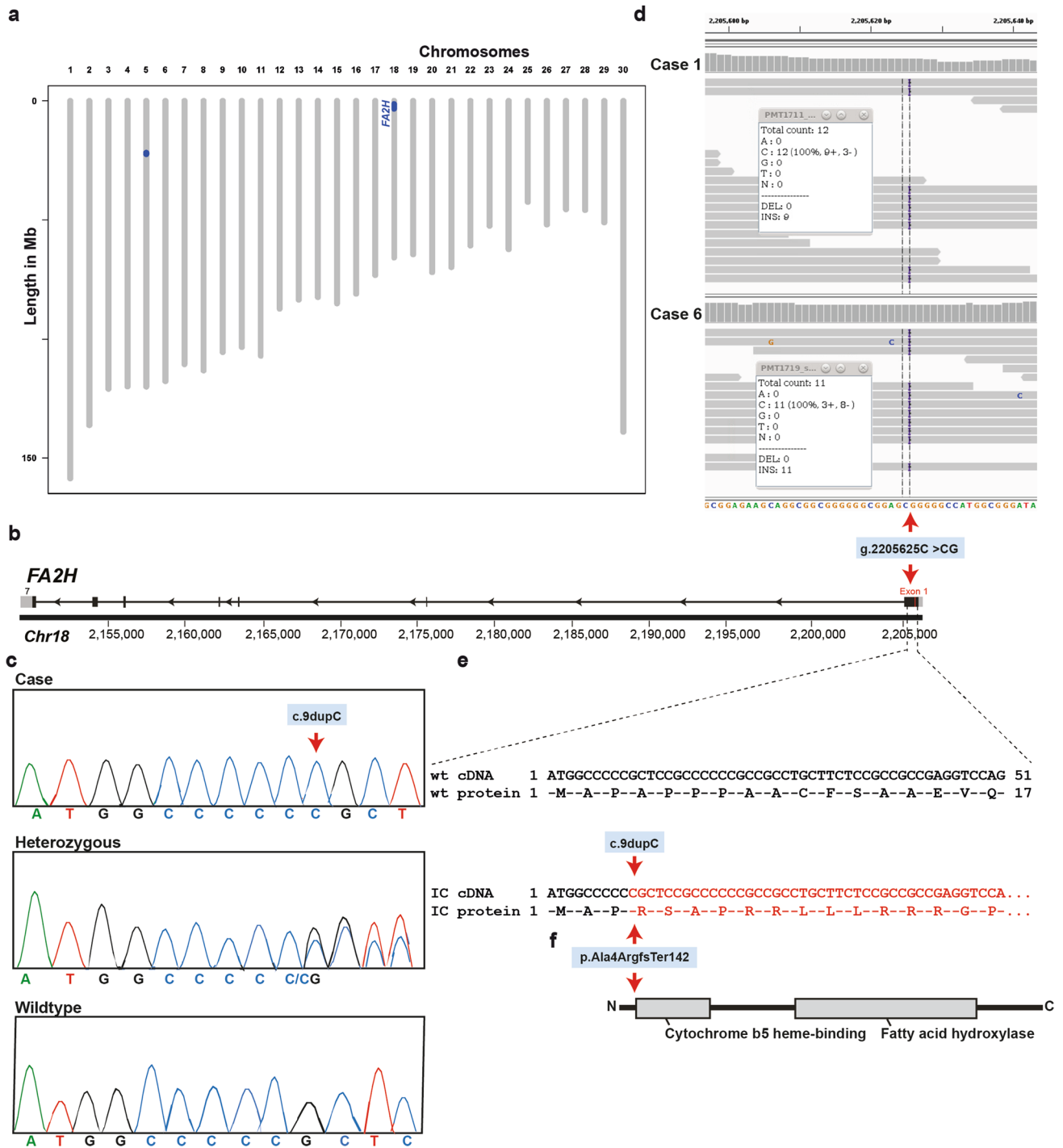


Fig. 3 Ichthyosis congenita (IC) *FA2H* frameshift variant in Chianina cattle. **a** Genetic mapping of the IC locus in the cattle genome. The two regions of shared homozygosity of seven cases are displayed in blue. Note that the largest segment of 1.92 Mb on chromosome 18 containing the, *FA2H* gene. **b** *FA2H* gene structure showing the variant located in exon 1. **c** Electropherograms of a case, heterozygous

and wild-type genotypes. **d** Integrative Genomics Viewer (IGV) screenshot presenting the g.2205625C>CG variant in the two whole-genome sequenced cases. **e** Predicted wild-type (wt) and IC cDNA e protein. **f** Schematic representation of the bovine *FA2H* protein and its two domains and the identified pathogenic frameshift variant (p.Ala4fsTer142; red arrow)

Table 1 Association of the 1 bp duplication (c.9dupC) variant in *FA2H* with ichthyosis congenita (IC) in Chianina cattle

	Genotype		
	wt/wt	wt/dup	dup/dup
IC-affected cattle	0	0	10
Obligate carriers ^a	0	10	0
Chianina top sires	96	17	0
Normal control cattle from various breeds	4707	0	0

^aParents of the affected animal

Discussion

Here we describe the clinicopathological phenotype displayed by nine Italian Chianina cattle with IC and present the results of the genetic analysis that identified a recessively inherited frameshift mutation in *FA2H*, providing a novel candidate gene for skin disorders in both humans and animals. Furthermore, we provide a DNA-based diagnostic test that enables the selection against this sub-lethal allele that show an estimated frequency of ~7.5% in Chianina top sires.

Clinicopathological resemblances between familial forms of ichthyosis in humans and animals and the keratinization defect observed histologically in IC-affected Italian Chianina cattle led to the hypothesis that genetic variants in candidate genes for ichthyosis could be responsible for this disease in cattle. However, protein-changing variants within these more than 30 known candidate genes (Oji et al. 2010) were not found within the two mapped IBD regions, thereby excluding these as likely candidates. We then performed whole-genome sequencing of two IC-affected cattle that led to the identification of a frameshift mutation in *FA2H* (c.9dupC; p.Ala4ArgfsTer142). The genetic association of this variant with the bovine familial IC phenotype was confirmed by the homozygous genotype in eight additionally affected cattle, including an older case presented in 2006, and by its absence in all other sequenced genomes. Furthermore, reported expression of *FA2H* transcripts in the urinary tract supports the associated urolithiasis and cystitis seen in some of the IC-affected cattle. Finally, the predicted consequence of the frameshift variant demonstrating a loss-of-function supports causality. This variant is therefore the first in any domestic animal species to be associated with IC, and *FA2H* should be considered an additional candidate gene for syndromic forms of ichthyosis in humans.

While genetic analysis strongly suggested the association of p.Ala4ArgfsTer142 allele with IC in affected Italian Chianina cattle, the frameshift variant lies very near the N-terminal end of the protein. Therefore, the impact of such a significant truncation on protein function is probably high, thus the variant represents a most likely pathogenic

loss-of-function mutation. Within a representative cohort of the current Italian Chianina population, a moderate allele frequency and the absence of the homozygous genotype for the deleterious allele was noticed.

In humans, mutations in *FA2H* (OMIM611026) are associated with recessively inherited spastic paraplegia type 35 (Dick et al. 2010), leukodystrophy with spasticity and dystonia (Edvardson et al. 2008), and fatty acid hydroxylase-associated neurodegeneration, a rare subtype neurodegeneration with brain iron accumulation (Kruer et al. 2010). So far, more than 40 different mutations have been associated with these neurological phenotypes (Rattay et al. 2019; Kawaguchi et al. 2020). However, to the best of our knowledge, no pathogenic variant in the *FA2H* associated to a form of ichthyosis has been reported in both animal and human species. Therefore, our study in cattle provides the first large-animal model of an *FA2H*-related congenital skin disorder.

FA2H encodes the endoplasmic reticulum enzyme fatty acid 2-hydroxylase, which plays a major role in the de novo synthesis of sphingolipids containing 2-hydroxy fatty acids (Alderson et al. 2004, 2005; Maldonado et al. 2008). 2-Hydroxy sphingolipids are very plentiful in neural tissue since the major components of myelin are galactolipids (galactosylceramide and sulfatide) with 2-hydroxy fatty acids (Alderson et al. 2005; Maldonado et al. 2008). However, the function of 2-hydroxyl modification of sphingolipids is still poorly known, although several studies evidently demonstrated that these compounds (including ceramides) play important roles in signal transduction (Hannun and Obeid 2008). Particularly, a study demonstrated that absence of FA2H lead to the impairment of cAMP-dependent cell cycle exit of Schwannoma cells, suggesting that FA2H sphingolipids may negatively regulate the cell cycle (Alderson and Hama 2009). Moreover, *FA2H* is highly expressed in the epidermis (Uchida et al. 2007). Notably, mammalian skin contains reasonably large amounts of 2-hydroxylated sphingolipids, which are involved in cell–cell recognition, signal transduction, and intercellular adhesion (Hakomori 2002; Uchida et al. 2007). The sphingolipids' ceramide backbone also plays a role as an intracellular signal of cell arrest, cellular senescence, and apoptosis in several types of cell, including keratinocytes (Hannun and Luberto 2000). Besides these ubiquitous bioregulatory functions, ceramide are abundant components of the extracellular lamellar membranes in the outermost layers of the epidermis, such as the stratum corneum, where they play an important role in the epidermal permeability barrier function (Holleran et al. 2006). Also, a notable increase in ceramide is noticed during epidermal differentiation (Holleran et al. 2006). In humans, it is known that differentiation-dependent up-regulation of ceramide synthesis and fatty acid elongation is accompanied by up-regulation of FA2H. Furthermore, the 2-hydroxylation of fatty acid by FA2H occurs prior to generation of

ceramides/glucosylceramides, and 2-hydroxyceramides/2-hydroxyglucosylceramides are essential for epidermal lamellar membrane formation (Uchida et al. 2007). Such findings suggest that the expression of FA2H is essential for epidermal permeability barrier homeostasis and responsible for synthesis of 2-hydroxylated sphingolipids in keratinocytes of mammalian skin. Therefore, the severe orthokeratotic hyperkeratosis observed in the Chianina cattle with IC could be a consequence of the frameshift insertion in the *FA2H* gene. Notably, lack of FA2H in *Fa2h*^{-/-} mice leads to hyperproliferation of sebocytes and enlarged sebaceous glands during hair follicle morphogenesis and anagen (active growth phase) in adult mice (Maier et al. 2011). Interestingly, the IC-affected animals included in this study often displayed intracytoplasmic, spindle-shaped, optically empty clefts within the sebocytes, although the sebaceous glands were similar in size to the ones observed in control animals. Sebaceous glands are holocrine glands that secrete a viscous, lipid-rich fluid rich in cholesterol and wax esters, triglycerides, squalene and cholesterol playing an important role in thermoregulation (Porter 2001). The rate of sebum is associated with the number and size of glands, and low production of sebum might lead to sebatosis or xerosis (Porter 2001; Shamloul and Khachemoune 2020). The major functions of sebum are to lubricate the skin and hair conferring impermeability to water, and in thermoregulation (Shamloul and Khachemoune 2020). Moreover, sebaceous glands play a role in immunity since sebum is thought to have antibacterial and antifungal properties (Strauss et al. 1983). Consequently, our findings may suggest that cattle affected by IC might be predisposed to develop skin secondary infections and present thermoregulation deficits due to this genetic defect. These situations were evidently suspected for two of our patients. Moreover, in *Fa2h*^{-/-} mice, deficiency in *Fa2h* caused a delay in emergence of the fur during morphogenesis and depilation-induced anagen and a cyclic alopecia (Maier et al. 2011). Herein, the cases revealed a localized alopecia, but the hair follicles present in the biopsies taken from the IC cutaneous lesions were unremarkable.

In mice, depletion of FA2H decreases the protein levels of GLUT4 leading to reduced glucose uptake and lipogenesis under basal and insulin-stimulated conditions (Guo et al. 2010). GLUT4 deficiency in mice (*Slc2a4*^{tm1Mch}/*Slc2a4*^{tm1Mch}) leads to retarded growth, decreased expected longevity and abnormal cellular glucose and fat metabolism (Katz et al. 1995). Intriguingly, all Chianina cattle homozygous for the *FA2H* mutation showed retarded growth and decreased expected longevity. Unfortunately, metabolic analysis to access the glucose metabolism was not performed.

Beside the skin lesions that were displayed in all the cases, four out of ten cases showed urolithiasis and three out of ten revealed cystitis. It is worth to highlight that in the six animals where these findings were not recorded: one was

ethanized 2 days after birth, and consequently, the absence of these findings might be explain by the young age of the calf; the remaining five were clinically examined only at the farms and, therefore, it was not possible to have a follow-up of the clinical status. On the contrary, the cases where we observed urolithiasis and cystitis were recovered at the clinic allowing the performance of a more detailed examination. Urolithiasis is a multifactorial disease resulting from complex interactions between environmental and genetic factors. Interestingly, *FA2H* in humans is also expressed in the urinary bladder and kidney (Fagerberg et al. 2014). However, physiological functions of FA2H in these organs are largely unknown.

Conclusions

Rare disorders like IC in livestock are usually not reported or are mis-diagnosed. Based on the known function of *FA2H* and its role in the skin, the predicted impact of the identified variant and its perfect co-segregation with the disease phenotype in the studied pedigree, we conclude that inherited IC in Chianina cattle is caused by a homozygous loss-of-function variant in *FA2H*. Thereby, this study represents an outstanding animal model for the understanding of similar conditions in different species and adds *FA2H* to the list of candidate genes for ichthyosis in humans. This example highlights the utility of precision diagnostics including genomics, for understanding rare disorders and the value of surveillance of cattle breeding populations for harmful genetic disorders.

Moreover, this study provides a DNA-based diagnostic test that allows selection against the identified pathogenic variant in the Chianina cattle population. Due to the high economic value of many Chianina cattle, including their skin for leather production, genetic testing should be pursued to prevent breeding of carriers that produce affected calves.

Supplementary Information The online version contains supplementary material available at <https://doi.org/10.1007/s00438-021-01824-8>.

Acknowledgements The Next Generation Sequencing Platform and the Interfaculty Bioinformatics Unit of the University of Bern are acknowledged for performing the WGS experiments and providing high-performance computing infrastructure. The technical assistance of Nathalie Besuchet Schmutz, Manuela Bozzo, Erika Bürgi, and Francesca Caravello is acknowledged.

Author contributions JGPJ performed all clinical and genetic analyses and drafted the manuscript. IMH carried out bioinformatics. AL assisted in the genetic analyses. AG collected samples and drafted parts of the manuscript. IMBV performed histopathology and drafted parts of the manuscript. AG and CD designed the study, supervised the project and finalized the manuscript. All authors participated in writing the manuscript and have read and approved the final version.

Funding Open Access funding provided by Universität Bern. This study was partially funded by the Swiss National Science Foundation.

Data availability The whole-genome data of our group have been made freely available under study accession number PRJEB28191 in the European Nucleotide Archive (<http://www.ebi.ac.uk/ena>). All accession numbers of the WGS are available in the Online Resource 2. SAMEA7690197 and SAMEA7690198 are the samples accession number of case 1 and case 6, respectively. All references to the bovine FA2H gene correspond to the NCBI accessions NC_037345.1 (chromosome 18, ARS-UCD1.2), NM_001192455.1 (FA2H gene), and NP_001179384.1 (FA2H protein). For the protein structure of FA2H, the UniProt database accession number E1BGC2 was used.

Code availability Not applicable.

Declarations

Conflict of interest The authors have no relevant financial or non-financial interests to disclose.

Ethics approval This study did not require official or institutional ethical approval as ‘non-experimental clinical veterinary practices’ are specifically excluded from being considered regulated procedures under The Animals (Scientific Procedures) Act (ASPA), 1986, Section 2(8) (<https://www.rcvs.org.uk/setting-standards/advice-and-guidance/code-of-professional-conduct-for-veterinary-surgeons/supporting-guidance/recognised-veterinary-practice/>). The cattle were handled according to good ethical standards and all live animals were blood sampled by a veterinary for diagnostic purposes on the farm to determine the cause of the disease. All other sampling was carried out postmortem on affected animals after euthanasia on humane grounds. The aim was to identify the cause of the congenital disorder and thereby improve the animal welfare situation on the Chianina cattle population by identifying the underlying genetic cause and preventing breeding of further cases.

Consent to participate Not applicable.

Consent for publication Not applicable.

Open Access This article is licensed under a Creative Commons Attribution 4.0 International License, which permits use, sharing, adaptation, distribution and reproduction in any medium or format, as long as you give appropriate credit to the original author(s) and the source, provide a link to the Creative Commons licence, and indicate if changes were made. The images or other third party material in this article are included in the article's Creative Commons licence, unless indicated otherwise in a credit line to the material. If material is not included in the article's Creative Commons licence and your intended use is not permitted by statutory regulation or exceeds the permitted use, you will need to obtain permission directly from the copyright holder. To view a copy of this licence, visit <http://creativecommons.org/licenses/by/4.0/>.

References

- Alderson NL, Hama H (2009) Fatty acid 2-hydroxylase regulates cAMP-induced cell cycle exit in D6P2T Schwannoma cells. *J Lipid Res* 50:1203–1208. <https://doi.org/10.1194/jlr.M800666-JLR200>
- Alderson NL, Rembiosa BM, Walla MD et al (2004) The human FA2H gene encodes a fatty acid 2-hydroxylase. *J Biol Chem* 279:48562–48568. <https://doi.org/10.1074/jbc.M406649200>
- Alderson NL, Walla MD, Hama H (2005) A novel method for the measurement of in vitro fatty acid 2-hydroxylase activity by gas chromatography–mass spectrometry. *J Lipid Res* 46:1569–1575. <https://doi.org/10.1194/jlr.D500013-JLR200>
- Bauer A, Waluk DP, Galichet A et al (2017) A de novo variant in the ASPRV1 gene in a dog with ichthyosis. *PLoS Genet* 13:1–13. <https://doi.org/10.1371/journal.pgen.1006651>
- Câmara ACL, Borges PAC, Paiva SA et al (2017) Ichthyosis fetalis in a cross-bred lamb. *Vet Dermatol* 28:125–156. <https://doi.org/10.1111/vde.12459>
- Casal ML, Wang P, Mauldin EA et al (2017) A Defect in NIPAL4 is associated with autosomal recessive congenital ichthyosis in American bulldogs. *PLoS ONE* 12:1–9. <https://doi.org/10.1371/journal.pone.0170708>
- Chang CC, Chow CC, Tellier LCAM et al (2015) Second-generation PLINK: rising to the challenge of larger and richer datasets. *Gigascience* 4:1–16. <https://doi.org/10.1186/s13742-015-0047-8>
- Charlier C, Coppie W, Rollin F et al (2008) Highly effective SNP-based association mapping and management of recessive defects in livestock. *Nat Genet* 40:449–454. <https://doi.org/10.1038/ng.96>
- Chen S, Zhou Y, Chen Y, Gu J (2018) Fastp: an ultra-fast all-in-one FASTQ preprocessor. *Bioinformatics* 34:i884–i890. <https://doi.org/10.1093/bioinformatics/bty560>
- Chittick EJ, Olivry T, Dalldorf F et al (2002) Harlequin ichthyosis in two greater Kudu (*Tragelaphus strepsiceros*). *Vet Pathol* 39:751–756. <https://doi.org/10.1354/vp.39-6-751>
- Credille KM, Minor JS, Barnhart KF et al (2009) Transglutaminase 1-deficient recessive lamellar ichthyosis associated with a LINE-1 insertion in Jack Russell terrier dogs. *Br J Dermatol* 161:265–272. <https://doi.org/10.1111/j.1365-2133.2009.09161.x>
- Dick KJ, Eckhardt M, Paisán-Ruiz C et al (2010) Mutation of FA2H underlies a complicated form of hereditary spastic paraplegia (SPG35). *Hum Mutat* 31:1251–1260. <https://doi.org/10.1002/humu.21205>
- Eager KLM, Conyers LE, Woolley SA et al (2020) A novel ABCA12 frameshift mutation segregates with ichthyosis fetalis in a Polled Hereford calf. *Anim Genet* 51:837–838. <https://doi.org/10.1111/age.12973>
- Edvardson S, Hama H, Shaag A et al (2008) Mutations in the fatty acid 2-hydroxylase gene are associated with leukodystrophy with spastic paraparesis and dystonia. *Am J Hum Genet* 83:643–648. <https://doi.org/10.1016/j.ajhg.2008.10.010>
- Fagerberg L, Hallström BM, Oksvold P et al (2014) Analysis of the human tissue-specific expression by genome-wide integration of transcriptomics and antibody-based proteomics. *Mol Cell Proteom* 13:397–406
- Grall A, Guaguère E, Planchais S et al (2012) PNPLA1 mutations cause autosomal recessive congenital ichthyosis in golden retriever dogs and humans. *Nat Genet* 44:140–147. <https://doi.org/10.1038/ng.1056>
- Guo L, Zhou D, Pryse KM et al (2010) Fatty acid 2-hydroxylase mediates diffusional mobility of raft-associated lipids, GLUT4 level, and lipogenesis in 3T3-L1 adipocytes. *J Biol Chem* 285:25438–25447. <https://doi.org/10.1074/jbc.M110.119933>
- Häfliger IM, Wiedemar N, Švara T et al (2020) Identification of small and large genomic candidate variants in bovine pulmonary hypoplasia and anasarca syndrome. *Anim Genet* 51:382–390. <https://doi.org/10.1111/age.12923>
- Hakomori SI (2002) The glycosynapse. *Proc Natl Acad Sci USA* 99:225–232. <https://doi.org/10.1073/pnas.012540899>

- Hannun YA, Luberto C (2000) Ceramide in the eukaryotic stress response. *Trends Cell Biol* 10:73–80. <https://doi.org/10.1080/00397911.2014.916302>
- Hannun YA, Obeid LM (2008) Principles of bioactive lipid signalling: lessons from sphingolipids. *Nat Rev Mol Cell Biol* 9:139–150. <https://doi.org/10.1038/nrm2329>
- Hayes BJ, Daetwyler HD (2019) 1000 bull genomes project to map simple and complex genetic traits in cattle: applications and outcomes. *Annu Rev Anim Biosci* 7:89–102. <https://doi.org/10.1146/annurev-animal-020518-115024>
- Holleran WM, Takagi Y, Uchida Y (2006) Epidermal sphingolipids: metabolism, function, and roles in skin disorders. *FEBS Lett* 580:5456–5466. <https://doi.org/10.1016/j.febslet.2006.08.039>
- Jacinto JGP, Häfliger IM, Veiga IMB et al (2020) A heterozygous missense variant in the COL5A2 in Holstein cattle resembling the classical Ehlers–Danlos syndrome. *Animals* 10:1–14. <https://doi.org/10.3390/ani10112002>
- Katz EB, Stenbit AE, Hatton K, DePinho R, Charron MJ (1995) Cardiac and adipose tissue abnormalities but not diabetes in mice deficient in GLUT4. *Nature* 377(6545):151–155
- Kawaguchi M, Sassa T, Kidokoro H et al (2020) Novel biallelic FA2H mutations in a Japanese boy with fatty acid hydroxylase-associated neurodegeneration. *Brain Dev* 42:217–221. <https://doi.org/10.1016/j.braindev.2019.11.006>
- Kruer MC, Paisán-Ruiz C, Boddart N et al (2010) Defective FA2H leads to a novel form of neurodegeneration with brain iron accumulation (NBIA). *Ann Neurol* 68:611–618. <https://doi.org/10.1002/ana.22122>
- Leeb T, Müller EJ, Roosje P, Welle M (2017) Genetic testing in veterinary dermatology. *Vet Dermatol* 28:4–e1. <https://doi.org/10.1111/vde.12309>
- Maier H, Meixner M, Hartmann D et al (2011) Normal fur development and sebum production depends on fatty acid 2-hydroxylase expression in sebaceous glands. *J Biol Chem* 286:25922–25934. <https://doi.org/10.1074/jbc.M111.231977>
- Maldonado EN, Alderson NL, Monje PV et al (2008) FA2H is responsible for the formation of 2-hydroxy galactolipids in peripheral nervous system myelin. *J Lipid Res* 49:153–161. <https://doi.org/10.1194/jlr.M700400-JLR200>
- Marukian NV, Choate KA (2016) Recent advances in understanding ichthyosis pathogenesis [version 1; referees: 2 approved]. *F1000Research* 5:1–9
- Metzger J, Wöhlke A, Mischke R et al (2015) A novel SLC27A4 splice acceptor site mutation in Great Danes with ichthyosis. *PLoS ONE* 10:1–13. <https://doi.org/10.1371/journal.pone.0141514>
- Molteni L, Dardano S, Parma P et al (2006) Ichthyosis in Chianina cattle. *Vet Rec* 158:412–414. <https://doi.org/10.1136/vr.158.12.412>
- Oji V, Tadani G, Akiyama M et al (2010) Revised nomenclature and classification of inherited ichthyoses: results of the First Ichthyosis Consensus Conference in Sorze 2009. *J Am Acad Dermatol* 63:607–641. <https://doi.org/10.1016/j.jaad.2009.11.020>
- Pope E (2020) Epidermolysis bullosa: a 2020 perspective. *Br J Dermatol* 183:603. <https://doi.org/10.1111/bjd.19125>
- Porter AMW (2001) Why do we have apocrine and sebaceous glands? *J R Soc Med* 94:236–237. <https://doi.org/10.1177/014107680109400509>
- Purcell S, Neale B, Todd-Brown K et al (2007) PLINK: a tool set for whole-genome association and population-based linkage analyses. *Am J Hum Genet* 81:559–575. <https://doi.org/10.1086/519795>
- Rattay TW, Lindig T, Baets J et al (2019) FAHN/SPG35: a narrow phenotypic spectrum across disease classifications. *Brain* 142:1561–1572. <https://doi.org/10.1093/brain/awz102>
- Robinson JT, Thorvaldsdóttir H, Wenger AM et al (2017) Variant review with the integrative genomics viewer. *Cancer Res* 77:e31–e34. <https://doi.org/10.1158/0008-5472.CAN-17-0337>
- Rosen BD, Bickhart DM, Schnabel RD et al (2020) De novo assembly of the cattle reference genome with single-molecule sequencing. *Gigascience* 9:1–9. <https://doi.org/10.1093/gigascience/giaa021>
- Shamloul G, Khachemoune A (2020) An updated review of the sebaceous gland and its role in health and diseases Part 1: embryology, evolution, structure, and function of sebaceous glands. *Dermatol Ther*. <https://doi.org/10.1111/dth.14695>
- Strauss J, Downing D, Ebling F (1983) Sebaceous glands. In: Goldsmith L (ed) *Biochemistry and physiology of the skin*. Oxford University Press, New York, pp 569–595
- Testoni S, Zappulli V, Gentile A (2006) Ichthyosis in two Chianina calves. *Dtsch Tierarztl Wochenschr* 113:351–354
- Uchida Y, Hama H, Alderson NL et al (2007) Fatty acid 2-hydroxylase, encoded by FA2H, accounts for differentiation-associated increase in 2-OH ceramides during keratinocyte differentiation. *J Biol Chem* 282:13211–13219. <https://doi.org/10.1074/jbc.M611562200>
- Wang X, Cao C, Li Y et al (2019) A harlequin ichthyosis pig model with a novel ABCA12 mutation can be rescued by acitretin treatment. *J Mol Cell Biol* 11:1029–1041. <https://doi.org/10.1093/jmcb/mjz021>
- Woolley SA, Eager KLM, Häfliger IM et al (2019) An ABCA12 missense variant in a Shorthorn calf with ichthyosis fetal. *Anim Genet* 50:749–752. <https://doi.org/10.1111/age.12856>
- Ye J, Coulouris G, Zaretskaya I et al (2012). *BMC Bioinform*. <https://doi.org/10.1186/1471-2105-13-134>

Publisher's Note Springer Nature remains neutral with regard to jurisdictional claims in published maps and institutional affiliations.

4.1.4.5 A *KRT71* Loss-of-Function Variant Results in Inner Root Sheath Dysplasia and Recessive Congenital Hypotrichosis of Hereford Cattle

Journal: Genes

Manuscript status: published

Contributions: phenotype description, whole-genome sequencing data analysis, figures, writing original draft and revisions

Displayed version: published version

DOI: [10.3390/genes12071038](https://doi.org/10.3390/genes12071038)

Article

A *KRT71* Loss-of-Function Variant Results in Inner Root Sheath Dysplasia and Recessive Congenital Hypotrichosis of Hereford Cattle

Joana G. P. Jacinto ^{1,2,†} , Alysta D. Markey ^{3,†}, Inês M. B. Veiga ⁴ , Julia M. Paris ² , Monika Welle ⁴, Jonathan E. Beever ^{3,5,‡}  and Cord Drögemüller ^{2,*,‡} 

¹ Department of Veterinary Medical Sciences, University of Bologna, 40064 Ozzano Emilia, Italy; joana.goncalves2@studio.unibo.it

² Institute of Genetics, Vetsuisse Faculty, University of Bern, 3012 Bern, Switzerland; julia-1991@hotmail.com

³ Laboratory of Molecular Genetics, Department of Animal Sciences, University of Illinois at Urbana-Champaign, Urbana, IL 61801, USA; alysta.markey@gmail.com (A.D.M.); jbeever@utk.edu (J.E.B.)

⁴ Institute of Animal Pathology, Vetsuisse Faculty, University of Bern, 3012 Bern, Switzerland; ines.veiga@vetsuisse.unibe.ch (I.M.B.V.); monika.welle@vetsuisse.unibe.ch (M.W.)

⁵ UTIA Genomics Center for the Advancement of Agriculture, Institute of Agriculture, University of Tennessee, Knoxville, TN 37996, USA

* Correspondence: cord.droegemueller@vetsuisse.unibe.ch; Tel.: +41-31-684-2529

† These authors contributed equally.

‡ These authors jointly supervised this work.



Citation: Jacinto, J.G.P.; Markey, A.D.; Veiga, I.M.B.; Paris, J.M.; Welle, M.; Beever, J.E.; Drögemüller, C. A *KRT71* Loss-of-Function Variant Results in Inner Root Sheath Dysplasia and Recessive Congenital Hypotrichosis of Hereford Cattle. *Genes* **2021**, *12*, 1038. <https://doi.org/10.3390/genes12071038>

Academic Editor: Anna V Kukekova

Received: 2 June 2021

Accepted: 2 July 2021

Published: 4 July 2021

Publisher's Note: MDPI stays neutral with regard to jurisdictional claims in published maps and institutional affiliations.



Copyright: © 2021 by the authors. Licensee MDPI, Basel, Switzerland. This article is an open access article distributed under the terms and conditions of the Creative Commons Attribution (CC BY) license (<https://creativecommons.org/licenses/by/4.0/>).

Abstract: Genodermatoses, such as heritable skin disorders, mostly represent Mendelian conditions. Congenital hypotrichosis (HY) characterize a condition of being born with less hair than normal. The purpose of this study was to characterize the clinicopathological phenotype of a breed-specific non-syndromic form of HY in Hereford cattle and to identify the causative genetic variant for this recessive disorder. Affected calves showed a very short, fine, wooly, kinky and curly coat over all parts of the body, with a major expression in the ears, the inner part of the limbs, and in the thoracic-abdominal region. Histopathology showed a severely altered morphology of the inner root sheath (IRS) of the hair follicle with abnormal Huxley and Henle's layers and severely dysplastic hair shafts. A genome-wide association study revealed an association signal on chromosome 5. Homozygosity mapping in a subset of cases refined the HY locus to a 690 kb critical interval encompassing a cluster of type II keratin encoding genes. Protein-coding exons of six positional candidate genes with known hair or hair follicle function were re-sequenced. This revealed a protein-changing variant in the *KRT71* gene that encodes a type II keratin specifically expressed in the IRS of the hair follicle (c.281delTGTGCCCA; p.Met94AsnfsX14). Besides obvious phenocopies, a perfect concordance between the presence of this most likely pathogenic loss-of-function variant located in the head domain of *KRT71* and the HY phenotype was found. This recessive *KRT71*-related form of hypotrichosis provides a novel large animal model for similar human conditions. The results have been incorporated in the Online Mendelian Inheritance in Animals (OMIA) database (OMIA 002114-9913).

Keywords: *Bos taurus*; congenital hypotrichosis; hair; head domain; keratin 71; precision medicine

1. Introduction

Hair is one of the distinguishing characteristics of mammals, and is involved in a wide range of functions such as thermoregulation, physical protection, and sensory activity [1]. The hair follicle (HF) is responsible for the production of hair [2–4]. Moreover, the HF represents an ectodermal appendage of the skin and is a complex structure [5]. The growing hair shaft is molded by the inner root sheath (IRS), which is surrounded by the companion layer, the outer root sheath, and the fibrous sheath. The IRS is composed of three layers: the IRS cuticle, the Huxley layer, and the Henle layer [6]. Many genes and signaling are known to be involved in HF development [1].

Keratins are the main structural component of the HF and some epithelial keratins are highly specific for the IRS of the HF, such as a set of four type I keratins (KRT25-KRT28) and five type II keratins (KRT71-KRT75) [7]. In particular, KRT71 is known to play a major role in hair shaft molding [6]. All keratins belong to the family of intermediate filament (IF) proteins and therefore share a common structural organization composed of three domains: the N-terminal head domain; the central α -helical rod domain; and the C-terminal tail domain [8].

Heritable hair disorders similar to many other genodermatoses mostly follow a monogenic mode of inheritance, e.g., congenital hypotrichosis (HY). HY belong to a group of human diseases, which are largely classified into syndromic and non-syndromic forms. HY is a condition generally characterized by the presence of less than the normal amount of hair and abnormal hair follicles and shafts, which can be completely absent or are dysplastic. The extent of body hair involvement can be very variable [6]. Thus, HY encompasses a clinically- pathologically- and heritably-heterogeneous group of hair disorders. Currently, human non-syndromic HY classification distinguishes 14 subtypes and 12 different associated genes (OMIM PS605389). Human HY following a dominant inheritance have been associated with causative variants in eight different genes (*EPS8L3*, *SNRPE*, *CDSN*, *HR*, *KRT71*, *KRT74*, *RPL21*, *APCDD1*) [6,9–15]. Whereas, autosomal recessive HY is related to mutations in four different genes (*LIPH*, *LPAR6*, *DSG4*, *LSS*) [16–19].

Forms of non-syndromic HY have been reported in many animal species (OMIA 000540), including American minks [20], cats [21,22], dogs [23], horses [24], macaques [25], meadow voles [26], Mongolian gerbils [27], golden hamsters [28], guinea pigs [29], pigs [30], sheep [31] and cattle [32]. Pathogenic variants causing forms of HY in animals have been identified in known candidate genes for HY (*HR* and *KRT71*) [21,22], or novel genes (*TSR2*, *SGK3* and *SP6*) [23,24,32] in HY-affected domestic animals. This highlights the potential of studying inherited conditions in such species to assign a role or function to previously uncharacterized genes or to add additional functions to known genes in regard to hair development.

In Hereford cattle, the occurrence of HY has been previously reported [33]. Hereford animals affected with the HY phenotype are born with partial or complete absence of hair that later becomes “fuzzy or kinky” in appearance [33]. This Hereford phenotype appears to be limited to the hair coat with microscopic analysis showing abnormal hair development. Characteristic large, atypical trichohyalin granules form in the IRS and are associated with premature breakup of the sheath and loss of the hair [34–36]. Furthermore, pedigree analysis indicates an autosomal recessive mode of inheritance [33,35]. Therefore, a monogenic cause for this breed-specific form of bovine HY affecting a functional candidate gene was hypothesized.

The aim of this study was to characterize the clinical and histopathological phenotypes of HY in Hereford cattle and to map the responsible genetic locus in the bovine genome and to identify the causative genetic variant associated with the disorder.

2. Materials and Methods

2.1. Animals and Samples

Clinical and pathological investigations were performed in 2021 at the University of Bern using two affected animals (cases 1 and 2) noted at the same farm in Switzerland. In addition, blood samples of 31 unaffected animals including both dams were sampled at this farm for subsequent genotyping.

Genetic investigation that leads to the identification of the pathogenic variant associated with the disease was performed earlier at the University of Illinois. The mapping population in this study consisted of 17 suspected affected calves born in the USA reported by eleven different farmers between 2007 and 2010, with eight of those having a single common male ancestor suspected to be a carrier of hypotrichosis (cases 24, 21, 111, 70, 109, 105, 107 and 110; group A). In addition, 22 suspected carrier animals were collected from these farms. The remaining affected calves were from two separate groups, with the first

being comprised of three affected half siblings and two distantly related calves (cases 22, 27, 341, 68, 237; group B). The second group contained four affected calves from three herds with unknown relatedness (cases 101, 287, 23, 286; group C). Finally, a population cohort consisting of 174 apparently normal cattle of the US purebred Hereford population was used to determine the absence/presence and frequency of the detected *KRT71* variant in the breed.

DNA was isolated from EDTA blood and semen samples using a simple salting out procedure [37].

2.2. Clinical and Histopathological Investigations

Two Hereford calves born in Switzerland, a two-month-old male (case 1) and an 11-month-old female (case 2), were referred by a breeder to the Institute of Genetics at the University of Bern because of congenital abnormal hair coat. The farm was a cow-calf-operation of Hereford cattle utilizing natural mating. Both cases were offspring from the same sire and both dams had a common ancestor. The two animals were reported to be born almost hairless and then started to develop short hair with age. The breeder reported that in the last four years, there were three additional cases in his herd.

Both affected calves were clinically examined. Furthermore, skin biopsies using an 8 mm punch were obtained from the neck skin from case 1 and a healthy control (1.5-month-old Simmental calf). The collected samples were fixed in 10% neutral buffered formalin and submitted to the Institute of Animal Pathology at the University of Bern, where these were trimmed, processed, embedded in paraffin wax, sectioned at 4 μ m, and stained with hematoxylin and eosin (H&E) for further histological evaluation.

2.3. Genetic Investigations

2.3.1. SNP Genotyping and GWAS

Seventeen affected animals and 54 normal breed controls were genotyped using the BovineSNP50 v1 Beadchip (Illumina, San Diego, CA, USA).

The whole genome association study (GWAS) and homozygosity mapping were completed using PLINK [38]. The “-assoc” and “-mperm” commands were used for GWAS and to obtain the corrected empirical P-value (max(T)) with 10,000 permutations. The commands “-homozyg-group” and “-homozyg-verbose” were used to group the pools of overlapping segments and display the genotypes for each pool. The command “-mind 0.15” allowed 15% missing genotypes per individual while the command “-maf 0.01” set the minor allele frequency to 1%. The command “-cow” set the chromosome codes for the cow. The command “-allow-no-sex” was used to allow ambiguously sexed individuals. The command “-homozyg-density 100” was used to allow one SNP per 100 kb.

During the genomic analysis, three different groups of affected animals were considered: group (A) represented eight cases that appeared in the verbose file using the homozygosity analysis commands described in Section 2.1; group (B) represents five cases that also appeared in the verbose file using relaxed homozygosity analysis commands; and group (C) represents four cases that did not appear in a verbose file from homozygosity analysis.

2.3.2. Microsatellite Genotyping

Microsatellite mapping was completed with 17 affected and 22 suspected carrier animals. Microsatellites were selected with the simple sequence repeat identification tool (SSRIT) [39], sequences were masked using RepeatMasker [40] and primers were designed using Primer Designer v 2.0 (Scientific and Educational Software). PCR products were fluorescently tagged via an M13 protocol [41], amplified in multiplex PCR and fragment analysis performed using an ABI3730xl DNA Analyzer (Applied Biosystems, Foster City, CA, USA). Microsatellite genotypes were analyzed with GeneMarker™ (Softgenetics®, LLC, State College, PA, USA).

2.3.3. Candidate Gene Analysis, Targeted Genotyping, Occurrence of the KRT71 Variant in a Global Control Cohort

Resequencing of candidate genes was completed for two normal, three suspected carrier and three affected animals. Six keratin genes (*KRT72*, *KRT71*, *KRT74*, *KRT83*, *KRT86*, and *KRT81*) were selected as candidates based on known function in hair and location relative to the homozygous region identified in the HY-affected calves on chromosome 5. Exon annotation based on computational methods was manually validated using mRNA sequences from NCBI and the software SPIDEY [42]. All references to the bovine *KRT71* gene correspond to the NCBI accessions NM_001075970.1 (*KRT71* mRNA), NP_001069438.1 (*KRT71* protein), NC_037332.1 (ARS-UCD1.2 assembly, chromosome 5). For the protein structure of *KRT71* the Uniprot accession Q148H5 was used.

Primers were designed as describe above to amplify protein coding exons in 1kb fragments (Table S1). Subsequent Sanger sequencing was performed on an ABI3730xl capillary sequencer and sequence assemblies were viewed and analyzed for polymorphisms using a Codon Code Aligner (Codon Code Corporation).

A diagnostic PCR and subsequent Sanger sequencing as described above were used to validate and genotype the variant in further animals. Therefore, the region containing the 8-bp deletion in *KRT71* (g.27331221delTGTGCCCA) was amplified using the following primers: 5'-CAGTGGGAAGAGTGGAGGTT-3' (forward primer) and 5'-CAATCCCTCTTGCTGCAACA-3' (reverse primer).

The most likely pathogenic 8-bp deletion in *KRT71* was searched for its occurrence in a global control cohort of 4110 genomes of a variety of breeds (1000 Bull Genomes Project run 8; www.1000bullgenomes.com (accessed on 1 July 2021)) [43]. Therefore we inspected the provided Variant Call Format (VCF) file of bovine chromosome 5 (PRJEB42783 is the project accession number at the European Variation Archive; <http://www.ebi.ac.uk/en> (accessed on 1 July 2021)) to evaluate the genotypes of the g.27331221delTGTGCCCA variant using an awk command on a local Linux server at the University of Bern.

3. Results

3.1. Clinical Phenotype

Particularly, the clinical examination of the cardiovascular, respiratory, urinary, musculoskeletal, and nervous systems showed no abnormalities. Moreover, no abnormalities in dentition were noticed as previously seen in cattle affected by ectodermal dysplasia, which is characterized by sparse hair and abnormal teeth [44].

The examination of the integument of both calves showed very short, fine, wooly, kinky and curly hair when compared to healthy animals (Figure 1a–c). The curly hair was more prominent in case 2, mostly on the head (Figure 1d). Kinky hair appeared over all parts of the body, with a major expression in ears, inner part of the limbs, and in the thoracic-abdominal region (Figure 1a,c,d). In the older animal (case 2), the observed lesions were more obvious (Figure 1c,d). No ectoparasites were observed in either case. Clinically, the calves were found to be healthy, with the exception of the hair coat changes.

Based on these clinical observations, the calves were suspected to have a congenital hypotrichosis.

3.2. Histopathological Phenotype

Histologically, the proximal portions of the hair follicles presented with dysplastic changes of the inner root sheath, characterized by large and irregularly sized trichohyalin granules and vacuolated cytoplasm of the non-cornified IRS cells (Figure 2b). The cornified IRS of the Henley layer in the inferior portion and of the Henley and Huxley layer of the isthmus region displayed irregular staining characteristics, and the remaining nuclei present in the isthmus were distributed irregularly (Figure 2b,d), whereas in normal bovine skin they are equally distributed (Figure 2a). Hair shafts were often shaped irregularly with an altered outer contour and were occasionally thinner than normal (Figure 2c,d). The histological findings were compatible with the clinical suspicion of a congenital hypotrichosis.



Figure 1. Congenital hypotrichosis in Hereford cattle. (a) Case 1: note the short, fine, woolly, kinky and curly hair, particularly in the thoracic-abdominal region. (b) Healthy control: 2-month-old Hereford calf with a normal coat. (c) Case 2: note the short, fine, woolly, kinky and curly hair, which is more severe than in case 1. (d) Case 2: note the evident curly hair in the head and the short, fine and kinky hair in the ears.

3.3. Genetic Analysis

Based on pedigree records, a monogenic recessive mode of inheritance was hypothesized. Initial GWAS using all 17 cases and 54 controls revealed evidence for association with the HY phenotype on chromosomes 5 and 7 (Figure 3a). Subsequent manual inspection of SNP genotyping data in both genome regions revealed a 690 kb region of shared homozygosity only for chromosome 5 from 26.91 Mb to 27.60 Mb in thirteen affected calves of group A and B (Figure 3c) while microsatellite genotyping of all 13 cases confirmed the region as homozygous between 26.58 Mb and 27.56 Mb (Table S2). The four HY-suspicious calves (group C) were excluded from this inspection, as they were heterozygous at different markers flanking this region (Table S2). Subsequent removal of these four calves from GWAS resulted in greater statistical significance of the association on chromosome 5 (Figure 3b) when compared to the GWAS including all reported calves (Figure 3a).

Positional candidate genes within the critical region were selected based on function and location relative to the homozygosity analysis of the HY-affected calves. A cluster of type II keratin encoding genes is annotated in that region (Figure 3d) and a total of 40 protein coding exons of six positional candidate genes were re-sequenced: *KRT72*, *KRT71*, *KRT74*, *KRT83*, *KRT86*, and *KRT81*. Only variants that were predicted to alter the coding sequences or that were located within the splice sites were considered. An eight base pair deletion was found in the first exon of the *KRT71* gene (chr5: g.27331221delTGTGCCCA)

(Figure 4a), which was consistent with expected genotype status of the animals sequenced. At the level of translation, the detected deletion (c.281delTGTGCCCA) is predicted to result in a frameshift in the head domain of KRT71 after methionine 94 with a premature stop codon at threonine 108 (p.Met94AsnfsX14) (Figure 4b,c). Consequently, the mutant protein, if expressed, is predicted to be significantly shorter than the normal KRT71 protein of 525 amino acids in length lacking the central α -helical rod and the terminal tail-domains important for dimerization (Figure 4c).

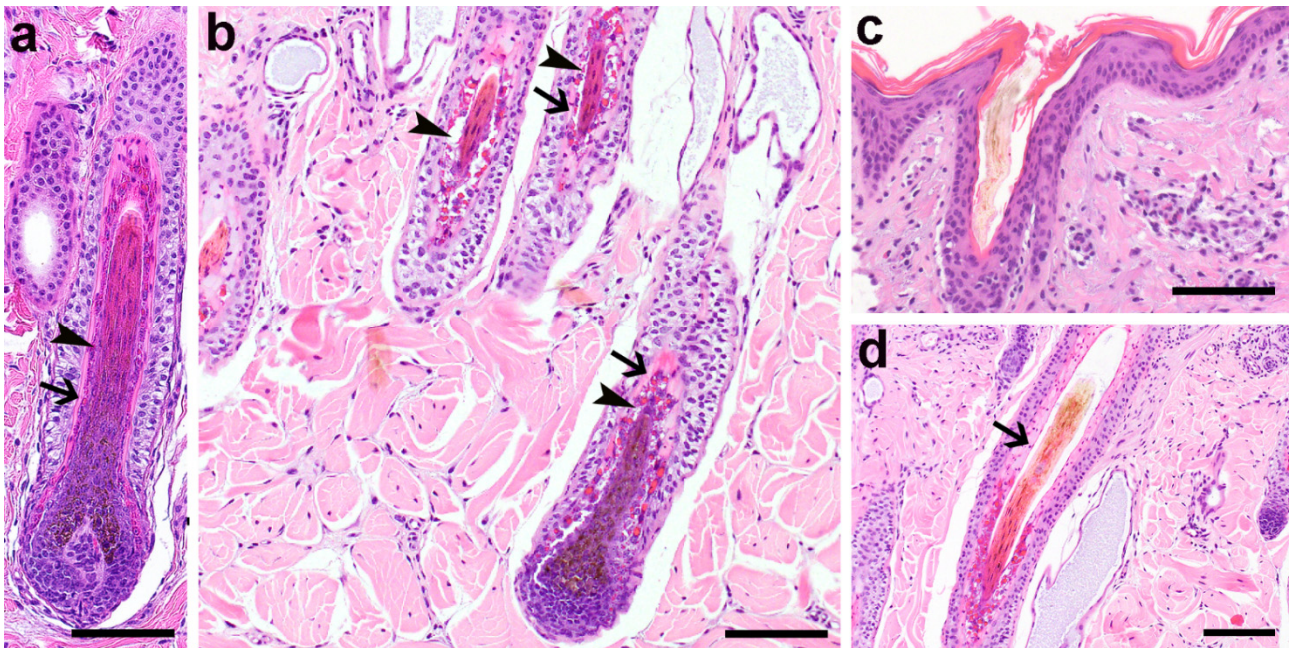


Figure 2. Histological changes displayed by a Hereford calf with congenital hypotrichosis. (a) Proximal portion of an anagen HF of a 1,5-month-old Simmental calf with a normal, non-cornified Huxley layer (arrowheads) and an already cornified Henle layer of the IRS (arrows) for comparison purposes. H&E staining, 200 \times . (b) Proximal portion of the anagen hair follicles of an affected Hereford calf (case 1) with a severely altered morphology of the inner root sheath. The cells of the non-cornified Huxley layer present with large, irregular sized trichohyalin granules and large vacuoles (arrowheads) in the cytoplasm. The already cornified Henle's layer (arrows) presents with large corneocytes with irregular staining characteristics. H&E staining, 200 \times . (c) Infundibulum with a dysplastic hair shaft from case 1, characterized by an irregular outer contour. H&E staining, 200 \times . (d) Altered cornification of the IRS in the isthmus region in case 1. The cornified IRS appears wider than normal and displays irregular staining characteristics. Nuclei were not arranged orderly (arrow) and the hair shaft has an irregular contour. H&E staining, 200 \times , bar 100 μ m in (a,b,d); bar 50 μ m in (c).

The 8-bp frameshift deletion in *KRT71* was validated by Sanger sequencing (Figure 4d). Genotyping of all 72 animals of the mapping cohort including the HY-suspicious calves, carriers and controls originating from the US Hereford population plus the cases, carriers and controls of the affected herd from Switzerland revealed perfect concordance between the presence of this deletion and the HY phenotype (Table 1). Among the HY- cases, all but four from the mapping cohort were homozygous mutants and all available carriers were heterozygous. These four HY-suspicious calves (case 110 of group A and cases 287, 23, 286 of group C) did not show the deleterious variant in *KRT71* nor a protein-changing variant in any further exon of the six candidate genes that were re-sequenced. It is probable that these four calves were misclassified based on phenotype and were not affected with the same type of congenital hypotrichosis and therefore were considered to represent phenocopies. Calf 101 (group C) was homozygous for the 8-bp frameshift deletion in *KRT71* but showed a shorter region of homozygosity, limiting the critical interval to 301 kb. Altogether, the mutant allele frequency was estimated as 2.2% in the studied unrelated 235 normal Hereford cattle.

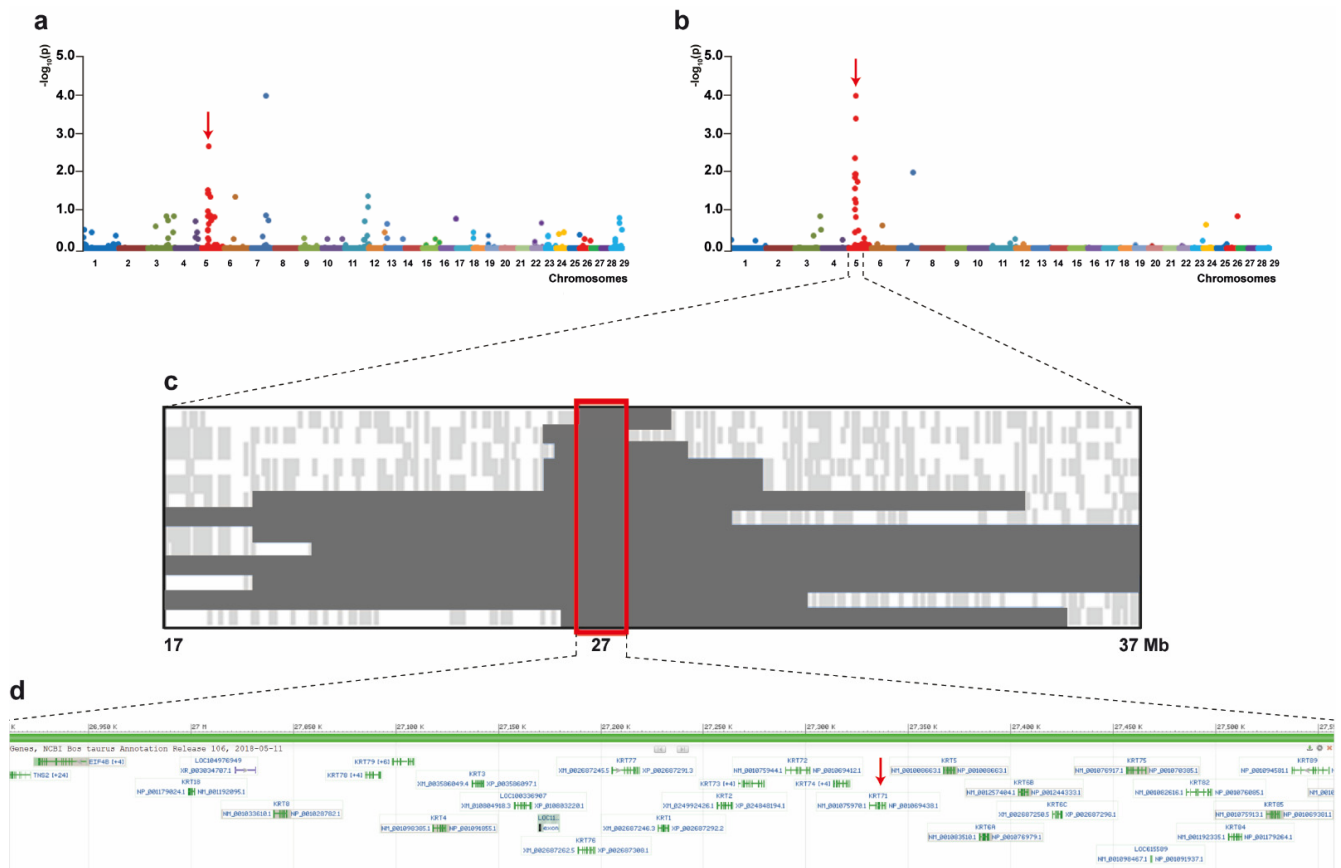


Figure 3. Positional cloning of the locus for recessive congenital hypotrichosis (HY) in Hereford cattle. (a) GWAS case/control results considering all purported HY-suspicious calves. Each chromosome is color coded along the X axis. The Y axis represents the $-\log_{10}$ of the corrected empirical P-value (max(T)) after 10,000 permutations from PLINK. (b) GWAS case/control results excluding calves from group C. Each chromosome is color coded along the X axis. The Y axis represents the $-\log_{10}$ of the corrected empirical P-value (max(T)) after 10,000 permutations from PLINK. (c) Schematic representing the genotypes of 13 HY-affected calves on chromosome 5. Each horizontal lane represents one calf with dark grey shading, indicating shared homozygosity. Light grey shading indicates a heterozygous genotype and white indicates an alternative homozygous genotype. The approximate Mb position is indicated below the figure. The red box encompasses the consensus homozygous region which spans approximately 690 kb. (d) Gene content of the critical region. Screen shot of NCBI Genome Data Viewer (ARS-UCD1.2 assembly, *Bos taurus* annotation release 106) shows the cluster of keratin II encoding genes including *KRT71* (red arrow).

Table 1. Association of the 8-bp deletion with the hypotrichosis phenotype.

	wt/wt	wt/del	del/del
HY-affected calves			
Swiss cases ^b			2
US cases	4 ^a		13
Obligate carriers ^c			
Swiss ^b		2	
US		22	
Unrelated normal Hereford cattle			
Swiss ^b	21	8	
US	197	9	
Global cohort included in the 1000 Bull Genomes Project	117		
Normal control cattle from various different breeds	3993		

^a these animals were assumed to represent phenocopies (see main text). ^b these animals were collected in a single farm. ^c parents of affected animals were classified as obligate carriers.

Additionally, the identified *KRT71* variant was absent in a global control cohort of 4110 cattle genomes, including 117 Hereford animals, of a variety of breeds included in the run 8 of the 1000 Bull Genomes Project [43].

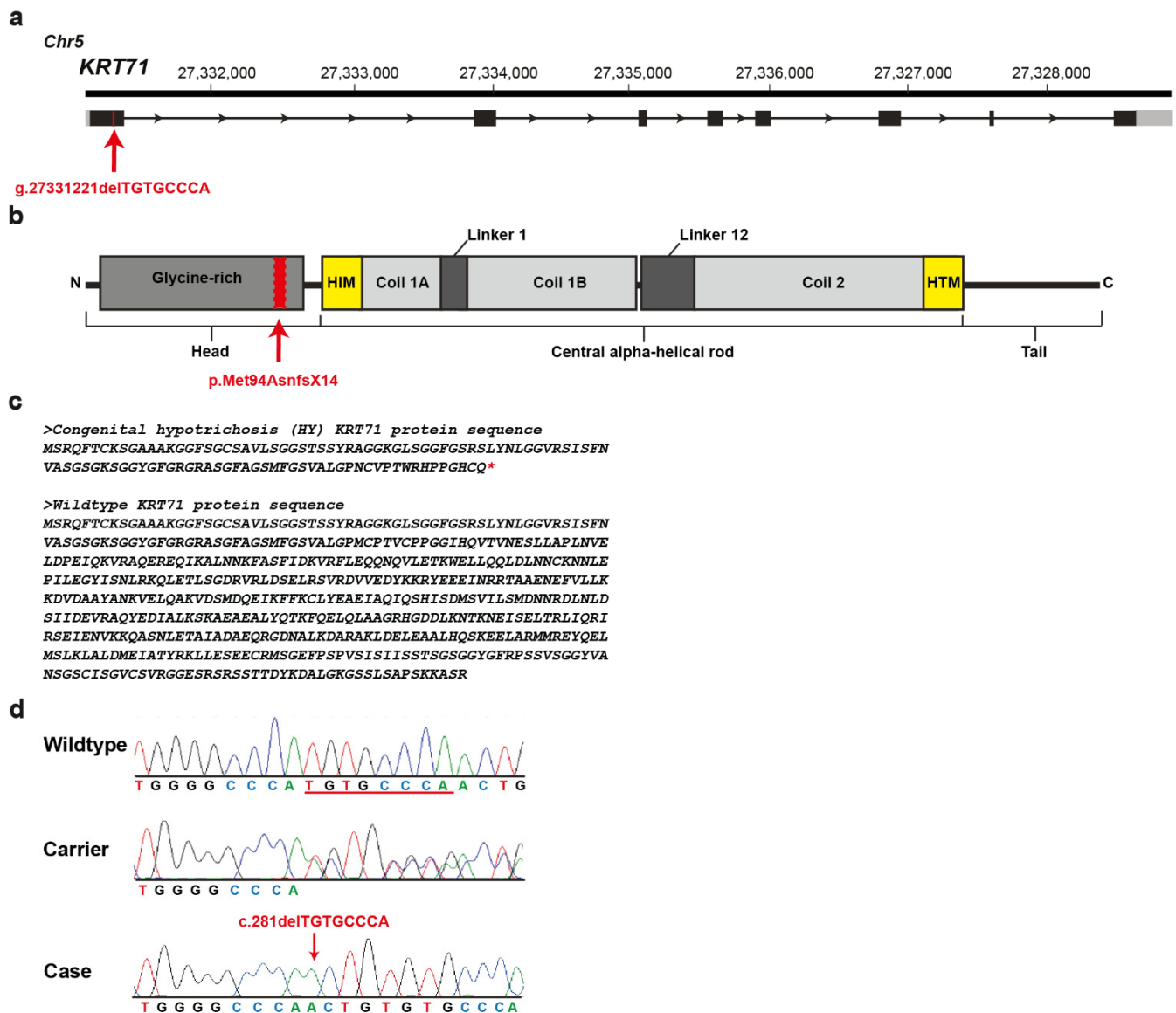


Figure 4. *KRT71* deletion in Hereford cattle affected by congenital hypotrichosis. (a) *KRT71* gene structure showing the location of the exon 1 variant on cattle chromosome 5. (b) Schematic representation of *KRT71* protein with its three functional domains. (c) Predicted protein sequences of an HY and wildtype *KRT71* protein. The red star (*) represents a stop codon. The normal protein is 525 amino acid residues in length. The HY protein is expected to be 108 amino acid residues in length due to the premature induction of a stop codon. (d) Electropherograms showing the different genotypes identified via Sanger sequencing.

4. Discussion

The identified deletion in *KRT71* resulting in a frameshift and early truncation of the protein affects a functionally important site of an obvious candidate gene and thus represents the most likely pathogenic variant associated with the observed recessively inherited congenital hypotrichosis (HY) phenotype in Hereford cattle. The HY-affected Hereford cattle herein presented clinically showed short, fine, wooly, kinky and curly hair and the skin biopsies examined from one of the affected calves showed a severely altered morphology of the IRS and the hair shafts.

Type I keratins have an acidic charge and are generally smaller while type II keratins, including *KRT71*, have a basic charge and are larger. These keratins form obligate type I-type II heterodimers [7,8]. Particularly, cytoplasmic IF proteins, such as keratins, undergo post-translational modifications (PMTs), including phosphorylation, glycosylation, sumoylation, acetylation, prenylation, ubiquitylation and transamidation, which regulate each other through crosstalk and binding of IFs to other proteins [45]. The structure of these proteins is highly dynamic and is able to reorganize in specific physiological conditions, e.g., during mitosis, cell stress situations and mutation response. The specific site of phosphorylation in the head and tail residues is the main facilitator of IF reorganization. Additionally, IF undergo other PMTs with target residues seated in the head, tail and central α -helical rod domains. PMTs of the central α -helical rod domain are most likely facilitated by the head and tail domain. It is known that many PMTs are altered in the context of disease-causing IF mutant [45]. The mutation identified in this study was positioned in the head domain of the protein. Taking into account that the identified pathogenic variant is a frameshift deletion resulting in a significantly shorter mutant transcript, and since this domain plays an essential role in the regulation of the protein, we speculate that the identified deletion disturbs the function. In fact, if the mutant mRNA transcript were to escape nonsense-mediated decay [46], the resultant truncated protein would not contain the α -helical rod domain or the helix boundary motifs that are integral to heterodimer formation of keratin molecules. This truncated protein would likely be unable to participate in filament formation, resulting in instability in the cytoskeletal network and a lack of tissue integrity [47].

So far, *KRT71* variants have been identified and studied at a molecular level in humans (OMIM 608245), mice, rats, dogs (OMIA 000245-9615) and cats (OMIA 001581-9685, OMIA 001712-9685, OMIA 001583-9685). In veterinary medicine, just one autosomal recessive splice site variant in *KRT71*-related hypotrichosis has been reported in cats in the coil 2 region of the central α -helical rod domain [22] and the histological findings in the hair follicles of Sphinx cats, which are a hairless cat breed, are identical to those found in the presented case [48]. In human medicine, a single, dominantly inherited *KRT71* missense variant associated with hypotrichosis has been reported affecting the helix initiation motif of the central α -helical rod domain [6]. Moreover, in mice models, several pathogenic *Krt71* variants affecting a single amino acid placed in the α -helical rod domain, mostly following an autosomal dominant inheritance, have been reported [49,50]. Interestingly, in mice, just one variant was positioned in the head domain and also showed recessive inheritance (*Rco3* mutation) [51]. The *Rco3* mutation is a 10 base pair deletion, resulting in a frameshift after amino acid residue 58 and, therefore, the absence of 422 carboxyl-terminal amino acid residues containing the complete α -helical rod domain [51]. The amino acid residues 59–134 show no similarity to any known or predicted protein. Similarly, the herein identified deletion is predicted to result in truncation of the *KRT71* protein after amino acid residue 108 with residues 95–108 showing no similarity to keratin proteins. Both truncated proteins would lack the rod and tail domains as well as the helix boundary motifs that are critical for heterodimer formation. Thus, if a truncated *KRT71* protein is produced, it is unlikely that the mutant protein would participate in correct heterodimer formation. As there were no detectable levels of *KRT71* in the IRS of the *Rco3* mice, it is more likely that the aberrant bovine *KRT71* transcript was removed by nonsense-mediated decay [46,51]. The same can be assumed for the variant identified here in cattle.

Further similarities between the *Rco3* and bovine variants are seen comparing the HY-phenotypes. The *Rco3* mutation is also autosomal and is recessively inherited and affects the skin, coat and nails, as well as the touch and vibrissae systems. The first body coat of *Rco3* homozygous mice was curly in nature, while the second body coat displayed progressive alopecia that was severe and patchy. Hair texture was abnormal with the cortex displaying frequent kinks and twists. The homozygous *Rco3* mice showed defective keratinization of the Henle's and Huxley's layers of the IRS, similar to what was observed in HY-affected Hereford cattle. Furthermore, the Henle's layer of *Rco3* mutants displayed

accumulation of electron-dense material, as well as lack of normal filament bundles that is likely due to either the inability of the truncated or the lack of the entire KRT71 protein to form heterodimers and intermediate filaments [51]. However, as described before in Sphinx and Devon Rex cats, also in the herein presented Hereford cattle, nails (respective hooves) and vibrissae system abnormalities as shown in *Rco3* mice were absent.

The hair anomalies reported here in Hereford cattle differ from those recently described in *HEPHL1*-related HY of Galloway cattle [52].

5. Conclusions

Rare non-lethal disorders such as hypotrichosis in livestock are usually not reported or diagnosed when the animals show mild to moderate phenotype, but they affect animal welfare through secondary wounds and may result in UV-induced skin cancer in grazing animals, thus lower the value of the affected animals. Additionally, molecular diagnosis is often not performed because of a lack of resources and diagnostic tools. Furthermore, this study provides a DNA-based diagnostic test that allows selection against the identified pathogenic variant in the international Hereford population. Investigation of these cases allowed a clinical, histopathological, and molecular genetic study, enabling for the first time the diagnosis of a *KRT71*-related recessively inherited form of HY in Hereford cattle. The loss-of-function variant most likely results to nonoccurrence of KRT71 during hair shaft molding, explaining the hair disorder. This study represents the first large animal model for similar human conditions. This example highlights the utility of precision diagnostics for understanding rare disorders and the neglected value of livestock populations for studying genetic disorders.

Supplementary Materials: The following are available online at <https://www.mdpi.com/article/10.3390/genes12071038/s1>. Table S1: Primer Sequences. Table S2: Genotypes of reported HY-suspicious calves on chromosome 5.

Author Contributions: Conceptualization, J.E.B. and C.D.; validation, J.E.B., M.W. and C.D.; formal analysis, J.G.P.J., A.D.M. and M.W.; investigation, J.G.P.J., A.D.M., I.M.B.V., and J.M.P.; writing—original draft preparation, J.G.P.J. and A.D.M.; writing—review and editing, J.G.P.J., A.D.M., I.M.B.V., M.W., J.E.B. and C.D.; visualization, J.G.P.J., A.D.M. and M.W.; supervision, J.E.B. and C.D.; project administration, J.E.B. and C.D.; funding acquisition, J.E.B. and C.D. All authors have read and agreed to the published version of the manuscript.

Funding: This research received no external funding.

Institutional Review Board Statement: This study did not require official or institutional ethical approval as it was not experimental, but rather part of clinical and pathological veterinary diagnostics. All animals in this study were examined with the consent of their owners and handled according to good ethical standards.

Informed Consent Statement: Not applicable.

Data Availability Statement: Not applicable.

Conflicts of Interest: The authors declare no conflict of interest.

References

1. Schneider, M.R.; Schmidt-Ullrich, R.; Paus, R. The Hair Follicle as a Dynamic Miniorgan. *Curr. Biol.* **2009**, *19*, R132–R142. [[CrossRef](#)] [[PubMed](#)]
2. Aoki, N.; Sawada, S.; Rogers, M.A.; Schweizer, J.; Shimomura, Y.; Tsujimoto, T.; Ito, K.; Ito, M. A novel type II cytokeratin, mK6irs, is expressed in the Huxley and Henle layers of the mouse inner root sheath. *J. Investig. Dermatol.* **2001**, *116*, 359–365. [[CrossRef](#)] [[PubMed](#)]
3. Porter, R.M.; Gandhi, M.; Wilson, N.J.; Wood, P.; McLean, W.H.I.; Lane, E.B. Functional analysis of keratin components in the mouse hair follicle inner root sheath. *Br. J. Dermatol.* **2004**, *150*, 195–204. [[CrossRef](#)] [[PubMed](#)]
4. Higgins, C.A.; Westgate, G.E.; Jahoda, C.A.B. Modulation in proteolytic activity is identified as a hallmark of exogen by transcriptional profiling of hair follicles. *J. Investig. Dermatol.* **2011**, *131*, 2349–2357. [[CrossRef](#)]
5. Shimomura, Y.; Christiano, A.M. Biology and genetics of hair. *Annu. Rev. Genom. Hum. Genet.* **2010**, *11*, 109–132. [[CrossRef](#)]

6. Fujimoto, A.; Farooq, M.; Fujikawa, H.; Inoue, A.; Ohyama, M.; Ehama, R.; Nakanishi, J.; Hagihara, M.; Iwabuchi, T.; Aoki, J.; et al. A missense mutation within the helix initiation motif of the keratin K71 gene underlies autosomal dominant woolly hair/hypotrichosis. *J. Investig. Dermatol.* **2012**, *132*, 2342–2349. [[CrossRef](#)] [[PubMed](#)]
7. Moll, R.; Divo, M.; Langbein, L. The human keratins: Biology and pathology. *Histochem. Cell Biol.* **2008**, *129*, 705–733. [[CrossRef](#)]
8. Coulombe, P.A.; Omary, M.B. “Hard” and “soft” principles defining the structure, function and regulation of keratin intermediate filaments. *Curr. Opin. Cell Biol.* **2002**, *14*, 110–122. [[CrossRef](#)]
9. Zhang, X.; Guo, B.R.; Cai, L.Q.; Jiang, T.; Sun, L.D.; Cui, Y.; Hu, J.C.; Zhu, J.; Chen, G.; Tang, X.F.; et al. Exome sequencing identified a missense mutation of EPSL3 in Marie Unna hereditary hypotrichosis. *J. Med. Genet.* **2012**, *49*, 727–730. [[CrossRef](#)]
10. Pasternack, S.M.; Refke, M.; Paknia, E.; Hennies, H.C.; Franz, T.; Schäfer, N.; Fryer, A.; Van Steensel, M.; Sweeney, E.; Just, M.; et al. Mutations in SNRPE, which encodes a core protein of the spliceosome, cause autosomal-dominant hypotrichosis simplex. *Am. J. Hum. Genet.* **2013**, *92*, 81–87. [[CrossRef](#)]
11. Betz, R.C.; Lee, Y.A.; Bygum, A.; Brandrup, F.; Bernal, A.I.; Toribio, J.; Alvarez, J.I.; Kukuk, G.M.; Ibsen, H.H.W.; Rasmussen, H.B.; et al. A gene for hypotrichosis simplex of the scalp maps to chromosome 6p21.3. *Am. J. Hum. Genet.* **2000**, *66*, 1979–1983. [[CrossRef](#)]
12. Kim, J.K.; Kim, E.; Baek, I.C.; Kim, B.K.; Cho, A.R.; Kim, T.Y.; Song, C.W.; Seong, J.K.; Yoon, J.B.; Stenn, K.S.; et al. Overexpression of Hr links excessive induction of Wnt signaling to Marie Unna hereditary hypotrichosis. *Hum. Mol. Genet.* **2009**, *19*, 445–453. [[CrossRef](#)] [[PubMed](#)]
13. Wasif, N.; Naqvi, S.K.U.H.; Basit, S.; Ali, N.; Ansar, M.; Ahmad, W. Novel mutations in the keratin-74 (KRT74) gene underlie autosomal dominant woolly hair/hypotrichosis in Pakistani families. *Hum. Genet.* **2011**, *129*, 419–424. [[CrossRef](#)] [[PubMed](#)]
14. Zhou, C.; Zang, D.; Jin, Y.; Wu, H.; Liu, Z.; Du, J.; Zhang, J. Mutation in ribosomal protein L21 underlies hereditary hypotrichosis simplex. *Hum. Mutat.* **2011**, *32*, 710–714. [[CrossRef](#)]
15. Shimomura, Y.; Agalliu, D.; Vonica, A.; Luria, V.; Wajid, M.; Baumer, A.; Belli, S.; Petukhova, L.; Schinzel, A.; Brivanlou, A.H.; et al. APCDD1 is a novel Wnt inhibitor mutated in hereditary hypotrichosis simplex. *Nature* **2010**, *464*, 1043–1047. [[CrossRef](#)]
16. Kazantseva, A.; Goltsov, A.; Zinchenko, R.; Grigorenko, A.P.; Abrukova, A.V.; Moliaka, Y.K.; Kirillov, A.G.; Guo, Z.; Lyle, S. Human hair growth deficiency is linked to a genetic defect in the phospholipase gene LIPH. *Science* **2006**, *314*, 2004–2007. [[CrossRef](#)] [[PubMed](#)]
17. Pasternack, S.M.; Von Kügelgen, I.; Al Aboud, K.; Lee, Y.-A.; Rüschemdorf, F.; Voss, K.; Hillmer, A.M.; Molderings, G.J.; Franz, T.; Ramirez, A.; et al. G protein-coupled receptor P2Y5 and its ligand LPA are involved in maintenance of human hair growth. *Nat. Genet.* **2008**, *40*, 329–334. [[CrossRef](#)] [[PubMed](#)]
18. Shimomura, Y.; Sakamoto, F.; Kariya, N.; Matsunaga, K.; Ito, M. Mutations in the desmoglein 4 gene are associated with monilethrix-like congenital hypotrichosis. *J. Investig. Dermatol.* **2006**, *126*, 1281–1285. [[CrossRef](#)]
19. Romano, M.T.; Tafazzoli, A.; Mattern, M.; Sivalingam, S.; Wolf, S.; Rupp, A.; Thiele, H.; Altmüller, J.; Nürnberg, P.; Ellwanger, J.; et al. Bi-allelic mutations in LSS, encoding lanosterol synthase, cause autosomal-recessive hypotrichosis simplex. *Am. J. Hum. Genet.* **2018**, *103*, 777–785. [[CrossRef](#)]
20. Johansson, I. Congenital defects in mink. *Vara Palsdjur.* **1965**, *36*, 93–94.
21. Buckley, R.M.; Gandolfi, B.; Creighton, E.K.; Pyne, C.A.; Bouhan, D.M.; Leroy, M.L.; Senter, D.A.; Gobble, J.R.; Abitbol, M.; Lyons, L.A. Werewolf, there wolf: Variants in hairless associated with hypotrichia and roaring in the lykoi cat breed. *Genes* **2020**, *11*, 682. [[CrossRef](#)] [[PubMed](#)]
22. Gandolfi, B.; Outerbridge, C.A.; Beresford, L.G.; Myers, J.A.; Pimentel, M.; Alhaddad, H.; Grahn, J.C.; Grahn, R.A.; Lyons, L.A. The naked truth: Sphynx and Devon Rex cat breed mutations in KRT71. *Mamm. Genome* **2010**, *21*, 509–515. [[CrossRef](#)] [[PubMed](#)]
23. Parker, H.G.; Harris, A.; Dreger, D.L.; Davis, B.W.; Ostrander, E.A. The bald and the beautiful: Hairlessness in domestic dog breeds. *Philos. Trans. R. Soc. B Biol. Sci.* **2017**, *372*. [[CrossRef](#)]
24. Thomer, A.; Gottschalk, M.; Christmann, A.; Naccache, F.; Jung, K.; Hewicker-Trautwein, M.; Distl, O.; Metzger, J. An epistatic effect of KRT25 on SP6 is involved in curly coat in horses. *Sci. Rep.* **2018**, *8*, 6374. [[CrossRef](#)] [[PubMed](#)]
25. Ratterree, M.S.; Baskin, G.B. Congenital hypotrichosis in a rhesus monkey. *Lab. Anim. Sci.* **1992**, *42*, 410–412.
26. Pinter, A.J.; McLean, A.K. Hereditary hairlessness in the montane vole. *J. Hered.* **1970**, *61*, 112–118. [[CrossRef](#)]
27. Swanson, H. The “hairless” gerbil: A new mutant. *Lab. Anim.* **1980**, *14*, 143–147. [[CrossRef](#)]
28. Nixon, C. Hereditary hairlessness in the Syrian golden hamster. *J. Hered.* **1972**, *63*, 215–217. [[CrossRef](#)]
29. Bolognia, J.L.; Murray, M.S.; Pawelek, J.M. Hairless pigmented guinea pigs: A new model for the study of mammalian pigmentation. *Pigment Cell Res.* **1990**, *3*, 150–156. [[CrossRef](#)]
30. Lemus-Flores, C.; Ulloa-Arvizu, R.; Ramos-Kuri, M.; Estrada, F.J.; Alonso, R.A. Genetic analysis of Mexican hairless pig populations. *J. Anim. Sci.* **2001**, *79*, 3021–3026. [[CrossRef](#)]
31. Finocchiaro, R.; Portolano, B.; Damiani, G.; Caroli, A.; Budelli, E.; Bolla, P.; Pagnacco, G. The hairless (hr) gene is involved in the congenital hypotrichosis of Valle del Belice sheep. *Genet. Sel. Evol.* **2003**, *35*, S147–S156. [[CrossRef](#)] [[PubMed](#)]
32. Murgiano, L.; Shirokova, V.; Welle, M.M.; Jagannathan, V.; Plattet, P.; Oevermann, A.; Pienkowska-Schelling, A.; Gallo, D.; Gentile, A.; Mikkola, M.; et al. Hairless streaks in cattle implicate TSR2 in early hair follicle formation. *PLoS Genet.* **2015**, *11*, 1–22. [[CrossRef](#)] [[PubMed](#)]
33. Craft, W.A.; Blizzard, W.L. The inheritance of semi-hairless ness in cattle. *J. Hered.* **1934**, *25*, 385–390. [[CrossRef](#)]

34. Bracho, G.A.; Beeman, K.; Johnson, J.L.; Leipold, H.W. Further studies of congenital hypotrichosis in Hereford cattle. *Zent. Vet.* **1984**, *31*, 72–80. [[CrossRef](#)] [[PubMed](#)]
35. Olson, T.A.; Hargrove, D.D.; Leipold, H.W. Occurrence of Hypotrichosis in Polled Hereford Cattle. *Bov. Pract.* **1985**, *20*, 4–8. [[CrossRef](#)]
36. Jayasekara, M.U.; Leipold, H.W.; Cook, J.E. Pathological changes in congenital hypotrichosis in Hereford cattle. *Zentralbl. Veterinarmed. A* **1979**, *26*, 744–753. [[CrossRef](#)]
37. Miller, S.A.; Dykes, D.D.; Polesky, H.F. A simple salting out procedure for extracting DNA from human nucleated cells. *Nucleic Acids Res.* **1988**, *16*, 1215. [[CrossRef](#)]
38. Purcell, S.; Neale, B.; Todd-Brown, K.; Thomas, L.; Ferreira, M.A.R.; Bender, D.; Maller, J.; Sklar, P.; De Bakker, P.I.W.; Daly, M.J.; et al. PLINK: A tool set for whole-genome association and population-based linkage analyses. *Am. J. Hum. Genet.* **2007**, *81*, 559–575. [[CrossRef](#)]
39. Temnykh, S.; DeClerck, G.; Lukashova, A.; Lipovich, L.; Cartinhour, S.; McCouch, S. Computational and experimental analysis of microsatellites in rice (*Oryza sativa* L.): Frequency, length variation, transposon associations, and genetic marker potential. *Genome Res.* **2001**, *11*, 1441–1452. [[CrossRef](#)]
40. Saha, S.; Bridges, S.; Magbanua, Z.V.; Peterson, D.G. Computational Approaches and Tools Used in Identification of Dispersed Repetitive DNA Sequences. *Trop. Plant Biol.* **2008**, *1*, 85–96. [[CrossRef](#)]
41. Boutin-Ganache, I.; Raposo, M.; Raymond, M.; Deschepper, C.F. M13-tailed primers improve the readability and usability of microsatellite analyses performed with two different allele-sizing methods. *Biotechniques* **2001**, *31*, 24–28. [[CrossRef](#)]
42. Wheelan, S.J.; Church, D.M.; Ostell, J.M. Spidey: A tool for mRNA-to-genomic alignments. *Genome Res.* **2001**, *11*, 1952–1957. [[CrossRef](#)] [[PubMed](#)]
43. Hayes, B.J.; Daetwyler, H.D. 1000 Bull Genomes Project to Map Simple and Complex Genetic Traits in Cattle: Applications and Outcomes. *Annu. Rev. Anim. Biosci.* **2019**, *7*, 89–102. [[CrossRef](#)] [[PubMed](#)]
44. O'Toole, D.; Häfliger, I.M.; Leuthard, F.; Schumaker, B.; Steadman, L.; Murphy, B.; Drögemüller, C.; Leeb, T. X-linked hypohidrotic ectodermal dysplasia in crossbred beef cattle due to a large deletion in *EDA*. *Animals* **2021**, *11*, 657. [[CrossRef](#)] [[PubMed](#)]
45. Snider, N.T.; Omary, M.B. Post-translational modifications of intermediate filament proteins: Mechanisms and functions. *Nat. Rev. Mol. Cell Biol.* **2014**, *15*, 163–177. [[CrossRef](#)] [[PubMed](#)]
46. Arin, M.J. The molecular basis of human keratin disorders. *Hum. Genet.* **2009**, *125*, 355–373. [[CrossRef](#)]
47. Langbein, L.; Rogers, M.A.; Praetzel, S.; Winter, H.; Schweizer, J. K6irs1, K6irs2, K6irs3, and K6irs4 represent the inner-root-sheath-specific type II epithelial keratins of the human hair follicle. *J. Investig. Dermatol.* **2003**, *120*, 512–522. [[CrossRef](#)]
48. Genovese, D.W.; Johnson, T.L.; Lamb, K.E.; Gram, W.D. Histological and dermatoscopic description of sphynx cat skin. *Vet. Dermatol.* **2014**, *25*, 523–e90. [[CrossRef](#)]
49. Fairfield, H.; Srivastava, A.; Ananda, G.; Liu, R.; Kircher, M.; Lakshminarayana, A.; Harris, B.S.; Karst, S.Y.; Dionne, L.A.; Kane, C.C.; et al. Exome sequencing reveals pathogenic mutations in 91 strains of mice with Mendelian disorders. *Genome Res.* **2015**, *25*, 948–957. [[CrossRef](#)]
50. Runkel, F.; Klaften, M.; Koch, K.; Böhnert, V.; Büssow, H.; Fuchs, H.; Franz, T.; De Angelis, M.H. Morphologic and molecular characterization of two novel Krt71 (Krt2-6g) mutations: Krt71rco12 and Krt71rco13. *Mamm. Genome* **2006**, *17*, 1172–1182. [[CrossRef](#)]
51. Peters, T.; Sedlmeier, R.; Büssow, H.; Runkel, F.; Lüers, G.H.; Korthaus, D.; Fuchs, H.; Hrabé De Angelis, M.; Stumm, G.; Russ, A.P.; et al. Alopecia in a novel mouse model RCO3 is caused by mK6irs1 deficiency. *J. Investig. Dermatol.* **2003**, *121*, 674–680. [[CrossRef](#)] [[PubMed](#)]
52. Kuca, T.; Marron, B.M.; Jacinto, J.G.P.; Paris, J.M.; Gerspach, C.; Beever, J.E.; Drögemüller, C. A nonsense variant in hephaestin like 1 (*HEPHL1*) is responsible for congenital hypotrichosis in Belted Galloway cattle. *Genes.* **2021**, *12*, 643. [[CrossRef](#)] [[PubMed](#)]

4.1.4.6 A Nonsense Variant in Hephaestin Like 1 (*HEPHL1*) Is Responsible for Congenital Hypotrichosis in Belted Galloway Cattle

Journal: Genes

Manuscript status: published

Contributions: SNP data analyses, methodology, writing original draft and revisions

Displayed version: published version

DOI: [10.3390/genes12050643](https://doi.org/10.3390/genes12050643)

Article

A Nonsense Variant in Hephaestin Like 1 (*HEPHL1*) Is Responsible for Congenital Hypotrichosis in Belted Galloway Cattle

Thibaud Kuca^{1,†}, Brandy M. Marron^{2,†}, Joana G. P. Jacinto^{3,4,†}, Julia M. Paris^{4,†}, Christian Gerspach¹, Jonathan E. Beever^{2,5,‡} and Cord Drögemüller^{4,*,‡}

¹ Department of Farm Animals, Vetsuisse-Faculty, University of Zurich, 8057 Zurich, Switzerland; thibaud.kuca@uzh.ch (T.K.); cgerspach@vetclinics.uzh.ch (C.G.)

² Laboratory of Molecular Genetics, Department of Animal Sciences, University of Illinois at Urbana-Champaign, Urbana, IL 61801, USA; bmarron@dacc.edu (B.M.M.); jbeever@utk.edu (J.E.B.)

³ Department of Veterinary Medical Sciences, University of Bologna, 40064 Ozzano Emilia, Italy; joana.goncalves2@studio.unibo.it

⁴ Institute of Genetics, Vetsuisse Faculty, University of Bern, 3012 Bern, Switzerland; julia-1991@hotmail.com

⁵ UTIA Genomics Center for the Advancement of Agriculture, Institute of Agriculture, University of Tennessee, Knoxville, TN 37996, USA

* Correspondence: cord.droegemueller@vetsuisse.unibe.ch; Tel.: +41-31-684-2529

† These authors contributed equally.

‡ These authors jointly supervised this work.



Citation: Kuca, T.; Marron, B.M.; Jacinto, J.G.P.; Paris, J.M.; Gerspach, C.; Beever, J.E.; Drögemüller, C. A Nonsense Variant in Hephaestin Like 1 (*HEPHL1*) Is Responsible for Congenital Hypotrichosis in Belted Galloway Cattle. *Genes* **2021**, *12*, 643. <https://doi.org/10.3390/genes12050643>

Academic Editor: Emilia Bagnicka

Received: 6 April 2021

Accepted: 19 April 2021

Published: 26 April 2021

Publisher's Note: MDPI stays neutral with regard to jurisdictional claims in published maps and institutional affiliations.



Copyright: © 2021 by the authors. Licensee MDPI, Basel, Switzerland. This article is an open access article distributed under the terms and conditions of the Creative Commons Attribution (CC BY) license (<https://creativecommons.org/licenses/by/4.0/>).

Abstract: Genodermatosis such as hair disorders mostly follow a monogenic mode of inheritance. Congenital hypotrichosis (HY) belong to this group of disorders and is characterized by abnormally reduced hair since birth. The purpose of this study was to characterize the clinical phenotype of a breed-specific non-syndromic form of HY in Belted Galloway cattle and to identify the causative genetic variant for this recessive disorder. An affected calf born in Switzerland presented with multiple small to large areas of alopecia on the limbs and on the dorsal part of the head, neck, and back. A genome-wide association study using Swiss and US Belted Galloway cattle encompassing 12 cases and 61 controls revealed an association signal on chromosome 29. Homozygosity mapping in a subset of cases refined the HY locus to a 1.5 Mb critical interval and subsequent Sanger sequencing of protein-coding exons of positional candidate genes revealed a stop gain variant in the *HEPHL1* gene that encodes a multi-copper ferroxidase protein so-called hephaestin like 1 (c.1684A>T; p.Lys562*). A perfect concordance between the homozygous presence of this most likely pathogenic loss-of-function variant and the HY phenotype was found. Genotyping of more than 700 purebred Swiss and US Belted Galloway cattle showed the global spread of the mutation. This study provides a molecular test that will permit the avoidance of risk matings by systematic genotyping of relevant breeding animals. This rare recessive *HEPHL1*-related form of hypotrichosis provides a novel large animal model for similar human conditions. The results have been incorporated in the Online Mendelian Inheritance in Animals (OMIA) database (OMIA 002230-9913).

Keywords: *Bos taurus*; hypotrichosis simplex; hair; development; dermatology; monogenic; genodermatosis

1. Introduction

Heritable hair disorders frequently follow a monogenic mode of inheritance, e.g., congenital hypotrichosis (HY), and they belong to a group of human diseases, which are classified into syndromic and non-syndromic forms [1]. Generally, HY is characterized by a paucity or the presence of a less than normal amount of hair and abnormal hair follicles and shafts, which are thin and atrophic, and the lesion extension and the affected areas of the body can be very variable [2,3]. Therefore, HY includes a clinically-, pathologically-

and heritably-heterogeneous group of hair disorders. At present, 14 subtypes and 12 different associated genes are encompassed in the classification of human non-syndromic HY (OMIM PS605389). These disorders in humans follow mostly a dominant inheritance and are associated with causative variants in eight different genes (*EPS8L3*, *SNRPE*, *CDSN*, *HR*, *KRT71*, *KRT74*, *RPL21*, *APCDD1*) [2,4–10]. Whereas, autosomal recessive HY is related to mutations in only four different genes (*LIPH*, *LPAR6*, *DSG4*, *LSS*) [11–14].

Several forms of non-syndromic HY have been reported in many animal species (OMIA 000540), including American mink [15], cats [16,17], dogs [18], horses [19], macaques [20], meadow voles [21], Mongolian gerbils [22], golden hamsters [23], guinea pigs [24], pigs [25], sheep [26] and cattle [27]. Mutations causing forms of HY in animals have been identified in known candidate genes for HY such as *HR* and *KRT71* [16,17], or novel genes such as *TSR2*, *SGK3*, and *SP6* [18,19,27] discovered in HY-affected domestic animals. This highlights the potential of studying inherited conditions in such species to assign a role or function to previously uncharacterized genes or to add additional functions to known genes in regard to hair development.

In Hereford cattle, non-syndromic recessively inherited HY has been reported and it is characterized by the partial or complete absence of hair at birth that later becomes “fuzzy or kinky” in appearance [28]. To the best of our knowledge, in Belted Galloway cattle no forms of HY have been previously reported. Therefore, this study aimed to characterize the clinical phenotype of HY in Belted Galloway cattle and to identify the causative genetic variant associated with the disorder.

2. Materials and Methods

2.1. Animals and Samples

The clinical investigation was performed in 2020 at the University of Zurich using one affected red Belted Galloway calf from a farm in Switzerland. The original genetic investigation that led to the identification of the pathogenic variant associated with the disease was performed in 2011 at the University of Illinois.

The final mapping population of this study consisted of twelve HY-suspected Belted Galloway calves, eleven of them born in the USA and reported by five different farmers between 2009 to 2011 (cases HYG_0046, HYG_0047, HYG_0048, HYG_0049, HYG_0050, HYG_0051, HYG_0053, HYG26, HYG33, HYG34, HYG-54) and a single HY-suspected calf born in Switzerland (case RM3402). As controls, a total of 61 phenotypically normal Belted Galloway cattle including 21 animals that were collected from US farms and 40 Swiss cattle were used. Eighteen out of the 21 US animals were suspected carriers for HY.

Finally, a population cohort consisting of 156 and 541 apparently normal cattle of the respective Swiss and US purebred Belted Galloway populations were used to determine the absence/presence and frequency of the detected *HEPHL1* variant in the breed.

DNA was isolated from EDTA-blood and semen samples using a simple salting out procedure [29].

2.2. Clinicopathological Investigations

An 11-day-old male calf, weighing 43 kg, was admitted to the Clinic for Ruminants of the University of Zurich for a history of progressive hair loss beginning three days after birth. Hair loss was first noticed to affect the head and subsequently the limbs. The calf was born without assistance, weighing 37 kg. The dam was apparently healthy and had previously given birth to three healthy calves. The calf was reported to have nursed and gained weight normally since birth. The affected animal was clinically examined. Furthermore, blood was collected for a complete blood count (CBC), plasma biochemical analysis, and venous blood gas (VBG) analysis. A skin biopsy sample was also collected from the left ear and assayed for bovine viral diarrhoea virus (BVDV) by an independent laboratory using a commercially available ELISA kit (IDEXX BVDV Ag/Serum Plus, IDEXX Switzerland AG, Liebefeld-Bern, Switzerland) according to the manufacturer’s instructions.

2.3. Genetic Investigations

2.3.1. SNP Genotyping and GWAS

Twelve HY-suspected affected animals (cases) and 61 normal Belted Galloway cattle (controls) were genotyped using the BovineSNP50 v1 Beadchip (Illumina, San Diego, CA, USA). The generated SNP data was prepared for a genome-wide association study (GWAS) and subsequent haplotype analysis using PLINK v1.9 [30]. GWAS using 39,014 informative SNP markers was performed using a linear mixed model while adjusting for population stratification as implemented in GEMMA v0.98 [31] and the significance threshold was estimated by Bonferroni correction. Manhattan and Q–Q plots of the corrected p-values were generated in R environment v3.6.0 [32], using the qqman package [33]. Haplotypes around the significantly associated locus were constructed using fastPHASE [34].

2.3.2. Candidate Gene Analysis

Three genes (*CEP295*, *C29H11orf54*, *HEPHL1*) were selected as candidates based on known function in hair and location relative to the homozygous region identified in the HY-affected calves on chromosome 29. Exon annotation based on computational methods was manually validated using mRNA sequences from NCBI and the software SPIDEY [35]. Primers were designed as described above to amplify protein-coding exons in 1kb fragments (Table S1). Subsequent Sanger sequencing was performed on an ABI3730xl capillary sequencer and sequence assemblies viewed and analyzed for polymorphisms using Codon Code Aligner (Codon Code Corporation).

2.3.3. Targeted Genotyping

A diagnostic PCR and subsequent Sanger sequencing as described above were used to validate and genotype the variant in further animals. Therefore, the region containing the stop gain variant in *HEPHL1* (Chr29: g. 721234T>A) was amplified using the following primers: 5'-TGAAAGTGTGTCAGCCCAACAG-3' (forward primer) and 5'-TCGATTCGAGAGCACTGAG-3' (reverse primer).

2.3.4. Occurrence of the HEPHL1 Variant in the 1000 Bull Genomes Project Cohort

The most likely pathogenic stop gain variant in *HEPHL1* was searched for its occurrence in a global control cohort of 4110 genomes of a variety of breeds (1000 Bull Genomes Project run 8; www.1000bullgenomes.com accessed on 4 April 2021) [36].

2.3.5. Sequence Accessions

All references to the bovine *HEPHL1* gene correspond to the NCBI accessions NM_001192511.2 (*HEPHL1* mRNA), NP_001179440.1 (*HEPHL1* protein), NC_037356.1 (ARS-UCD1.2 assembly, chromosome 29). For the protein structure of *HEPHL1*, the Uniprot accession F1N752 was used.

3. Results

3.1. Clinicopathological Findings

On clinical examination, the Swiss calf was found to be clinically healthy except for the skin abnormalities. Particular clinical examination of the cardiovascular, respiratory, genitourinary, musculoskeletal, and nervous systems showed no abnormalities. Moreover, no abnormalities in dentition were noticed as previously seen in cattle affected by ectodermal dysplasia characterized by sparse hair and abnormal teeth [37].

The integumentary system examination revealed multiple small to large areas of alopecia on the limbs and the dorsal part of the head, neck, and back (Figure 1a,b). The largest alopecic lesions were located on the lateral and medial aspects of the tarsal joints and the dorsal aspect of the fetlock and carpal joints. Moderate scaling was also present on the dorsal aspect of the head and neck. Excoriations were also present on the dorsal aspect of the fetlock and carpal joints and the lateral aspect of the tarsal joints. There was no evidence of erythema, pruritus, crusting, or thickening of the skin.

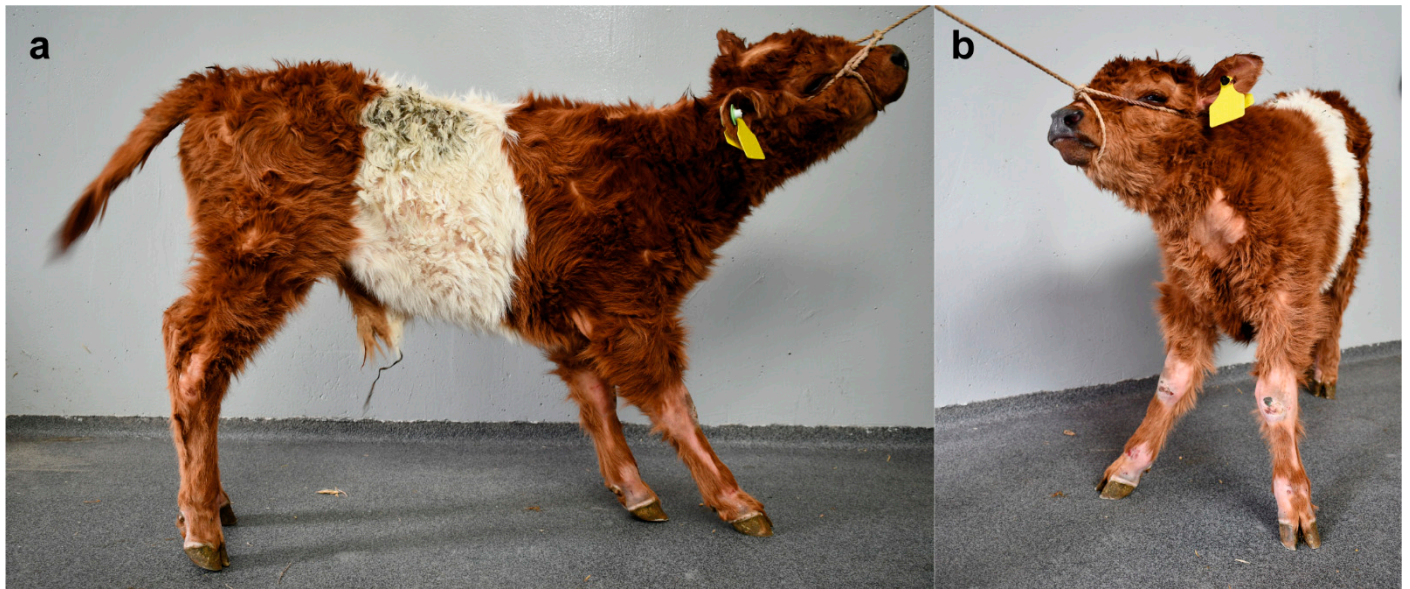


Figure 1. Congenital hypotrichosis in a Swiss Belted Galloway cattle. (a) Note the multiple areas of alopecia on the limbs and the dorsal part of the head. (b) Note the large alopecic lesions located on the neck and the dorsal aspect of the fetlock and carpal joints. Note also the excoriations on the dorsal aspect of the fetlock and carpal joints.

Complete blood count revealed mild erythrocytosis, hypochromia, thrombocytosis, and leukocytosis due to mature neutrophilia and monocytosis. Plasma biochemistry revealed mild hyperbilirubinemia, hypercalcemia, hyperphosphatemia, severely increased GGT activity, mildly increased GLDH and SDH activities, and mildly decreased BUN concentration. VBG analysis revealed mild hyperglycemia and hyperlactatemia (Table S2). The calf was confirmed to be negative for BVDV.

Considering the age of the calf, the distribution of skin lesions, and the absence of other clinically relevant clinical abnormalities, congenital non-syndromic hypotrichosis was suspected.

3.2. Genetic Analysis

A monogenic recessive mode of inheritance was hypothesized. GWAS using 12 cases and 61 controls revealed a region of genome-wide significance for association with the HY phenotype on chromosome 29 (Figure 2a). The best-associated SNP marker maps to position 1,045,388 bp ($p_{\text{corrected}} = 1.22 \times 10^{-6}$). Haplotype analysis on this location revealed one region encompassing 21 markers of shared homozygosity in 11 affected calves located at the top of chromosome 29, with exception of one calf (case HYG_0050) (Figure 2c). It could be assumed that this single HY-suspected case was misclassified based on phenotype and was not affected with the same form of HY and therefore was considered to represent most likely a phenocopy. Recombinant haplotypes present in three cases (HYG33, HYG34, and HYG-54) allowed us to narrow the critical region for the HY-associated locus to a 1549-kb segment (Figure 2c).

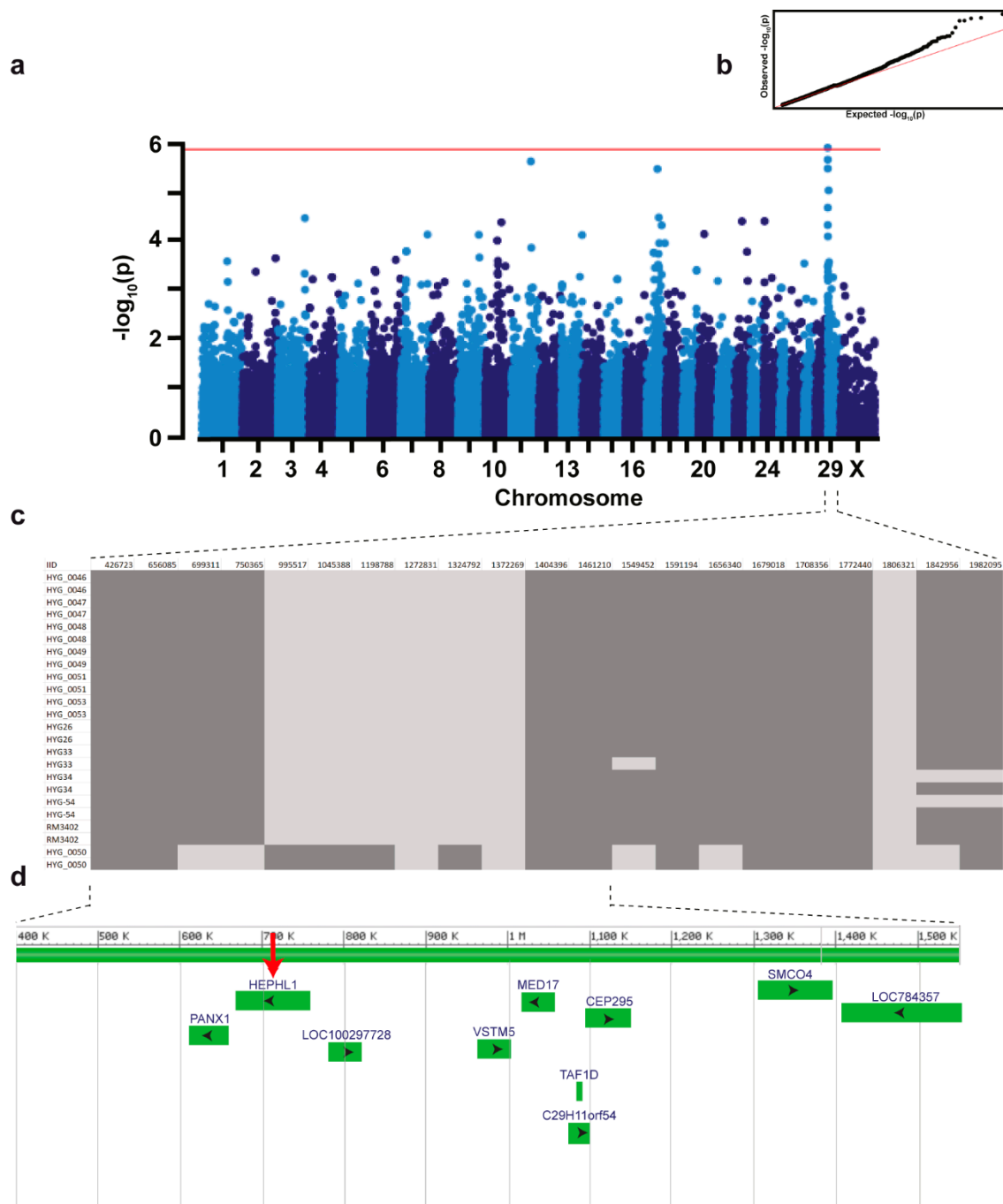


Figure 2. A region on chromosome 29, including the *HEPHL1* gene, is associated with recessive congenital hypotrichosis in Belted Galloway cattle. **(a)** Manhattan plot for the GWAS using 12 HY-suspected calves and 61 control cattle is shown and indicates a signal with multiple associated SNPs on chromosome 29. Each chromosome is represented along the X-axis. The Y-axis represents the $-\log_{10}$ of the corrected empirical p -value. The red line indicates the Bonferroni-corrected significance with a $-\log_{10}p = 5.88$ ($\alpha = 0.05$). **(b)** The quantile-quantile plots showing the observed vs. expected log p -values are shown. **(c)** Schematic representing the haplotypes of 12 HY-suspected calves on chromosome 29. The exact positions of the SNP markers are indicated above. **(d)** Gene content of the 1.5 Mb-sized critical regions located at the proximal end of the chromosome. Screenshot of NCBI Genome Data Viewer (ARS-UCD1.2 assembly, *Bos taurus* annotation release 106) shows the annotated genes and loci including *HEPHL1* (red arrow).

Positional candidate genes within the 1549-kb critical region were selected based on function and location relative to the homozygosity analysis of the HY-affected calves. The coding exons and flanking splice regions of three positional candidate genes were

subsequently re-sequenced: *CEP295*, *C29H11orf54*, and *HEPHL1*. Only variants that were predicted to alter the coding sequences or that were located within the splice sites were considered. A nonsense pathogenic variant was found in the ninth exon of the *HEPHL1* gene (chr29: g.721234A>T) (Figure 3a) which was consistent with the expected genotype status of the animals sequenced. At the level of translation, the detected single nucleotide substitution (c.1684A>T) is predicted to result in a premature stop codon in the Domain 3 (Cu-oxidase type 3) of *HEPHL1* after lysine 562 (p.Lys562*) (Figure 3b,c). Consequently, the mutant protein, if expressed, is predicted to be significantly shorter than the wild-type *HEPHL1* protein of 1157 amino acids in length lacking the Domains 4 (Cu-oxidase type 3) and 5 (Cu-oxidase type 2), and C-terminal domain. The HY protein is expected to be 562 amino acid residues in length due to the premature induction of a stop codon.

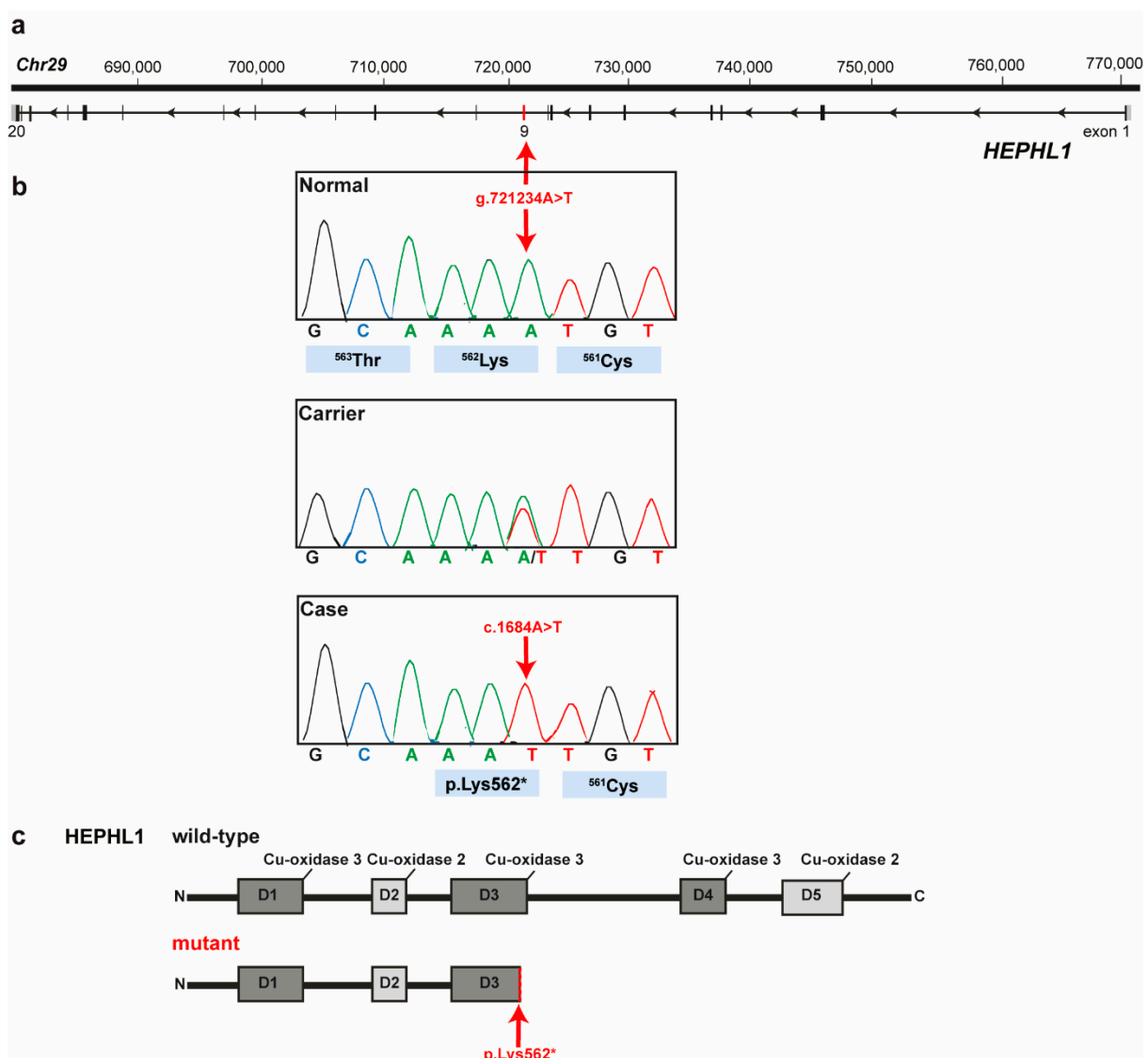


Figure 3. *HEPHL1* nonsense variant in Belted Galloway cattle affected by congenital hypotrichosis. (a) *HEPHL1* gene structure showing the location of the exon 9 variant on cattle chromosome 29. (b) Electropherograms showing the different genotypes identified via Sanger sequencing. (c) Schematic representation of *HEPHL1* wild-type protein with its functional domains and the mutant protein. The wild-type protein is 1157 amino acid residues in length. The mutant protein is expected to be 562 amino acid residues in length due to the premature induction of a stop codon. D, domain.

The nonsense variant in *HEPHL1* was further validated by Sanger sequencing (Figure 3b). Genotyping of all animals of the mapping cohort including the HY-calves and

controls originating from the US Belted Galloway population plus the case and obligatory carrier (dam) and controls from Swiss herds, revealed almost perfect concordance between the presence of this nonsense variant and the HY phenotype (Table 1). As expected, 11 HY-affected calves were homozygous mutants and the available obligatory carriers were heterozygous. A single HY-suspected calf (case HyG_0050) did not show the deleterious variant in *HEPHL1*. It is highly probable that this calf was misclassified based on phenotype and was not affected with the same type of congenital hypotrichosis and therefore, as speculated before during haplotype analysis, indeed represent a phenocopy. By genotyping of almost 700 animals the mutant allele frequency was estimated as 2.2% and 6.7% in the studied Swiss and US Belted Galloway cattle populations, respectively. The higher allele frequency in the US population is probably biased as many animals submitted for diagnostics were of suspect pedigree, thus increasing the allele frequency artificially. Additionally, the identified *HEPHL1* variant was absent in a global control cohort of 4110 cattle genomes of a variety of breeds included in the run 8 of the 1000 Bull Genomes Project [36].

Table 1. Association of the nonsense variant in *HEPHL1* with the hypotrichosis phenotype in Belted Galloway cattle.

	TT	AT	AA
HY-affected calves			
Swiss case			1
US cases	1 ^a		10
Obligate carriers^b			
Swiss		1	
US		18	
Unrelated normal Belted Galloway cattle			
Swiss	148	7	
US	471	73	
Normal control cattle from various breeds	4110		

^a this animal was assumed to represent a phenocopy (see main text) ^b these parents of HY-affected animals were classified as obligate carriers.

4. Discussion

The identified nonsense variant in *HEPHL1* resulting in a premature stop codon and consequent early truncation of the protein affects a functionally important site of a candidate gene and thus represents the most likely pathogenic variant associated with the observed recessively inherited congenital hypotrichosis (HY) phenotype in Belted Galloway cattle. This breed-specific disorder has not been reported before and we found purebred Belted Galloway calves from two different continents indicating that the mutant allele occurs worldwide segregating at different frequencies. To the best of our knowledge, no pathogenic variant in the *HEPHL1* gene has been reported in domestic animal species. Therefore, this study in cattle provides the first example of a *HEPHL1*-related congenital hair disorder in domestic animals.

In fact, iron represents an essential element and constituent of important cellular proteins such as myoglobin, hemoglobin, flavoproteins, cytochromes, and various non-heme enzymes [38]. Multi-copper ferroxidases play a major role in maintaining iron homeostasis in humans and mice [39–41]. In particular, these proteins present an important role in oxidizing ferrous iron [Fe (II)], released from the cells, into ferric iron [Fe (III)], which is subsequently distributed by transferrin [42]. Ceruloplasmin (CP) and hephaestin (HEPH) are well-known ferroxidases that facilitate this reaction in different tissues while the hephaestin like 1 (*HEPHL1*), another member of the multicopper oxidase family have an uncertain role in iron transport [39]. In humans, recessively inherited biallelic *HEPHL1* variants are associated with a phenotype characterized by abnormal hair (pili torti and trichorrhesis nodosa), joint laxity, severe heat intolerance, and developmental delay (OMIM 261990) [39]. In mice, recessively inherited mutations in *HEPHL1* are responsible for the so-called “hephaestin like 1; curly whiskers” (*Heph1^{cw}*) and “hephaestin like 1; curly whiskers 2 Jackson”

(*Heph11^{cw-2j}*) phenotypes that are associated with abnormal hair-follicle development and immunogenetic disorders [40]. Remarkably, *HEPHL1*-homozygous mutant Belted Galloway cattle, clinically presented exclusively hair abnormalities and a slight alteration on hepatic parameters, supporting an important role for the ferroxidase activity of *HEPHL1* in hair development and suggesting a possible role in iron homeostasis. The hair abnormalities described herein in Galloway cattle are distinguishable from those of HY in Hereford cattle [43]. Moreover, most changes detected in hematological and biochemical variables (i.e., erythrocytosis, hypochromasia, thrombocytosis, leukocytosis, neutrophilia, monocytosis, increased GGT activity, decreased BUN concentration, hyperglycemia, hypercalcemia, and hyperphosphatemia) were deemed age-related as similar changes were demonstrated in healthy calves during the first months of life [44]. Leukocytosis, neutrophilia, monocytosis, thrombocytosis, hyperlactatemia, and hyperglycemia could also have resulted from the endogenous release of catecholamines and glucocorticoids in response to transport and handling. Hypochromasia could also have been secondary to iron or copper deficiency. However, in the absence of anemia and microcytosis, this was deemed less likely. An increase in GGT activity in association with a normal plasma protein concentration was consistent with an adequate colostrum intake and transfer of passive immunity. Increased GLDH and SDH activities were consistent with mild acute hepatocellular injury. In the absence of increased AST activity, a primary hepatic disease was deemed unlikely while hyperbilirubinemia was consistent with cholestasis. Interestingly, mutations in CP are associated with aceruloplasminemia in humans (OMIM604290) and mice leading to a decrease in iron export and an increase of iron retention in the liver [45,46]. Given the retrieved hepatic parameters of the homozygous mutant calf in this study, we hypothesize by the similarity that a deficiency in *HEPHL1* may also lead to an alteration of iron transport in the liver.

The pathogenic variant herein identified was positioned in Domain 3, a Cu-oxidase type 3, of the *HEPHL1* bovine protein. Taking into account that the identified pathogenic variant is a nonsense variant resulting in a significantly shorter mutant protein since it encodes an early stop codon, we speculate that the identified amino-acid substitution disturbs the protein. In fact, if the mutant mRNA transcript were to escape nonsense-mediated decay [47], even if this truncated protein was produced, it would lack Domains 4 and 5, and C-terminal membrane-spanning domain, and therefore it is not expected to contribute any membrane ferroxidase function. Therefore, it is very unlikely that the mutant protein, if expressed, fulfills any physiological function. Possibly nonsense-mediated decay selectively recognizes and degrades truncated transcripts. We were not able to get skin biopsies for studying either RNA expression e.g., by RT-PCR or *HEPHL1* protein expression e.g., by immunofluorescence.

5. Conclusions

Rare non-lethal disorders such as HY in livestock are commonly not reported or are misdiagnosed when the animals show mild to moderate phenotype. However, these disorders affect negatively animal welfare due to the development of secondary infections. Additionally, molecular diagnosis is often not performed because of a lack of resources and diagnostic tools. Moreover, this study provides a DNA-based diagnostic test that allows selection against the identified pathogenic variant in the international Belted Galloway cattle population. This diagnostic test will permit the avoidance of risk matings by systematic genetic testing of potential breeding animals and in particular top sires used in artificial insemination. Investigation of this phenotype allowed a clinical and molecular genetic study, enabling for the first time the diagnosis of a *HEPHL1*-related recessively inherited form of HY in domestic animals. This study represents the first large animal model for similar human conditions. Furthermore, this example highlights the utility of precision diagnostics for understanding rare disorders and the neglected value of livestock populations for studying genetic disorders.

Supplementary Materials: The following are available online at <https://www.mdpi.com/article/10.3390/genes12050643/s1>, Table S1: Primer Sequences. Table S2: Blood analysis results of a Swiss Belted Galloway calf affected by congenital hypotrichosis.

Author Contributions: Conceptualization, J.E.B. and C.D.; validation, T.K., J.M.P., J.G.P.J., B.M.M., J.E.B. and C.D.; formal analysis, T.K., J.M.P., J.G.P.J. and B.M.M.; investigation, T.K., J.M.P., J.G.P.J. and B.M.M.; resources, C.G., J.E.B., and C.D.; writing—original draft preparation, T.K., J.M.P., J.G.P.J. and B.M.M.; writing—review and editing, T.K., J.M.P., J.G.P.J., B.M.M., J.E.B. and C.D.; visualization, T.K., J.M.P. and J.G.P.J.; supervision, J.E.B. and C.D.; project administration, J.E.B. and C.D.; funding acquisition, J.E.B. and C.D. All authors have read and agreed to the published version of the manuscript.

Funding: This research received no external funding.

Institutional Review Board Statement: This study did not require official or institutional ethical approval as it was not experimental, but rather part of clinical and pathological veterinary diagnostics. All animals in this study were examined with the consent of their owners and handled according to good ethical standards.

Informed Consent Statement: Not applicable.

Data Availability Statement: Not applicable.

Acknowledgments: We thank Anna Letko and Nathalie Besuchet Schmutz for their expert technical assistance.

Conflicts of Interest: The authors declare no conflict of interest.

References

- Betz, R.C.; Cabral, R.M.; Christiano, A.M.; Sprecher, E. Unveiling the roots of monogenic genodermatoses: Genotrichoses as a paradigm. *J. Investig. Dermatol.* **2012**, *132*, 906–914. [[CrossRef](#)]
- Fujimoto, A.; Farooq, M.; Fujikawa, H.; Inoue, A.; Ohyama, M.; Ehama, R.; Nakanishi, J.; Hagihara, M.; Iwabuchi, T.; Aoki, J.; et al. A missense mutation within the helix initiation motif of the keratin K71 gene underlies autosomal dominant woolly hair/hypotrichosis. *J. Investig. Dermatol.* **2012**, *132*, 2342–2349. [[CrossRef](#)] [[PubMed](#)]
- Ahmed, A.; Almohanna, H.; Griggs, J.; Tosti, A. Genetic Hair Disorders: A Review. *Dermatol. Ther.* **2019**, *9*, 421–448. [[CrossRef](#)] [[PubMed](#)]
- Zhang, X.; Guo, B.R.; Cai, L.Q.; Jiang, T.; Sun, L.D.; Cui, Y.; Hu, J.C.; Zhu, J.; Chen, G.; Tang, X.F.; et al. Exome sequencing identified a missense mutation of EPSL3 in Marie Unna hereditary hypotrichosis. *J. Med. Genet.* **2012**, *49*, 727–730. [[CrossRef](#)]
- Pasternack, S.M.; Refke, M.; Paknia, E.; Hennies, H.C.; Franz, T.; Schäfer, N.; Fryer, A.; Van Steensel, M.; Sweeney, E.; Just, M.; et al. Mutations in SNRPE, which encodes a core protein of the spliceosome, cause autosomal-dominant hypotrichosis simplex. *Am. J. Hum. Genet.* **2013**, *92*, 81–87. [[CrossRef](#)]
- Betz, R.C.; Lee, Y.A.; Bygum, A.; Brandrup, F.; Bernal, A.I.; Toribio, J.; Alvarez, J.I.; Kukuk, G.M.; Ibsen, H.H.W.; Rasmussen, H.B.; et al. A gene for hypotrichosis simplex of the scalp maps to chromosome 6p21.3. *Am. J. Hum. Genet.* **2000**, *66*, 1979–1983. [[CrossRef](#)]
- Kim, J.K.; Kim, E.; Baek, I.C.; Kim, B.K.; Cho, A.R.; Kim, T.Y.; Song, C.W.; Seong, J.K.; Yoon, J.B.; Stenn, K.S.; et al. Overexpression of Hr links excessive induction of Wnt signaling to Marie Unna hereditary hypotrichosis. *Hum. Mol. Genet.* **2009**, *19*, 445–453. [[CrossRef](#)] [[PubMed](#)]
- Wasif, N.; Naqvi, S.K.U.H.; Basit, S.; Ali, N.; Ansar, M.; Ahmad, W. Novel mutations in the keratin-74 (KRT74) gene underlie autosomal dominant woolly hair/hypotrichosis in Pakistani families. *Hum. Genet.* **2011**, *129*, 419–424. [[CrossRef](#)] [[PubMed](#)]
- Zhou, C.; Zang, D.; Jin, Y.; Wu, H.; Liu, Z.; Du, J.; Zhang, J. Mutation in ribosomal protein L21 underlies hereditary hypotrichosis simplex. *Hum. Mutat.* **2011**, *32*, 710–714. [[CrossRef](#)]
- Shimomura, Y.; Agalliu, D.; Vonica, A.; Luria, V.; Wajid, M.; Baumer, A.; Belli, S.; Petukhova, L.; Schinzel, A.; Brivanlou, A.H.; et al. APCDD1 is a novel Wnt inhibitor mutated in hereditary hypotrichosis simplex. *Nature* **2010**, *464*, 1043–1047. [[CrossRef](#)]
- Kazantseva, A.; Goltsov, A.; Zinchenko, R.; Grigorenko, A.P.; Abrukova, A.V.; Moliaka, Y.K.; Kirillov, A.G.; Guo, Z.; Lyle, S. Human Hair Growth Deficiency Is Linked to a Genetic Defect in the Phospholipase Gene LIPH. *Science* **2006**, *314*, 2004–2007. [[CrossRef](#)] [[PubMed](#)]
- Pasternack, S.M.; Von Kügelgen, I.; Aboud, K.A.; Lee, Y.A.; Rüschenhoff, F.; Voss, K.; Hillmer, A.M.; Molderings, G.J.; Franz, T.; Ramirez, A.; et al. G protein-coupled receptor P2Y5 and its ligand LPA are involved in maintenance of human hair growth. *Nat. Genet.* **2008**, *40*, 329–334. [[CrossRef](#)] [[PubMed](#)]
- Shimomura, Y.; Sakamoto, F.; Kariya, N.; Matsunaga, K.; Ito, M. Mutations in the desmoglein 4 gene are associated with monilethrix-like congenital hypotrichosis. *J. Investig. Dermatol.* **2006**, *126*, 1281–1285. [[CrossRef](#)]

14. Romano, M.T.; Tafazzoli, A.; Mattern, M.; Sivalingam, S.; Wolf, S.; Rupp, A.; Thiele, H.; Altmüller, J.; Nürnberg, P.; Ellwanger, J.; et al. Bi-allelic Mutations in LSS, Encoding Lanosterol Synthase, Cause Autosomal-Recessive Hypotrichosis Simplex. *Am. J. Hum. Genet.* **2018**, *103*, 777–785. [[CrossRef](#)]
15. Johansson, I. Congenital defects in mink. *Vara Palsdjur* **1965**, *36*, 93–94.
16. Buckley, R.M.; Gandolfi, B.; Creighton, E.K.; Pyne, C.A.; Bouhan, D.M.; Leroy, M.L.; Senter, D.A.; Gobble, J.R.; Abitbol, M.; Lyons, L.A. Werewolf, there wolf: Variants in hairless associated with hypotrichia and roaring in the lykoi cat breed. *Genes* **2020**, *11*, 682. [[CrossRef](#)] [[PubMed](#)]
17. Gandolfi, B.; Outerbridge, C.A.; Beresford, L.G.; Myers, J.A.; Pimentel, M.; Alhaddad, H.; Grahn, J.C.; Grahn, R.A.; Lyons, L.A. The naked truth: Sphynx and Devon Rex cat breed mutations in KRT71. *Mamm. Genome* **2010**, *21*, 509–515. [[CrossRef](#)]
18. Parker, H.G.; Harris, A.; Dreger, D.L.; Davis, B.W.; Ostrander, E.A. The bald and the beautiful: Hairlessness in domestic dog breeds. *Philos. Trans. R. Soc. B Biol. Sci.* **2017**, *372*. [[CrossRef](#)]
19. Thomer, A.; Gottschalk, M.; Christmann, A.; Naccache, F.; Jung, K.; Hewicker-Trautwein, M.; Distl, O.; Metzger, J. An epistatic effect of KRT25 on SP6 is involved in curly coat in horses. *Sci. Rep.* **2018**, *8*, 6374. [[CrossRef](#)]
20. Ratterree, M.S.; Baskin, G.B. Congenital hypotrichosis in a rhesus monkey. *Lab. Anim. Sci.* **1992**, *42*, 410–412.
21. Pinter, A.J.; McLean, A.K. Hereditary hairlessness in the montane vole. *J. Hered.* **1970**, *61*, 112–118. [[CrossRef](#)] [[PubMed](#)]
22. Swanson, H. The “hairless” gerbil: A new mutant. *Lab. Anim.* **1980**, *14*, 143–147. [[CrossRef](#)]
23. Nixon, C. Hereditary hairlessness in the Syrian golden hamster. *J. Hered.* **1972**, *63*, 215–217. [[CrossRef](#)] [[PubMed](#)]
24. Bologna, J.L.; Murray, M.S.; Pawelek, J.M. Hairless pigmented guinea pigs: A new model for the study of mammalian pigmentation. *Pigment Cell Res.* **1990**, *3*, 150–156. [[CrossRef](#)] [[PubMed](#)]
25. Lemus-Flores, C.; Ulloa-Arvizu, R.; Ramos-Kuri, M.; Estrada, F.J.; Alonso, R.A. Genetic analysis of Mexican hairless pig populations. *J. Anim. Sci.* **2001**, *79*, 3021–3026. [[CrossRef](#)]
26. Finocchiaro, R.; Portolano, B.; Damiani, G.; Caroli, A.; Budelli, E.; Bolla, P.; Pagnacco, G. The hairless (hr) gene is involved in the congenital hypotrichosis of Valle del Belice sheep. *Genet. Sel. Evol.* **2003**, *35*, S147–S156. [[CrossRef](#)]
27. Murgiano, L.; Shirokova, V.; Welle, M.M.; Jagannathan, V.; Plattet, P.; Oevermann, A.; Pienkowska-Schelling, A.; Gallo, D.; Gentile, A.; Mikkola, M.; et al. Hairless Streaks in Cattle Implicate TSR2 in Early Hair Follicle Formation. *PLoS Genet.* **2015**, *11*, 1–22. [[CrossRef](#)] [[PubMed](#)]
28. Craft, W.A.; Blizzard, W.L. The inheritance of semi-hairless ness in cattle. *J. Hered.* **1934**, *25*, 385–390. [[CrossRef](#)]
29. Miller, S.A.; Dykes, D.D.; Polesky, H.F. A simple salting out procedure for extracting DNA from human nucleated cells. *Nucleic Acids Res.* **1988**, *16*, 1215. [[CrossRef](#)] [[PubMed](#)]
30. Purcell, S.; Neale, B.; Todd-Brown, K.; Thomas, L.; Ferreira, M.A.R.; Bender, D.; Maller, J.; Sklar, P.; De Bakker, P.I.W.; Daly, M.J.; et al. PLINK: A tool set for whole-genome association and population-based linkage analyses. *Am. J. Hum. Genet.* **2007**, *81*, 559–575. [[CrossRef](#)]
31. Zhou, X.; Stephens, M. Genome-wide efficient mixed-model analysis for association studies. *Nat. Genet.* **2012**, *44*, 821–824. [[CrossRef](#)]
32. R Core Team. *R: A Language and Environment for Statistical Computing*; R Core Team: Vienna, Austria, 2018.
33. Turner, S.D. qqman: An R package for visualizing GWAS results using Q-Q and manhattan plots. *bioRxiv* **2014**, 5165. [[CrossRef](#)]
34. Scheet, P.; Stephens, M. A fast and flexible statistical model for large-scale population genotype data: Applications to inferring missing genotypes and haplotypic phase. *Am. J. Hum. Genet.* **2006**, *78*, 629–644. [[CrossRef](#)] [[PubMed](#)]
35. Wheelan, S.J.; Church, D.M.; Ostell, J.M. Spidey: A tool for mRNA-to-genomic alignments. *Genome Res.* **2001**, *11*, 1952–1957. [[CrossRef](#)] [[PubMed](#)]
36. Hayes, B.J.; Daetwyler, H.D. 1000 Bull Genomes Project to Map Simple and Complex Genetic Traits in Cattle: Applications and Outcomes. *Annu. Rev. Anim. Biosci.* **2019**, *7*, 89–102. [[CrossRef](#)]
37. O’toole, D.; Häfliger, I.M.; Leuthard, F.; Schumaker, B.; Steadman, L.; Murphy, B.; Drögemüller, C.; Leeb, T. X-linked hypohidrotic ectodermal dysplasia in crossbred beef cattle due to a large deletion in eda. *Animals* **2021**, *11*, 657. [[CrossRef](#)]
38. Mackenzie, E.L.; Iwasaki, K.; Tsuji, Y. Intracellular iron transport and storage: From molecular mechanisms to health implications. *Antioxidants Redox Signal.* **2008**, *10*, 997–1030. [[CrossRef](#)] [[PubMed](#)]
39. Sharma, P.; Reichert, M.; Lu, Y.; Markello, T.C.; Adams, D.R.; Steinbach, P.J.; Fuqua, B.K.; Parisi, X.; Kaler, S.G.; Vulpe, C.D.; et al. Biallelic HEPHL1 variants impair ferroxidase activity and cause an abnormal hair phenotype. *PLoS Genet.* **2019**, *15*, e1008143. [[CrossRef](#)] [[PubMed](#)]
40. Eragene, S.; Stewart, J.J.; Samuel-Constanzo, J.I.; Tan, T.; Esgdaille, N.Z.; Bigiarelli, K.J.; DaCosta, V.D.; Jimenez, H.; King, T.R. The mouse curly whiskers (cw) mutations are recessive alleles of hephaestin-like 1 (Heph1l). *Mol. Genet. Metab. Rep.* **2019**, *20*, 100478. [[CrossRef](#)] [[PubMed](#)]
41. Chen, H.; Attieh, Z.K.; Syed, B.A.; Kuo, Y.M.; Stevens, V.; Fuqua, B.K.; Andersen, H.S.; Naylor, C.E.; Evans, R.W.; Gambling, L.; et al. Identification of zyklopen, a new member of the vertebrate multicopper ferroxidase family, and characterization in rodents and human cells. *J. Nutr.* **2010**, *140*, 1728–1735. [[CrossRef](#)]
42. De Domenico, I.; McVey Ward, D.; Kaplan, J. Regulation of iron acquisition and storage: Consequences for iron-linked disorders. *Nat. Rev. Mol. Cell Biol.* **2008**, *9*, 72–81. [[CrossRef](#)]
43. Olson, T.A.; Hargrove, D.D.; Leipold, H.W. Occurrence of Hypotrichosis in Polled Hereford Cattle. *Bov. Pract.* **1985**, *4–8*. [[CrossRef](#)]

44. Brun-Hansen, H.C.; Kampen, A.H.; Lund, A. Hematologic values in calves during the first 6 months of life. *Vet. Clin. Pathol.* **2006**, *35*, 182–187. [[CrossRef](#)] [[PubMed](#)]
45. Harris, Z.L.; Durley, A.P.; Man, T.K.; Gitlin, J.D. Targeted gene disruption reveals an essential role for ceruloplasmin in cellular iron efflux. *Proc. Natl. Acad. Sci. USA* **1999**, *96*, 10812–10817. [[CrossRef](#)] [[PubMed](#)]
46. Xu, X.; Pin, S.; Gathinji, M.; Fuchs, R.; Harris, Z.L. Aceruloplasminemia: An inherited neurodegenerative disease with impairment of iron homeostasis. *Ann. N. Y. Acad. Sci.* **2004**, *1012*, 299–305. [[CrossRef](#)]
47. Chang, Y.F.; Imam, J.S.; Wilkinson, M.F. The Nonsense-mediated decay RNA surveillance pathway. *Annu. Rev. Biochem.* **2007**, *76*, 51–74. [[CrossRef](#)]

4.1.5 Ocular and auricular disorders

- **Achromatopsia:** “*CNGB3* missense variant causes recessive achromatopsia in Original Braunvieh cattle”, International Journal of Molecular Sciences, 2021, 22, pp. 12440 – 12440 (see [chapter 4.1.5.1](#))
- **Hemifacial microsomia:** “A homozygous missense variant in laminin subunit beta 1 as candidate causal mutation of hemifacial microsomia in Romagnola cattle”, Journal of Veterinary Internal Medicine, 2021, online, pp. 1 – 8 (see [chapter 4.1.5.2](#)).

4.1.5.1 *CNGB3* missense variant causes recessive achromatopsia in Original Braunvieh cattle

Journal: International Journal of Molecular Sciences

Manuscript status: published

Contributions: phenotype investigation

Displayed version: published version

DOI: [10.3390/ijms222212440](https://doi.org/10.3390/ijms222212440)



Article

CNGB3 Missense Variant Causes Recessive Achromatopsia in Original Braunvieh Cattle

Irene M. Häfliger ^{1,†} , Emma Marchionatti ^{2,†} , Michele Stengård ^{3,†} , Sonja Wolf-Hofstetter ¹ , Julia M. Paris ¹ , Joana G. P. Jacinto ⁴ , Christine Watté ³ , Katrin Voelter ⁵ , Laurence M. Ocelli ⁶ , András M. Komáromy ⁶ , Anna Oevermann ⁷ , Christine Goepfert ⁸ , Angelica Borgo ⁹ , Raphaël Roduit ⁹ , Mirjam Spengeler ¹⁰ , Franz R. Seefried ¹⁰ and Cord Drögemüller ^{1,*}

- ¹ Institute of Genetics, Vetsuisse Faculty, University of Bern, Bremgartenstrasse 109a, 3001 Bern, Switzerland; irene.haefli@vetsuisse.unibe.ch (I.M.H.); hofstettersonja@hotmail.com (S.W.-H.); julia-1991@hotmail.com (J.M.P.)
 - ² Clinic for Ruminants, Department of Clinical Veterinary Medicine, Vetsuisse Faculty, University of Bern, Bremgartenstrasse 109a, 3001 Bern, Switzerland; emma.marchionatti@vetsuisse.unibe.ch
 - ³ Division of Ophthalmology, Department of Clinical Veterinary Medicine, Vetsuisse Faculty, University of Bern, Länggassstrasse 128, 3001 Bern, Switzerland; michele.stengard@vetsuisse.unibe.ch (M.S.); christine.watte@vetsuisse.unibe.ch (C.W.)
 - ⁴ Department of Veterinary Medical Sciences, University of Bologna, 50 Ozzano Emilia, 40064 Bologna, Italy; joana.goncalves2@studio.unibo.it
 - ⁵ Ophthalmology Section, Vetsuisse Faculty, University of Zurich, Winterthurerstrasse 260, 8057 Zurich, Switzerland; kvoelter@vetclinics.uzh.ch
 - ⁶ College of Veterinary Medicine, Michigan State University, 736 Wilson Rd., East Lansing, MI 48824, USA; ocelli@msu.edu (L.M.O.); komaromy@msu.edu (A.M.K.)
 - ⁷ Division of Neurological Sciences, Vetsuisse Faculty, University of Bern, Bremgartenstrasse 109a, 3001 Bern, Switzerland; anna.oevermann@vetsuisse.unibe.ch
 - ⁸ COMPATH, Institute of Animal Pathology, Vetsuisse Faculty, University of Bern, Länggassstrasse 122, 3001 Bern, Switzerland; christine.goepfert@vetsuisse.unibe.ch
 - ⁹ Department of Ophthalmology, University of Lausanne, Jules-Gonin Eye Hospital, Av. de France 15, 1004 Lausanne, Switzerland; angelica.borgo@fa2.ch (A.B.); raphael.rodut@fa2.ch (R.R.)
 - ¹⁰ Qualitas AG, Chamerstrasse 56, 6300 Zug, Switzerland; mirjam.spengeler@qualitasag.ch (M.S.); franz.seefried@qualitasag.ch (F.R.S.)
- * Correspondence: cord.droegemueller@vetsuisse.unibe.ch; Tel.: +41-(0)31-684-25-29
† Contributed equally.



Citation: Häfliger, I.M.; Marchionatti, E.; Stengård, M.; Wolf-Hofstetter, S.; Paris, J.M.; Jacinto, J.G.P.; Watté, C.; Voelter, K.; Ocelli, L.M.; Komáromy, A.M.; et al. *CNGB3* Missense Variant Causes Recessive Achromatopsia in Original Braunvieh Cattle. *Int. J. Mol. Sci.* **2021**, *22*, 12440. <https://doi.org/10.3390/ijms222212440>

Academic Editor: Akiko Maeda

Received: 29 October 2021

Accepted: 17 November 2021

Published: 18 November 2021

Publisher's Note: MDPI stays neutral with regard to jurisdictional claims in published maps and institutional affiliations.



Copyright: © 2021 by the authors. Licensee MDPI, Basel, Switzerland. This article is an open access article distributed under the terms and conditions of the Creative Commons Attribution (CC BY) license (<https://creativecommons.org/licenses/by/4.0/>).

Abstract: Sporadic occurrence of inherited eye disorders has been reported in cattle but so far pathogenic variants were found only for rare forms of cataract but not for retinopathies. The aim of this study was to characterize the phenotype and the genetic aetiology of a recessive form of congenital day-blindness observed in several cases of purebred Original Braunvieh cattle. Electroretinography in an affected calf revealed absent cone-mediated function, whereas the rods continue to function normally. Brain areas involved in vision were morphologically normal. When targeting cones by immunofluorescence, a decrease in cone number and an accumulation of beta subunits of cone cyclic-nucleotide gated channel (CNGB3) in the outer plexiform layer of affected animals was obvious. Achromatopsia is a monogenic Mendelian disease characterized by the loss of cone photoreceptor function resulting in day-blindness, total color-blindness, and decreased central visual acuity. After SNP genotyping and subsequent homozygosity mapping with twelve affected cattle, we performed whole-genome sequencing and variant calling of three cases. We identified a single missense variant in the bovine *CNGB3* gene situated in a ~2.5 Mb homozygous genome region on chromosome 14 shared between all cases. All affected cattle were homozygous carriers of the p.Asp251Asn mutation that was predicted to be deleterious, affecting an evolutionary conserved residue. In conclusion, we have evidence for the occurrence of a breed-specific novel *CNGB3*-related form of recessively inherited achromatopsia in Original Braunvieh cattle which we have designated OH1 showing an allele frequency of the deleterious allele of ~8%. The identification of carriers will enable selection against this inherited disorder. The studied cattle might serve as an animal model to further elucidate the function of *CNGB3* in mammals.

Keywords: *Bos taurus*; animal model; day-blindness; retina; development; mendelian genetics; rare disease; precision medicine

1. Introduction

Food animal ophthalmology is a neglected area of veterinary medicine [1,2]. In farm animal practice, conditions such as visual impairment or even blindness, despite having a negative impact on behavior and welfare, are rarely considered, as there is usually no profoundly damaging economic impact on animal production [3].

Sporadic occurrence of inherited eye disorders in livestock species such as cattle has been reported [4–6]. However, many affected newborns go unreported or escape surveillance systems [4]. In addition to hereditary reasons, environmental causes such as vitamin A deficiency and bacterial or viral infections must also be taken into account [5–7]. Although congenital eye defects are rare, they are important and should be considered because they often follow monogenic recessive inheritance [4,6]. Therefore, such inherited disorders can rapidly gain in prevalence due to the undetected use of carriers, especially in the course of artificial insemination in cattle. So far pathogenic variants were found only for rare breed-specific recessive forms of cataract in Romagnola (OMIA 001936-9913) and Holstein (OMIA 002111-9913) cattle [8,9]. Such findings enable selection against these disorders within the affected populations. Furthermore, the *NID1*-related cataract observed in Romagnola was the first report of a naturally occurring mutation leading to a non-syndromic form of cataract in a mammalian species [8]. Therefore, the genetic study performed in cattle added the affected gene to the list of candidate genes for inherited forms of nuclear cataract in humans, illustrating the impact of studying eye conditions in domestic animals.

Achromatopsia, an inherited retinal disease characterized by the loss of cone photoreceptor function resulting in day-blindness, total color-blindness, and decreased central visual acuity, has not yet been described in cattle. Pathogenic variants in six genes (*CNGA3*, *CNGB3*, *GNAT2*, *ATF6*, *PDE6C*, and *PDE6H*) have been identified in humans with achromatopsia (OMIM 216900) [10]. In sheep, a form of *CNGA3*-related achromatopsia has been characterized (OMIA 001481-9940) [11]. This ovine condition was intensively used for functional restoration of cone function [12], highlighting the biomedical value of such large animal models [13,14] in addition to the direct benefits for animal breeding and animal health.

The aim of this study was to characterize the phenotype and the underlying causative genetic defect for this presumably new form of congenital day-blindness observed in several cases of purebred Original Braunvieh cattle from Switzerland.

2. Results

2.1. Clinical Description

Initially, in 2017, a four-month-old calf (case 2) was presented to the University of Zurich for evaluation of suspected day blindness. Ocular examination revealed bilaterally absent menace responses and dazzle reflexes. Pupillary responses were positive. Chromatic light stimulation (Melan) revealed bilaterally minimal dazzle reflexes with red and blue light, pupillary responses were normal with blue and reduced with red light stimulation. The remainder of the ocular exam (slit-lamp biomicroscopy, indirect and direct ophthalmoscopy, intraocular pressure) was within normal limits with the optic nerve head showing a deep physiologic cup. The calf was able to complete an obstacle course in dim light, but not in bright light.

In 2020, a 5.5-month-old calf (case 12) was presented to the University of Bern for evaluation of a suspected vision disturbance. The farmer noted that the calf was hesitant to walk and often collided with obstacles in its environment, especially when separated from the mother (Video S1). Observation of the calf revealed extremely poor navigation

of large and small objects in the examination hall in ambient room light. Navigation of obstacles and recognition of large high-contrast obstacles after room lights were turned off was slightly improved. Ophthalmic examination revealed absent menace response in both eyes (OU) in dim, ambient and bright (outdoor) light conditions. The direct and consensual pupillary light responses as well as dazzle reflexes to white light were reduced in both eyes. A slightly reduced pupillary light response was noted with bright blue light stimulation and severely reduced to bright red light stimulation. Slit-lamp biomicroscopic examination of the eyelids, conjunctiva, cornea, anterior chamber, lens and anterior vitreous was normal in both eyes with the exception of mild mydriasis OU. The pupils were symmetrical OU. Fluorescein staining of the cornea was negative OU. Indirect ophthalmoscopy revealed normal appearance to the optic nerve, tapetal and non-tapetal retina, and retinal vessels bilaterally. Intraocular pressure was measured within normal limits (11 mmHg OD, 14 mmHg OS).

Electroretinography in the affected calf revealed severely reduced light-adapted single cone and cone flicker responses, while the dark-adapted mixed cone-rod response was considered normal (Figure 1). Combined with the behavioral observations and clinical findings, the ERGs support an achromatopsia diagnosis based on the specific loss of cone-mediated retinal function without any retinal degenerative changes.

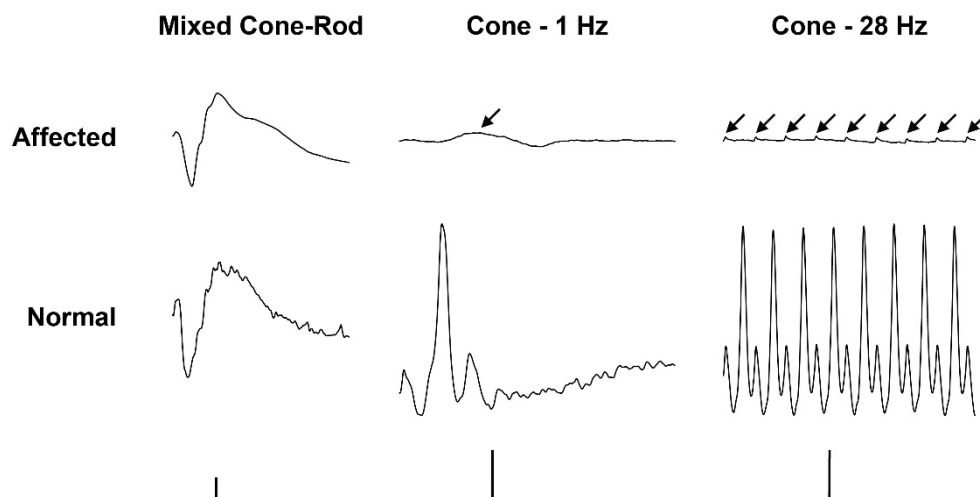


Figure 1. Electroretinogram (ERG) of a 5.5-month old achromatopsia-affected Original Braunvieh (case 12) and a seven-month old Hereford control cattle. Dark-adaptation responses in representative normal and affected calves. While the dark-adapted mixed cone-rod responses were comparable between the two animals, the light-adapted single cone (1 Hz) and cone flicker (28 Hz) responses were severely reduced (arrows). Calibration bars: vertical = 100 μ V, horizontal = 50 ms.

2.2. Pathological Phenotype

During necropsy of case 12 no gross lesions were detectable and brain areas involved in vision were morphologically normal.

The retina were targeted by immunofluorescence. We observed the expression of CNGB3 in the outer segment (OS) of cones in the control animal, while this expression was decreased in the affected animal. We also detected a significant difference of staining in the outer nuclear layer (ONL), where the CNGB3 protein seemed to be concentrated in the affected animal. This may suggest a mislocalization of the mutated CNGB3. Immunoreactivity of CNGB3 in the outer plexiform layer (OPL) may be due to an unspecific signal as the localization is observed in both control and affected animals. (Figure 2a). Further experiments on other affected calves (we analysed only one) or by transfection of the mutated CNGB3 in cells will confirm the potential higher stability of the mutated cyclic nucleotide-gated channel.

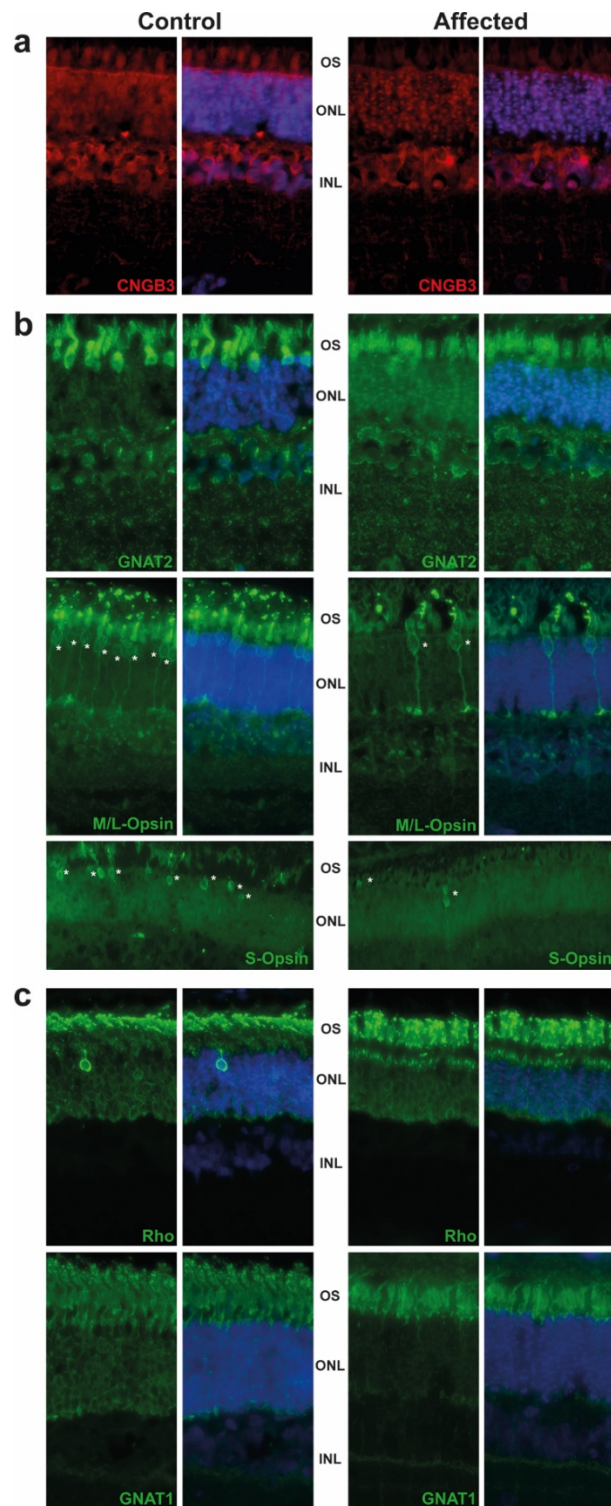


Figure 2. Immunostaining of retinal markers in a five-month old achromatopsia-affected cattle (case 12) and a control cattle of the same age. Cyclic nucleotide gated channel subunit beta 3 (CNGB3) (a), Cones markers (GNAT2, M/L-OPSIN, S-OPSIN) (b) and rods markers (GNAT1, RHODOPSIN) (c) are immunostained in both control and affected animals accordingly to conditions described in Table S2. Cell nuclei are shown in blue with DAPI. Images acquired at equal distances from the optic nerve head for each protein. Asterisks (*) show M/L- and S-Opsin cones present in both control and affected animal. Negative controls without primary antibody were performed (not shown).

Based on GNAT2 and cone opsins staining, we clearly observed a decrease in the cone OS, which are shorter and abnormally shaped. Although we did not count the number of cones per retina, we observed a decrease in their number, in affected animal in comparison to control, as shown in M/L- and S-Opsin staining (Figure 2b, white asterisk). These results are in correlation with the ERG and are consistent with the progressive loss of cone outer segments seen in other species with achromatopsia. We also observed a slight decrease of the rod OS length in affected animals and a mislocalization of Rho (Figure 2c).

2.3. Pedigree Analysis

The initially studied cases 1 and 2 were both the only affected animals in two different Swiss herds of purebred Original Braunvieh cattle. The sire of these two cases was a natural service purebred Original Braunvieh bull, which sired a further 24 apparently normal offspring within two years. A query to the Original Braunvieh breeders in Switzerland revealed further evidence of ten similar cases sired by different bulls collected over a period of three years. The available pedigree records of all 12 cases were analyzed and multiple inbreeding loops between the parents were found (Figure 3). We detected a single common ancestor occurring 8–11 generations ago. Due to the obvious history of inbreeding, a recessive inherited condition was considered. In light of the obvious consanguinity as well as the apparently unaffected parents, we hypothesize that the achromatopsia-affected calves might be explained by a recessively inherited variant. The founding mutation thus probably occurred many generations before the cases occurred. The causal variant was probably spread by the common ancestor, an artificial insemination bull born in 1961, as well as by some of his male descendants.

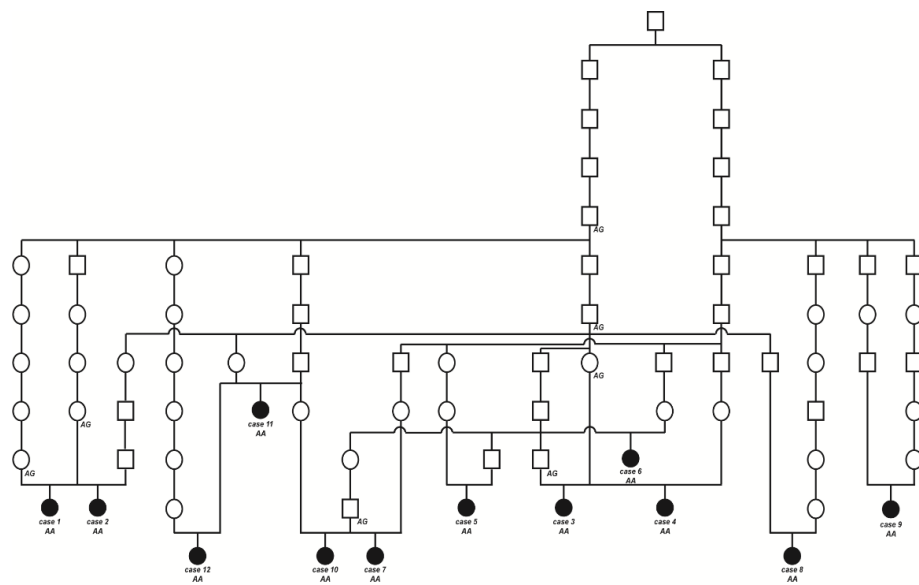


Figure 3. Pedigree of the Original Braunvieh cattle family segregating for achromatopsia suggested monogenic autosomal recessive inheritance. Affected animals are filled symbols. Open symbols represent normal cattle. DNA samples were available from animals with genotypes for the *CNGB3* XM_015474554.2:c.751G>A variant are given below the symbols.

2.4. Genetic Analysis

SNP genotyping data for twelve affected cattle identified two shared ROHs between all cases on chromosome 11 and 14 (Figure 4a). On chromosome 11 all animals were homozygous for 101 SNP markers from 66,668,989 to 68,938,216 corresponding to a repeatedly detected strong selection signature of the Original Braunvieh breed encompassing a genome region with 24 protein-coding genes [15–17]. As no candidate gene for a retinopathy was contained in that region, we focused on the second ROH found on chromosome 14. All twelve affected cattle were homozygous at 28 SNP markers on chromosome 14 from

74,306,245 to 76,800,429, which allowed the identification of a single disease-associated IBD haplotype shared by all cases, limiting the critical region to 2,494,184 bp on chromosome 14 (Table S1; Figure 4a,b). Interestingly, the bovine homolog of *CNGB3*, a gene that causes achromatopsia in other species, maps to that genome region at 76 Mb (Figure 4c).

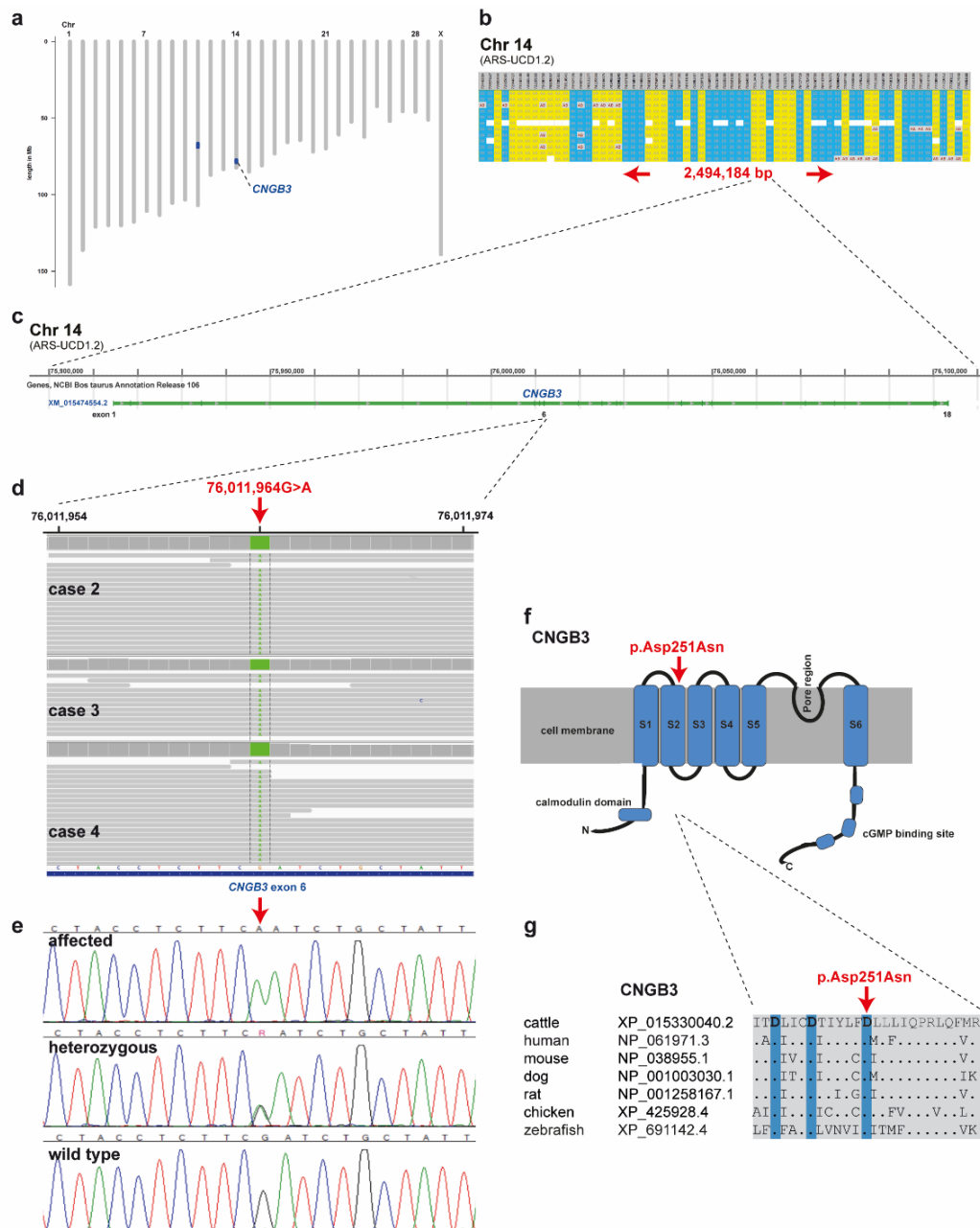


Figure 4. Achromatopsia-associated *CNGB3* missense variant in Original Braunvieh. (a) Genome-wide homozygosity mapping presenting the two homozygous blocks shared in 12 affected calves in blue. Note the red arrow highlighting the *CNGB3* gene on cattle chromosome 14. (b) Schematic representing the SNP genotypes of 12 affected calves on chromosome 14. Each horizontal lane represents one calf with yellow and blue shading, indicating shared homozygosity. Grey shading indicates a heterozygous genotype and white indicates missing genotypes. The genome positions of markers are indicated above the figure. The red arrows indicate the consensus homozygous region that spans approximately 2.5 Mb. (c) *CNGB3* gene structure showing the location of the exon 6 variant. (d) Genome viewer screenshot presenting the homozygous Chr14: g.76011964A>G variant in three affected calves. (e) Electropherograms showing the different genotypes identified via Sanger sequencing. (f) Localization of the missense variant (red arrow) with respect to the topological model of the *CNGB3* protein. (g) Across species sequence alignment of the affected *CNGB3* S2 domain. Note that the missense variant (red arrow) affects the evolutionary conserved Tri-Asp motif that is highlighted in blue.

Subsequently, we sequenced the genomes of three of the affected cattle (cases 2, 3 and 4) and searched for private variants that were exclusively present in a homozygous state in all three affected cattle and absent or only heterozygous in the genomes of 567 other cattle. Beside 34 non-coding variants, all located in the critical region on chromosome 14, this analysis identified a single homozygous private protein-changing variant in *CNGB3*, a known candidate gene for achromatopsia. The variant can be designated as chr14: 76011964G>A (ARS-UCD1.2 assembly) (Figure 4d). It is a missense variant, XM_015474554.2: c.751G>A, predicted to change a highly conserved aspartic acid residue in the second S2 domain of *CNGB3*, XP_015330040.2: p.Asp251Asn (Figure 4f,g). In silico analysis predicted the functional effect of p.Asp251Asn as deleterious using PROVEAN software (score -4.985) [18].

We confirmed the presence of the *CNGB3* missense variant by Sanger sequencing (Figure 4e). The genotypes at the variant co-segregated with the achromatopsia phenotype as expected for a monogenic autosomal recessive mode of inheritance (Figure 3). All twelve available DNA samples from the achromatopsia-affected cattle carried the mutant allele in a homozygous state, while their parents were heterozygous, as expected for obligate carriers (Figure 3; Table 1).

Table 1. Association of the missense variant in *CNGB3* with the achromatopsia phenotype in Original Braunvieh cattle.

	GG	AG	AA
Achromatopsia-affected calves			12
Obligate carriers ^a		5	
Other Original Braunvieh cattle ^{b,c}	2477	463	12
Brown Swiss cattle ^c	14,976	52	
Holstein cattle ^c	14,825		
Simmental cattle ^c	2021		
Sequenced cattle genomes from various breeds (local Swiss cohort) ^d	552	15	
Control cattle from various breeds (1000 Bull Genomes project) ^e	3298	7 ^f	1 ^g

^a parents of affected animals were classified as obligate carriers. ^b phenotypes are unknown. ^c Axiom[®] genotype data from population-wide routine genomic testing. ^d 567 genomes of the Swiss Comparative Bovine Resequencing project including 92 Original Braunvieh cattle. ^e run 8: 3306 genomes including 58 Original Braunvieh cattle. ^f exclusively Original Braunvieh. ^g case 2 was added to the 1000 Bull Genomes project.

We also genotyped the *CNGB3*: c.751G>A variant in a population control cohort comprising 2952 Original Braunvieh cattle without any phenotypic records. The mutant *CNGB3* allele was detected in the homozygous state in 12 of the cattle, whereas 463 were heterozygous carriers revealing an allele frequency of the mutant allele of 8.2% (Table 1). Interestingly, the mutant allele was absent from more than 35,000 cattle of various other breeds (Table 1). We found some rare heterozygous carriers with an allele frequency of 0.2% only in the Brown Swiss population of Switzerland (Table 1).

3. Discussion

To date, no genetic mutations have been associated with retinopathies in cattle. Affected Original Braunvieh calves with suspected vision disturbance suffer from day-blindness due to congenitally reduced cone-mediated function of the retina. Our clinicopathological evaluation of affected calves supported a diagnosis of achromatopsia based on abnormally appearing cone outer segments and normal rod photoreceptors. Furthermore, neither retinal degenerative changes nor abnormalities in the central visual pathways were observed. Pedigree and ROH analysis suggested an autosomal recessive mode of

inheritance. Genome-wide homozygosity mapping using SNP array data was used successfully for high-resolution mapping of two critical regions of shared homozygosity. We performed whole-genome sequencing on three affected Original Braunvieh calves with day-blindness to identify variants associated with the phenotype. The similar clinical presentation between familial achromatopsia in humans and bovine recessive day-blindness led to the hypothesis that a protein-changing variant within *CNGA3*, *CNGB3*, *GNAT2*, *ATF6*, *PDE6C*, and *PDE6H* would be associated with achromatopsia of Original Braunvieh calves. Whereas only *CNGB3* was located in an IBD segment, we identified a missense variant in *CNGB3*: c.751G>A, p.Asp251Asn that significantly associated with the phenotype. Nine additional affected calves were subsequently genotyped and homozygous for the missense variant. Therefore, the cattle studied could serve as an animal model to further investigate the function of *CNGB3* in mammals.

In domestic animals, to this point in sheep [11–13] and dogs [19–22] (previously reported as cone degeneration and canine hemeralopia), the underlying genetics of different forms of achromatopsia are reported. Cones alone are affected in Alaskan Malamute (OMIA 001365-9615) and the German shorthaired pointers (OMIA 001676-9615) because of breed specific mutations in *CNGB3*, a cone-specific gene. Cone cyclic nucleotide-gated channels (CNG) are tetramers formed by three *CNGA3* and one *CNGB3* subunit; *CNGA3* subunits can function as homotetrameric channels but *CNGB3* exhibits channel function only when co-expressed with *CNGA3* [23]. A 140-kb deletion and a missense mutation in *CNGB3* occurs in achromatopsia-affected dogs of multiple breeds [20]. Interestingly, the described canine missense variant also leads to an exchange of an aspartic acid with an asparagine residue, compromising a critical functional domain, and the phenotype seen in homozygous dogs represents a loss of function. Similar to what we found in Original Braunvieh cattle, the *CNGB3* missense mutation causing achromatopsia in German shorthaired pointers is also located in exon 6 (c.784G, p.Asp262Asn), affecting the corresponding residue of a conserved region of the same gene, suggesting an important role for this aspartate residue in channel biogenesis and/or function [21]. The flanking region surrounding these missense mutations is well conserved between species and is predicted to encode the second transmembrane domain of the *CNGB3* protein containing three Asp residues designated the *tri-Asp motif* and conserved in all CNG channels [21]. Mutations of these conserved aspartate residues result in the absence of nucleotide-activated currents in heterologous expression. Aspartate is a negatively charged, polar amino acid found in both dogs and cattle with achromatopsia replaced by asparagine (Asn), another polar amino acid, which differs only in that it contains an amino group in place of one of the oxygens found in aspartate (Asp) and thus lacks a negative charge. Obviously, retinopathies associated with missense mutations draw attention to amino acids important for understanding the structure-function properties of functionally important channels. By in vitro follow-up studies of *CNGB3*-related canine achromatopsia it was found that Asp/Asn mutations affect the heteromeric subunit assembly of the six transmembrane-spanning helices (S1–S6), resulting in the loss of these inter-helical interactions altering the electrostatic equilibrium within in the S1–S4 bundle [21]. Although disease-causing variants within the S2 segment of human *CNGB3* have not been reported (OMIM 605080), a study involving a missense mutation p.Asp211Glu at S2 of *CNGA3* confirmed that variations in a conserved region could lead to cone dysfunction [24].

In Switzerland, the Original Braunvieh population is the ancestor of the world-renowned Brown Swiss population, which originated in North America from animals obtained in Switzerland at the turn of the century around 1900 [25]. Therefore, we speculate that the sporadic occurrence of *CNGB3*-carriers in the current Brown Swiss population indicates that the mutation might have arisen before that time and predates modern pedigree records. In recent decades, outbreaks of four undesirable genetic defects (weaver disease, spinal dysmyelination, spinal muscular atrophy, and arachnomelia) have occurred in Brown Swiss cattle. This report represents the first genetic disorder known in Original

Braunvieh cattle which we have designated OH1, and the obtained results enable targeted selection to avoid the occurrence of further affected animals in future.

In summary, this study highlights the strong genetic similarities between human and bovine achromatopsia, suggesting that bovine achromatopsia, similar to that found in dogs, could serve as an excellent model for developing treatment strategies for humans.

4. Materials and Methods

4.1. Animal Selection for Genetic Analysis

This study was conducted with 248 Original Braunvieh cattle samples. The case cohort of this study consisted of twelve purebred Original Braunvieh cattle with suspected congenital vision disturbance reported to the breeding organization by different farmers between 2017 and 2020 (Table S1). In addition, either hair root or EDTA blood samples of three dams and two sires were collected for the genetic analysis, and genomic DNA was extracted using the Promega Maxwell[®] RSC system (Promega, Dübendorf, Switzerland). The remaining 231 male Original Braunvieh cattle were used as population controls. These bulls had reliable phenotype records on normal vision because they were very carefully examined by veterinarians before being used for artificial insemination. Before admission to the insemination station, these young bulls are carefully examined and these examinations include, in particular, the consideration of the presence of possible congenital disorders, including a standard ophthalmological examination of the eyes.

Once the most likely causative variant was discovered, it was added to two Swiss Axiom[®] genotyping arrays (Thermo Fisher Scientific, Waltham, MA, USA) routinely used for genomic selection. Thus, after two years of population-wide genotyping in Swiss dairy populations for the purpose of genomic selection, more than 30,000 genotypes for the CNGB3 variant were available. These were mainly determined in the four largest Swiss dairy cattle populations (Brown Swiss, Holstein, Original Braunvieh and Simmental).

4.2. Ophthalmological Examination including Electroretinography

A four-month-old calf (case 2) was presented to the University of Zürich Food Animal Clinic and the Ophthalmology Section in summer 2017 for evaluation of suspected vision disturbance.

A 5.5-month-old calf (case 12) was presented to the University of Bern Food Animal Clinic and the Division of Ophthalmology in the year 2020 for evaluation of suspected vision disturbance. Pupillary light responses were examined with bright red and blue light stimulation (Melan-100, 200–250 kcd, Iris-vet series, BioMed Vision Technologies, Ames, IA, USA). Furthermore, slit-lamp biomicroscopic examination (SL-17 Portable Slit Lamp, Kowa, Japan) of the adnexa and anterior segments, fluorescein staining (Contacare Ophthalmics and Diagnostics, Gujarat, India) of the corneas and indirect ophthalmoscopy (Omega 500 Binocular Indirect Ophthalmoscope, Heine Optotechnik GmbH, Gilching, Germany) of the ocular fundi were carried out. Intraocular pressures were measured by rebound tonometry (Tonovet Rebound Tonometer, Icare, Finland).

Electroretinograms (ERGs) were recorded under general anesthesia in case 12 following clinical and behavioural examinations. A jugular intravenous catheter was placed and the calf was sedated with xylazine 0.2 mg/kg IM. Induction was performed with ketamine 4 mg/kg intravenous, and 10 min after sedation the calf was placed in lateral recumbency. The head was positioned with cushions to facilitate access to the eye for testing. Anesthesia was maintained using ketamine continuous-rate infusion 3 mg/kg/h and xylazine continuous-rate infusion 0.05 mg/kg/hr. Flow-by oxygen was administered continuously via nasal oxygen catheter. All recordings were conducted on the right eye, following dilation of the pupil with 1% tropicamide ophthalmic solution. ERGs were recorded using the RetiPORT ERG system (Roland Consult, Brandenburg an der Havel, Germany). Two platinum subdermal needle electrodes (Grass Safelead Needle electrodes, Grass Technologies, West Warwick, RI, USA) were used: The reference electrode was placed subcutaneously approximately 10 mm from the lateral canthus, and the ground electrode

was placed over the occipital protuberance. An ERG-Jet[®] corneal electrode (Fabrinal SA, La Chaux-de-Fonds, Switzerland) was used as the active electrode and applied with 2.5% hypromellose ophthalmic demulcent solution. Flash stimuli and light adaptation were delivered using a handheld Mini Ganzfeld (Roland Consult).

Following 20 min of dark adaptation, mixed cone-rod responses were recorded with a flash intensity of 0.096 cd.s/m² (average of 3 sweeps at 0.1 Hz). Subsequently, the eye was light-adapted for 5 min to a white uniform background light of 30 cd/m² and single cone (average of 3 sweeps at 1.0 Hz) and cone flicker (average of 3 sweeps at 28 Hz) responses were recorded with a 3.0 cd.s/m² flash intensity. For all recordings, the filters were set to allow a bandpass of 1 to 300 Hz.

4.3. Targeting Cones by Immunofluorescence

After slaughtering, the enucleated calf eyes of case 12 were fixed in Bouin's solution for 24 h, trimmed and paraffin embedded. The 3 µm-embedded paraffin sections were further processed for immunofluorescence. Briefly, retina sections were first deparaffinized by successive baths (three different Xylol baths of 5 min, 3 min, 3 min respectively; and six ethanol baths: from 100% to 70%; then washed several times in water). Sections were then boiled 30 min in a Dako antigen retrieval solution (Agilent S169984-2) and left to cool down for 45 min. Retina sections were incubated for 1 h in blocking solution and incubated with primary antibodies as indicated in Table S2. Following incubation with primary antibodies, sections were washed 3 times in PBS and incubated for 1.5 h at RT with the secondary antibodies (Table S2). After three successive washing steps in PBS, sections were treated for 25 min in 0.1% Sudan black B (Sigma 380B)/70% ethanol. Then, sections were washed again twice in ethanol 70%, and three times in PBS 0.02% Tween and counterstained with 49,6-Diamidino-2-phenylindole (DAPI) to identify retinal cell layers. After three washing steps in PBS, sections were mounted with antifadent citifluor solution (Electron microscopy sciences, Hatfield, PA, USA). Immunostaining was visualized under a fluorescence microscope (Leica, Switzerland). Incubation with the secondary antibody alone was used as a negative control, and every image acquisition of the retina was made at the same distance from the optic nerve head for each antigen.

4.4. Morphology and Histopathology of the Visual Pathway

The head of case 1 was taken for gross and histopathological evaluation after slaughtering at the age of five months. The visual pathways of the affected cattle were evaluated and biopsies fixed in 4% formaldehyde for routine histopathological evaluation with haematoxylin and eosin (H&E) staining of the optic nerve, optic tract, optic chiasm, lateral geniculate nucleus and the visual cortex.

4.5. SNP Genotyping and Subsequent Homozygosity Mapping with 12 Affected Cattle

Genotype data for the twelve achromatopsia-affected cattle (cases 1–12) were obtained with an Illumina BovineHD BeadChip array. The PLINK v1.9 software [26] was used to perform basic quality filtering of the dataset. For homozygosity mapping, the genotype data for the twelve affected cattle were used. Markers on the sex chromosomes were excluded. The following PLINK option parameters were applied (`-homozyg-snp 10`; `-homozyg group`; `-homozyg-density 30`; `-homozyg-gab 1000`; `-homozyg-window-het 0`; `-homozyg-window-missing 0`) to search for extended regions of homozygosity (ROH) indicating chromosomal region of identity-by-descent (IBD). ROH analyses were performed using an imputed dataset that included the entire Swiss genotype archive for Original Braunvieh. Animals were genotyped using several routinely available array chips that included between nine and 777 k SNPs. The available genotype archive was used in a two-step imputation approach and was imputed first to a density of 150 k. Subsequently, imputation to 777 k-density was carried out using 150 k data. A number of 2507 and 351 Original Braunvieh reference animals were available for 150 k and 777 k imputation, respectively. FImpute v2.2 software was used with default parameters for both steps [27]. In each step, SNPs

with a minor allele frequency (MAF) lower than 1% were removed from the dataset. The final marker set included 114891 and 681179 SNPs for each density (150 k and 777 k), respectively. SNPs were filtered using the following thresholds: MAF higher than 0.01 and an SNP call rate higher than 0.99 in the genotype data from the reference population. The output interval was displayed in Excel spreadsheets to find overlapping regions (Table S1). All positions correspond to the ARS-UCD1.2 reference genome assembly.

4.6. Whole-Genome Resequencing and Variant Calling

Three Illumina TruSeq PCR-free libraries with ~500 bp insert size were prepared from three affected cattle (cases 2, 3 and 4). We collected 2×150 bp paired-end reads on a NovaSeq 6000 instrument. Mapping to ARS-UCD1.2 reference genome assembly was performed as described [28]. The sequence data were deposited under study accession PRJEB28191 and sample accessions SAMEA4644768, SAMEA6528889 and SAMEA6528891 at the European Nucleotide Archive.

Variant calling including single-nucleotide variants (SNVs) and small indels was performed as described [29]. To predict the functional effects of the called variants, SnpEff software v4.3 [30] together with the ARS-UCD1.2 reference genome assembly and NCBI Annotation Release 106 (https://www.ncbi.nlm.nih.gov/genome/annotation_euk/Bos_taurus/106/; accessed on 30 June 2021) was used. For private variant filtering we used control genome sequences from 567 cattle of diverse breeds including 119 Original Braunvieh animals. These genomes were produced during the Swiss Comparative Bovine Resequencing project and made publicly available (<https://www.ebi.ac.uk/ena/browser/view/PRJEB18113/>; accessed on 30 June 2021). The most likely pathogenic missense variant in *CNGB3* was inspected for its presence in a global control cohort of 3306 genomes with a sequence depth of at least 8x from a variety of breeds including 92 Original Braunvieh animals (1000 Bull Genomes Project run 8; www.1000bullgenomes.com accessed on 30 June 2021) [29].

4.7. Genotyping Assays

Two genotyping tests were developed for the XM_015474554.2:c.751G > A missense variant in the *CNGB3* gene to confirm segregation with disease and to estimate the allele frequency in the population.

4.7.1. PCR and Sanger Sequencing

We designed a specific PCR for the targeted genotyping of the chr14:76011964G>A variant. PCR was performed for 30 cycles using Amplitaq Gold Master Mix (ThermoFisher, Rotkreuz, Switzerland) in a 10 μ L reaction containing 10 ng genomic DNA and 5 pmol of each primer (F 5'-CCTGTGGCTCTCACTTGTC-3' and R 5'-CTCCCGAGCCCCTACTTACT-3'). After treatment with exonuclease I and alkaline phosphatase, PCR amplicons were sequenced on an ABI 3730 DNA Analyzer (ThermoFisher, Rotkreuz, Switzerland). Sanger sequences were analyzed using the Sequencher 5.1 software (GeneCodes, Ann Arbor, MI, USA).

4.7.2. Axiom[®] Genotyping Array

Two fully customized Axiom[®] genotyping arrays (Thermo Fisher Scientific, Rotkreuz, Switzerland) designed for genomic selection purpose in Swiss dairy cattle populations designated as SWISScow (96-array layout with 314,744 markers) and SWISSLD1 (384-array layout with 64,212 markers) both included the chr14:76011964G>A variant.

Supplementary Materials: The following are available online at <https://www.mdpi.com/article/10.3390/ijms222212440/s1>.

Author Contributions: Conceptualization, F.R.S. and C.D.; validation, I.M.H., E.M., M.S. (Michele Stengård) and J.M.P.; formal analysis, I.M.H., S.W.-H., M.S. (Michele Stengård), C.W., E.M., J.G.P.J., K.V., L.M.O., A.M.K., A.O., C.G., A.B., R.R. and M.S. (Mirjam Spengeler); investigation, I.M.H., S.W.-

H., E.M., M.S. (Michele Stengård) and R.R.; data curation, I.M.H.; writing—original draft preparation, I.M.H., E.M., M.S. (Michele Stengård), A.M.K., R.R. and C.D.; writing—review and editing, I.M.H., S.W.-H., J.M.P., M.S. (Michele Stengård), C.W., E.M., J.G.P.J., K.V., L.M.O., A.M.K., A.O., C.G., A.B., R.R., M.S. (Mirjam Spengeler), F.R.S. and C.D.; supervision, C.D.; project administration, C.D.; funding acquisition, R.R. and C.D. All authors have read and agreed to the published version of the manuscript.

Funding: This research was partially funded by Swiss National Science foundation, grant number 172911 to CD and 166119 to RR, and the APC was funded by the Swiss National Science foundation. RR and AB were funded by Art & Vie foundation.

Institutional Review Board Statement: This study did not require official or institutional ethical approval as it was not experimental but part of clinical and pathological veterinary diagnostics. The animals were handled according to good ethical standards and Swiss legislation (Animal Welfare regulation: Tierschutzverordnung from 23 April 2008, last amended on 4 September 2018). The tissue for pathological examinations were collected after slaughtering. The aim was to identify the cause of the congenital disorder. All animals in this study were examined with the consent of their owners. Collection of blood samples was approved by the Cantonal Committee for Animal Experiments (Canton of Bern; permit 71/19).

Informed Consent Statement: Not applicable.

Data Availability Statement: The WGS data of the three sequenced cases can be found in the European Nucleotide Archive under the sample accession nos. SAMEA4644768 (case 2), SAMEA6528889 (case 3), and SAMEA6528891 (case 4).

Acknowledgments: The authors are grateful to Brauvieh Schweiz for assistance in sampling and organization of cattle for the clinical exams as well as for SNP array genotyping of all cases. The authors also wish to thank Swissgenetics for providing semen. Furthermore we thank Nathalie Besuchet and Simon Pot for expert assistance. We also acknowledge all bovine researchers contributing to the 1000 Bull Genomes Project and those who deposited cattle whole genome sequencing data into public databases.

Conflicts of Interest: Authors declare no conflict of interest.

References

1. Lavach, J.D. *Large Animal Ophthalmology*; Mosby: St. Louis, MO, USA, 1990.
2. Williams, D.L. Production animal ophthalmology. *Vet. Clin. N. Am. Food Anim. Pract.* **2010**, *26*, xi–xii. [[CrossRef](#)]
3. Williams, D.L. Welfare issues in farm animal ophthalmology. *Vet. Clin. N. Am. Food Anim. Pract.* **2010**, *26*, 427–435. [[CrossRef](#)] [[PubMed](#)]
4. Leipold, H.W. Congenital ocular defects in food-producing animals. *Vet. Clin. N. Am. Large Anim. Pract.* **1984**, *6*, 577–595. [[CrossRef](#)]
5. Gelatt, K.N.; Ben-Shlomo, G.; Gilger, B.C.; Hendrix, D.V.; Kern, T.J.; Plummer, C.E. *Veterinary Ophthalmology*, 6th ed.; John Wiley & Sons: Hoboken, NJ, USA, 2021; pp. 1983–2054.
6. Williams, D.L. Congenital abnormalities in production animals. *Vet. Clin. N. Am. Food Anim. Pract.* **2010**, *26*, 477–486. [[CrossRef](#)]
7. He, X.; Li, Y.; Li, M.; Jia, G.; Dong, H.; Zhang, Y.; He, C.; Wang, C.; Deng, L.; Yang, Y. Hypovitaminosis A coupled to secondary bacterial infection in beef cattle. *BMC Vet. Res.* **2012**, *8*, 222. [[CrossRef](#)]
8. Murgiano, L.; Jagannathan, V.; Calderoni, V.; Joehler, M.; Gentile, A.; Drögemüller, C. Looking the cow in the eye: Deletion in the NID1 gene is associated with recessive inherited cataract in Romagnola cattle. *PLoS ONE* **2014**, *9*, e110628. [[CrossRef](#)] [[PubMed](#)]
9. Hollmann, A.K.; Dammann, I.; Wemheuer, W.M.; Wemheuer, W.E.; Chilla, A.; Tipold, A.; Schulz-Schaeffer, W.J.; Beck, J.; Schütz, E.; Brenig, B. Morgagnian cataract resulting from a naturally occurring nonsense mutation elucidates a role of CPAMD8 in mammalian lens development. *PLoS ONE* **2017**, *12*, e0180665.
10. Sun, W.; Li, S.; Xiao, X.; Wang, P.; Zhang, Q. Genotypes and phenotypes of genes associated with achromatopsia: A reference for clinical genetic testing. *Mol. Vis.* **2020**, *26*, 588–602. [[PubMed](#)]
11. Reicher, S.; Seroussi, E.; Gootwine, E. A mutation in gene CNGA3 is associated with day blindness in sheep. *Genomics* **2010**, *95*, 101–104. [[CrossRef](#)]
12. Ross, M.; Ofri, R.; Aizenberg, I.; Abu-Siam, M.; Pe'er, O.; Arad, D.; Rosov, A.; Gootwine, E.; Dvir, H.; Honig, H.; et al. Naturally-occurring myopia and loss of cone function in a sheep model of achromatopsia. *Sci. Rep.* **2020**, *10*, 19314. [[CrossRef](#)]
13. Komáromy, A.M. Day blind sheep and the importance of large animal disease models. *Vet. J.* **2010**, *185*, 241–242. [[CrossRef](#)] [[PubMed](#)]
14. Winkler, P.A.; Occelli, L.M.; Petersen-Jones, S.M. Large animal models of inherited retinal degenerations: A review. *Cells* **2020**, *9*, 882. [[CrossRef](#)] [[PubMed](#)]

15. Rothhammer, S.; Seichter, D.; Förster, M.; Medugorac, I. A genome-wide scan for signatures of differential artificial selection in ten cattle breeds. *BMC Genom.* **2013**, *14*, 908. [[CrossRef](#)]
16. Signer-Hasler, H.; Burren, A.; Neuditschko, M.; Frischknecht, M.; Garrick, D.; Stricker, C.; Gredler, B.; Bapst, B.; Flury, C. Population structure and genomic inbreeding in nine Swiss dairy cattle populations. *Genet. Sel. Evol.* **2017**, *49*, 83. [[CrossRef](#)]
17. Bhati, M.; Kadri, N.K.; Crysnanto, D.; Pausch, H. Assessing genomic diversity and signatures of selection in Original Braunvieh cattle using whole-genome sequencing data. *BMC Genom.* **2020**, *21*, 27. [[CrossRef](#)]
18. Choi, Y.; Chan, A.P. PROVEAN web server: A tool to predict the functional effect of amino acid substitutions and indels. *Bioinformatics* **2015**, *31*, 2745–2747. [[CrossRef](#)]
19. Miyadera, K.; Acland, G.M.; Aguirre, G.D. Genetic and phenotypic variations of inherited retinal diseases in dogs: The power of within- and across-breed studies. *Mamm. Genome* **2012**, *23*, 40–61. [[CrossRef](#)] [[PubMed](#)]
20. Yeh, C.Y.; Goldstein, O.; Kukekova, A.V.; Holley, D.; Knollinger, A.M.; Huson, H.J.; Pearce-Kelling, S.E.; Acland, G.M.; Komáromy, A.M. Genomic deletion of CNGB3 is identical by descent in multiple canine breeds and causes achromatopsia. *BMC Genet.* **2013**, *14*, 27. [[CrossRef](#)]
21. Tanaka, N.; Delemotte, L.; Klein, M.L.; Komáromy, A.M.; Tanaka, J.C. A cyclic nucleotide-gated channel mutation associated with canine daylight blindness provides insight into a role for the S2 segment tri-Asp motif in channel biogenesis. *PLoS ONE* **2014**, *9*, e88768. [[CrossRef](#)]
22. Tanaka, N.; Dutrow, E.V.; Miyadera, K.; Delemotte, L.; MacDermaid, C.M.; Reinstein, S.L.; Crumley, W.R.; Dixon, C.J.; Casal, M.L.; Klein, M.L.; et al. Canine CNGA3 Gene Mutations Provide Novel Insights into Human Achromatopsia-Associated Channelopathies and Treatment. *PLoS ONE* **2015**, *10*, e0138943. [[CrossRef](#)]
23. Sidjanin, D.J.; Lowe, J.K.; McElwee, J.L.; Milne, B.S.; Phippen, T.M.; Sargan, D.R.; Aguirre, G.D.; Acland, G.M.; Ostrander, E.A. Canine CNGB3 mutations establish cone degeneration as orthologous to the human achromatopsia locus ACHM3. *Hum. Mol. Genet.* **2002**, *11*, 1823–1833. [[CrossRef](#)]
24. Chen, X.T.; Huang, H.; Chen, Y.H.; Dong, L.J.; Li, X.R.; Zhang, X.M. Achromatopsia caused by novel missense mutations in the CNGA3 gene. *Int. J. Ophthalmol.* **2015**, *8*, 910–915.
25. Hagger, C. Estimates of genetic diversity in the brown cattle population of Switzerland obtained from pedigree information. *J. Anim. Breed. Genet.* **2005**, *122*, 405–413. [[CrossRef](#)] [[PubMed](#)]
26. Purcell, S.; Neale, B.; Todd-Brown, K.; Thomas, L.; Ferreira, M.A.R.; Bender, D.; Maller, J.; Sklar, P.; De Bakker, P.I.W.; Daly, M.J.; et al. PLINK: A tool set for whole-genome association and population-based linkage analyses. *Am. J. Hum. Genet.* **2007**, *81*, 559–575. [[CrossRef](#)] [[PubMed](#)]
27. Sargolzaei, M.; Chesnais, J.P.; Schenkel, F.S. FImpute—An efficient imputation algorithm for dairy cattle populations. *J. Dairy Sci.* **2011**, *94*, 421.
28. Häfliger, I.M.; Wiedemar, N.; Švara, T.; Starič, J.; Cociancich, V.; Šest, K.; Gombač, M.; Paller, T.; Agerholm, J.S.; Drögemüller, C. Identification of small and large genomic candidate variants in bovine pulmonary hypoplasia and anasarca syndrome. *Anim. Genet.* **2020**, *51*, 382–390. [[CrossRef](#)] [[PubMed](#)]
29. Hayes, B.J.; Daetwyler, H.D. 1000 Bull Genomes Project to Map Simple and Complex Genetic Traits in Cattle: Applications and Outcomes. *Annu. Rev. Anim. Biosci.* **2019**, *7*, 89–102. [[CrossRef](#)]
30. Cingolani, P.; Platts, A.; Wang, L.L.; Coon, M.; Nguyen, T.; Wang, L.; Land, S.J.; Lu, X.; Ruden, D.M. A program for annotating and predicting the effects of single nucleotide polymorphisms, SnpEff: SNPs in the genome of *Drosophila melanogaster* strain w1118; iso-2; iso-3. *Fly* **2012**, *6*, 80–92. [[CrossRef](#)] [[PubMed](#)]

4.1.5.2 A homozygous missense variant in laminin subunit beta 1 as candidate causal mutation of hemifacial microsomia in Romagnola cattle

Journal: Journal of Veterinary Internal Medicine

Manuscript status: published

Contributions: phenotype description, whole-genome sequencing data analysis, figures, writing original draft and revisions

Displayed version: published version

DOI: [10.1111/jvim.16316](https://doi.org/10.1111/jvim.16316)

A homozygous missense variant in laminin subunit beta 1 as candidate causal mutation of hemifacial microsomia in Romagnola cattle

Joana G. P. Jacinto^{1,2}  | Irene M. Häfliger² | Marco Bernardini^{3,4}  |
 Maria Teresa Mandara⁵  | Ezio Bianchi⁶ | Marilena Bolcato¹  |
 Noemi Romagnoli¹ | Arcangelo Gentile¹  | Cord Drögemüller² 

¹Department of Veterinary Medical Sciences, University of Bologna, Ozzano, Italy

²Institute of Genetics, Vetsuisse Faculty, University of Bern, Bern, Switzerland

³Anicura Portoni Rossi Veterinary Hospital, Zola Predosa, Bologna, Italy

⁴Department of Animal Medicine, Productions and Health, University of Padua, Padua, Italy

⁵Department of Veterinary Medicine, Neuropathology Laboratory, University of Perugia, Perugia, Italy

⁶Department of Veterinary Medical Sciences, University of Parma, Parma, Italy

Correspondence

Joana G. P. Jacinto, Department of Veterinary Medical Sciences, University of Bologna, Ozzano, Italy.
 Email: joana.goncalves2@studio.unibo.it

Funding information

This research was partially funded by Swiss National Science foundation, Grant/Award Number: 172911

Abstract

Hemifacial microsomia (HFM) was diagnosed in a 9-day-old Romagnola calf. The condition was characterized by microtia of the left ear, anotia of the right ear, asymmetry of the face, and deafness. Magnetic resonance imaging revealed agenesis of the right pinna and both tympanic bullae, asymmetry of the temporal bones and temporomandibular joints, and right pontine meningocele. Brainstem auditory evoked responses confirmed the impaired auditory capacity. At gross post mortem examination, there was agenesis and hypoplasia of the right and the left external ear, respectively. No histological abnormalities were detected in the inner ears. A trio whole-genome sequencing approach was carried out and identified a private homozygous missense variant in *LAMB1* affecting a conserved residue (p.Arg668Cys). Genotyping of 221 Romagnola bulls revealed a carrier prevalence <2%. This represents a report of a *LAMB1*-related autosomal recessive inherited disorder in domestic animals and adds *LAMB1* to the candidate genes for HFM.

KEYWORDS

Bos taurus, development, microtia, precision medicine, rare disease, WGS

1 | INTRODUCTION

Microtia is a congenital malformation of the external ear and can range in severity from mild structural abnormalities to complete absence of the ear (anotia).¹ It occurs as an isolated malformation (nonsyndromic form) or as a part of a spectrum of anomalies

(syndromic form). Hemifacial microsomia (HFM) is the term used to describe a syndromic form that might be characterized by microtia, facial asymmetry, oral clefts, and eyelid defects. Renal abnormalities, cardiac defects, polydactyly, and vertebral deformities are ancillary malformations.^{2,3}

The causes of microtia are poorly understood in both humans and animals,⁴ although evidence supports contribution of genetic and environmental components. In humans, there are several monogenic inherited mostly syndromic forms of microtia (OMIM 600674 occur associated with disease-causing variants in genes such as *HOXA1*,⁵

Abbreviations: BAs, brachial arches; BAERs, brainstem auditory evoked responses; CNCCs, cranial neural crest cells; H&E, hematoxylin and eosin; HFM, hemifacial microsomia; IGV, Integrative Genomics Viewer; MRI, magnetic resonance imaging; NCCs, neural crest cells; NHL, normal hearing level; WGS, whole-genome sequencing; EGF, epidermal growth factor.

This is an open access article under the terms of the Creative Commons Attribution-NonCommercial-NoDerivs License, which permits use and distribution in any medium, provided the original work is properly cited, the use is non-commercial and no modifications or adaptations are made.

© 2021 The Authors. *Journal of Veterinary Internal Medicine* published by Wiley Periodicals LLC on behalf of American College of Veterinary Internal Medicine.

HOXA2,^{6,7} *ORC1*, *ORC6*, *CDT1*,⁸ *ORC4*,⁹ *CDC6*,¹⁰ *MCM5*,¹¹ *TCOF1*,¹² *POLR1C*, *POLR1D*,¹³ *POLR1B*,¹⁴ and *FGF3*.¹⁵ Mouse model studies identify a list of genes associated with microtia, and illustrated several signaling pathways, including BMP, WNT, FGF, and retinoic acid, that present an important function in outer-ear development.² Furthermore, in cattle and sheep dominantly inherited nonsyndromic forms of anomalies affecting the outer ear are associated with regulatory variants affecting the expression of *HMX1*^{16,17} (OMIA 000317-9913 and OMIA 001952-9940). A recessive syndromic form of microtia in pigs is associated with a deletion in *HOXA1*⁴ (OMIA 001952-9823).

The aims of this study were to describe the clinical and disease phenotype observed in a Romagnola calf affected by HFM, to identify the suspected genetic etiology by a trio-based whole-genome

sequencing (WGS) approach, and to estimate the prevalence of the deleterious allele in Romagnola cattle.

2 | CASE DESCRIPTION

A 9-day-old female Romagnola calf, weighting 43 kg, was admitted to the Department of Veterinary Medical Sciences, University of Bologna because absence of the auricles and facial asymmetry.

At the time of admission, the calf had asymmetry of the face with deviation to the right side and lingual ptosis (Figure 1A). The right pinna was absent (anotia), while the left 1 was a rudiment of soft tissue with absence of the ear canal (aural atresia) and covered by long hair

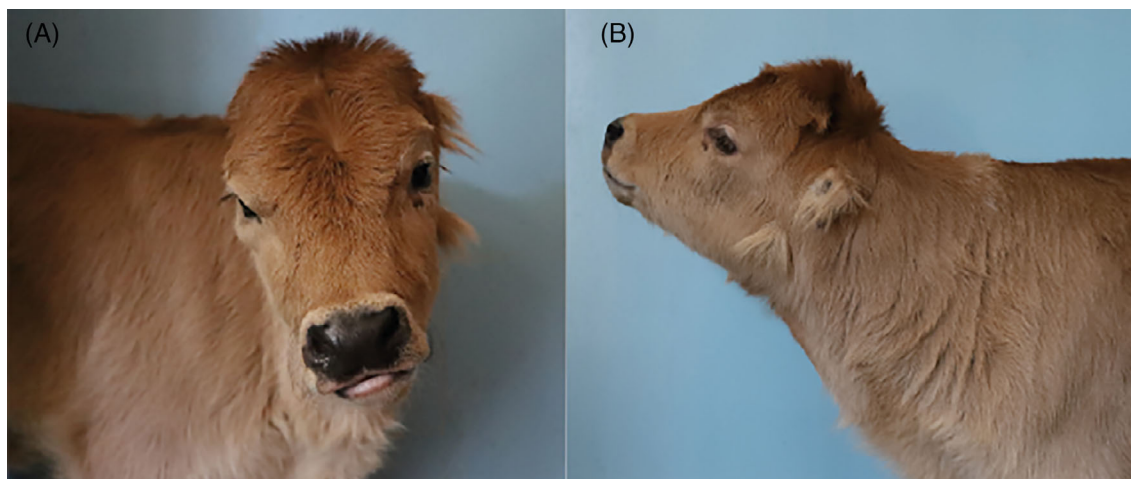


FIGURE 1 Hemifacial microsomia (HFM) in the Romagnola calf demonstrating: (A) note the abnormal conformation of the splanchnocranium with slight right deviation from the sagittal plan and (B) note that the left pinna is a rudiment of soft tissue with absence of the ear canal (aural atresia) and covered by long hair

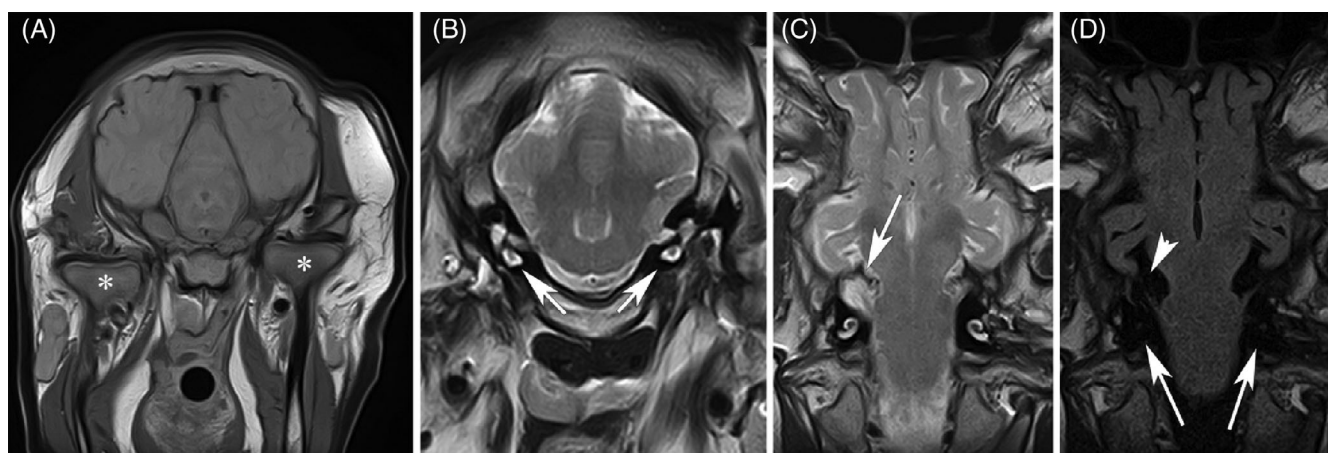


FIGURE 2 Magnetic resonance imaging of the head in the Romagnola calf with hemifacial microsomia (HFM). (A) Transverse proton density image at the level of the caudal mesencephalon. There is marked asymmetry of the temporomandibular joints (asterisks) and the surrounding soft tissues. (B) Transverse T2-weighted image at the level of the pons. There is a normal hyperintense signal of the perilymph and endolymph in both inner ears (arrows). Note the bilateral agenesis of the tympanic bullae. (C) Dorsal T2-weighted image at the level of the inner ears. An enlargement of the subarachnoidal space (meningocele) is seen on the right side at the level of the pons (arrow). (D) Dorsal fluid-attenuated inversion recovery (FLAIR) image at the same level as (C). The T2-weighted hyperintense signal from the inner ears (long arrows) and cerebrospinal fluid in the meningocele (arrow head) is suppressed

hair (Figure 1B). The neurological examination revealed reduced mental status characterized by decreased level of consciousness with listlessness and drowsiness. Notably, the calf did not respond to loud noises and hand clapping. It had a normal stance and gait. A deficit of proprioception was detected in the forelimbs.

Hematology revealed lymphocytosis ($6030/\text{mm}^3$; reference interval, $4250\text{--}5850/\text{mm}^3$) with monocytosis ($1430/\text{mm}^3$) and neutrophilia ($6490/\text{mm}^3$; reference interval, $290\text{--}950/\text{mm}^3$), and hypoproteinemia (5.68 g/dL ; reference interval, $6.74\text{--}7.46\text{ g/dL}$) with hypoalbuminemia (2.79 g/dL ; reference interval, $3.03\text{--}3.55\text{ g/dL}$). Blood samples were tested for bovine viral diarrhea virus, Schmallenberg virus, bluetongue virus, *Neospora caninum*, and *Toxoplasma gondii* using PCR and ELISA for detecting antigens and antibodies, respectively. Tests were negative for all these pathogens using both PCR and ELISA.

The calf underwent general anesthesia for magnetic resonance imaging (MRI) of the head. Magnetic resonance imaging was obtained using a 1.5 T scanner. T2-weighted images were acquired in transverse, sagittal, and dorsal planes, T1-weighted images were acquired in the transverse plane, fluid attenuated inversion recovery (T2-FLAIR) images were acquired in the dorsal plane, and proton density images were acquired in the transverse plane. Slice thickness was 3 to 4 mm, with a 10% interslice gap. Field of view was 16 to 18 cm. No contrast medium was administered. Magnetic resonance imaging revealed: asymmetry of the temporal bones and the temporomandibular joints associated with a right pontine meningocele (Figure 2A,C,D); agenesis of the right external ear canal and both tympanic bullae (Figure 2B). Moreover, on the left side, a structure resembling the innermost part of the external ear canal in shape and location was detected. There was no cavitation. T2-weighted images showed bilaterally a normally shaped, hyperintense signal of the endolymphatic and perilymphatic fluids contained in the inner ear.

Brainstem auditory evoked responses (BAERs) were examined. The signal was amplified 200 000 times, filtered with a bandwidth of 160 to 2000 Hz, and averaged 500 times. Automatic artifact rejection was used with an analysis time of 10 ms. The recording montage was vertex (noninverting input of the amplifier) and ipsilateral mastoid (inverting input). Ground electrode was inserted at the base of the neck. Recording and ground electrodes were stainless steel needles. Acoustic and bone stimuli, produced by electrical square waves of 0.1 ms with a delivery rate of 10/s, were used. Acoustic stimuli were alternating clicks of 95 dB normal hearing level (NHL) delivered monaurally using an audiometric earphone. Bone stimulation was performed with a specific transducer applied to the ipsilateral mastoid bone at a stimulus intensity of 95 dB NHL. For each ear and type of stimulation, 2 tracings were obtained and superimposed to show reproducibility of the responses. The BAERs confirmed the impaired auditory capacity with no evidence of acoustic or bone stimulation at high intensities in ear.

Three months after hospitalization the calf was euthanized because of a severe pneumonia not apparently related to the primary disease.

The calf was subsequently submitted for necropsy. Macroscopically, the left pinna was hypoplastic and the opening of the external

ear canal closed by haircoat while the right pinna was absent and no anatomical remains were found. After decalcification on formalin fixed tissue, macroscopic examination was performed on cut surface having cochlea and semicircular canals aligned. On transversal cut surface, it was completely occupied by chondroid tissue. No abnormalities were detected in the inner ears and brain. Due to the absence of cerebrospinal fluid pressure after detachment of the head, the pontine meningocele observed on the right side by MRI was not detected. Additional findings were severe bronchopneumonia, complete ectopia of the spiral loop of the ascending colon, and numerous nonperforated abomasal ulcers.

Both the ear regions and brain were collected for histopathology. They were fixed in 10% neutral buffered formalin and 5 μm paraffin embedded sections were routinely stained with hematoxylin and eosin (H&E). Formalin-fixed paraffin-embedded 5 μm transverse sections of the brain were stained with H&E and Luxol-fast blue-periodic acid-Schiff methods. Histological abnormalities were not observed in both brain tissue and inner ears. The clinical and pathological findings resembled a form of HFM.

Several inbreeding loops between the unaffected parents were found in the pedigree of the calf. In light of this obvious consanguinity, the presented case of bovine HFM was hypothesized to be a rare recessively inherited variant. Therefore, WGS using the Illumina NovaSeq6000 was performed on DNA extracted from EDTA-blood of the HFM-affected calf, its dam, and from semen of its sire. The sequenced reads were mapped to the ARS-UCD1.2¹⁸ reference genome resulting in an average read depth of approximately $18.1\times$ in the calf, $17.9\times$ in the dam, and $19.2\times$ in the sire and subsequently single-nucleotide variants and small indel variants were called. The applied software and steps to process fastq-files into binary alignment map and genomic variant call format files were in accordance with the

TABLE 1 Results of variant filtering of the HFM-affected calf using the whole-genome sequence data of both parents and 4706 control genomes

Filtering step	Homozygous variants	Heterozygous variants
All variants in the affected calf	3 896 484	4 757 749
Private variants in the affected calf	104 207	1423
Private variants in the affected calf with obligatory carrier parents (protein-changing)	99 443 (245)	NA
Protein-changing private variants with obligatory carrier parents (recessive inheritance)	5	NA
Protein-changing private variants absent in both parents (de novo mutations)	NA	0

Abbreviations: HFM, hemifacial microsomia; NA, not applicable.

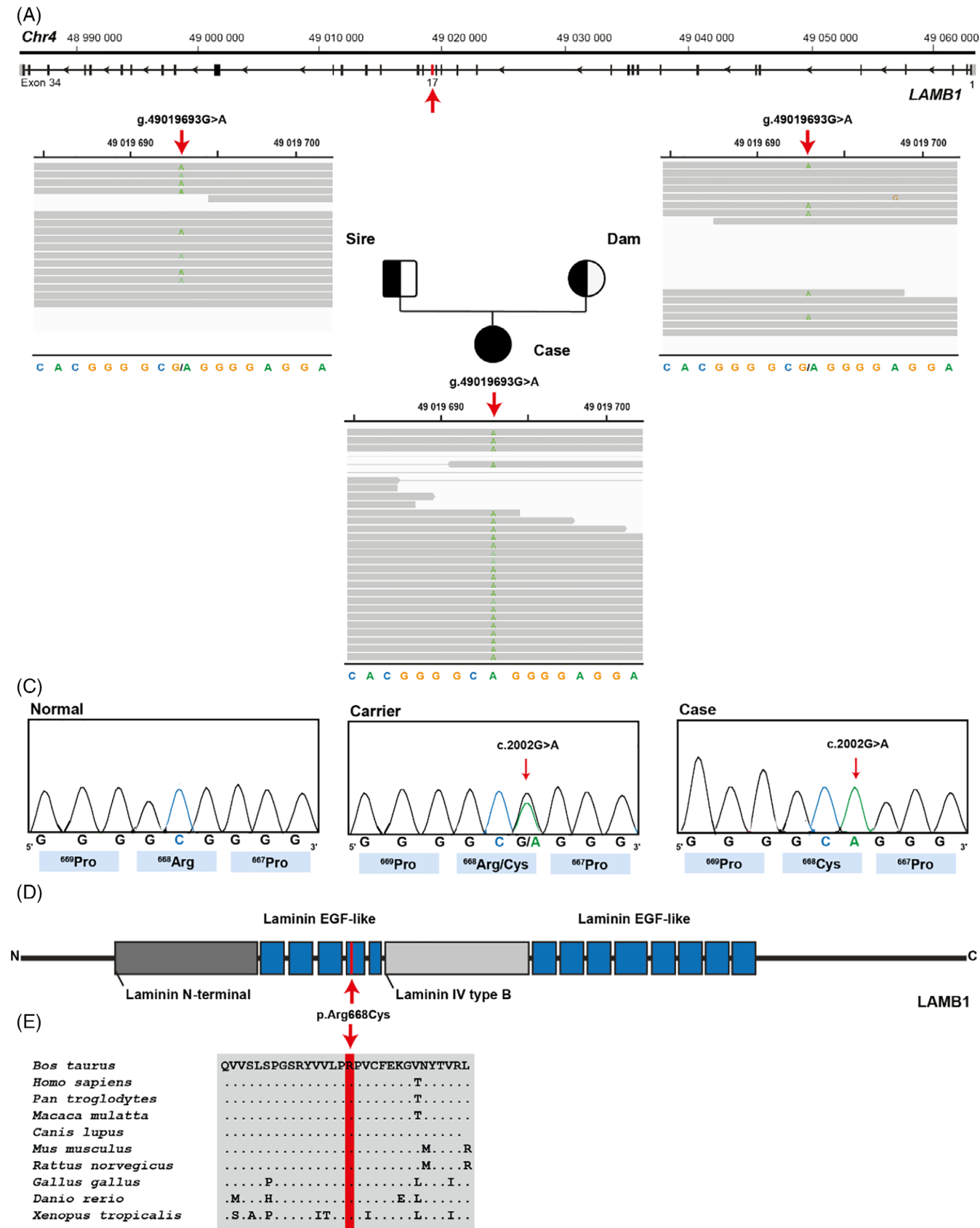


FIGURE 3 Legend on next page.

TABLE 2 Pathogenicity prediction results for the 5 homozygous protein-changing variants exclusively present in the genome of the affected calf and absent in the global control cohort of more than 4700 genomes of a variety of breeds

Gene	OMIM	Associated disorder/gene function	Protein change	Predicted effect	Provean impact and score
<i>LAMB1</i>	150240	Lissencephaly 5	p.Arg668Cys	Deleterious	-4.544
<i>PDCD7</i>	608138	Ceramide-mediated signaling	p.Pro28Leu	Neutral	-1.677
<i>CLMN</i>	611121	Specifically expressed at the final stage of spermatogenesis	p.Lys988Arg	Neutral	-0.310
<i>MEX3C</i>	611005	Phosphoproteins that bound RNA	p.Ala12Pro	Neutral	-0.087
<i>DCC</i>	120470	Colorectal cancer; esophageal carcinoma; Gaze palsy, familial horizontal, with progressive scoliosis, 2	p.Cys36Arg	Neutral	1.322

TABLE 3 Association of the p.Arg668Cys missense variant in *LAMB1* with the hemifacial macrosomia (HFM) phenotype in Romagnola cattle

	Genotype (R = Arg; C = Cys)		
	RR	RC	CC
HFM affected calf	0	0	1
Obligate carriers ^a	NA	2	0
Normal Romagnola control bulls	216	5	0
Normal control cattle from various breeds	4706	0	0

Abbreviation: NA, not applicable.

^aParents of the affected animal.

1000 Bull Genomes Project processing guidelines of run 7 (www.1000bullgenomes.com),¹⁹ except for the trimming, which was performed using fastp.²⁰ Further preparation of the genomic data was done as reported earlier.²¹ In order to find private variants, the genotype of the affected calf was compared with 4706 controls, including 596 cattle genomes of various breeds that had been sequenced in the course of other ongoing studies at the Institute of Genetics of the University of Bern (Table S1) as well as 4110 genomes of a variety of breeds included in run 8 of the 1000 Bull Genomes Project.¹⁸ The generated sequence data are publicly available in the European Nucleotide Archive (SAMEA7015114 is the sample accession number of the affected calf; SAMEA7690202 is the sample accession number of the dam and SAMEA7690203 of the sire; <http://www.ebi.ac.uk/en>).

Integrative Genomics Viewer (IGV)²² software version 2.0 was used for visual inspection of genome regions containing candidate variants. Assuming recessive inheritance in a trio-based approach, filtering of WGS data for homozygous coding variants present in the calf and heterozygous in the parental genomes identified 99 443 variants of which 245 were protein-changing with a predicted high or moderate impact (Table 1). These 245 variants were further investigated for their occurrence in a global control cohort of 4706 genomes of a variety of breeds, which revealed 5 remaining protein-changing variants that were exclusively homozygous in the genome of the affected calf and heterozygous in its parents (Tables 1 and S2).

Among these 5 remaining private variants, 1 single variant affects an interesting candidate gene for the observed phenotype (Figure 3A; Table 2). This homozygous variant at chr4:49019693G>A represents a missense variant in *LAMB1* (NM_001206519.1: c.2002C>T; Figure 3B,C). It alters the encoded amino acid of *LAMB1* residue 668 (NP_001193448.1:p.Arg668Cys) located in the laminin epidermal growth factor (EGF)-like 4 domain (Figure 3D). Furthermore, the arginine to cysteine substitution affects an evolutionary conserved amino acid (Figure 3E) and was predicted to be deleterious²³ (Table 2). To confirm and evaluate the presence of the *LAMB1* variant, the affected genomic region was amplified by PCR and Sanger sequenced in the calf, its dam and sire. Additionally, DNA was extracted from EDTA-blood of 221 Romagnola bulls and genotyping of the *LAMB1* variant was performed. The *LAMB1* missense variant was genotyped using the following primers: 5'- GTAGATGCACGTTGTCTGCC -3' (forward primer) and 5'- AGCCAAAACCAGACAGACTA -3' (reverse primer). Analyzing the sequencing data, it was confirmed that the calf was

FIGURE 3 A homozygous *LAMB1* missense variant in the HFM-affected Romagnola calf. (A) *LAMB1* gene structure showing the variant location on chromosome 4, exon 17 (red arrow). References to the bovine *LAMB1* gene correspond to the NCBI accessions NC_037331.1 (chromosome 4, ARS-UCD1.2), NM_001206519.1 (bovine *LAMB1* mRNA). (B) IGV screenshot presenting the Chr4: g. 49019693G>A variant homozygous in the affected calf (shown below) and heterozygous in both parents (top left: sire; top right: dam) revealed by whole-genome sequencing. (C) Electropherograms showing the normal, carrier, and case genotypes obtained by Sanger sequencing. (D) Schematic representation of the bovine *LAMB1* protein and its functional domains obtained from the UniProt database (<http://www.uniprot.org/>; accession number: A0A3S5ZPX3). Laminin N-terminal domain is represented in dark gray; laminin epidermal growth factor (EGF)-like domains are represented in blue; laminin IV type B domain is represented in light gray. (E) Multiple sequence alignment of the laminin EGF-like of *LAMB1* protein encompassing the region of the p.Arg668Cys variant demonstrates complete evolutionary conservation across species. Protein sequences accession numbers in NCBI for each species are NP_001193448.1 (*Bos taurus*), NP_002282.2 (*Homo sapiens*), XP_001165667.2 (*Pan troglodytes*), XP_001090393.2 (*Macaca mulatta*), XP_533089.4 (*Canis lupus*), NP_032508.2 (*Mus musculus*), XP_003750185.1 (*Rattus norvegicus*), XP_415943.3 (*Gallus gallus*), XP_002933140.2 (*Xenopus tropicalis*), NP_775382.1 (*Danio rerio*). HFM, hemifacial macrosomia; IGV, Integrative Genomics Viewer

homozygous and the sire and dam heterozygous for the detected *LAMB1* variant. Furthermore, the genotyping of the 221 Romagnola bulls revealed no homozygous mutant animal and a total of 5 heterozygous carriers (1.13%; Table 3).

Variant filtering revealed no private heterozygous protein-changing variants present in the genome of the HFM-affected calf and absent in both parental genomes and in 4706 controls.

3 | DISCUSSION

In this study, a comprehensive clinical, pathologic, and genetic investigation of a deaf Romagnola calf displaying a form of congenital microtia associated with craniofacial anomalies revealed a putative genetic cause for the abnormality. In humans, 50% of microtia cases are associated with ancillary findings, mostly craniofacial anomalies.^{24,25} Hemifacial microsomia is 1 of the major microtia-related diagnoses in human medicine with an incidence of 1:5600 live births²⁶ and is estimated as the most common birth defect of the human face, after cleft lip and cleft palate. Features of HFM include unilaterally as well as bilaterally deformity of the external ear and small ipsilateral half of the face with epibulbar dermoid and vertebral anomalies (OMIM 164210), leading to asymmetrical appearance.²⁷ Due to a marked phenotypic diversification, no typical clinical picture can be assigned to HFM: it might present from minor asymmetry with deformed auricle or microtia, until complete anotia, with conductive type hearing loss.²⁴

A genetic origin was evaluated assuming either a recessively inherited mutation or alternatively the hypothesis of a dominant acting *de novo* mutation (which occurred in a single parental gamete or happened during early embryonic development of the calf) as the possible cause for this novel congenital phenotype. The trio-based WGS approach identified 5 homozygous and no heterozygous protein-changing variants exclusively present in the genome of the affected calf and absent in a global control cohort. Consequently, a *de novo* mutation as a possible cause for the observed phenotype seems unlikely. After *in silico* effect predictions just the homozygous variant affecting the fourth laminin EGF-like domain of *LAMB1* was predicted to be deleterious. Moreover, within a representative control cohort of the current Italian Romagnola population, a very low allele frequency and the absence of the homozygous genotype for the deleterious allele was noticed. Considering the rarity of this coding variant, the *in silico* effect prediction and the known function of *LAMB1* gene, the identified variant was considered to represent the most likely genetic cause for the observed phenotype. Furthermore, it might be assumed that this pathogenic variant affecting a functional candidate gene is the most plausible explanation.

The candidate gene *LAMB1* encodes laminin subunit beta 1 belonging to laminins that are large molecular weight glycoproteins found in the basal lamina, playing an important role in cell proliferation, differentiation, migration, and adhesion.²⁸ They are cross-shaped heterotrimeric proteins constituted by the assembly of 3 disulfide-linked polypeptides, the α , β , and γ chains from the *LAMA*, *LAMB*, and *LAMC* families, respectively.²⁹ Each individual laminin subunit demonstrates a

specific spatial and temporal expression pattern.³⁰ In mammals, there are at least 15 laminins, and *LAMB1* is present in 6 of them.³¹ Moreover, *LAMB1* is 1 of the earliest laminin subunits expressed during embryogenesis at several sites, including neuroectoderm.^{29,32} The calf in this study had several malformations deriving from neuroectoderm such as the pontine meningocele and malformations of the auricle, middle ear, and temporomandibular region. Hemifacial microsomia affects most structures of the craniofacial region that derive from the first and second brachial arches (BAs). Arising from the neuroectoderm, neural crest cells (NCCs) follow stereotypical migratory pathways and populate the BAs, and cranial NCCs (CNCCs) form the first and second BAs, which contribute to most craniofacial skeleton and connective tissues.³³ Cranial neural crest cells in the first BA form the maxilla, zygomatic bone, mandible, malleus, incus, and trigeminal nerve, which might be affected in HFM. Cranial neural crest cells of the second BA form the stapes and facial nerve.³⁴ Therefore the described phenotype displayed by the calf in this study, including microtia of the left ear and anotia of the right ear, absence of tympanic bullae, deafness and asymmetry of the temporal bones and the temporomandibular joints, strongly resembles human HFM. In veterinary medicine, so far, rare forms of HFM are reported only in cats.³⁵

Mutations in the *LAMB1* gene have been identified and studied at a molecular level in humans (OMIM 150240) and mice (MGI 96743). Pathogenic variants affecting the human *LAMB1* are associated with autosomal recessive diseases such as: cobblestone brain malformation with congenital hydrocephalus, severe developmental delay, and an increased head circumference³⁶; progressive leukoencephalopathy with seizures, ocular abnormalities, and porencephalic lesions³⁷; childhood-onset epilepsy, macrocephaly, and intellectual development arrest³⁸; and adult-onset leukoencephalopathy.³⁹ In mice, heterozygous dominant acting variants in *lamb1* are associated with dystonia-like movement disorder with brain and spinal neuronal defects,⁴⁰ while recessively inherited pathogenic variants are related with embryonic lethality between implantation and somite formation.⁴¹ The calf presented in this study had malformation of the skull; however, no signs of leukoencephalopathy, cobblestone brain malformation, or dystonia were noticed.

This is a report of a pathogenic *LAMB1* variant in domestic animals and of the *LAMB1*-related recessively inherited form of HFM. Therefore, it represents an animal model for the understanding of similar human conditions and adds *LAMB1* to the list of candidate genes for HFM. Humans show developmental, anatomical, and physiological features of the auditory system that are more similar with cattle than with mice. Among these, the fact that compared to mice, cattle and humans can hear at birth. The cattle model thus fits better than the mouse model for understanding human hearing diseases.

In conclusion, this study provides a DNA-based diagnostic test that enables selection against the identified pathogenic variant in Romagnola cattle.

ACKNOWLEDGMENT

This research was partially funded by Swiss National Science foundation, grant number 172911. The authors acknowledge the Interfaculty

Bioinformatics Unit of the University of Bern for providing computational infrastructure. The WGS data are available under the study accession no. PRJEB18113 at the European Nucleotide Archive (www.ebi.ac.uk/ena; sample accessions SAMEA7015114 [affected calf], SAMEA7690202 [dam], and SAMEA7690203 [sire]). We thank Nathalie Besuchet-Schmutz for expert technical assistance. [Correction added on 16 Dec 2021, after the first online publication: Acknowledgement section has been updated]

CONFLICT OF INTEREST DECLARATION

Authors declare no conflicts of interest.

OFF-LABEL ANTIMICROBIAL DECLARATION

Authors declare no off-label use of antimicrobials.

INSTITUTIONAL ANIMAL CARE AND USE COMMITTEE (IACUC) OR OTHER APPROVAL DECLARATION

Authors declare no IACUC or other approval was needed.

HUMAN ETHICS APPROVAL DECLARATION

Authors declare human ethics approval was not needed for this study.

ORCID

Joana G. P. Jacinto  <https://orcid.org/0000-0002-6438-7975>

Marco Bernardini  <https://orcid.org/0000-0002-8572-0271>

Maria Teresa Mandara  <https://orcid.org/0000-0003-1501-6163>

Marilena Bolcato  <https://orcid.org/0000-0002-0605-3344>

Arcangelo Gentile  <https://orcid.org/0000-0002-6091-8978>

Cord Drögemüller  <https://orcid.org/0000-0001-9773-522X>

REFERENCES

- Suutarla S, Rautio J, Ritvanen A, Ala-Mello S, Jero J, Klockars T. Microtia in Finland: comparison of characteristics in different populations. *Int J Pediatr Otorhinolaryngol*. 2007;71(8):1211-1217.
- Luquetti DV, Heike CL, Hing AV, Cunningham ML, Cox TC. Microtia: epidemiology and genetics. *Am J Med Genet A*. 2012;158A(1):124-139.
- Mastroiacovo P, Corchia C, Botto LD, Lanni R, Zampino G, Fusco D. Epidemiology and genetics of microtia-antia: a registry based study on over one million births. *J Med Genet*. 1995;32(6):453-457.
- Qiao R, He Y, Pan B, et al. Understanding the molecular mechanisms of human microtia via a pig model of HOXA1 syndrome. *Dis Model Mech*. 2015;8(6):611-622.
- Tischfield MA, Bosley TM, Salih MAM, et al. Homozygous HOXA1 mutations disrupt human brainstem, inner ear, cardiovascular and cognitive development. *Nat Genet*. 2005;37(10):1035-1037.
- Alasti F, Sadeghi A, Sanati MH, et al. A mutation in HOXA2 is responsible for autosomal-recessive microtia in an Iranian family. *Am J Hum Genet*. 2008;82(4):982-991.
- Brown KK, Viana LM, Helwig CC, et al. HOXA2 haploinsufficiency in dominant bilateral microtia and hearing loss. *Hum Mutat*. 2013;34(10):1347-1351.
- Bicknell LS, Bongers EMHF, Leitch A, et al. Mutations in the pre-replication complex cause Meier-Gorlin syndrome. *Nat Genet*. 2011;43(4):356-360.
- Guernsey DL, Matsuoka M, Jiang H, et al. Mutations in origin recognition complex gene ORC4 cause Meier-Gorlin syndrome. *Nat Genet*. 2011;43(4):360-365.
- Fenwick AL, Kliszczak M, Cooper F, et al. Mutations in CDC45, encoding an essential component of the pre-initiation complex, cause Meier-Gorlin syndrome and craniosynostosis. *Am J Hum Genet*. 2016;99(1):125-138.
- Vetro A, Savasta S, Russo Raucchi A, et al. MCM5: a new actor in the link between DNA replication and Meier-Gorlin syndrome. *Eur J Hum Genet*. 2017;25(5):646-650.
- Edwards SJ, Gladwin AJ, Dixon MJ. The mutational spectrum in Treacher Collins syndrome reveals a predominance of mutations that create a premature-termination codon. *Am J Hum Genet*. 1997;60(3):515-524.
- Schaefer E, Collet C, Genevieve D, et al. Autosomal recessive POLR1D mutation with decrease of TCOF1 mRNA is responsible for Treacher Collins syndrome. *Genet Med*. 2014;16(9):720-724.
- Sanchez E, Laplace-Builhé B, Mau-Them FT, et al. POLR1B and neural crest cell anomalies in Treacher Collins syndrome type 4. *Genet Med*. 2020;22(3):547-556.
- Tekin M, Öztürkmen Akay H, Fitoz S, et al. Homozygous FGF3 mutations result in congenital deafness with inner ear agenesis, microtia, and microdontia. *Clin Genet*. 2008;73(6):554-565.
- He S, Zhang Z, Sun Y, et al. Genome-wide association study shows that microtia in Altay sheep is caused by a 76 bp duplication of HMX1. *Anim Genet*. 2020;51(1):132-136.
- Koch CT, Bruggmann R, Tetens J, Drögemüller C. A non-coding genomic duplication at the HMX1 locus is associated with crop ears in highland cattle. *PLoS One*. 2013;8(10):e77841.
- Rosen BD, Bickhart DM, Schnabel RD, et al. De novo assembly of the cattle reference genome with single-molecule sequencing. *Gigascience*. 2020;9(3):1-9.
- Hayes BJ, Daetwyler HD. 1000 bull genomes project to map simple and complex genetic traits in cattle: applications and outcomes. *Annu Rev Anim Biosci*. 2019;7:89-102.
- Chen S, Zhou Y, Chen Y, Gu J. Fastp: an ultra-fast all-in-one FASTQ preprocessor. *Bioinformatics*. 2018;34(17):i884-i890.
- Häfliger IM, Wiedemar N, Švara T, et al. Identification of small and large genomic candidate variants in bovine pulmonary hypoplasia and anasarca syndrome. *Anim Genet*. 2020;51(3):382-390.
- Robinson JT, Thorvaldsdóttir H, Wenger AM, Zehir A, Mesirov JP. Variant review with the integrative genomics viewer. *Cancer Res*. 2017;77(21):e31-e34.
- Choi Y, Chan AP. PROVEAN web server: a tool to predict the functional effect of amino acid substitutions and indels. *Bioinformatics*. 2015;31(16):2745-2747.
- Paul MA, Opyrchał J, Knakiewicz M, Jaremków P, Bajtek J, Chrapusta A. Hemifacial microsomia review: recent advancements in understanding the disease. *J Craniofac Surg*. 2020;31(8):2123-2127.
- Hartzell LD, Chinnadurai S. Microtia and related facial anomalies. *Clin Perinatol*. 2018;45(4):679-697.
- Wolford LM, Perez DE. Surgical management of congenital deformities with temporomandibular joint malformation. *Oral Maxillofac Surg Clin North Am*. 2015;27(1):137-154.
- Gougoutas AJ, Singh DJ, Low DW, Bartlett SP. Hemifacial microsomia: clinical features and pictographic representations of the OMENS classification system. *Plast Reconstr Surg*. 2007;120(7):112e-113e.
- Lee J, Gross JM. Laminin beta1 and gamma1 containing laminins are essential for basement membrane integrity in the zebrafish eye. *Invest Ophthalmol Vis Sci*. 2007;48(6):2483-2490.
- Roediger M, Miosge N, Gersdorff N. Tissue distribution of the laminin $\beta 1$ and $\beta 2$ chain during embryonic and fetal human development. *J Mol Histol*. 2010;41(2-3):177-184.
- Sharif KA, Li C, Gudas LJ. cis-acting DNA regulatory elements, including the retinoic acid response element, are required for tissue specific

- laminin B1 promoter/lacZ expression in transgenic mice. *Mech Dev.* 2001;103(1-2):13-25.
31. Sharif KA, Baker H, Gudas LJ. Differential regulation of laminin b1 transgene expression in the neonatal and adult mouse brain. *Neuroscience.* 2004;126(4):967-978.
 32. Baldarelli RM, Smith CM, Finger JH, et al. The mouse Gene Expression Database (GXD): 2021 update. *Nucleic Acids Res.* 2021;49(D1):D924-D931.
 33. Minoux M, Rijli FM. Molecular mechanisms of cranial neural crest cell migration and patterning in craniofacial development. *Development.* 2010;137(16):2605-2621.
 34. Johnson JM, Moonis G, Green GE, Carmody R, Burbank HN. Syndromes of the first and second branchial arches, part 1: embryology and characteristic defects. *AJNR Am J Neuroradiol.* 2011;32(1):14-19.
 35. Song RB, Kent M, Glass EN, Davis GJ, Castro FA, de Lahunta A. Hemifacial microsomia in a cat. *Anat Histol Embryol.* 2017;46(5):497-501.
 36. Radmanesh F, Caglayan AO, Silhavy JL, et al. Mutations in LAMB1 cause cobblestone brain malformation without muscular or ocular abnormalities. *Am J Hum Genet.* 2013;92(3):468-474.
 37. Tonduti D, Dorboz I, Renaldo F, et al. Cystic leukoencephalopathy with cortical dysplasia related to LAMB1 mutations. *Neurology.* 2015; 84(21):2195-2197.
 38. Okazaki T, Saito Y, Hayashida T, et al. Bilateral cerebellar cysts and cerebral white matter lesions with cortical dysgenesis: expanding the phenotype of LAMB1 gene mutations. *Clin Genet.* 2018;94:391-392.
 39. Yasuda R, Yoshida T, Mizuta I, et al. Adult-onset leukoencephalopathy with homozygous LAMB1 missense mutation. *Neurol Genet.* 2020; 6(4):4-7.
 40. Liu YB, Tewari A, Salameh J, et al. A dystonia-like movement disorder with brain and spinal neuronal defects is caused by mutation of the mouse laminin β 1 subunit, Lamb1. *Elife.* 2015;4:e11102.
 41. Miner JH, Li C, Mudd JL, Go G, Sutherland AE. Compositional and structural requirements for laminin and basement membranes during mouse embryo implantation and gastrulation. *Development.* 2004; 131(10):2247-2256.

SUPPORTING INFORMATION

Additional supporting information may be found in the online version of the article at the publisher's website.

How to cite this article: Jacinto JGP, Häfliger IM, Bernardini M, et al. A homozygous missense variant in laminin subunit beta 1 as candidate causal mutation of hemifacial microsomia in Romagnola cattle. *J Vet Intern Med.* 2022;36(1): 292-299. doi:10.1111/jvim.16316

4.2 Results of the estimation of the frequency of deleterious alleles

The results of the frequency estimation of deleterious alleles and carrier frequencies for the investigated disorders in the respective breed populations are presented in **Table 3**.

Table 3: Estimation of the deleterious alleles and carrier frequencies.

Disorder	Gene	Variant	Breed	AF	CF
Pseudomyotonia congenita	<i>ATP2A1</i> exon 6	Missense g.25940510C>T c.491G>A p.R164H	Chianina	6%	12%
			Marchigiana	9.1%	18.2%
			Romagnola	1.1%	2.1%
	<i>ATP2A1</i> exon 8	Missense (compound heterozygous): g.25939141C>A c.857G>T p.G286V + g.25939366C>A c.632G>T p.G211V	Romagnola	3.4%	6.8%
Paunch Calf Syndrome	<i>KDM2B</i>	Missense g.53761149G>A c.2503G>A p.D835N	Marchigiana	2%	3.9%
			Romagnola	12%	24%
Hemifacial microsomia	<i>LAMB1</i>	Missense g.49019693G>A c.2002C>T p.R668C	Romagnola	3.1%	6.1%
Congenital Bilateral Cataract	<i>NID1</i>	855 bp deletion c.3579_3604+829del	Romagnola	1.6%	3.2%
Ichthyosis Congenita	<i>FA2H</i>	2 bp insertion g.2205625_2205626insG c.9dupC p.A4Rfs*142	Chianina	5.1%	10.1%
Ichthyosis Fetalis	<i>ABCA12</i>	Missense g.103025585T>C c.5804A>G p.H1935R	Chianina	1.4%	2.8%
Achromatopsia	<i>CNGB3</i>	Missense g.76011964G>A	Braunvieh	8.2%	16.4%

		c.751G>A p.D251N			
Hypotrichosis	<i>KRT71</i>	7bp deletion g.27331221_27331228d el c.281_288del p.M94Nfs*14	Hereford	2.2%	4.4%
	<i>HEPHL1</i>	Nonsense g.721234T>A c.1684A>T p.K562*	Belted- Galloway	5.7%	11.4%

AF = allelic frequency; CF= carrier frequency

4.3 Contribution of the Biobank for Genetic Disorders

Around 16.000 samples were deposited in the Biobank for Genetic Disorder. They correspond to the clinical cases shown in **Table 1** and their available relatives, and the controls indicated in **Table 2**.

5 Discussion and Perspectives

The current study was based on clinical cases of genetic disorders deriving from the past or current caseload available as well as presented or submitted to the Clinic for Ruminants of DIMEVET and to the IGVFB. The study allowed a comprehensive clinical and/or pathological characterization of the cases. A wide spectrum of phenotypes affecting different organ systems such as skeletal, neuromuscular, metabolic, integumentary, eyes and ears were investigated and identified causative variants and associated genes varied greatly. The application of the FGA led to the identification of candidate variants for seven recessive and seven *de novo* dominant disorders in different breeds.

Unfortunately, FGA was not such far conclusive for the identification of a definitive causing variant in a form of Generalized Juvenile Angiomatosis in a Simmental calf. Assuming a spontaneous *de novo* mutation event, four variants, respectively in the *PREX1*, *UBE3B*, *PCDHGA2*, and *ZSWIM6* genes, were identified, and one of them may represent a possible candidate pathogenic variant for this rare form of vascular malformation.

While SNV can cause lethal phenotypes, it is even more understandable that larger structural variants (insertions and deletions) might cause severe phenotypes.

In regard to the recessive disorders, the research output included routine DNA-based diagnostic tests for six recessive disorders allowing the selection against the identified pathogenic variants in the international population of the affected breeds (e.g. targeted genotyping and avoidance of high-risk matings of carrier animals) and adds a complete clinicopathological characterization of a case of congenital *APOB*-associated cholesterol deficiency in a Holstein calf to the literature. When routine screenings are not performed, recessive deleterious variants can quickly spread through a population by widespread use of popular carrier AI sires [47]. This fact highlights that the systematic genotyping, principally in AI sires, whenever enforceable, is of paramount importance to control deleterious alleles in cattle populations. In this way, the identified causal recessive could be considered within the breeding program of the respective breeds. Across the forthcoming generations, the allelic frequency of the presented recessive deleterious variants could be reduced or even better eliminated, contributing to improved animal welfare and prevention of economic losses and finally to overall improvement of the breed.

In regard to dominant disorders, the research output included the identification of novel causal variants for previously reported as well as new phenotype-genotype correlations. Moreover, the examples presented, highlight that spontaneous *de novo* mutations might be more common than perceived.

The quite elevated number of clinical cases experienced during the study period supports the growing concerns of the associations of bovine breeders on the increasing frequency of genetic diseases. However, it is my personal conviction that the number of genetic defects brought to the attention of the scientific world does not represent their real occurrence in the population. This is due to different reasons:

- a) low value of calves (especially male of dairy breeds) that prevent them to receive attention or consultation by a veterinarian;
- b) misdiagnosis by the veterinarian, mostly due to lack of experience, lack of specific symptoms or the lack of diagnostic tools in the field;
- c) difficulties in seeking assistance to local diagnostic centers;
- d) cost of transporting sick animals to diagnostic centers.

An additional factor is the tendency of some breeders not to report, or even to hide, pathologies suspected of being of genetic origin that might penalize their professional reputation. In the case of congenital malformations, some farmers might also be concerned of being singled out as disseminators of strange diseases and even monstrosities.

The inability to recognize the presence of genetic defects at an early stage of dissemination in the population compromises the adoption of plans to control or eliminate the carriers and the propagators of the pathogenic variants, thus favoring an exponential increase in the population. Thus, it is crucial to encourage farmers, breeding associations and veterinary practitioners to regularly refer and submit potential cases of genetic disorders to reference centers for investigation. This was achieved during this study program thus creating a successful caseload.

Interestingly, in some cases the clinical and/or pathological investigations showed similar genotype-phenotype correlations between affected cattle and human patients with causal recessive and dominant pathogenic variants affecting the same genes (e.g. for Achondrogenesis type II and *COL2A1*; Osteogenesis imperfecta and *COL1A1*; Congenital cholesterol deficiency and *APOB*; Classical Ehlers-Danlos syndrome and *COL5A2*; Epidermolysis bullosa simplex and *KRT5*; Hypotrichosis and *KRT71*;

Achromatopsia and *CNGB3*). This confirms that cattle might represent useful model for comparative studies. Furthermore, clinical and/or pathological investigations also revealed novel phenotype-genotype correlations in affected cattle not previously being reported in human patients with causal recessive and dominant pathogenic variants affecting novel genes (e.g., for Skeletal-cardio-enteric dysplasia and *MAP2K2*; Congenital neuromuscular channelopathy and *KCNQ1*; Ichthyosis congenita and *FA2H*; Hypotrichosis and *HEPHL1*; Hemifacial microsomia and *LAMB1*). In particular, it is worth to highlight the discovery of a most likely pathogenic variant in *KCNQ1* causing a syndromic form of a Congenital neuromuscular channelopathy in a Belgian Blue x Holstein crossbred calf; thus, representing the first disorder associated with the *KCNQ1* gene.

In human medicine, it is often difficult to identify genetic causes of rare diseases due the limited number of patients. Therefore, novel phenotype-genotype correlations might help as a model for human genetics to identify the cause of disorders in human patients showing similar phenotypes. Livestock animals are predestined as model organisms due to the breeding management system. The intensive use of few AI sires implies the risk of the spread of a disorder-causing variant, which can also be (hopefully) quite quickly detected in a larger cohort [48]. In addition, cattle are particularly interesting, as the use of genomic information is widespread, pedigree information is recorded attentively, and farmers are (hopefully) encouraged to regularly report any anomalies in newborn animals. Especially with the use of WGS in single cases affected by *de novo* mutations, novel genetic correlations and findings important for human health can be detected [48].

Furthermore, the identification of pathogenic variants also highlights the utility of precision diagnostics including genomics, for understanding rare disorders and the value of surveillance of cattle breeding populations for harmful genetic disorders.

In regard to the study of the estimation of the frequency of deleterious alleles the results create awareness to the breeders, breeding associations and veterinarians. It is important that the carrier frequency for the Paunch calf syndrome *KDM2B*-related in Romagnola (lethal phenotype) was considerable high (24%) even with the inclusion of this condition in the breeding programs. An often-mentioned reason why deleterious alleles keep segregating at a considerable allele frequency is balancing selection [49, 50]. Thereby the disease-associated variant has a desirable effect on production traits and is therefore under positive selection. Within the presented research, production traits such as milk yield or

contents were not investigated. Therefore, balancing selection might play a role in the more frequently occurring disorder-causing alleles.

In regard to the enrichment of the Biobank for Genetic Disorders, the storage of samples together with phenotypical data represent a large-scale biomedical database and research resource for cattle, containing in-depth genetic and phenotypical information. It is a major contributor to the advancement of precision medicine and enabled scientific discoveries presented in this thesis.

6 Appendix

Table A1: Genetic congenital skeletal disorders of cattle: brief description of the phenotype, the associated genes and types of variants.

Disorder	IM	Phenotype	Gene	OMIA	Type of variant	Breed(s)	Ref
Achondrogenesis type II	AD*, AD ⁺	Disproportionate growth retardation with fascial dysplasia and shortening of the vertebral column and the abaxial skeleton. Disrupted endochondral osteogenesis with disorganization of epiphyseal plate chondrocytes (chondrodysplasia).	<i>COL2A1</i>	001926-9913	SNV (splice site, missense), gross deletion	Holstein, crossbred	[48, 51–55]
Arachnomelia	ARL	Facial deformities (short lower jaw and concave rounding of the dorsal profile of the maxilla), long and thin legs (dolichostenomelia), marked bilateral hyperextension of fetlocks.	<i>MOCSI</i>	001541-9913	2bp deletion (frameshift)	Fleckvieh	[56, 57]
			<i>SUOX</i>	000059-9913	1bp insertion (frameshift)	Brown Swiss	[58]
Brachyspina	ARL	Extensive malformation of almost all vertebrae causing significant shortening of the spine, reduced body size and disproportion between legs and vertebral column, inferior brachygnatism, hypoplasia of abdominal organs, e.g. kidneys, gonads and intestine (atresia),	<i>FANCI</i>	000151-9913	gross deletion	Holstein	[59, 60]

		high rate of embryonic and foetal mortality, full term cases rare.					
Caprine-like generalized hypoplasia syndrome	AR	Low birth weight, muscular insufficiency and delayed development during the entire life, long and thin head ('deer head' or 'sheep head') and partial coat depigmentation in the red zones.	<i>CEP250</i>	<u>001502-9913</u>	SNV (nonsense)	Montbeliarde	[61]
Complex vertebral malformation (CVM)	AR	Reduced body size, symmetrical arthrogryposis, cervical and/or thoracic vertebral column malformations (misshapen and fused vertebrae), high rate of embryonic and fetal mortality, full term cases rare.	<i>SLC35A3</i>	<u>001340-9913</u>	SNV (missense)	Holstein	[62, 63]
Chondrodysplasia	AD	Brachygnathia superior, movement disabilities, severe skeletal shortening of long bones and joint hyperextension.	<i>FGFR3</i>	<u>001703-9913</u>	SNV (stop-lost)	Holstein	[64]
Crooked tail	AR	Crooked tail, short head, growth retardation, extreme muscularity and spastic paresis.	<i>MRC2</i>	<u>001452-9913</u>	2bp deletion (frameshift); SNV (missense)	Belgian Blue	[65, 66]
Developmental duplications	AR	Cranioschisis, myolipoma or teratoma, dermoid cysts and/or dermoid sinuses, exencephaly, vertebral dysraphism, Chiari malformations, cerebral dysmorphogenesis, diprosopus,	<i>NHLRC2</i>	<u>002103-9913</u>	SNV (missense)	Angus	[67]

		microphthalmia, cleft palate, polymelia, heteropagus conjoined twins, diastematomyelia, gastroschisis with intestinal eventration.					
Dwarfism - Bulldog calf	ARL	Extremely disproportionate dwarfism, short vertebral column, marked micromelia, large abdominal hernia, large head with retracted muzzle, cleft palate, and protruding tongue.	<i>ACAN</i>	<u>001271-9913</u>	4bp insertion (frameshift); 1bp insertion (frameshift); SNV (regulatory)	Dexter, Scottish Highland, Zebu	[68, 69]
Dwarfism	AR	Low birth weight and size, multiple craniofacial abnormalities (, brachygnathia inferior, narrow head, structural deformities of the muzzle), spinal distortions, wrinkled skin, disproportionately large head evident during rearing, poor growth.	<i>GON4L</i>	<u>001985-9913</u>	1bp deletion (frameshift)	Fleckvieh	[70]
		Reduced endochondral ossification of growth plates, protrusions of the alar wing of the basis phenoid bone into the cranial cavity, abnormalities of the ventral vertebral bodies and curvature of the vertebral processes, poor growth.	<i>PRKG2</i>	<u>001485-9913</u>	SNV (nonsense)	Angus	[71]
Dwarfism - proportionate with inflammatory lesions	AR	Proportionate growth retardation with onset of age 5–6 months (not observed at birth), normal muscular development, close forehead, long and thin neck,	<i>RNF11</i>	<u>001686-9913</u>	SNV (splice site)	Belgian Blue	[72]

		hairy, long and thin head; compromised disease resistance.					
Ellis-van Creveld Syndrome	AR	Reduced endochondral ossification of growth plates, abnormal cartilaginous matrix and epiphyseal growth plate, short limbs, joint abnormalities.	<i>EVC2</i>	<u>000187-9913</u>	2bp deletion (frameshift); SNV (splice site); 2bp deletion and 1bp insertion (frameshift)	Tyrolean Grey, Japanese Brown	[73, 74]
Hereditary perinatal weak calf syndrome	AR	Intrauterine growth retardation, neonatal weakness. Post-natal, embryonic or fetal death.	<i>IARS</i>	<u>001817-9913</u>	SNV (missense)	Japanese Black	[75]
Facial dysplasia syndrome	AD*	Stillbirth or post-natal death, facial dysplasia and complete prolapse of the eyes. Brain malformations (e.g. microencephaly, hydrocephalus).	<i>FGFR2</i>	<u>002090-9913</u>	SNV (missense)	Holstein	[76]
Frontonasal dysplasia	AD [†]	Stillbirth, craniofacial malformations with upwardly curved mandibles, cleft palate was evident, absence of eyes, optic nerve and orbital cavities, aprosencephaly short tail.	<i>ZIC2</i>	<u>002307-9913</u>	1bp deletion (frameshift)	Limousin	[77]
Marfan syndrome	AD*	Disproportionately long limbs and digits, joint laxity, cardiovascular defect (aortic and mitral valves), ocular disease (myopia and ectopia lentis).	<i>FBNI</i>	<u>000628-9913</u>	SNV (missense, splice site)	Limousin, Japanese Black	[78, 79]

Osteogenesis imperfecta type II	AD*,AD ⁺	Congenital. Stillbirth or post-natal death, bone and dental fragility, blue sclera, and evidence of in utero fractures.	<i>COL1A1</i>	<u>002127-9913</u>	4bp deletion + 1bp insertion (in-frame deletion + missense); SNV (missense)	Fleckvieh, Red Angus	[48, 80, 81]
Osteopetrosis	AR	Premature calves (10-30 days before expected date), multiple craniofacial abnormalities (e.g., brachygnathia inferior, impacted molars), long and fragile bones, marked reduction of osteoclasts. If the calf is born alive, death occurs within 24 hours after birth.	<i>SLC4A2</i>	<u>002443-9913</u>	3.8kb deletion	Red Angus	[82]
Lethal multi-organ developmental dysplasia (paunch calf syndrome)	ARL	Splanchnocranium malformation (enlarged, shortened and flattened head - bulldog-like), absence of medial dewclaws, ascites, hepatic fibrosis.	<i>KDM2B</i>	<u>001722-9913</u>	SNV (missense)	Romagnola, Marchigiana	[83, 84]
Mandibulofacial dysostosis	AR	Facial deformities due mandibulofacial dysostosis, short and/or asymmetric lower mandible and bilateral skin tags 2–10 cm caudal to the commissure of the lips.	<i>CYP26C1</i>	<u>002288-9913</u>	SNV (missense)	Hereford	[85]
Polled and multisystemic syndrome	AD*	Retarded growth, polledness, facial dysmorphism, chronic diarrhea,	<i>ZEB2</i>	<u>001736-9913</u>	gross deletion;	Charolais, Fleckvieh	[86, 87]

		premature ovarian failure, and variable neurological and cardiac anomalies.			11bp deletion (frameshift)		
Skeletal-cardio-enteric dysplasia	AD [†]	Stillbirth, reduced fetal growth, short-spine, long and narrow face, cardiac defects and heterotopy of spiral colon.	<i>MAP2K2</i>	<u>002381-9913</u>	SNV (missense)	Romagnola	[88]
Syndactyly (mule foot)	AR	Fusion of the functional digits.	<i>LRP4</i>	<u>000963-9913</u>	SNV (missense, splice site); 2bp deletion + insertion (2bp missense)	Simmental Charrolais cross, Simmental, Angus, Holstein	[89–91]
Tetradysmelia	ARL	Abortion or stillbirth, severe limb malformations of all limbs with absence of distal parts of the fore and hindlimbs, mandibular malformation, brachygnathia superior.	<i>RSPO2</i>	<u>002297-9913</u>	gross deletion (frameshift)	Holstein	[92]
Tibial hemimelia syndrome	ARL	Tibial hemimelia, preaxial polydactyly, malformation of pelvis, abdominal hernia, arthrogryposis multiplex, and syndromic acerebral macrocephaly.	<i>ALX4</i>	<u>001009-9913</u>	gross deletion; 20bp duplication (frameshift)	Shorthorn, Galloway	[93, 94]
Vertebral and spinal dysplasia	AD ^{&}	Vertebral (specifically tail) deformities and neurological syndrome with gait abnormalities of hindlimbs. Variable phenotype severity: from very mild (only tail deformities) to severe (paraparesis).	<i>T</i>	<u>001951-9913</u>	SNV (missense)	Holstein	[95]

IM = inheritance mode, **AD** = autosomal dominant, **AR** = autosomal recessive, **ARL**= autosomal recessive lethal, **OMIA** = Online mendelian inheritance in animals [10], **ref** = references, * = *de novo* in mosaic sire, + = *de novo* in the embryo, † = *de novo* in the germline of one parent or in the embryo, & = incomplete penetrance

Table A2: Genetic neuromuscular disorders of cattle: brief description of the phenotype, the associated genes and types of variants.

Disorder	IM	Phenotype	Gene	OMIA	Type of variant	Breed(s)	Ref
Arthrogryposis, distal type 1B	AD ⁺	Congenital. Difficult quadrupedale stance, tremor, ataxia, only backward movement with hypermetria in hindlimbs and tip-toe-standing of forelimbs, increase muscle tone in limbs, reduced spinal reflexes and sensibility in limbs.	<i>MYBPCI</i>	001978-9913	SNV (missense)	Holstein	[96]
Arthrogryposis (lethal syndrome)	AR	Congenital. Arthrogryposis of all limbs, severe scoliosis (curved spine), stocky head, macroglossy, impaired tooth eruption, cleft palate and upper lip, omphalocele (abdominal wall defect with umbilical hernia) and corneal clouding.	<i>PIGH</i>	001953-9913	SNV (splice site)	Belgian Blue	[97]
Arthrogryposis multiplex congenita	ARL	Congenital. Arthrogryposis or joint contracture of multiple joints, reduced body weight, severe torticollis and kypho-scoliosis, mild lordosis, joints with fibro-osseous ankyloses, palatoschisis, lateral deviation of viscerocranium, narrow thorax and	<i>CHRNBI</i>	002022-9913	1bp insertion (frameshift)	Red Danish	[98]
			<i>AGRN</i>	002135-9913	gross deletion	Angus	[99]

		abdomen, ribs with uneven course, generalized severe lipomatous muscular atrophy, multiple internal organ lesions due to narrowing of body cavities.					
Bovine Progressive Degenerative Myeloencephalopathy (Weaver syndrome)	AR	Onset from 6-8 months of age. Progressive bilateral hind leg weakness (paresis) and ataxia, resulting in weaving gait and recumbency. Degenerative changes in the white matter of spinal cord and degeneration of the Purkinje cells in cerebellum.	<i>PNPLA8</i>	<u>000827-9913</u>	SNV (missense)	Brown Swiss	[100–102]
Charcot Marie Tooth disease	AR	Congenital. Loss of coordination. Lesions of axonal degeneration, Schwann cell hyperplasia and demyelination.	<i>FGD4</i>	<u>002374-9913</u>	SNV (splice site)	Holstein, Jersey	[103]
Congenital hypomyelination	AR	Congenital. Inability to rise, and severe muscle tremor with periods of spasticity. Deficiency of myelin, especially in the cerebellum and brainstem (failure of formation of myelin, plus incomplete and delayed myelination of axons).	<i>KIF1C</i>	<u>000527-9913</u>	SNV (missense)	Charolais	[104]
Congenital myasthenic syndrome	AR	Onset from first months of age. Progressive muscular weakness. Weakness exacerbated by exercise and improve with rest.	<i>CHRNE</i>	<u>000685-9913</u>	20bp deletion (frameshift)	Brahman	[105]

Congenital muscular dystonia 1	AR	Variable onset (from birth to several months of age). Seizure episodes lasting from several minutes to more than one hour, occurrence and persistence of seizures influenced by environmental stressors (extreme cold temperature) or increased physical activity (processing at vaccination or weaning). During seizure episodes individuals typically lie on their side with all limbs extended in a rigid state.	<i>ATP2A1</i>	<u>001450-9913</u>	SNV (missense)	Belgian Blue	[106]
Congenital muscular dystonia 2	ARL	Congenital. Severe episodes of myoclonus upon acoustic or tactile stimulation. Death within a few hours of birth.	<i>LOC528050</i>	<u>001451-9913</u>	SNV (missense)	Belgian Blue	[106]
Congenital neuromuscular channelopathy	AD [†]	Congenital. Episodes of exercise-induced generalized myotonic muscle stiffness accompanied by increase in serum potassium, flattening of splanchnocranium with deviation.	<i>KCNGB1</i>	<u>002483-9913</u>	SNV (missense)	Crossbred (Belgian Blue x Holstein)	[107]
Congenital pseudomyotonia	AR	Congenital. Exercise-induced muscle contracture preventing animals from performing muscular activities.	<i>ATP2A1</i>	<u>001464-9913</u>	SNV (missense)	Chianina, Romagnola	[108, 109]
Congenital Myoclonus	AR	Congenital. Hyperesthesia and myoclonic jerks of skeletal musculature occurring both	<i>GLRA1</i>	<u>000689-9913</u>	SNV (nonsense)	Hereford	[110]

		spontaneously and in response to tactile, visual and auditory stimuli. Death within few days of birth.					
Contractural arachnodactyly (Fawn calf syndrome)	AR	Congenital. Proximal limb contracture, distal limb hyperextension, kyphosis. Findings decrease as calves' growth.	<i>ADAMTSL3</i>	<u>001511-9913</u>	gross deletion	Angus	[111]
Degenerative axonopathy	AR	Onset first weeks of age. Impaired coordination during movement beginning Axonal degeneration in the central nervous system and femoral nerve.	<i>MFN2</i>	<u>001106-9913</u>	SNV (splice site)	Tyrolean Grey	[112]
Mucopolysaccharidosis IIIB	AR	Onset within the first two years of age with progressive increase over lifespan. Progressive ataxia, stumbling gait, swaying and difficulty in balance and walking.	<i>NAGLU</i>	<u>001342-9913</u>	SNV (missense)	unknown	[113]
Neurocristopathy	AD*	Congenital. Hypotonia, lack of balance and coordination in, facial abnormalities, heart defects and retarded growth.	<i>CHD7</i>	<u>002125-9913</u>	5bp deletion (frameshift)	Montbeliard	[48]
Neuronal ceroid lipofuscinosis 5	AR	Onset from 1.5 years of age. Blindness, ataxia, seizures. Accumulation of lysosome derived fluorescent storage bodies in neurons and most other cells.	<i>CLN5</i>	<u>001482-9913</u>	1bp duplication (frameshift)	Devon	[114]

Neuropathy with splayed forelimbs	AR	Not available.	<i>UCHL1</i>	<u>002298-9913</u>	SNV (missense)	Jersey	[115]
Niemann-Pick disease, type C1	AR	Onset from 3 months of age. Hindlimb weakness, dysmetria, incoordination, head tremors, wide based stance, walking sideways or falling over and recumbency followed by death, exacerbated by stress. Neurons degeneration and widespread foamy vacuolation of cytoplasm and glia of central nervous system.	<i>NPCI</i>	<u>000725-9913</u>	SNV (missense)	Angus	[116]
Spinal muscular atrophy (SMA)	AR	Onset from first weeks of age. Progressive weakness, severe neurogenic muscular atrophy, paraparesis and sternal recumbency.	<i>KDSR (FVT1)</i>	<u>002390-9913</u>	SNV (missense)	Brown Swiss	[117, 118]
Spinal dysmyelination	AR	Congenital. Lateral recumbency with slight to moderate opisthotonos, body tremor, and spastic extension of the limbs, general muscle atrophy. Bilateral symmetrical hypo- and demyelination of axons in the cervical and thoracic segments of spinal cord.	<i>SPAST</i>	<u>001247-9913</u>	SNV (missense)	Brown Swiss	[119, 120]
Turning calves syndrome	AR	Onset from 2-6 weeks of age. Ataxia (especially of hindlimbs) and paraparesis. Nervous symptoms progress over the next months of age, leading to repetitive falls and	<i>SLC25A46</i>	<u>002150-9913</u>	SNV (missense)	Rouge-des-Prés	[121]

		ultimately resulting in permanent recumbency and inevitably euthanasia. Degenerative lesions of general proprioceptive sensory and upper motor neuron motor systems.					
--	--	--	--	--	--	--	--

IM = inheritance mode, **AD** = autosomal dominant, **AR** = autosomal recessive, **ARL**= autosomal recessive lethal, **OMIA** = Online mendelian inheritance in animals [10], **ref** = references, * = *de novo* in mosaic sire, + = *de novo* in the embryo, † = *de novo* in the germline of one parent or in the embryo, & = incomplete penetrance

Table A3: Genetic metabolic disorders of cattle: brief description of the phenotype, the associated genes and types of variants

Disorder	IM	Phenotype	Gene	OMIA	Type of variant	Breed(s)	Ref
Bovine leukocyte adhesion deficiency (BLAD)	AR	Congenital. Diarrhea, periodontal gingivitis with gingival recession and tooth loss, tendency to recurrent and prolonged mucosal and epithelial infections, persistent and pronounced mature neutrophilia, increased susceptibility to infection in young calves.	<i>ITGB2</i>	000595-9913	SNV (missense)	Holstein	[122]
Chediak-Higashi syndrome	AR	Congenital. Tendency to bleed and prolonged bleeding time due to insufficient platelet aggregation, oculocutaneous hypopigmentation, partial albinism, increased hemorrhagic predisposition and reduced resistance to infection.	<i>LYST</i>	000185-9913	SNV (missense)	Japanese Black	[123]

Cholesterol deficiency (CDH)	AD&	Congenital. Homozygous mutant: diarrhea, buccal lesions, hypocholesterolemia and hypolipidemia, failure to thrive (die within the first 6-12 months age). Heterozygous carrier: unspecific symptoms of reduced fertility, growth, and health, reduced levels of blood cholesterol and triglycerides.	<i>APOB</i>	<u>001965-9913</u>	1.3kb ERV insertion (frameshift)	Holstein	[124–126]
Citrullinaemia	ARL	Congenital. Depression, lack of appetite, unsteady gait and aimless wandering, tongue protrusion, frothing at mouth, head-pressing, rapid progression with appearance of blindness and death within 3-5 days.	<i>ASS1</i>	<u>000194-9913</u>	SNV (nonsense)	Holstein	[127]
Congenital disorder of glycosylation	AR	Congenital. Reduced growth parameters, reduced levels of blood triglycerides.	<i>GALNT2</i>	<u>002375-9913</u>	SNV (splice site)	Holstein, Jersey	[103]
Congenital erythropoietic porphyria	AR	Congenital. Photosensitization with subepidermal blistering and dermal necrosis of unpigmented areas, diffuse systemic brown discoloration of bones and teeth, hemolytic anemia.	<i>UROS</i>	<u>001175-9913</u>	NA	Holstein	[128]
Deficiency of uridine monophosphate synthase (DUMPS) (embryonic lethality)	AD&	Congenital. Homozygous mutant: embryonic lethality (approximately at day 40). Heterozygous cows: high orotic acid levels in the milk due to the reduced activity of UMPS.	<i>UMPS</i>	<u>000262-9913</u>	SNV (nonsense)	Holstein	[129, 130]

Dwarfism, growth-hormone deficiency	AR	Congenital. Reduced growth parameters (proportioned growth), abnormal insulin sensitivity, abnormal ovarian follicular growth, smaller diameter of the corpus luteum.	<i>GHI</i>	<u>001473-9915</u>	SNV (missense)	Brahman	[131]
Factor XI deficiency (blood coagulation)	AR	Congenital. Impaired coagulability of the blood with strong tendency to bleed due to deficiency of clotting factor IX, bloody milk, and anemia.	<i>F11</i>	<u>000363-9913</u>	76bp insertion (frameshift); 15bp insertion (missense + in-frame)	Holstein, Sahiwal, Japanese Black	[132, 133]
Glycogen storage disease II	AR	Congenital. Reduced growth parameters, progressive muscular weakness, lethargy, expected lifespan less than 12 months.	<i>GAA</i>	<u>000419-9913</u>	SNV (missense, nonsense)	Shorthorn, Brahman, Droughtmaster	[134]
Glycogen storage disease V	AR	Onset from first months of age. Exercise intolerance, recumbency post-exercise, elevated serum CK and AST, rhabdomyolysis accompanied by myoglobinuria.	<i>PYGM</i>	<u>001139-9913</u>	SNV (missense)	Charolais	[135]
Hemophilia A	XR	Congenital. Impaired coagulability of the blood with strong tendency to bleed due to deficiency of clotting factor VIII.	<i>F8</i>	<u>000437-9913</u>	SNV (missense)	Japanese Brown, Fleckvieh	[136, 137]
Mannosidosis, alpha	ARL	Congenital. Stillbirth, postnatal death or rapidly progressive neurological syndrome (intentional tremors, ataxia and aggression). Accumulation of partially degraded mannose rich	<i>MAN2B1</i>	<u>000625-9913</u>	SNV (missense)	Galloway, Angus, Murray Grey	[138]

		oligosaccharides within the lysosomes (lysosomal storage disease) with cytoplasmic vacuolation in central nervous system and parenchymatous organs.					
Mannosidosis, beta	ARL	Congenital. Inability to stand up, intentional tremors, hidebound skin, domed calvaria, prognathism, narrow palpebral fissures. Variable dilatation of lateral cerebral ventricles, marked pallor and paucity of white matter of cerebrum and cerebellum, bilateral renomegaly.	<i>MANBA</i>	<u>000626-9913</u>	SNV (nonsense)	Salers	[139]
Maple syrup urine disease	AR	Onset within first week of age. Progressive neurological dysfunction with opisthotonus and forelimb rigidity.	<i>BCKDHA</i>	<u>000627-9913</u>	SNV (missense, nonsense)	Hereford, Shorthorn	[140, 141]
Thrombopathia	AR	Beeding episodes, including epistaxis, gingival bleeding, and hematuria. Impaired platelet aggregation.	<i>RASGRP2</i>	<u>002433-9913</u>	SNV (missense)	Fleckvieh, Simmental	[142]

IM = inheritance mode, **AD** = autosomal dominant, **AR** = autosomal recessive, **ARL**= autosomal recessive lethal, **OMIA** = Online mendelian inheritance in animals [10], **ref** = references, **XR** = X-linked recessive, **&**= incomplete penetrance

Table A4: Congenital genodermatosis of cattle: brief description of the phenotype, the associated genes and types of variants.

Disorder	IM	Phenotype	Gene	OMIA	Type of variant	Breed(s)	Ref
Acrodermatitis enteropathica	AR	Parakeratosis and dermatitis in areas of continual skin flexion or in regions particularly subjected to abrasion (e.g. around the mouth, eyes, base of the ear, joints and lower part of the thorax, abdomen and limbs) stomatitis, diarrhea, immunodeficiency due to impairment of the immune system (included thymus hypoplasia), growth retardation.	<i>SLC39A4</i>	<u>000593-9913</u>	SNV (splice site)	Holstein	[143]
Anhidrotic ectodermal dysplasia	AR, XR	Abnormalities in two or more ectodermal derivatives, including hair, teeth, nails, and eccrine glands (e.g. sparse hair, abnormal teeth, and anhidrosis or hypohidrosis), recurrent respiratory disease.	<i>EDAR</i>	<u>002128-9913</u>	1bp insertion (frameshift)	Charolais	[48]
			<i>EDA</i>	<u>000543-9913</u>	gross deletion; gross inversion; 161bp insertion, 19bp deletion, 4bp insertion (frameshift); SNV (splice site, nonsense)	Holstein, Japanese Black, crossbred	[144–153]

Coat colour dilution and hypotrichosis	AR	Black diluted to charcoal or chocolate-coloured coat, variable degrees of hypotrichosis (especially tail-switch = rat-tail syndrome) and white areas of coat, including tail-switch with normal hair.	<i>PMEL17</i>	<u>001545-9913</u>	SNV (missense), 2bp deletion	Charolais, Galloway, Hereford, Highland, Simmental	[154, 155]
Coat colour, oculocutaneous albinism type I	AR	Complete lack of pigment in the skin, hair, eyes, horns and hooves.	<i>TYR</i>	<u>000202-9913</u>	1bp insertion (frameshift)	Brown Swiss	[156]
Coat colour, albinism, oculocutaneous type IV	AR	Complete lack of pigment in the skin, hair, eyes, horns and hooves.	<i>SLC45A2</i>	<u>001821-9913</u>	SNV (missense)	Brown Swiss	[157]
Ehlers-Danlos syndrome, classical type II	AD	Skin fragility and hyperextensibility, atrophic scarring. Skin collagen dysplasia.	<i>COL5A2</i>	<u>002295-9913</u>	SNV (missense)	Holstein	[158]
Ehlers-Danlos syndrome, type VII (dermatosparaxis)	ARL	Stillbirth or post-natal death, extreme skin fragility (multiple fissures) and hyperextensibility.	<i>ADAMTS2</i>	<u>000328-9913</u>	3bp insertion + 17bp deletion (premature stop-codon)	Belgian Blue	[159]
Ehlers-Danlos syndrome, spondylodysplastic type I	AR	Skin fragility and hyperextensible, delayed wound healing. Absence of dermatan sulphate proteoglycan in skin connective tissue.	<i>EPYC</i>	<u>001716-9913</u>	SNV (missense)	Holstein	[160]
Epidermolysis bullosa, dystrophic	AR	Loss of skin distal to fetlocks and mucosa of muzzle, diminished cohesion of skin layers, blister formation, and fragility, marked cutaneous pain.	<i>COL7A1</i>	<u>000341-9913</u>	SNV (nonsense)	Rotes Höhenvieh, Vorderwald	[161, 162]

Epidermolysis bullosa, junctionalis	AR	Dysungulation of hooves, skin erosions and ulcers of from carpal and tarsal joints, fetlocks, ears, eyes, and muzzle and oral cavity (e.g. nares, tongue, buccal and labial sides of the mucosa and palate), ear deformities (atrophied pinna and closed ears), anorexia, apathy, emaciation and marked cutaneous pain.	<i>ITGB4</i>	<u>001948-9913</u>	gross deletion	Charolais	[163, 164]
Epidermolysis bullosa junctionalis	AR	Extensive skin blistering predominantly located at pressure points and on limb extremities and articulations, hoof exungulation with erythema and multiple mucosal ulcerations in oral cavity and on the tongue, marked cutaneous pain.	<i>LAMA3</i>	<u>001677-9913</u>	SNV (nonsense)	Belgian Blue	[165]
Epidermolysis bullosa junctionalis	AR	Extensive skin blistering predominantly located at pressure points and on limb extremities and articulations, hoof exungulation with erythema and multiple mucosal ulcerations in oral cavity and on the tongue, marked cutaneous pain.	<i>LAMC2</i>	<u>001678-9913</u>	gross deletion	Hereford	[166]
Epidermolysis bullosa, simplex	AD*,AD ⁺	Skin alopecia, erosion and crusting especially at distal part of limbs, multifocal erosion and ulceration of tongue and oral mucosa, marked cutaneous pain. Segmental separation of full thickness epidermis from dermis.	<i>KRT5</i>	<u>002081-9913</u>	SNV (missense)	Friesian X Jersey crossbred	[167, 168]

Hypotrichosis congenita	AR	Multiple small to large areas of alopecia on limbs, dorsal part of head, neck, and back, retarded growth.	<i>HEPHL1</i>	<u>002230-9913</u>	SNV (nonsense)	Belted Galloway	[169]
		Very short, fine, wooly, kinky and curly coat over all parts of body, with a major expression in t ears, inner part of the limbs, and in thoracic-abdominal region.	<i>KRT71</i>	<u>002114-9913</u>	8bp deletion (frameshift)	Hereford	[170]
Hypotrichosis with coat-colour dilution (rat-tail syndrome)	AD	Hypotrichosis exclusively in diluted coloured hair, thermoregulation disruption which impairs health and growth performance.	<i>MC1R</i>	<u>001544-9913</u>	SNV (missense)	Crossbred	[171]
			<i>PMEL</i>	<u>001544-9913</u>	3bp deletion (in-frame)	Crossbred	[171]
Ichthyosis fetalis	ARL	Stillbirth or post-natal death. Skin hyperkeratosis resulting in deep fissures, eversion of the mucocutaneous junctions (ectropion and eclabium).	<i>ABCA12</i>	<u>002238-9913</u>	SNV (missense, frameshift)	Chianina, Shorthorn, Polled Hereford	[106, 172, 173]
Ichthyosis congenita	AR	Skin xerosis, hyperkeratosis and scaling, urolithiasis and cystitis, retarded growth	<i>FA2H</i>	<u>002450-9913</u>	2bp insertion (frameshift)	Chianina	[174]
Immunodeficiency with psoriasis-like skin alterations	AR	Retarded growth, ulcerative dermatitis with hyperkeratosis, alopecia furunculosis, subcutaneous abscess formation, leukocytosis with neutrophilia.	<i>IL17RA</i>	<u>002271-9913</u>	1bp deletion (frameshift)	Holstein	[175]
Streaked hypotrichosis	XD ^{&}	Hairless lesions across lines of Blaschko and head with fishbone-like pattern (steaked hypotrichosis), udder with non-streaked hypotrichosis, skin lesions without association to coat color.	<i>TSR2</i>	<u>000542-9913</u>	SNV (splice site)	Pezzata Rossa	[176]

Tricho-dento-osseous-like syndrome	AD*	Dull tousled hair coat with mild hypotrichosis of the ventral neck and legs, curly eyelashes, pinnae hypotrichosis, dry skin and covered with fine scale, slight brown discoloration. Trichogram: irregular shaped hair shafts characterized by multiple indentations of cuticle, cortex and medulla.	<i>DLX3</i>	<u>002109-9913</u>	10bp insertion (frameshift)	Brown Swiss	[177]
Zinc deficiency-like syndrome (genodermatosis)	AR	Skin scaling and crusting most evident in muzzle, eyes, sternum and extremities, seborrhoea in inguinal region, enlargement of palpable lymph nodes, erosive or ulcerative lesions of the oral mucosa and interdigital spaces, retarded growth, recurrent diarrhea and pneumonia.	<i>PLD4</i>	<u>001935-9913</u>	SNV (nonsense)	Fleckvieh	[178]

IM = inheritance mode, **AD** = autosomal dominant, **AR** = autosomal recessive, **ARL** = autosomal recessive lethal, **OMIA** = Online mendelian inheritance in animals [10], **ref** = references, **XR** = X-linked recessive, **XD** = X-linked dominant, * = *de novo* in mosaic sire, + = *de novo* in the embryo, † = *de novo* in the germline of one parent or in the embryo, & = incomplete penetrance.

Table A5: Genetic ocular and auricular disorders of cattle: brief description of the phenotype, the associated genes and types of variants.

Disorder	IM	Phenotype	Gene	OMIA	Type of variant	Breed(s)	Ref
Achromatopsia	AR	Congenital. Day-blindness, absent cone-mediated function.	<i>CNGB3</i>		SNV (missense)	Original Braunvieh	[179]
Congenital Morgagnian cataract	AR	Congenital. Bilateral complete mature to hypermature cataract.	<i>CPAMD8</i>	<u>002111-9913</u>	SNV (nonsense)	Holstein	[180]
Congenital bilateral cataract	AR	Congenital. Bilateral incomplete immature nuclear cataract.	<i>NID1</i>	<u>001936-9913</u>	855bp deletion (frameshift)	Romagnola	[181]
Congenital multiple ocular defects	AR	Congenital. Microphthalmia, torsion of the eye, complete blindness	<i>WFDC1</i>	<u>002423-9913</u>	1bp insertion (frameshift)	Japanese Black	[182]
Crop ears	AD ^{&}	Crop ears bilaterally symmetrically. Phenotypic severity of crop ears varies greatly.	<i>HMX1</i>	<u>000317-9913</u>	76bp duplication	Highland cattle	[183]
Depigmentation associated with microphthalmia	AD*	Congenital. Complete absence of pigment, small eyes and musculoskeletal malformations affecting all four limbs, muscular atrophy.	<i>MITF</i>	<u>001931-9913</u>	gross deletion	Holstein	[184]
Dominant white with bilateral deafness	AD*	Congenital. Hypopigmentation, heterochromia irides, colobomatous eyes and bilateral hearing loss.	<i>MITF</i>	<u>001680-9913</u>	3bp deletion (in-frame); SNV (missense)	Holstein, Fleckvieh	[48, 185]
Hemifacial microsomia	AR	Congenital. Microtia and anotia, face asymmetry, deafness, tympanic bullae agenesis, temporal bones and temporomandibular joints asymmetry, pontine meningocele.	<i>LAMB1</i>	<u>002479-9913</u>	SNV (missense)	Romagnola	[186]

Retinitis pigmentosa 1	AR	Onset from 4.5 years. Blindness due bilateral retinal degeneration with a heterogeneous color, multiple focal areas of hyper reflectivity in the tapetal area. Absence of photoreceptor outer segments along with a marked thinning and disorganization of outer nuclear layer with very few remaining nuclei.	<i>RPI</i>	<u>002029-9913</u>	1bp insertion (frameshift)	Angus, Beef Booster Composite, Belgian Blue, Charolais, Gelbvieh, Holstein, Maine Anjou, Normande, Red Angus	[30]
------------------------	----	--	------------	--------------------	----------------------------	--	------

IM = inheritance mode, **AD** = autosomal dominant, **AR** = autosomal recessive, **OMIA** = Online mendelian inheritance in animals [10], **ref** = references, * = *de novo* in mosaic sire, & = incomplete penetrance.

Table A6: Genetic cardiac and diaphragmatic muscle disorders of cattle: brief description of the phenotype, the associated genes and types of variants

Disorder	IM	Phenotype	Gene	OMIA	Type of variant	Breed(s)	Ref
Cardiomyopathy and woolly haircoat syndrome	AR	Congenital. Woolly haircoat, arrhythmogenic cardiomyopathy, prominent forehead, exophthalmus, bilateral serous ocular discharge, ulcerative ocular keratitis, death within the first 12 weeks of age.	<i>PPP1R13L</i>	000161-9913	7bp duplication (frameshift)	Hereford	[187]
Dilated cardiomyopathy	AR	Onset from 2-4 years of age. Right side heart failure due to systolic dysfunction, cardiomegaly with ventricular, atrial dilation and hypertrophy.	<i>OPA3</i>	000162-9913	SNV (missense)	Fleckvieh	[188]
Myopathy of the diaphragmatic muscles	AR	Late onset. Ruminal tympany and respiratory insufficiency.	<i>HSPA1A</i>	001319-9913	gross deletion	Holstein Friesian	[189]

IM = inheritance mode, **AR** = autosomal recessive, **OMIA** = Online mendelian inheritance in animals [10], **ref** = references.

Table A7: Genetic congenital renal and genitourinary disorders of cattle: brief description of the phenotype, the associated genes and types of variants.

Disorder	IM	Phenotype	Gene	OMIA	Type of variant	Breed(s)	Ref
Fanconi syndrome	AR	Retarded growth, polyuria and polydipsia, glycosuria, poor claw, horn and coat quality. Pale cortex of the kidneys, unilateral renal hypoplasia, tubulonephrosis of the proximal tubules with protein and glucose-rich contents.	<i>SLC2A2</i>	000366-9913	7bp deletion+4bp insertion (frameshift)	Braunvieh, Fleckvieh	[190]

Gonadal hypoplasia	AR	Incomplete development or underdevelopment of the gonads (testes or ovaries).	<i>KIT</i>	<u>000426-9913</u>	structural rearrangement	Northern Finncattle; Swedish Mountain	[191]
Renal dysplasia	AR	Dullness, retarded growth, overgrowth of hooves and severe renal failure (increased blood urea nitrogen and creatinine). Atrophic renal tubules and extensive interstitial fibrosis with inflammatory cell infiltration in kidney parenchyma.	<i>CLDN16</i>	<u>001135-9913</u>	gross deletion	Japanese Black	[192, 193]
Xanthinuria type II	AR	Lethal growth retardation at approximately 6 months of age, elevated xanthine secretion in urine associated. Expanded renal tubules containing xanthine calculi ranging from 1–3 mm in diameter.	<i>MOCOS</i>	<u>001819-9913</u>	1bp deletion (frameshift)	Tyrolean Grey; Japanese Black	[41, 194]

IM = inheritance mode, **AR** = autosomal recessive, **OMIA** = Online mendelian inheritance in animals [10], **ref** = references.

7 Curriculum Vitae

Full name Joana Gonçalves Pontes Jacinto
E-mail address joana.goncalves2@studio.unibo.it
ORCID orcid.org/0000-0002-6438-7975
Date of birth 27th of April 1994
Nationality Portuguese
Languages Portuguese, English, Italian, Spanish



Academic education

- Feb. 2022 – Mar. 2022 **Research stay**, group of Prof. Dr. med. vet. Cord Drögemüller, Institute of Genetics, University of Bern, CH. Genomic studies on genetic cattle disorders applying a whole-genome approach.
- Oct. 2021 – Dec. 2021 **Research stay**, group of Prof. Dr. med. vet. Cord Drögemüller, Institute of Genetics, University of Bern, CH. Genomic studies on genetic cattle disorders applying a whole-genome approach.
- Jan. 2021 – Feb. 2021 **Research stay**, group of Prof. Dr. med. vet. Cord Drögemüller, Institute of Genetics, University of Bern, CH. Genomic studies on genetic cattle disorders applying a whole-genome approach.
- Jul. 2020 – Dec. 2020 **Research stay**, group of Prof. Dr. med. vet. Cord Drögemüller, Institute of Genetics, University of Bern, CH. Genomic studies on genetic cattle disorders applying a whole-genome approach.
- Since May 2020 **Standard residency - European College of Bovine Health Management (ECBHM)**, Clinic for Ruminants, Department of Veterinary Medical Sciences, University of Bologna, IT. Practical and theoretical training in cattle medicine.
- Feb. 2020 – Mar. 2020 **Research stay**, group of Prof. Dr. med. vet. Cord Drögemüller, Institute of Genetics, University of Bern, CH. Genomic studies on genetic cattle disorders applying a whole-genome approach.
- Nov. 2019 – Dec. 2019 **Collaboration stay in the project Vetbome**, Veterinary Faculty of Mekelle, ET. Project funded by the Emilia Romagna region (IT), Vet for Africa and Department of Veterinary Medical Sciences of the University of Bologna in the context of decentralized cooperation projects and regional interventions for cooperation with developing countries and countries in transition, international solidarity and the promotion of a culture of peace. Personal contribution providing Veterinary training in the Tigray region for both undergraduate and graduate veterinary students.

- Since Oct. 2018 **PhD in Veterinary Sciences**, Department of Veterinary Medical Sciences, University of Bologna, IT. Practical and theoretical experience in cattle medicine (mainly internal medicine diseases and genetic diseases); active participation in all clinical activities at the Ruminants clinic or the Department of Veterinary Medical Sciences, University of Bologna; intensive training in bovine internal medicine, as well as basic training in surgery, zoonotic diseases, herd health, gross pathology, reproductive management and obstetrics.
- Mar. 2018 – Apr. 2018 **Internship**, Klinik für Wiederkäuer Mit Ambulanz und Bestandsbetreuung, Ludwig-Maximilians-Universität München, DE. Practical experience in ruminants medicine including internal medicine in beef and dairy cattle, cattle orthopedics and reproduction of cattle and small ruminants.
- Sep. 2017 – Dec. 2017 **ERASMUS+**, Clinic for Ruminants, Department of Veterinary Medical Sciences, University of Bologna, IT
- Sep. 2012 – Jul. 2018 **Master’s Degree in Veterinary Medicine**, Faculty of Veterinary Medicine, Lusofona University, PT

Research positions

- Since May. 2020 **ECBHM Residency project**: “Surveillance of genetic disorders in cattle”, supervised by Prof. Dr. med. vet. Arcangelo Gentile, Clinic for Ruminants, Department of Veterinary Medical Sciences, University of Bologna, IT
- Since Nov. 2018 **PhD thesis**: “Genetic disorders in cattle”, group of Prof. Dr. med. vet. Arcangelo Gentile, Clinic for Ruminants, Department of Veterinary Medical Sciences, University of Bologna, IT
- Sep. 2012 – Jul. 2018 **Master thesis**: “Autosomal Recessive Cholesterol Deficiency in a Holstein Calf”, with Dr. med. Vet. João Cannas da Silva, Faculty of Veterinary Medicine, Lusofona University, PT and Prof. Dr. med. vet. Arcangelo Gentile, Clinic for Ruminants, Department of Veterinary Medical Sciences, University of Bologna, IT

Scientific experience in private companies

- Jul. 2017 – Aug. 2017 **Internship** Associação Agrícola De São Miguel, Cooperativa União Agrícola, PT. Practical experience in cattle medicine including herd health management, nutrition, surgery, reproduction and internal medicine.
- Jan. 2018 – Feb. 2018 **Internship**, Associação Agrícola De São Miguel, Cooperativa União Agrícola, PT. Practical experience in cattle medicine including internal medicine of beef and dairy cattle, reproductive management and pregnancy diagnosis, herd health management and milk quality evaluation.

Memberships:

- **Circolo ACLI - VET FOR AFRICA, IT.** Active member.
- **Veterinari senza Frontiere (SIVtro-VSF Italia), IT.** Active member.
- **Società Italiana di Buiatria, IT.** Active member.

Additional skills: photography, running, travelling, volunteering work.

8 List of Publications

Jacinto J.G.P., Häfliger I.M., Veiga I.M.B., Letko A., Benazzi C., Bolcato M., Drögemüller C. **2020**. A heterozygous missense variant in the *COL5A2* in Holstein cattle resembling the classical Ehlers-Danlos syndrome. *Animals*. DOI: [10.3390/ani10112002](https://doi.org/10.3390/ani10112002)

Jacinto J.G.P., Bolcato M., Drögemüller C., Gentile A., Militerno G. **2020**. Autosomal cholesterol deficiency in a Holstein calf. *Pakistan Veterinary Journal*. DOI: [10.29261/pakvetj/2019.120](https://doi.org/10.29261/pakvetj/2019.120)

Jacinto J.G.P., Häfliger I. M., Letko A., Drögemüller C., Agerholm J. S. 2020. A large deletion in the *COL2A1* gene expands the spectrum of pathogenic variants causing bulldog calf syndrome in cattle. *Acta veterinaria Scandinavica*. DOI: [10.1186/s13028-020-00548-w](https://doi.org/10.1186/s13028-020-00548-w)

Jacinto J.G.P., Häfliger I.M., Gentile A., and Drögemüller C. **2020**. A 6.7kb deletion in the *COL2A1* gene in a Holstein calf with achondrogenesis type II and perosomus elumbis. *Animal Genetics*. DOI: [10.1111/age.13033](https://doi.org/10.1111/age.13033)

Jacinto J.G.P., Häfliger I.M., Veiga M.B., Drögemüller C., and Agerholm J.S. **2020**. A *de novo* mutation in *KRT5* in a crossbred calf with epidermolysis bullosa. *Journal of Veterinary Internal Medicine*. DOI: [10.1111/jvim.15943](https://doi.org/10.1111/jvim.15943)

Murgiano L., Militerno G., Sbarra F., Drogemuller C., **Jacinto J.G.P.**, Gentile A., Bolcato M. 2020. KDM2B-associated paunch calf syndrome in Marchigiana cattle. *Journal of Veterinary Internal Medicine*. DOI: [10.1111/jvim.15789](https://doi.org/10.1111/jvim.15789)

Gentile A., **Jacinto J.G.P.**, Benazzi C., Bolcato M. 2020. Malattie congenite del sistema nervoso del bovino. *Large Animals Review*. 26, pp. 305 – 315.

Bolcato M., **Jacinto J.G.P.**, Bolognini D., Gentile A. **2020**. Su di un caso di malformazione doppia (cefalotoracopagia) nel vitello. *Large Animals Review*. 26, pp. 259 – 264.

Jacinto J.G.P., Bolcato M., Gentile A., Benazzi C., Muscatello L.V. **2021**. Congenital Suborbital Undifferentiated Sarcoma in a Crossbred Calf. *Animals*. DOI: [10.3390/ani11020534](https://doi.org/10.3390/ani11020534)

Jacinto J.G.P., Bolcato M., Sheahan B.J., Muscatello L.V., Gentile A., Avallone G, Benazzi C. **2021**. Congenital Tumours and Tumour-Like Lesions in Calves: a Review. *Journal of Comparative Pathology*. DOI: [10.1016/j.jcpa.2021.02.003](https://doi.org/10.1016/j.jcpa.2021.02.003)

Jacinto J.G.P., Häfliger I.M., Akyürek E.E., Sacchetto R., Benazzi C., Gentile A., and Drögemüller C. **2021**. *KCNGL1*-related syndromic form of congenital neuromuscular channelopathy in a crossbred calf. *Genes*. DOI: [10.3390/genes12111792](https://doi.org/10.3390/genes12111792)

Jacinto J.G.P., Häfliger I.M., Bernardini M., Mandara M., Bianchi E., Bolcato M., Romagnoli N., Gentile A., and Drögemüller C. **2021**. A homozygous missense variant in laminin subunit beta 1 as candidate causal mutation of hemifacial microsomia in Romagnola cattle. *Journal of Veterinary Internal Medicine*. DOI: [10.1111/jvim.16316](https://doi.org/10.1111/jvim.16316)

Jacinto J.G.P., Häfliger I.M., Borel N., Zanolari P., Drögemüller C. and Veiga I.M.B. **2021**. Clinicopathological and Genomic Characterization of a Simmental Calf with Generalized Bovine Juvenile Angiomatosis. *Animals*. DOI: [10.3390/ani11030624](https://doi.org/10.3390/ani11030624)

Jacinto J.G.P., Markey A.D., Veiga I.M.B., Paris J.M., Welle M., Beever J.E., Drögemüller C. **2021**. A *KRT71* Loss-of-Function Variant Results in Inner Root Sheath Dysplasia and Recessive Congenital Hypotrichosis of Hereford Cattle. *Genes*. DOI: [10.3390/genes12071038](https://doi.org/10.3390/genes12071038)

Kuca T., Marron B.M., **Jacinto J.G.P.**, Paris J.M., Gerspach C., Beever J.E., Drögemüller C. **2021**. A Nonsense Variant in Hephaestin Like 1 (HEPHL1) Is Responsible for Congenital Hypotrichosis in Belted Galloway Cattle. *Genes*. doi: [10.3390/genes12050643](https://doi.org/10.3390/genes12050643)

Jacinto J.G.P., Häfliger I.M., Gentile A., and Drögemüller C. **2021**. A heterozygous missense variant in *MAP2K2* in a stillborn Romagnola calf with skeletal-cardio-enteric dysplasia. *Animals*. DOI: [10.3390/ani11071931](https://doi.org/10.3390/ani11071931)

Jacinto J.G.P., Häfliger I.M., McEvoy F., Drögemüller C., and Agerholm J.S. **2021**. A *de novo* mutation in *COL1A1* in a Holstein calf with osteogenesis imperfecta type II. *Animals*. DOI: [10.3390/ani11020561](https://doi.org/10.3390/ani11020561)

Jacinto J.G.P., Häfliger I.M., Veiga I.M.B., Letko A., Gentile A., and Drögemüller C. **2021**. A frameshift insertion in *FA2H* causes a recessively inherited form of ichthyosis congenita in Chianina cattle. *Molecular Genetics and Genomics*. DOI: [10.1007/s00438-021-01824-8](https://doi.org/10.1007/s00438-021-01824-8)

Häfliger I.M., Marchionatti E., Stengård M., Wolf-Hofstetter S., Paris J.M., **Jacinto G.P.J.**, Watté C., Voelter K., Occelli L.M., Komáromy A., Oevermann A., Goepfert C., Borgo A., Roduit R., Spengeler M., Seefried F., and Drögemüller C. **2021**. *CNGB3* missense variant causes recessive achromatopsia in Original Braunvieh cattle. *International Journal of Molecular Sciences*. DOI: [10.3390/ijms222212440](https://doi.org/10.3390/ijms222212440)

Jacinto J.G.P., Häfliger I.M., Christen M., Paris J.M., Seefried F.R., Drögemüller C. **2022**. Is a heterozygous missense variant in *SGSH* the cause of a syndromic form of congenital amastia in an Original Braunvieh calf? *Animal genetics*. Advance online publication. DOI: [10.1111/age.13207](https://doi.org/10.1111/age.13207)

Jacinto, J.G.P., Häfliger, I. M., Baes, C. F., de Oliveira, H. R., Drögemüller, C. **2022**. A *de novo* start-lost variant in *ANKRD28* in a Holstein calf with dwarfism. *Animal genetics*. Advance online publication. DOI: [10.1111/age.13204](https://doi.org/10.1111/age.13204)

Bolcato M., Roccaro M., **Jacinto J.G.P.**, Peli A., Gentile A., Bianchi E. **2022**. Use of Electrodiagnostics in the Diagnosis and Follow-Up of Brachial Plexus Syndrome in a Calf. *Veterinary Sciences*. DOI: [10.3390/vetsci9030136](https://doi.org/10.3390/vetsci9030136)

9 Conference oral communications and posters

Oral presentations presented by myself:

Jacinto J.G.P., Sbarra F., Drögemüller C., Bolcato M., Gentile A. Prevalenza di alleli patologici autosomici recessivi nei tori italiani di razza Chianina, Marchigiana e Romagnola. S.I.B. (Italian Buiatrics Society) Virtual Week, Online Congress, from 22 – 26 November 2021.

Jacinto, J.G.P., Häfliger, I.M., Veiga, I.M., Letko, A., Drögemüller, C., Gentile, A. A recessively inherited form of ichthyosis congenita in Chianina cattle is associated with a frameshift insertion in the *FA2H* gene. Proceedings of the European College of Bovine Health Management (ECBHM) Scientific Session 2021, Online, 23 September 2021.

Jacinto J.G.P., Gentile A., Sbarra F., Drögemüller C., Prevalence of known recessive disease alleles in Italian beef cattle. EAAP scientific committee, Book of abstracts of the 72nd Annual Meeting of the European Federation of Animal Science, 2021, pp. 349 - 349, Davos, Switzerland, 30.08.2021 – 02.09.2021.

Jacinto J.G.P., Veiga I.M.B., Häfliger I.M., Gentile A., Letko A., Benazzi C., Bolcato M., Drögemüller C. A heterozygous missense variant in the *COL5A2* in Holstein cattle resembling the classical Ehlers-Danlos syndrome. S.I.B. (Italian Buiatrics Society) Virtual Week, Online Congress 26 November 2020.

Jacinto J.G.P., Bolcato M., Petronelli C., Campanerut F., Gentile A., Famigli Bergamini P., Benazzi C. Tumors in calves: clinical experience. The 51st National S.I.B. (Italian Buiatrics Society) Congress, Parma, Italy from 7 – 8 November 2019.

Jacinto J.G.P., Bolcato M., Benazzi C., Petronelli C., Campanerut F., Gentile A., Famigli Bergamini P. Clinical findings and gross pathology in SBV (Schmallenberg Virus) seropositive calves. The 51st National S.I.B. (Italian Buiatrics Society) Congress, Parma, Italy from 7 – 8 November 2019.

Jacinto J.G.P. Tumors and tumor-like lesions in young cattle. Workshop Clínica de Ruminantes da FMV de Bolonha em colaboração com a FMV da ULHT, Lisbon, Portugal from 3 – 4 October 2019. Part of the organization committee.

Jacinto J.G.P. Genetic disorders in cattle. Workshop Clínica de Ruminantes da FMV de Bolonha em colaboração com a FMV da ULHT, Lisbon, Portugal from 3 – 4 October 2019. Part of the organization committee.

Jacinto J.G.P. Schmallenberg virus in cattle. Workshop Clínica de Ruminantes da FMV de Bolonha em colaboração com a FMV da ULHT, Lisbon, Portugal from 3 – 4 October 2019. Part of the organization committee.

Jacinto J.G.P., Bolcato M., Benazzi C., Petronelli C., Campanerut F., Gentile A., Famigli P.B. Clinical Findings and gross pathology in SBV (Schmallenberg Virus) seropositive calves. XXIV International Congress of the Mediterranean Federation for Health and Production of Ruminants (FeMeSPRum), León, Spain from 26 – 28 September 2019.

Oral Presentations presented by co-authors:

Gorrieri F., Gebrekidan B., **Jacinto J.G.P.**, Bolcato M. Su di una curiosa appendice osteo-fibro-lipomatosa nella regione cervicale dorsale di una manza. S.I.B. (Italian Buiatrics Society) Virtual Week, Online Congress, from 22 – 26 November 2021.

Bolcato M., **Jacinto J.G.P.**, Gentile A. Epileptic seizures in ruminants. XX Middle European Buiatric Congress, Terme Ptuj, Slovenia from 22 – 25 September 2021.

Häfliger I.M., Marchionatti E., Wolf-Hofstetter S., Paris J.M., **Jacinto J.G.P.**, Watté C., Stengard M., Voelter K., Ocelli L.M., Komáromy A.M., Oevermann A., Göpfert C., Borgo A., Roduit R., Seefried F., Drögemüller C. *CNGB3* missense variant causes recessive day-blindness (achromatopsia) in Original Braunvieh cattle, in: EAAP scientific committee, Book of Abstracts of the 72nd Annual Meeting of the European Federation of Animal Science, 2021, pp. 244 – 244.

Bolcato M., **Jacinto J.G.P.**, Militerno G., Dimitrijevic B., Famigli Bergamini P. Heterotopy (“Error loci”) of the spiral loop of the ascending colon in cattle predisposing intestinal injury. XXIV International Congress of the Mediterranean Federation for Health and Production of Ruminants (FeMeSPRum), León, Spain from 26 – 28 September 2019.

Bolcato M., **Jacinto J.G.P.**, Militerno G., Cannas da Silva J., Gentile A. Autosomal Recessive Cholesterol Deficiency in a Holstein Calf. The 50th National S.I.B. (Italian Buiatrics Society) Congress, Bologna, 10-13 October 2018.

Poster presentation:

Jacinto, J.G.P., Muscatello, L.V., Bolcato M., Benazzi, C., Gentile, A. Tumours and tumour-like lesions in calves: clinicopathological experience of 13 cases. XX Middle European Buiatric Congress, Terme Ptuj, Slovenia from 22 – 25 September 2021.

Masebo N.T., Bolcato M., **Jacinto J.G.P.**, Gentile A., Militerno G., Genital tract involvements in a bull affected by bovine besnoitiosis. XX Middle European Buiatric Congress, Terme Ptuj, Slovenia from 22 – 25 September 2021.

10 References

1. Roth TL, Marson A (2021) Genetic Disease and Therapy. *Annu Rev Pathol Mech Dis* 16:145–166
2. Richter T, Nestler-Parr S, Babela R, Khan ZM, Tesoro T, Molsen E, Hughes DA (2015) Rare Disease Terminology and Definitions-A Systematic Global Review: Report of the ISPOR Rare Disease Special Interest Group. *Value Heal J Int Soc Pharmacoeconomics Outcomes Res* 18:906–914
3. (2018) National Human Genome Research Institute. <https://www.genome.gov/For-Patients-and-Families/Genetic-Disorders>. Accessed 6 Dec 2021
4. Jackson M, Marks L, May GHW, Wilson JB (2018) The genetic basis of disease. *Essays Biochem* 62:643–723
5. Viotti M (2020) Preimplantation Genetic Testing for Chromosomal Abnormalities: Aneuploidy, Mosaicism, and Structural Rearrangements. *Genes (Basel)*. <https://doi.org/10.3390/genes11060602>
6. Mohr OL, Wriedt C (1928) Hairless, a new recessive lethal in cattle. *J Genet* 19:315–336
7. Wriedt C, Mohr OL (1928) Amputated, a recessive lethal in cattle; with a discussion on the bearing of lethal factors on the principles of live stock breeding. *J Genet* 20:187–215
8. Watson JD, Crick FHC (1953) The structure of DNA. In: *Cold Spring Harb. Symp. Quant. Biol.* pp 123–131
9. Consortium BGS and A, Elvik CG, Tellam RL, et al (2009) The genome sequence of taurine cattle: a window to ruminant biology and evolution. *Science* 324:522–528
10. OMIA (2022) Online Mendelian Inheritance in Animals.
11. Thornton PK (2010) Livestock production: recent trends, future prospects. *Philos Trans R Soc London Ser B, Biol Sci* 365:2853–2867
12. Georges M, Charlier C, Hayes B (2019) Harnessing genomic information for livestock improvement. *Nat Rev Genet* 20:135–156
13. Thibier M, Wagner H-G (2002) World statistics for artificial insemination in cattle. *Livest Prod Sci* 74:203–212
14. Doekes HP, Veerkamp RF, Bijma P, de Jong G, Hiemstra SJ, Windig JJ (2019) Inbreeding depression due to recent and ancient inbreeding in Dutch Holstein–Friesian dairy cattle. *Genet Sel Evol* 51:54
15. Bourneuf E, Otz P, Pausch H, et al (2017) Rapid Discovery of De Novo Deleterious Mutations in Cattle Enhances the Value of Livestock as Model Species. *Sci Rep* 7:11466
16. Häfliger IM, Seefried F, Drögemüller C (2020) Trisomy 29 in a stillborn Swiss Original Braunvieh calf. *Anim. Genet.*
17. Panter KE, Welch KD, Lee ST, Gardner, D. R. Stegelmeier BL, Ralphs MH, Davis TZ, Green BT, Pfister JA, Cook D (2011) Plants teratogenic to livestock in the United States. In: Riet-Correa F, Pfister J, Schild AL, Wierenga T (eds) *Poisoning by plants, mycotoxins Relat. toxins*. CABI, p 236
18. VanRaden PM, Olson KM, Null DJ, Hutchison JL (2011) Harmful recessive effects on fertility detected by absence of homozygous haplotypes. *J Dairy Sci* 94:6153–6161

19. Adams HA, Sonstegard TS, VanRaden PM, Null DJ, Van Tassell CP, Larkin DM, Lewin HA (2016) Identification of a nonsense mutation in APAF1 that is likely causal for a decrease in reproductive efficiency in Holstein dairy cattle. *J Dairy Sci* 99:6693–6701
20. McClure MC, Bickhart D, Null D, et al (2014) Bovine exome sequence analysis and targeted SNP genotyping of recessive fertility defects BH1, HH2, and HH3 reveal a putative Causative mutation in SMC2 for HH3. *PLoS One* 9:e92769
21. Fritz S, Hoze C, Rebours E, et al (2018) An initiator codon mutation in SDE2 causes recessive embryonic lethality in Holstein cattle. *J Dairy Sci* 101:6220–6231
22. Hozé C, Escouflaire C, Mesbah-Uddin M, Barbat A, Boussaha M, Deloche MC, Boichard D, Fritz S, Capitan A (2020) A splice site mutation in CENPU is associated with recessive embryonic lethality in Holstein cattle. *J Dairy Sci* 103:607–612
23. Sonstegard TS, Cole JB, VanRaden PM, Van Tassell CP, Null DJ, Schroeder SG, Bickhart D, McClure MC (2013) Identification of a nonsense mutation in CWC15 associated with decreased reproductive efficiency in Jersey cattle. *PLoS One* 8:e54872
24. Guarini AR, Sargolzaei M, Brito LF, Kroezen V, Lourenco DAL, Baes CF, Miglior F, Cole JB, Schenkel FS (2019) Estimating the effect of the deleterious recessive haplotypes AH1 and AH2 on reproduction performance of Ayrshire cattle. *J Dairy Sci* 102:5315–5322
25. Schütz E, Wehrhahn C, Wanjek M, Bortfeld R, Wemheuer WE, Beck J, Brenig B (2016) The Holstein Friesian lethal haplotype 5 (HH5) results from a complete deletion of TBF1M and cholesterol deficiency (CDH) from an ERV-(LTR) insertion into the coding region of APOB. *PLoS One* 11:e0154602
26. Michot P, Fritz S, Barbat A, et al (2017) A missense mutation in PFAS (phosphoribosylformylglycinamide synthase) is likely causal for embryonic lethality associated with the MH1 haplotype in Montbeliarde dairy cattle. *J Dairy Sci* 100:8176–8187
27. Venhoranta H, Pausch H, Flisikowski K, et al (2014) In frame exon skipping in UBE3B is associated with developmental disorders and increased mortality in cattle. *BMC Genomics* 15:1–9
28. Schwarzenbacher H, Burgstaller J, Seefried FR, et al (2016) A missense mutation in TUBD1 is associated with high juvenile mortality in Braunvieh and Fleckvieh cattle. *BMC Genomics* 17:400
29. Joller S, Stettler M, Locher I, Dettwiler M, Seefried F, Meylan M, Drögemüller C (2018) Fanconi-bickel-syndrom: A novel genetic disease in Original Braunvieh. *Schweiz Arch Tierheilkd* 160:179–184
30. Michot P, Chahory S, Marete A, et al (2016) A reverse genetic approach identifies an ancestral frameshift mutation in RP1 causing recessive progressive retinal degeneration in European cattle breeds. *Genet Sel Evol* 48:56
31. Risch N, Merikangas K (1996) The future of genetic studies of complex human diseases. *Science* 273:1516–1517
32. Teo YY (2008) Common statistical issues in genome-wide association studies: a review on power, data quality control, genotype calling and population structure. *Curr Opin Lipidol* 19:133–143
33. Benjamini Y, Yekutieli D (2001) The control of the false discovery rate in multiple testing

- under dependency. *Ann Stat* 29:1165–1188
34. Bland JM, Altman DG (1995) Multiple significance tests: the Bonferroni method. *Bmj* 310:170
 35. Turner S (2018) qqman: an R package for visualizing GWAS results using Q-Q and manhattan plots. *J Open Source Softw* 34:1–2
 36. R Core Team R: A language and environment for statistical computing.
 37. Teare MD, Santibañez Koref MF (2014) Linkage analysis and the study of Mendelian disease in the era of whole exome and genome sequencing. *Brief Funct Genomics* 13:378–383
 38. Ott J, Wang J, Leal SM (2015) Genetic linkage analysis in the age of whole-genome sequencing. *Nat Rev Genet* 16:275–284
 39. Vahidnezhad H, Youssefian L, Jazayeri A, Uitto J (2018) Research techniques made simple: Genome-wide homozygosity/autozygosity mapping Is a powerful tool for identifying candidate genes in autosomal recessive genetic diseases. *J Invest Dermatol* 138:1893–1900
 40. Purcell S, Neale B, Todd-Brown K, et al (2007) PLINK: A tool set for whole-genome association and population-based linkage analyses. *Am J Hum Genet* 81:559–575
 41. Bhati M, Kadri NK, Crysanto D, Pausch H (2020) Assessing genomic diversity and signatures of selection in Original Braunvieh cattle using whole-genome sequencing data. *BMC Genomics* 21:27
 42. Rosen BD, Bickhart DM, Schnabel RD, et al (2020) De novo assembly of the cattle reference genome with single-molecule sequencing. *Gigascience* 9:1–9
 43. National Center for Biotechnology Information (2018) ARS-UCD1.2 Assembly.
 44. National Center for Biotechnology Information (2018) NCBI *Bos taurus* Annotation Release 106.
 45. Smedley D, Smith KR, Martin A, et al (2021) 100,000 Genomes Pilot on Rare-Disease Diagnosis in Health Care - Preliminary Report. *N Engl J Med* 385:1868–1880
 46. Alfares A, Alsubaie L, Aloraini T, Alaskar A, Althagafi A, Alahmad A, Rashid M, Alswaid A, Alothaim A, Eyaid W (2020) What is the right sequencing approach? Solo VS extended family analysis in consanguineous populations. *BMC Med Genomics* 13:1–8
 47. Cole JB (2015) A simple strategy for managing many recessive disorders in a dairy cattle breeding program. *Genet Sel Evol* 47:94
 48. Bourneuf E, Otz P, Pausch H, et al (2017) Rapid Discovery of de Novo Deleterious Mutations in Cattle Enhances the Value of Livestock as Model Species. *Sci Rep* 7:1–19
 49. Kadri NK, Sahana G, Charlier C, et al (2014) A 660-kb deletion with antagonistic effects on fertility and milk production segregates at high frequency in Nordic Red cattle: additional evidence for the common occurrence of balancing selection in livestock. *PLoS Genet* 10:e1004049
 50. Derks MFL, Lopes MS, Bosse M, Madsen O, Dibbits B, Harlizius B, Groenen MAM, Megens HJ (2018) Balancing selection on a recessive lethal deletion with pleiotropic effects on two neighboring genes in the porcine genome. *PLoS Genet* 14:e1007661
 51. Reinartz S, Mohwinkel H, Surie C, Hellige M, Feige K, Eikelberg D, Beineke A, Metzger

- J, Distl O (2017) Germline mutation within COL2A1 associated with lethal chondrodysplasia in a polled Holstein family. *BMC Genomics* 18:1–10
52. Agerholm JS, Menzi F, McEvoy FJ, Jagannathan V, Drogemuller C (2016) Lethal chondrodysplasia in a family of Holstein cattle is associated with a de novo splice site variant of COL2A1. *BMC Vet Res* 12:1–9
 53. Daetwyler HD, Capitan A, Pausch H, et al (2014) Whole-genome sequencing of 234 bulls facilitates mapping of monogenic and complex traits in cattle. *Nat Genet* 46:858–865
 54. Jacinto JGP, Häfliger IM, Letko A, Drögemüller C, Agerholm JS (2020) A large deletion in the COL2A1 gene expands the spectrum of pathogenic variants causing bulldog calf syndrome in cattle. *Acta Vet Scand* 62:49
 55. Jacinto JGP, Häfliger IM, Gentile A, Drögemüller C, Bolcato M (2021) A 6.7 kb deletion in the COL2A1 gene in a Holstein calf with achondrogenesis type II and perosomus elumbis. *Anim Genet* 52:244–245
 56. Seichter D, Russ I, Förster M, Medugorac I (2011) SNP-based association mapping of Arachnomelia in Fleckvieh cattle. *Anim Genet* 42:544–547
 57. Buitkamp J, Semmer J, Götz K-U (2011) Arachnomelia syndrome in Simmental cattle is caused by a homozygous 2-bp deletion in the molybdenum cofactor synthesis step 1 gene (MOCS1). *BMC Genet* 12:11
 58. Drögemüller C, Tetens J, Sigurdsson S, Gentile A, Testoni S, Lindblad-Toh K, Leeb T (2010) Identification of the bovine arachnomelia mutation by massively parallel sequencing implicates sulfite oxidase (SUOX) in bone development. *PLOS Genet* 6:e1001079
 59. Agerholm JS, McEvoy F, Arnbjerg J (2006) Brachyspina syndrome in a Holstein calf. *J Vet Diagnostic Investig* 18:418–422
 60. Charlier C, Agerholm JS, Coppieters W, et al (2012) A deletion in the bovine FANCI gene compromises fertility by causing fetal death and brachyspina. *PLoS One* 7:e43085
 61. Floriot S, Vesque C, Rodriguez S, et al (2015) C-Nap1 mutation affects centriole cohesion and is associated with a Seckel-like syndrome in cattle. *Nat Commun* 6:6894
 62. Thomsen B, Horn P, Panitz F, Bendixen E, Petersen AH, Holm L-E, Nielsen VH, Agerholm JS, Arnbjerg J, Bendixen C (2006) A missense mutation in the bovine SLC35A3 gene, encoding a UDP-N-acetylglucosamine transporter, causes complex vertebral malformation. *Genome Res* 16:97–105
 63. Agerholm JS, Bendixen C, Andersen O, Arnbjerg J (2001) Complex vertebral malformation in Holstein calves. *J Vet Diagnostic Investig* 13:283–289
 64. Häfliger IM, Letko A, Murgiano L, Drögemüller C (2020) De novo stop-lost germline mutation in FGFR3 causes severe chondrodysplasia in the progeny of a Holstein bull. *Anim Genet* 51:466–469
 65. Fasquelle C, Sartelet A, Li W, et al (2009) Balancing selection of a frame-shift mutation in the MRC2 gene accounts for the outbreak of the crooked tail syndrome in Belgian Blue cattle. *PLOS Genet* 5:e1000666
 66. Sartelet A, Klingbeil P, Franklin CK, Fasquelle C, Geron S, Isacke CM, Georges M, Charlier C (2012) Allelic heterogeneity of Crooked Tail Syndrome: result of balancing selection? *Anim Genet* 43:604–607

67. Denholm LJ, Martin LE, Teseling CF, Parnell PF, Beever JE (2014) Developmental Duplications (DD): 2. Mutation of the NHLRC2 gene causes neural tube defects in Angus cattle with multiple congenital malformation phenotypes that include axial and limb duplications, heteropagus conjoined twins, midbrain and forebrain malfo. Proc. XXVIII World Buiatrics Congr. Cairns Aust. Abstr. 100:
68. Struck A-K, Dierks C, Braun M, Hellige M, Wagner A, Oelmaier B, Beineke A, Metzger J, Distl O (2018) A recessive lethal chondrodysplasia in a miniature zebu family results from an insertion affecting the chondroitin sulfat domain of aggrecan. BMC Genet 19:1–9
69. Cavanagh JAL, Tammen I, Windsor PA, Bateman JF, Savarirayan R, Nicholas FW, Raadsma HW (2007) Bulldog dwarfism in Dexter cattle is caused by mutations in ACAN. Mamm Genome 18:808–814
70. Schwarzenbacher H, Wurmser C, Flisikowski K, Misurova L, Jung S, Langenmayer MC, Schnieke A, Knubben-Schweizer G, Fries R, Pausch H (2016) A frameshift mutation in GON4L is associated with proportionate dwarfism in Fleckvieh cattle. Genet Sel Evol 48:1–10
71. Koltjes JE, Mishra BP, Kumar D, Kataria RS, Totir LR, Fernando RL, Cobbold R, Steffen D, Coppieters W, Georges M (2009) A nonsense mutation in cGMP-dependent type II protein kinase (PRKG2) causes dwarfism in American Angus cattle. Proc Natl Acad Sci 106:19250–19255
72. Sartelet A, Druet T, Michaux C, Fasquelle C, Géron S, Tamma N, Zhang Z, Coppieters W, Georges M, Charlier C (2012) A splice site variant in the bovine RNF11 gene compromises growth and regulation of the inflammatory response. PLoS Genet 8:e1002581–e1002581
73. Murgiano L, Jagannathan V, Benazzi C, Bolcato M, Brunetti B, Muscatello LV, Dittmer K, Piffer C, Gentile A, Drögemüller C (2014) Deletion in the EVC2 gene causes chondrodysplastic dwarfism in Tyrolean Grey cattle. PLoS One 9:e94861
74. Takeda H, Takami M, Oguni T, et al (2002) Positional cloning of the gene LIMBIN responsible for bovine chondrodysplastic dwarfism. Proc Natl Acad Sci U S A 99:10549–10554
75. Hirano T, Kobayashi N, Matsuhashi T, Watanabe D, Watanabe T, Takasuga A, Sugimoto M, Sugimoto Y (2013) Mapping and exome sequencing identifies a mutation in the IARS gene as the cause of hereditary perinatal weak calf syndrome. PLoS One 8:e64036
76. Agerholm JS, McEvoy FJ, Heegaard S, Charlier C, Jagannathan V, Drögemüller C (2017) A de novo missense mutation of FGFR2 causes facial dysplasia syndrome in Holstein cattle. BMC Genet 18:1–9
77. Braun M, Lehmecker A, Eikelberg D, Hellige M, Beineke A, Metzger J, Distl O (2021) De novo ZIC2 frameshift variant associated with frontonasal dysplasia in a Limousin calf. BMC Genomics 22:1–9
78. Singleton AC, Mitchell AL, Byers PH, Potter KA, Pace JM (2005) Bovine model of Marfan syndrome results from an amino acid change (c. 3598G> A, p. E1200K) in a calcium-binding epidermal growth factor-like domain of fibrillin-1. Hum Mutat 25:348–352
79. Hirano T, Matsuhashi T, Kobayashi N, Watanabe T, Sugimoto Y (2012) Identification of an FBN1 mutation in bovine Marfan syndrome-like disease. Anim Genet 43:11–17

80. Petersen JL, Tietze SM, Burrack RM, Steffen DJ (2019) Evidence for a de novo, dominant germ-line mutation causative of osteogenesis imperfecta in two Red Angus calves. *Mamm Genome* 30:81–87
81. Jacinto JGP, Häfliger IM, McEvoy FJ, Drögemüller C, Agerholm JS (2021) A de novo mutation in COL1A1 in a Holstein Calf with Osteogenesis Imperfecta Type II. *Animals* 11:561
82. Meyers SN, McDanel TG, Swist SL, Marron BM, Steffen DJ, O'Toole D, O'Connell JR, Beever JE, Sonstegard TS, Smith TPL (2010) A deletion mutation in bovine SLC4A2 is associated with osteopetrosis in Red Angus cattle. *BMC Genomics* 11:337
83. Murgiano L, Militerno G, Sbarra F, Drögemüller C, G. P. Jacinto J, Gentile A, Bolcato M (2020) KDM2B-associated paunch calf syndrome in Marchigiana cattle. *J Vet Intern Med* 34:1657–1661
84. Testoni S, Bartolone E, Rossi M, Patrignani A, Bruggmann R, Lichtner P, Tetens J, Gentile A, Drögemüller C (2012) KDM2B Is Implicated in Bovine Lethal Multi-Organic Developmental Dysplasia. *PLoS One* 7:1–8
85. Sieck RL, Fuller AM, Bedwell PS, Ward JA, Sanders SK, Xiang S-H, Peng S, Petersen JL, Steffen DJ (2020) Mandibulofacial dysostosis attributed to a recessive mutation of CYP26C1 in Hereford cattle. *Genes (Basel)* 11:1246
86. Capitan A, Allais-Bonnet A, Pinton A, et al (2012) A 3.7 Mb deletion encompassing ZEB2 causes a novel polled and multisystemic syndrome in the progeny of a somatic mosaic bull. *PLoS One* 7:e49084
87. Gehrke LJ, Upadhyay M, Heidrich K, et al (2020) A de novo frameshift mutation in ZEB2 causes polledness, abnormal skull shape, small body stature and subfertility in Fleckvieh cattle. *Sci Rep* 10:1–14
88. Jacinto JGP, Häfliger IM, Gentile A, Drögemüller C (2021) A heterozygous missense variant in MAP2K2 in a stillborn romagnola calf with skeletal-cardio-enteric dysplasia. *Animals* 11:1931
89. Drögemüller C, Leeb T, Harlizius B, Tammen I, Distl O, Höltershinken M, Gentile A, Duchesne A, Eggen A (2007) Congenital syndactyly in cattle: four novel mutations in the low density lipoprotein receptor-related protein 4 gene (LRP4). *BMC Genet* 8:1–12
90. Duchesne A, Gautier M, Chadi S, Grohs C, Floriot S, Gallard Y, Caste G, Ducos A, Eggen A (2006) Identification of a doublet missense substitution in the bovine LRP4 gene as a candidate causal mutation for syndactyly in Holstein cattle. *Genomics* 88:610–621
91. Johnson EB, Steffen DJ, Lynch KW, Herz J (2006) Defective splicing of Megf7/Lrp4, a regulator of distal limb development, in autosomal recessive mulefoot disease. *Genomics* 88:600–609
92. Becker D, Weikard R, Schulze C, Wohlsein P, Kühn C (2020) A 50-kb deletion disrupting the RSPO2 gene is associated with tetradysmelia in Holstein Friesian cattle. *Genet Sel Evol* 52:1–13
93. Brenig B, Schütz E, Hardt M, Scheuermann P, Freick M (2015) A 20 bp duplication in exon 2 of the aristaless-like homeobox 4 gene (ALX4) Is the candidate causative mutation for tibial hemimelia syndrome in Galloway cattle. *PLoS One* 10:e0129208
94. Beever JE, Marron BM (2012) Screening for the genetic defect causing tibial hemimelia in bovines. U.S. Pat. No. 8,158,356

95. Kromik A, Ulrich R, Kusenda M, et al (2015) The mammalian cervical vertebrae blueprint depends on the T (brachyury) gene. *Genetics* 199:873–883
96. Wiedemar N, Riedi A, Jagannathan V, Drögemüller C, Meylan M (2015) Genetic abnormalities in a calf with congenital increased muscular tonus. *J Vet Intern Med* 29:1418
97. Sartelet A, Li W, Pailhoux E, et al (2015) Genome-wide next-generation DNA and RNA sequencing reveals a mutation that perturbs splicing of the phosphatidylinositol glycan anchor biosynthesis class H gene (PIGH) and causes arthrogryposis in Belgian Blue cattle. *BMC Genomics* 16:1–9
98. Agerholm JS, McEvoy FJ, Menzi F, Jagannathan V, Drögemüller C (2016) A CHRN1B1 frameshift mutation is associated with familial arthrogryposis multiplex congenita in Red dairy cattle. *BMC Genomics* 17:1–10
99. Beever JE, Marron BM (2011) Screening for arthrogryposis multiplex in bovines. U.S. Pat. No. 20,110,151,440 A1
100. Leipold HW, Blaugh B, Huston K, Edgerly CG, Hibbs CM (1973) Weaver syndrome in Brown Swiss cattle: clinical signs and pathology. *Vet Med small Anim Clin* 68:645–647
101. McClure M, Kim E, Bickhart D, et al (2013) Fine mapping for weaver syndrome in Brown Swiss cattle and the identification of 41 concordant mutations across NRCAM, PNPLA8 and CTTNBP2. *PLoS One* 8:e59251
102. Kunz E, Rothhammer S, Pausch H, Schwarzenbacher H, Seefried FR, Matiasek K, Seichter D, Russ I, Fries R, Medugorac I (2016) Confirmation of a non-synonymous SNP in PNPLA8 as a candidate causal mutation for Weaver syndrome in Brown Swiss cattle. *Genet Sel Evol* 48:1–14
103. Reynolds EGM, Neeley C, Lopdell TJ, et al (2021) Non-additive association analysis using proxy phenotypes identifies novel cattle syndromes. *Nat Genet* 53:949–954
104. Duchesne A, Vaiman A, Frah M, et al (2018) Progressive ataxia of Charolais cattle highlights a role of KIF1C in sustainable myelination. *PLOS Genet* 14:e1007550
105. Kraner S, Sieb JP, Thompson PN, Steinlein OK (2002) Congenital myasthenia in Brahman calves caused by homozygosity for a CHRNE truncating mutation. *Neurogenetics* 4:87–91
106. Charlier C, Coppieeters W, Rollin F, et al (2008) Highly effective SNP-based association mapping and management of recessive defects in livestock. *Nat Genet* 40:449–454
107. Jacinto JGP, Häfliger IM, Akyürek EE, Sacchetto R, Benazzi C, Gentile A, Drögemüller C (2021) KCNG1-related syndromic form of congenital neuromuscular channelopathy in a crossbred calf. *Genes (Basel)* 12:1792
108. Drögemüller C, Drögemüller M, Leeb T, Mascarello F, Testoni S, Rossi M, Gentile A, Damiani E, Sacchetto R (2008) Identification of a missense mutation in the bovine ATP2A1 gene in congenital pseudomyotonia of Chianina cattle: An animal model of human Brody disease. *Genomics* 92:474–477
109. Murgiano L, Sacchetto R, Testoni S, Dorotea T, Mascarello F, Liguori R, Gentile A, Drögemüller C (2012) Pseudomyotonia in Romagnola cattle caused by novel ATP2A1 mutations. *BMC Vet Res* 8:1–9
110. Pierce KD, Handford CA, Morris R, Vafa B, Dennis JA, Healy PJ, Schofield PR (2001) A nonsense mutation in the $\alpha 1$ subunit of the inhibitory glycine receptor associated with

bovine myoclonus. *Mol Cell Neurosci* 17:354–363

111. Denholm LJ, Beever JE, Marron BM, Walker KH, Healy PJ, Dennis JA, O'Rourke BA, Teseling TF (2014) Contractural Arachnodactyly (CA): A congenital recessive marfanoid syndrome with reduced elasticity of muscle connective tissue resulting from a large (~58 kilobase pair) deletion affecting the ADAMTSL3 gene in Angus and Angus influenced cattle breeds. In: Proc. XXVIII World Buiatrics Congr. Cairns Aust. p 0305
112. Drögemüller C, Reichart U, Seuberlich T, et al (2011) An unusual splice defect in the mitofusin 2 gene (MFN2) is associated with degenerative axonopathy in Tyrolean Grey cattle. *PLoS One* 6:e18931
113. Karageorgos L, Hill B, Bawden MJ, Hopwood JJ (2007) Bovine mucopolysaccharidosis type IIIB. *J Inherit Metab Dis* 30:358–364
114. Houweling PJ, Cavanagh JAL, Palmer DN, Frugier T, Mitchell NL, Windsor PA, Raadsma HW, Tammen I (2006) Neuronal ceroid lipofuscinosis in Devon cattle is caused by a single base duplication (c.662dupG) in the bovine CLN5 gene. *Biochim Biophys Acta - Mol Basis Dis* 1762:890–897
115. American Jersey Cattle Association (2020) Jersey neuropathy with splayed forelimbs (JNS).
116. Woolley SA, Tsimnadis ER, Lenghaus C, et al (2020) Molecular basis for a new bovine model of Niemann-Pick type C disease. *PLoS One* 15:e0238697
117. El-Hamidi M, Leipold HW, Vestweber JGE, Saperstein G (1989) Spinal muscular atrophy in Brown Swiss calves. *Zentralblatt für Vet R A* 36:731–738
118. Krebs S, Medugorac I, Röther S, Strässer K, Förster M (2007) A missense mutation in the 3-ketodihydrosphingosine reductase FVT1 as candidate causal mutation for bovine spinal muscular atrophy. *Proc Natl Acad Sci* 104:6746–6751
119. Hafner A, Dahme E, Obermaier G, Schmidt P, Dirksen G (1993) Spinal dysmyelination in new-born Brown Swiss x Braunvieh calves. *J Vet Med Ser B* 40:413–422
120. Thomsen B, Nissen PH, Agerholm JS, Bendixen C (2010) Congenital bovine spinal dysmyelination is caused by a missense mutation in the SPAST gene. *Neurogenetics* 11:175–183
121. Duchesne A, Vaiman A, Castille J, et al (2017) Bovine and murine models highlight novel roles for SLC25A46 in mitochondrial dynamics and metabolism, with implications for human and animal health. *PLoS Genet* 13:e1006597–e1006597
122. Shuster DE, Kehrl Jr. ME, Ackermann MR, Gilbert RO (1992) Identification and prevalence of a genetic defect that causes leukocyte adhesion deficiency in Holstein cattle. *Proc Natl Acad Sci U S A* 89:9225–9229
123. Kunieda T, Nakagiri M, Takami M, Ide H, Ogawa H (1999) Cloning of bovine LYST gene and identification of a missense mutation associated with Chediak-Higashi syndrome of cattle. *Mamm Genome* 10:1146–1149
124. Menzi F, Besuchet-Schmutz N, Fragnière M, et al (2016) A transposable element insertion in APOB causes cholesterol deficiency in Holstein cattle. *Anim Genet* 47:253–257
125. Kipp S, Segelke D, Schierenbeck S, et al (2016) Identification of a haplotype associated with cholesterol deficiency and increased juvenile mortality in Holstein cattle. *J Dairy Sci* 99:8915–8931

126. Artesi M, Hahaut V, Cole B, Lambrechts L, Ashrafi F, Marçais A, Hermine O, Griebel P, Arsic N, van der Meer F (2019) Pooled CRISPR Inverse PCR sequencing (PCIP-seq): simultaneous sequencing of retroviral insertion points and the integrated provirus with long reads. *bioRxiv* 558130
127. Dennis JA, Healy PJ, Beaudet AL, O'Brien WE (1989) Molecular definition of bovine argininosuccinate synthetase deficiency. *Proc Natl Acad Sci USA* 86:7947–7951
128. Agerholm JS, Thulstrup PW, Bjerrum MJ, Bendixen C, Jørgensen CB, Fredholm M (2012) A molecular study of congenital erythropoietic porphyria in cattle. *Anim Genet* 43:210–215
129. Shanks RD, Dombrowski DB, Harpestad GW, Robinson JL (1984) Inheritance of UMP synthase in dairy cattle. *J Hered* 75:337–340
130. Schwenger B, Schöber S, Simon D (1993) DUMPS cattle carry a point mutation in the uridine monophosphate synthase gene. *Genomics* 16:241–244
131. McCormack BL, Chase CCJ, Olson TA, Elsasser TH, Hammond AC, Welsh THJ, Jiang H, Randel RD, Okamura CA, Lucy MC (2009) A miniature condition in Brahman cattle is associated with a single nucleotide mutation within the growth hormone gene. *Domest Anim Endocrinol* 37:104–111
132. Marron BM, Robinson JL, Gentry PA, Beever JE (2004) Identification of a mutation associated with factor XI deficiency in Holstein cattle. *Anim Genet* 35:454–456
133. Kunieda M, Tsuji T, Abbasi AR, Khalaj M, Ikeda M, Miyadera K, Ogawa H, Kunieda T (2005) An insertion mutation of the bovine F11 gene is responsible for factor XI deficiency in Japanese black cattle. *Mamm Genome* 16:383–389
134. Dennis JA, Moran C, Healy PJ (2000) The bovine α -glucosidase gene: coding region, genomic structure, and mutations that cause bovine generalized glycogenosis. *Mamm Genome* 11:206–212
135. Tsujino S, Shanske S, Valberg SJ, Cardinet GH, Smith BP, DiMauro S (1996) Cloning of bovine muscle glycogen phosphorylase cDNA and identification of a mutation in cattle with myophosphorylase deficiency, an animal model for McArdle's disease. *Neuromuscul Disord* 6:19–26
136. Khalaj M, Abbasi AR, Shimojo K, Moritomo Y, Yoneda K, Kunieda T (2009) A missense mutation (p. Leu2153His) of the factor VIII gene causes cattle haemophilia A. *Anim Genet* 40:763–765
137. Reinartz S, Weiß C, Mischke R, Distl O (2018) A mild form of haemophilia A is associated with two factor VIII missense mutations in German Fleckvieh cattle. *Anim Genet* 49:350–351
138. Tollersrud OK, Berg T, Healy P, Evjen G, Ramachandran U, Nilssen Ø (1997) Purification of bovine lysosomal α -mannosidase, characterization of its gene and determination of two mutations that cause α -mannosidosis. *Eur J Biochem* 246:410–419
139. Leipprandt JR, Chen H, Horvath JE, Qiao XT, Jones MZ, Friderici KH (1999) Identification of a bovine β -mannosidosis mutation and detection of two β -mannosidase pseudogenes. *Mamm Genome* 10:1137–1141
140. DENNIS JA, HEALY PJ (1999) Definition of the mutation responsible for maple syrup urine disease in poll shorthorns and genotyping poll shorthorns and poll herefords for maple syrup urine disease alleles. *Res Vet Sci* 67:1–6

141. Zhang B, Healy PJ, Zhao Y, Crabb DW, Harris RA (1990) Premature translation termination of the pre-E1 alpha subunit of the branched chain alpha-ketoacid dehydrogenase as a cause of maple syrup urine disease in Polled Hereford calves. *J Biol Chem* 265:2425–2427
142. Boudreaux MK, Schmutz SM, French PS (2007) Calcium diacylglycerol guanine nucleotide exchange factor I (CalDAG-GEFI) gene mutations in a thrombopathic Simmental calf. *Vet Pathol* 44:932–935
143. Yuzbasiyan-Gurkan V, Bartlett E (2006) Identification of a unique splice site variant in SLC39A4 in bovine hereditary zinc deficiency, lethal trait A46: An animal model of acrodermatitis enteropathica. *Genomics* 88:521–526
144. Drögemüller C, Distl O, Leeb T (2003) X-linked anhidrotic ectodermal dysplasia (ED1) in men, mice, and cattle. *Genet Sel Evol* 35:S137
145. Gargani M, Valentini A, Pariset L (2011) A novel point mutation within the EDA gene causes an exon dropping in mature RNA in Holstein Friesian cattle breed affected by X-linked anhidrotic ectodermal dysplasia. *BMC Vet Res* 7:35
146. Ogino A, Kohama N, Ishikawa S, Tomita K, Nonaka S, Shimizu K, Tanabe Y, Okawa H, Morita M (2011) A novel mutation of the bovine EDA gene associated with anhidrotic ectodermal dysplasia in Holstein cattle. *Hereditas* 148:46–49
147. Ogino A, Shimizu K, Tanabe Y, Morita M (2012) De novo mutation of the bovine EDA gene associated with anhidrotic ectodermal dysplasia in Japanese Black cattle. *Anim Genet* 43:646
148. Escoufflaire C, Rebours E, Charles M, Orellana S, Cano M, Rivière J, Grohs C, Hayes H, Capitan A (2019) A de novo 3.8-Mb inversion affecting the EDA and XIST genes in a heterozygous female calf with generalized hypohidrotic ectodermal dysplasia. *BMC Genomics* 20:715
149. Karlskov-Mortensen P, Cirera S, Nielsen OL, Arnbjerg J, Reibel J, Fredholm M, Agerholm JS (2011) Exonization of a LINE1 fragment implicated in X-linked hypohidrotic ectodermal dysplasia in cattle. *Anim Genet* 42:578–584
150. Drögemüller C, Barlund CS, Palmer CW, Leeb T (2006) A novel mutation in the bovine EDA gene causing anhidrotic ectodermal dysplasia (Brief report). *Arch Anim Breed* 49:615–616
151. Drögemüller C, Distl O, Leeb T (2001) Partial deletion of the bovine ED1 gene causes anhidrotic ectodermal dysplasia in cattle. *Genome Res* 11:1699–1705
152. Drögemüller C, Peters M, Pohlenz J, Distl O, Leeb T (2002) A single point mutation within the ED1 gene disrupts correct splicing at two different splice sites and leads to anhidrotic ectodermal dysplasia in cattle. *J Mol Med* 80:319–323
153. O’Toole D, Häfliger IM, Leuthard F, Schumaker B, Steadman L, Murphy B, Drögemüller C, Leeb T (2021) X-Linked Hypohidrotic Ectodermal Dysplasia in Crossbred Beef Cattle Due to a Large Deletion in EDA. *Anim*. <https://doi.org/10.3390/ani11030657>
154. Gutiérrez-Gil B, Wiener P, Williams JL (2007) Genetic effects on coat colour in cattle: dilution of eumelanin and pheomelanin pigments in an F2-Backcross Charolais × Holstein population. *BMC Genet* 8:56
155. Jolly RD, Wills JL, Kenny JE, Cahill JI, Howe L (2008) Coat-colour dilution and hypotrichosis in Hereford crossbred calves. *N Z Vet J* 56:74–77

156. Schmutz SM, Berryere TG, Ciobanu DC, Mileham AJ, Schmidtz BH, Fredholm M (2004) A form of albinism in cattle is caused by a tyrosinase frameshift mutation. *Mamm Genome* 15:62–67
157. Rothhammer S, Kunz E, Seichter D, Krebs S, Wassertheurer M, Fries R, Brem G, Medugorac I (2017) Detection of two non-synonymous SNPs in SLC45A2 on BTA20 as candidate causal mutations for oculocutaneous albinism in Braunvieh cattle. *Genet Sel Evol* 49:1–8
158. Jacinto JGP, Häfliger IM, Veiga IMB, Letko A, Benazzi C, Bolcato M, Drögemüller C (2020) A heterozygous missense variant in the COL5A2 in holstein cattle resembling the classical Ehlers–Danlos syndrome. *Animals* 10:2002
159. Colige A, Sieron AL, Li SW, et al (1999) Human Ehlers-Danlos syndrome type VII C and bovine dermatosparaxis are caused by mutations in the procollagen I N-proteinase gene. *Am J Hum Genet* 65:308–317
160. Tajima M, Miyake S, Takehana K, Kobayashi A, Yamato O, Maede Y (1999) Gene defect of dermatan sulfate proteoglycan of cattle affected with a variant form of Ehlers-Danlos syndrome. *J Vet Intern Med* 13:202–205
161. Pausch H, Ammermuller S, Wurmser C, Hamann H, Tetens J, Drogemuller C, Fries R (2016) A nonsense mutation in the COL7A1 gene causes epidermolysis bullosa in Vorderwald cattle. *BMC Genet* 17:149
162. Menoud A, Welle M, Tetens J, Lichtner P, Drögemüller C (2012) A COL7A1 mutation causes dystrophic epidermolysis bullosa in Rotes Höhenvieh cattle. *PLoS One* 7:e38823
163. Michot P, Fantini O, Braque R, et al (2015) Whole-genome sequencing identifies a homozygous deletion encompassing exons 17 to 23 of the integrin beta 4 gene in a Charolais calf with junctional epidermolysis bullosa. *Genet Sel Evol* 47:37
164. Peters M, Reber I, Jagannathan V, Raddatz B, Wohlsein P, Drögemüller C (2015) DNA-based diagnosis of rare diseases in veterinary medicine: A 4.4 kb deletion of ITGB4 is associated with epidermolysis bullosa in Charolais cattle. *BMC Vet Res* 11:1–8
165. Sartelet A, Harland C, Tamma N, Karim L, Bayrou C, Li W, Ahariz N, Coppieters W, Georges M, Charlier C (2015) A stop-gain in the laminin, alpha 3 gene causes recessive junctional epidermolysis bullosa in Belgian Blue cattle. *Anim Genet* 46:566–570
166. Murgiano L, Wiedemar N, Jagannathan V, Isling LK, Drögemüller C, Agerholm JS (2015) Epidermolysis bullosa in Danish Hereford calves is caused by a deletion in LAMC2 gene. *BMC Vet Res* 11:23
167. Ford CA, Stanfield AM, Spelman RJ, et al (2005) A mutation in bovine keratin 5 causing epidermolysis bullosa simplex, transmitted by a mosaic sire. *J Invest Dermatol* 124:1170–1176
168. Jacinto JGP, Häfliger IM, Veiga IMB, Drögemüller C, Agerholm JS (2020) A de novo mutation in KRT5 in a crossbred calf with epidermolysis bullosa simplex. *J Vet Intern Med* 34:2800–2807
169. Kuca T, Marron BM, Jacinto JGP, Paris JM, Gerspach C, Beever JE, Drögemüller C (2021) A nonsense variant in hephaestin like 1 (HEPHL1) is responsible for congenital hypotrichosis in Belted Galloway cattle. *Genes (Basel)* 12:643
170. Jacinto JGP, Markey AD, Veiga IMB, Paris JM, Welle M, Beever JE, Drögemüller C (2021) A KRT71 loss-of-function variant results in inner root sheath dysplasia and

- recessive congenital hypotrichosis of Hereford cattle. *Genes (Basel)* 12:1038
171. Knaust J, Hadlich F, Weikard R, Kuehn C (2016) Epistatic interactions between at least three loci determine the “rat-tail” phenotype in cattle. *Genet Sel Evol* 48:26
 172. Eager KLM, Conyers LE, Woolley SA, Tammen I, O’Rourke BA (2020) A novel ABCA12 frameshift mutation segregates with ichthyosis fetalis in a Polled Hereford calf. *Anim Genet* 51:837–838
 173. Woolley SA, Eager KLM, Häfliger IM, Bauer A, Drögemüller C, Leeb T, O’Rourke BA, Tammen I (2019) An ABCA12 missense variant in a Shorthorn calf with ichthyosis fetalis. *Anim Genet* 50:749–752
 174. Jacinto JGP, Häfliger IM, Veiga I, Letko A, Gentile A, Drögemüller C (2021) A frameshift insertion in FA2H causes a recessively inherited form of ichthyosis congenita in Chianina cattle. *Mol Genet Genomics* 296:1313–1322
 175. Häfliger IM, Sickinger M, Holsteg M, Raeder LM, Henrich M, Marquardt S, Drögemüller C, Lühken G (2020) An IL17RA frameshift variant in a Holstein cattle family with psoriasis-like skin alterations and immunodeficiency. *BMC Genet* 21:1–10
 176. Murgiano L, Shirokova V, Welle MM, et al (2015) Hairless streaks in cattle implicate TSR2 in early hair follicle formation. *PLOS Genet* 11:e1005427
 177. Hofstetter S, Welle M, Gorgas D, Balmer P, Roosje P, Mock T, Meylan M, Jagannathan V, Drögemüller C (2017) A de novo germline mutation of DLX 3 in a Brown Swiss calf with tricho-dento-osseus-like syndrome. *Vet Dermatol* 28:616-e150
 178. Jung S, Pausch H, Langenmayer MC, Schwarzenbacher H, Majzoub-Altweck M, Gollnick NS, Fries R (2014) A nonsense mutation in PLD4 is associated with a zinc deficiency-like syndrome in Fleckvieh cattle. *BMC Genomics* 15:623
 179. Häfliger IM, Marchionatti E, Stengård M, et al (2021) CNGB3 missense variant causes recessive achromatopsia in Original Braunvieh cattle. *Int J Mol Sci* 22:12440
 180. Hollmann AK, Dammann I, Wemheuer WM, Wemheuer WE, Chilla A, Tipold A, Schulz-Schaeffer WJ, Beck J, Schütz E, Brenig B (2017) Morgagnian cataract resulting from a naturally occurring nonsense mutation elucidates a role of CPAMD8 in mammalian lens development. *PLoS One* 12:e0180665–e0180665
 181. Murgiano L, Jagannathan V, Calderoni V, Joechler M, Gentile A, Drögemüller C (2014) Looking the cow in the eye: Deletion in the NID1 gene is associated with recessive inherited cataract in romagnola cattle. *PLoS One*. <https://doi.org/10.1371/journal.pone.0110628>
 182. Abbasi AR, Khalaj M, Tsuji T, Tanahara M, Uchida K, Sugimoto Y, Kunieda T (2009) A mutation of the WFDC1 gene is responsible for multiple ocular defects in cattle. *Genomics* 94:55–62
 183. Koch CT, Bruggmann R, Tetens J, Drögemüller C (2013) A non-coding genomic duplication at the HMX1 locus is associated with crop ears in highland cattle. *PLoS One* 8:e77841
 184. Wiedemar N, Drögemüller C (2014) A 19-Mb de novo deletion on BTA 22 including MITF leads to microphthalmia and the absence of pigmentation in a Holstein calf. *Anim Genet* 45:868–870
 185. Philipp U, Lupp B, Mömke S, Stein V, Tipold A, Eule JC, Rehage J, Distl O (2011) A

- MITF mutation associated with a dominant white phenotype and bilateral deafness in German Fleckvieh cattle. *PLoS One* 6:e28857
186. Jacinto JGP, Häfliger IM, Bernardini M, Mandara MT, Bianchi E, Bolcato M, Romagnoli N, Gentile A, Drögemüller C A homozygous missense variant in laminin subunit beta 1 as candidate causal mutation of hemifacial microsomia in Romagnola cattle. *J. Vet. Intern. Med.*
 187. Simpson MA, Cook RW, Solanki P, Patton MA, Dennis JA, Crosby AH (2009) A mutation in NF κ B interacting protein 1 causes cardiomyopathy and woolly haircoat syndrome of Poll Hereford cattle. *Anim Genet* 40:42–46
 188. Owczarek-Lipska M, Plattet P, Zipperle L, Drögemüller C, Posthaus H, Dolf G, Braunschweig MH (2011) A nonsense mutation in the optic atrophy 3 gene (OPA3) causes dilated cardiomyopathy in Red Holstein cattle. *Genomics* 97:51–57
 189. Sugimoto M, Furuoka H, Sugimoto Y (2003) Deletion of one of the duplicated Hsp70 genes causes hereditary myopathy of diaphragmatic muscles in Holstein-Friesian cattle. *Anim Genet* 34:191–197
 190. Burgstaller J, Url A, Pausch H, Schwarzenbacher H, Egerbacher M, Wittek T (2016) Clinical and biochemical signs in Fleckvieh cattle with genetically confirmed Fanconi-Bickel syndrome (cattle homozygous for Fleckvieh haplotype 2). *Berl Munch Tierarztl Wochenschr* 129:132–137
 191. Venhoranta H, Pausch H, Wysocki M, et al (2013) Ectopic KIT copy number variation underlies impaired migration of primordial germ cells associated with gonadal hypoplasia in cattle (*Bos taurus*). *PLoS One* 8:e75659–e75659
 192. Hirano T, Kobayashi N, Itoh T, Takasuga A, Nakamaru T, Hirotsune S, Sugimoto Y (2000) Null mutation of PCLN-1/Claudin-16 results in bovine chronic interstitial nephritis. *Genome Res* 10:659–663
 193. Hirano T, Hirotsune S, Sasaki S, Kikuchi T, Sugimoto Y (2002) A new deletion mutation in bovine Claudin-16 (CL-16) deficiency and diagnosis. *Anim Genet* 33:118–122
 194. Murgiano L, Jagannathan V, Piffer C, Diez-Prieto I, Bolcato M, Gentile A, Drögemüller C (2016) A frameshift mutation in MOCOS is associated with familial renal syndrome (xanthinuria) in Tyrolean Grey cattle. *BMC Vet Res* 12:1–10

11 Acknowledgements

In the late 2018 I decided to move to Bologna wishing to become a PhD candidate in cattle medicine. Prof. Dr. Arcangelo Gentile made this wish come true by mentoring, supporting and encouraging me in the last three years. Since the early 2020 Prof. Dr. Cord Drögemüller have gave me the possibility to join his group in the Institute of Genetics of the Vetsuisse Faculty, University of Bern. Without his exceptional support, concern and mentoring this thesis would not be possible.

Likewise, I want to acknowledge Prof. Dr. Cinzia Benazzi for her mentoring and continuous support.

Furthermore, I would like to acknowledge the support of bovine practitioners and farmers who were fundamental for the reported and submission of the cases. I would also like to thanks to the breeding associations such as the National Association of Italian Beef Cattle Breeders (ANABIC), in particular to Dr. Fiorella Sbarra, for providing the biological material of the Italian beef breeds.

Several of the presented studies were performed in collaboration with national and international researchers. I am very grateful to all their support and trust to collaborate. The given inputs inspired me and allowed me to growth personal- and professionally.

I also want to thank the lab technicians from the Institute of Genetics of the Vetsuisse Faculty, University of Bern, especially Nathalie Besuchet, who were extremely helpful for the success of this thesis.

An enormous thank you to the whole the team at the Institute of Genetics of the Vetsuisse Faculty, University of Bern who received me with open arms and to my colleagues form the Ruminants Clinic of the University of Bologna.

Finally, I want to thank my family and friends for all their support and faith on me.